High-resolution analysis of rapid climate change from Greenland ice cores

Thesis

High-resolution analysis of rapid climate change from Greenland ice cores

Elizabeth Ruth Thomas

Submitted for the degree of Doctor of Philosophy to the Open University
May 2006

Sponsoring establishment:
British Antarctic Survey
Cambridge
UK

BEST COPY AVAILABLE.

VARIABLE PRINT QUALITY

ORIGINAL COPY TIGHTLY BOUND

TEXT BOUND CLOSE TO THE SPINE IN THE ORIGINAL THESIS

PAGINATED BLANK PAGES ARE SCANNED AS FOUND IN ORIGINAL THESIS

NO INFORMATION IS MISSING

Abstract

Extreme shifts in the climate system have long been recognized but the timescales for most events are large, occurring over millennia or longer. There is however, growing evidence for abrupt shifts in the climate system on much shorter timescales of centuries, decades or even years. It is these abrupt climate changes that would have the biggest impact on modern society with a potentially large and catastrophic climate shift occurring within the human lifespan. In this thesis I investigate two large and abrupt climate oscillations, as observed in the Greenland ice core record. The first is the most prominent cold event to have occurred during the Holocene, the cold event 8,200 years ago (the 8.2 kyr event) and the second is one of the strongest and longest glacial oscillations, Dansgaard-Oeschger event 8 (DO-8).

I present a collection of high-resolution chemistry and stable isotope records from the plateau of the Greenland ice cap during the cold event 8,200 years ago. Using a composite of 4 records, the cold event is observed as a 160.5 year period during which decadal-mean isotopic values were below average, within which there is a central event of 69 years during which values were consistently more than one standard deviation below the average for the preceding period. The results show clear evidence for colder temperatures and a decrease in snow accumulation rate. However, the changes in chemical concentrations for the ions looked at here are small, suggesting only minor changes in atmospheric circulation for this event. Apart from the decrease in methane concentration, Greenland ice cores give only weak evidence for effects outside the North Atlantic region.

A new high-resolution chemical and stable isotope record is presented, from the North Greenland Ice Core Project (NGRIP) ice core, during Dansgaard-Oeschger event 8. The onset of DO-8 is first observed as a rapid decrease in chemical deposition to Greenland, indicating a large and abrupt shift in oceanic and atmospheric circulation. The change in the chemical deposition is followed over a decade later by an increase in temperature of approximately 13 °C, from extreme cold stadial conditions to warm interstadial conditions, accompanied by a 33 % increase in annual snow accumulation. The transition is observed in the deuterium excess record as an abrupt shift to warmer source water conditions in the period after the chemical transition but considerably earlier than interstadial temperatures have been reached.

Acknowledgements

When I decided I wanted to be a scientist, I had romantic ideas about working in the tropics on the back of a boat in a bikini, saving the world and getting a good tan in the process. So how did I end up working in a freezer in Cambridge?

Having spent over 2,160 hours shivering at –20°C (I have counted!), its a question I have asked myself frequently. However, when I look at my completed thesis I know it was worth it...besides, all those hours in the cold were a fantastic excuse to eat lots of cake!

I never imagined that I would gain the opportunities that I have and I am grateful to all those who helped make it possible. I would like to thank all three supervisors, Eric Wolff (BAS), Robert Mulvaney (BAS) and Jonathan Holmes (UCL) for their comments and support throughout, and my examiners David Peel and Jim Marshall for their valued suggestions and a long and thorough viva.

I would also like to thank my friends for keeping me positive and Sue Foord for her help in the cold room and for never actually cutting off her fingers!

Finally, to my parents I thank you for your constant and unwavering support, and encouragement. I dedicate this thesis to you.

Declaration

All chemical data (unless otherwise stated) has been solely produced by myself and has not been used to obtain any other academic qualification. All isotope data (unless otherwise stated) was sampled by myself and analysed by Carol Arrowsmith at NIGL, and Sigfus Johnsen at the University of Copenhagen. James White, Bruce Vaughn and Trevor Popp sampled and analysed isotope data at the University of Colorado.

Some of the results presented in this thesis have been published in a peer-reviewed journal, a copy of which is included at the end of the thesis.

The funding for this project was from the Natural Environment Research Councils Rapid climate change programme and the British Antarctic Survey. All data (unless otherwise stated) produced in this thesis is stored at the British Oceanographic Data Centre (BODC).

Aims

The aims of this thesis are to investigate the most prominent rapid climate change event of the Holocene, the 8.2 kyr event, and one of the strongest and longest events of the last glacial, Dansgaard-Oeschger event 8 (~35 kyr before present).

A new chemical and isotope record was produced from the analysis of two deep ice cores from Greenland to study the changes in deposition, temperature, accumulation and atmospheric circulation at a sub-seasonal resolution during the Holocene cold event and at the onset and termination of the glacial oscillation. Was a significant circulation or depositional change observed during the Holocene cooling and the glacial warming? If so, what changed first, the temperature, ocean or atmosphere? Was a change in seasonality observed and at what rate did the changes occur? Is it possible to obtain a sub-seasonal resolution record from the glacial ice when the annual layer thickness has been so strongly compressed?

This thesis starts with an introduction to rapid climate change from the last glacial to the present day highlighting the importance to the two events chosen in this study. The combined methods used in the investigation of both events, including the newly developed sample cutting and analysis techniques, are then discussed and the comprehensive quality control results presented. The two events are then discussed separately with both sections comprising of a critical review of the literature, presentation of the results and a discussion. The key findings and conclusions of both events are presented in the final chapter.

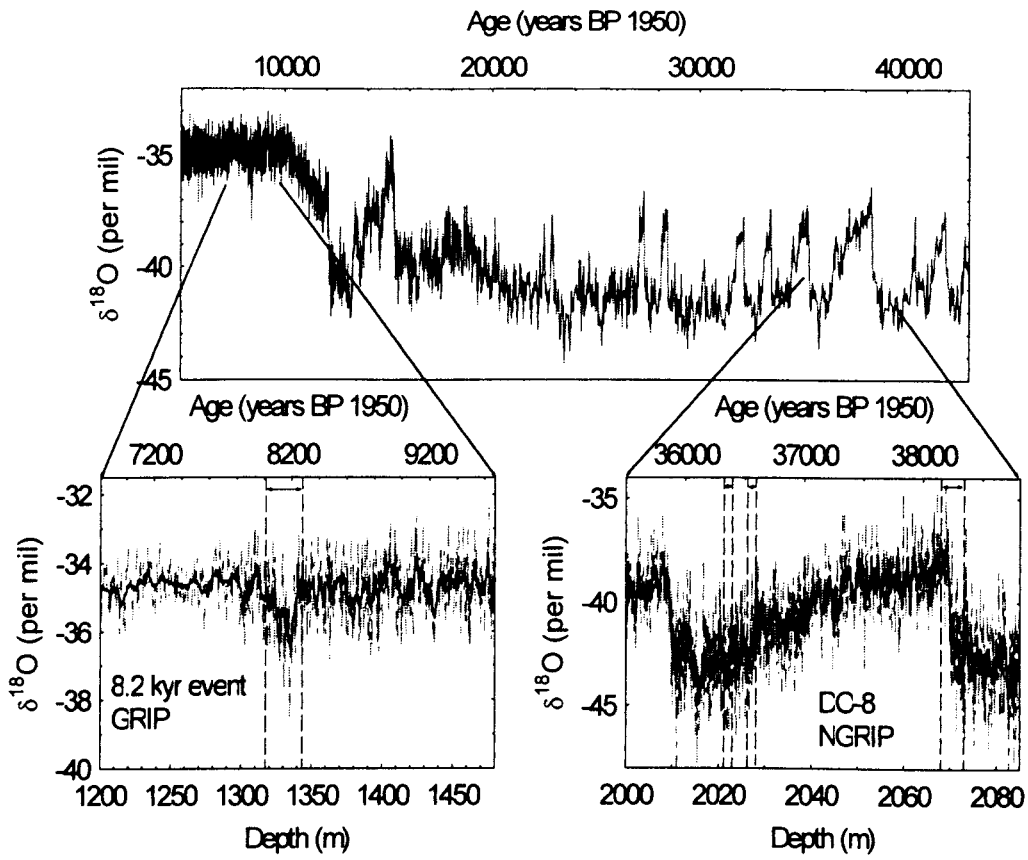

Figure i. Location of the 8.2 kyr event and DO-8. Top graph: Isotope record ($\delta^{18}O$ per mil) from GRIP [Johnsen et al., 1997] at 55 cm resolution. Bottom graphs: Expanded isotope record to show 8.2 kyr event (left) and DO-8 (right). Ice used in this thesis is shown by the vertical dashed lines and red arrows on bottom graphs. All graphs plotted using the GICCO5 age-scale [Rassmussen et al., 2005]

Chapter One

Introduction to Rapid Climate Change

Introduction to rapid climate change

Palaeoclimate records show that the climate system has existed in many different stable states from that of today. Large regional, hemispheric and global climate changes have occurred in the Earth's history as shown by numerous palaeoclimate records [Broecker, 1995, 1997]. Some of these occurred long ago when geological and astronomic conditions were substantially different from those of the present, such as the proposed "snowball earth" (when global glaciation persisted for millions of years) [Caldeira and Kasting, 1992], while others, such as the warm-polar "hothouse" pattern, were reached relatively recently, when geological conditions were similar to those of our modern Earth [Barron, 1987].

Extreme shifts in the climate system have long been recognized but the timescales are large for most events, occurring over millennia or longer. This is shown in figure 1.1; a comparison of the EPICA Dome C ice core, which covers eight glacial cycles, the Vostok ice core, and marine sediment cores [EPICA community members 2004]. There is however, growing evidence for abrupt shifts in the climate system on much shorter timescales of centuries, decades or even years. It is these abrupt climate changes that would have the biggest impact on modern society with a potentially large and catastrophic climate shift occurring within the human lifespan.

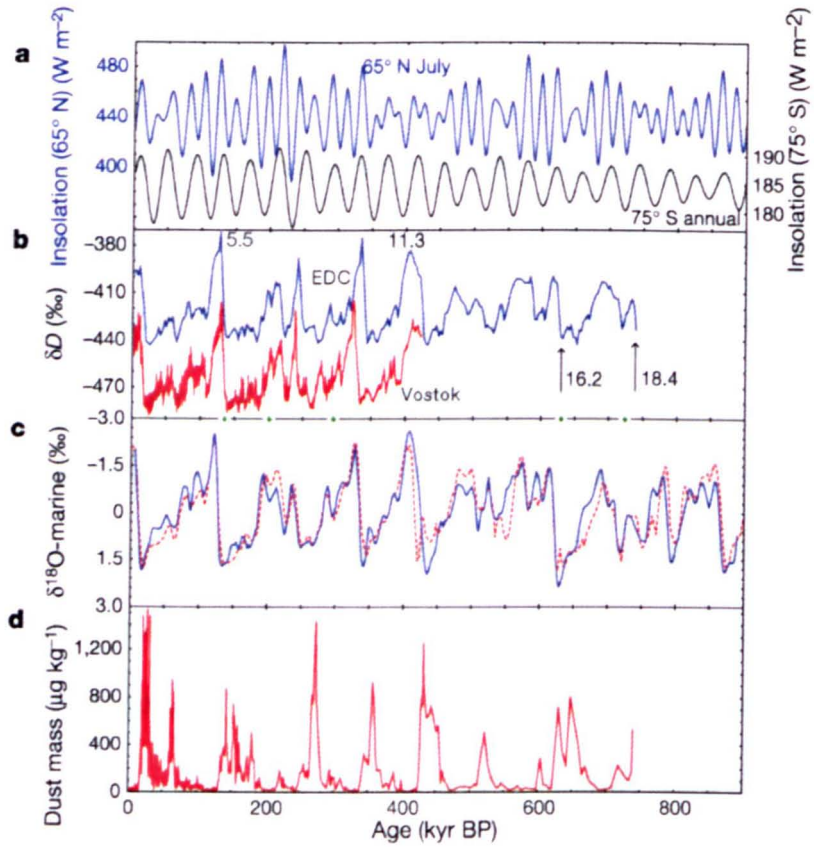

Figure 1.1. a Insolation records from Dome C. b Isotope record (δD) from Dome C (blue) and Vostok (red). c Marine oxygen isotope record. d Dust record from Dome C. [EPICA community members 2004]

Climate change has become a popular topic of debate in the scientific community and is gaining the attention of policy makers and governments through the possible socio-economic response to large-scale shifts in the climate system. Panels such as the IPCC (Inter governmental Panel on Climate Change) and the FCCC (Framework Convention on Climate Change) have been set up to assess the future impacts of global climate change and the possible "dangerous anthropogenic interferences" [IPCC 2001]. Alley (2003) concluded that past climate was especially unstable at times when the climate system was being forced to change from one state to another and that human activities may be driving the climate towards one of these thresholds. Although a substantial body of research has been collected on the potential ecological

and social impacts of climate change, nearly all studies assume a slow and gradual change.

Evidence from a wide range of palaeoclimate proxies has shown that the Earth's climate has been far from stable. The presence of large temperature variations is clearly observed in the Greenland ice core record with large and abrupt changes appearing frequently during the last glacial period [Bond et al., 1993; Dansgaard et al., 1993; Taylor et al., 1999]. In February 2004 concerns for climate change and, in particular, abrupt climate change led to the release of a report commissioned by the United States Department of Defence titled "An abrupt climate change scenario and its implications for United States security" [Schwartz and Randall, 2003]. The scenario was based on the implications of a continuation in the global temperatures recorded since the mid 20th century and the report speculated on the subsequent availability of food, water and energy. Substantial media coverage surrounded the report with "Doom and Gloom" cover stories highlighting the possible food shortages, mass population migrations and military conflict predicted in the report [Stipp, 2004]. The Hollywood dramatization of rapid climate change in the film "The day after tomorrow" [Emmerich, 2004] has further heightened public awareness on the possibility of substantial climate change within their lifetime. The focus of panels such as the FCCC is on the anthropogenic forcing and not the broader natural forcing which has caused past climate changes that are both large in scale and abrupt in time, with evidence to suggest regional changes of between 8 °C to 16 °C and a factor of two change in precipitation to have occurred in less than a decade.

Triggers for abrupt climate change:

According to the National Research Council (NRC) report "Abrupt climate change: Inevitable surprises", "an abrupt climate change occurs when the climate system is forced to cross some threshold, triggering a transition to a new state at a rate determined by the climate system itself and faster than the cause" [NCR 2002, p 14]. The forcings may be fast or chaotic but even a small forcing can create a large and abrupt response in the climate system [Alley et al., 2003].

Change in any measure of climate or its variability can be abrupt, including change in the intensity, duration, or frequency of extreme events. Floods, hurricanes, or volcanic eruptions have a large impact on humans and ecosystems, but their effects generally would not be considered abrupt climate changes unless the climate system is pushed over a threshold into a new state; however, a rapid, persistent change in the number or strength of floods or hurricanes might be regarded as an abrupt climate change.

Triggers may be fast, such as outburst floods associated with the termination of the last glaciation, or slow such as continental drift and orbital forcing. Solar activity and volcanic aerosols have been considered to explain the climate variability of the mid to late Holocene [Beer et al., 2000]. However they are considered too small to have triggered the larger climate changes observed during the early Holocene and the late glacial.

Within the palaeoclimate community the most popular explanation for abrupt climate change comes from the oceans, which following an initial trigger such as freshwater

flux to the north Atlantic, have the internal dynamics to latch the climate into a different state for centuries [Broecker et al., 2003].

The role of the oceans:

The high heat capacity of the oceans relative to the surrounding land modulates the earth's daily, seasonal, and inter-annual temperature fluctuations. The oceans act as a conveyor transporting heat from the equator toward the poles by a process known as Thermohaline Circulation (THC). A schematic of the global conveyor as described by Broecker et al., 1991 is shown in figure 1.2 showing the movement of warm saline waters around the globe. The North Atlantic currents, referred to as the Gulf Stream, are shown in figure 1.3, where the red arrows depict warm saline waters travelling north and blue arrows depict cold water travelling south. The strength of THC is primarily controlled by seawater density, which is a function of temperature and salinity, and the wind curl stress. Differential solar heating between high and low latitudes accelerates surface waters northwards towards the poles while the colder less saline waters produced in the high latitudes (as a result of freshwater input and low evaporation at high latitudes) sink southwards. The meridional overturning in the north Atlantic is dominated by the haline (freshwater) forcing from the Nordic seas, North Atlantic Deep Water (NADW) formation.

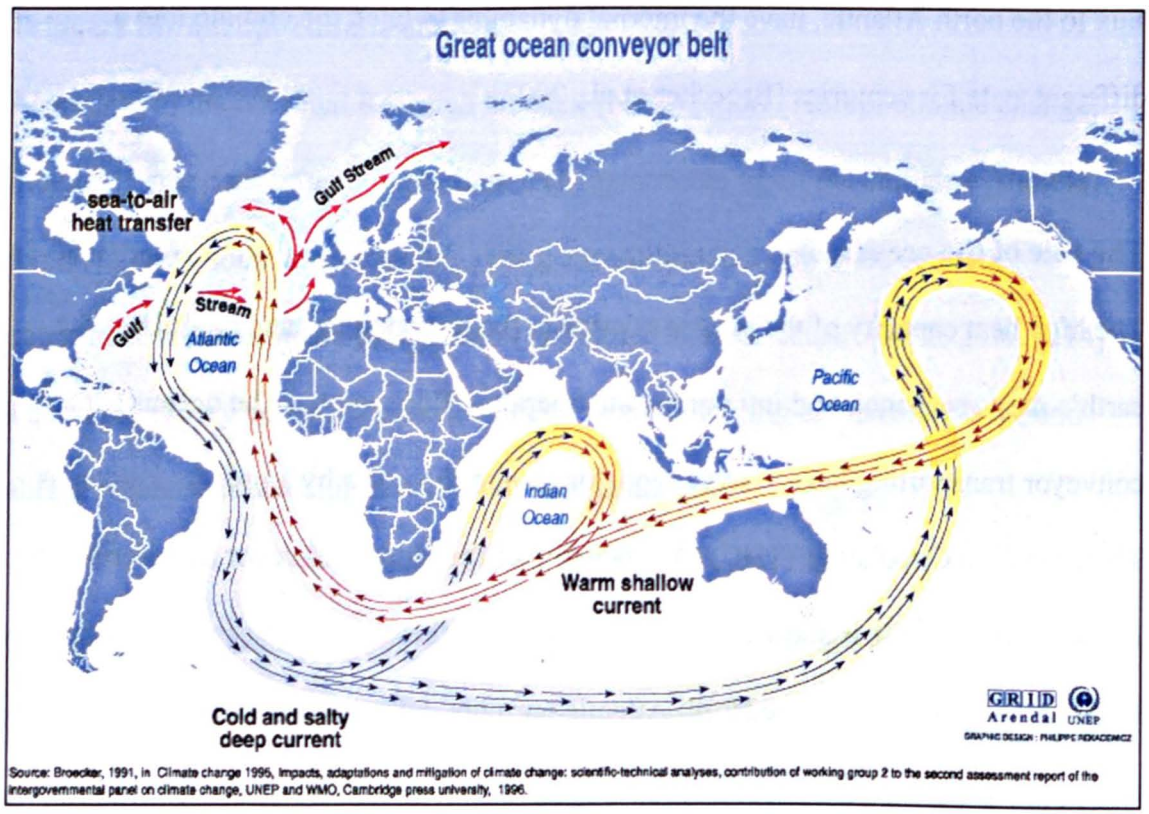

Figure 1.2. Global Conveyor [Broecker et al., 1991]. Red arrows indicate warm water currents and blue arrows indicate cold water currents.

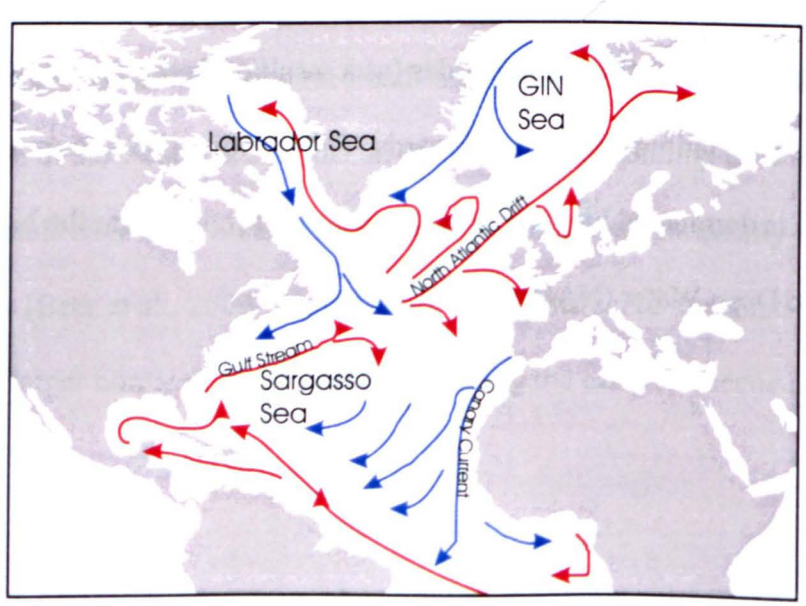

Figure 1.3. Schematic of North Atlantic "Gulf stream" currents. Red arrows indicate warm water current and blue arrows indicate cold water currents. (GIN refers to Greenland-Iceland-Norwegian seas)

THC is strongest in the North Atlantic, with only a small drive in the North Pacific where the high-latitude waters are too fresh to sink. The pole-ward heat transport associated with THC is also small in the southern ocean, where the lack of a meridional land barrier prevents the development of the strong east-west pressure gradient required to balance the southward surface flow. In the Southern Oceans it is the deep-water formation along the Antarctic continental shelf that produces the dense Antarctic Bottom water that heads towards lower latitudes. The dense water formed in the Weddell and Ross Seas is a result of high evaporation and brine rejection or the super-cooled water formed at the base of the thick floating ice shelves.

It is therefore the North Atlantic thermohaline circulation that is believed to hold the key to climatic oscillations during the last glacial period, and the abrupt changes within the Holocene.

It has long been believed that different states exist within the North Atlantic THC that can change abruptly as a result of even small changes in the hydrological cycle. Triggers such as an increase in freshwater input into the North Atlantic can slow the meridonal overturning by reducing the salinity and therefore the density of the NADW, thus reducing the southward flow resulting in a weakening of the THC. This has been shown in the many "hosing" experiments carried out using general circulation models (GCMs) with results ranging from significant weakening to a total shutdown of the THC [Renssen et al., 2001; 2002]. It is widely accepted that past climate oscillations were governed by three main THC modes; a modern mode, a glacial mode and a Heinrich mode [Labeyrie et al., 1992; Clark et al., 2002].

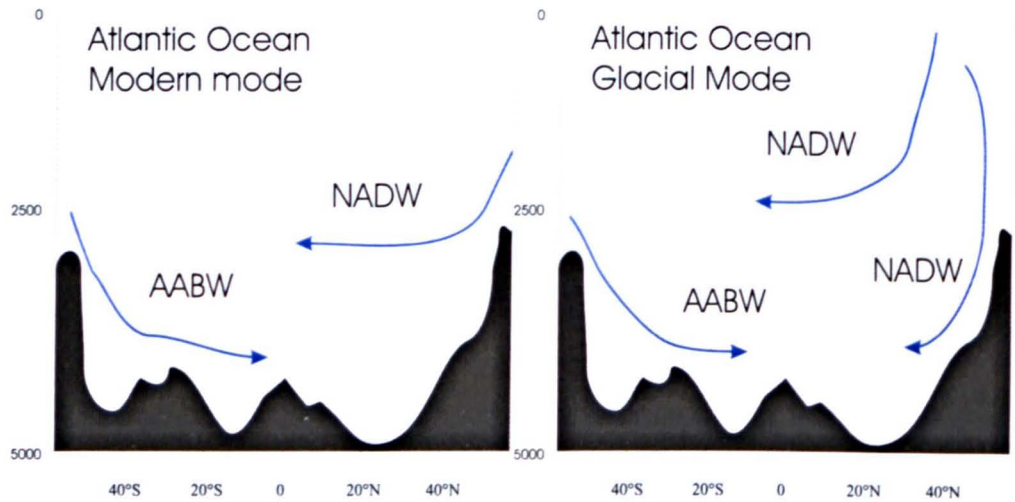

Figure 1.4 Schematic of Atlantic Ocean for the modern mode (NADW sinks to ~3000 m at high latitudes) and glacial mode (NADW sinks to ~2500 m in sub-polar North Atlantic). Based on figure 2 from Labeyrie et al., 1992, described by Clark et al., 2002.

In the modern mode the North Atlantic deep water (NADW) is formed in the Nordic seas and subsequently flows south over the Greenland-Scotland ridge towards the Labrador Sea. Upon meeting the relatively cold and fresh Labrador Sea intermediate waters, which are largely confined to the North Atlantic sub-polar gyre, recirculation occurs and the water mass continues southward.

In the glacial mode, the southward expansion of sea ice during the cold glacial periods switches the formation of NADW southward from the Nordic seas. Formation is probably dominated by open-ocean convection in the sub-polar North Atlantic, sinking to depths of 2500 meters. Possible buoyancy loss as a result of brine rejection under the Nordic sea ice may have provided an additional source of NADW in this mode. In the Heinrich mode, Antarctic-derived water fills the North Atlantic basin at depths as shallow as 1000 meters. In summary it is the changes in depth, location and volume of NADW that constrains the mode of THC.

Ocean and coupled atmosphere-ocean general climate models (GCMs) have been used to assess the rate of ocean overturning, with the aim of predicting future responses to possible switches in the mode of THC. Most of these coupled GCM model projections show a decrease in the strength of overturning as a result of increased greenhouse gas concentrations.

It is these future predictions from the climate models that are of most interest to governments and policy makers. However, it is only through the correct simulations of past climate oscillations, and a proper understanding of their cause and effect, that we will be able to confidently reconstruct large scale ocean-atmosphere reorganizations and predict future abrupt climate change.

Current climate change

Observational data indicate that abrupt climate changes have occurred within the last century with an abrupt warming recorded during the 1920s. A warming, in excess of 4°C, was recorded for the Atlantic side of the Arctic Ocean with the following decade bringing severe drought to the United States [Alley et al., 2003; and authors therein]. Observed sea surface temperatures (SST's) are also believed to have been increasing during the 1990s, coupled with a recent freshening of the North Atlantic. In recent work by Bryden et al (2005) it was reported that there has been a 30% decrease in the North Atlantic Meridional Overturning Circulation (MOC) at 25°N since 1957.

In the southern hemisphere the Antarctic Peninsula appears to have shown the greatest warming in the last 50 years, with an estimated increase in near surface air temperatures of 2.8 °C compared with the global mean warming of 0.3 °C [Vaughan

et al., 2001]. Sea ice extent in both the Arctic [Johannessen et al., 1999] and Antarctic [Curran et al., 2003] has also shown a considerable decrease since the 1950s according to satellite data, moreover, coupled atmosphere-ice-ocean-climate model simulations predict that the Arctic will be virtually ice free during the summer by the end of the 21st century [Johannessen et al., 1999].

Little doubt still exists that global temperatures have increased during the latter part of the 20th centaury. Despite decadal variability, recent warming is of much larger amplitude than anything observed during the last 1000 years (figure 1.5 and references therein). Evidence has been collected from a wide range of palaeoclimate proxies including tree rings, speleothem, ice cores and sediment records and compared with observational and historical records to provide a temperature reconstruction for northern Europe over the past 1000 years.

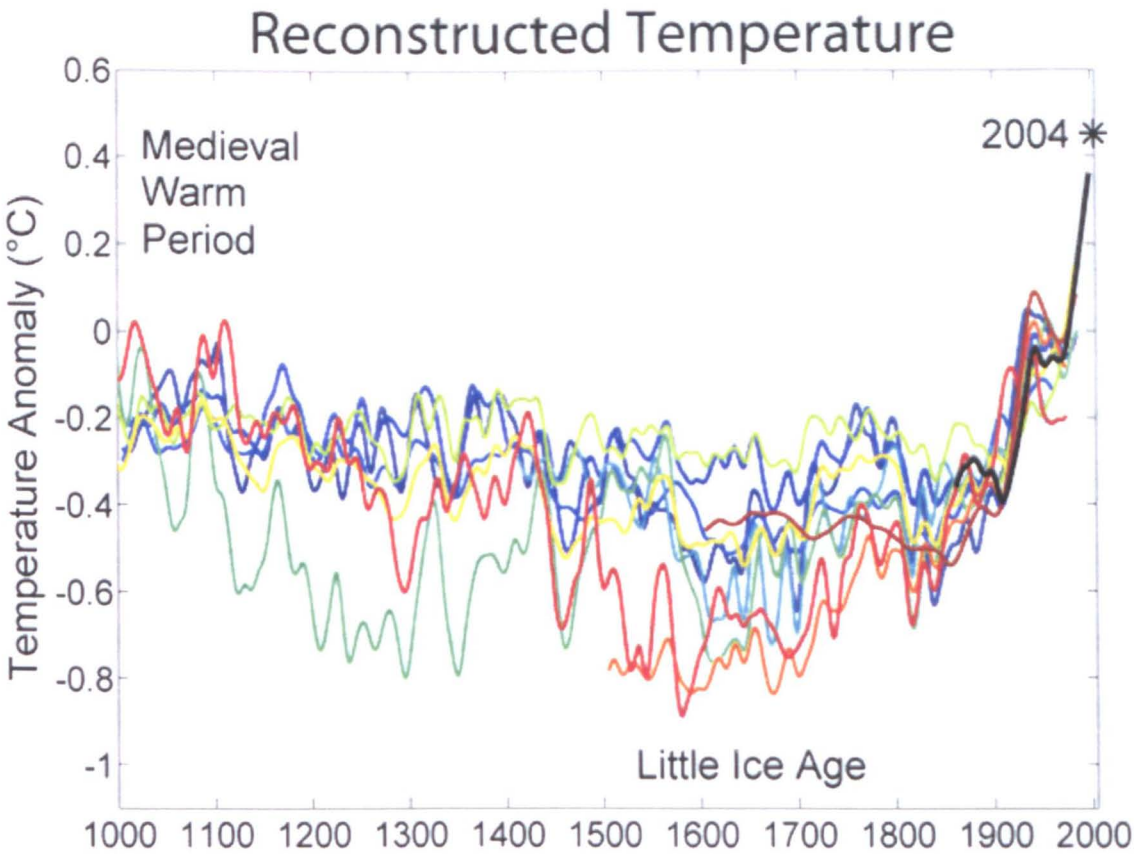

Figure 1.5 Climate reconstruction over the last 1000 years. Dark blue **P.D. Jones et al.,1998;** blue **M.E. Mann et al., 1999;** light blue **Crowley and Lowery 2000;** lightest blue **K.R. Briffa et al., 2001;** light green **J. Esper, et al ., 2002;** yellow **M.E. Mann and P.D. Jones (2003);** orange **P.D. Jones and M.E. Mann (2004);** red-orange **S. Huang (2004);** red **A. Moberg et al., 2005;** dark red **J.H. Oerlemans (2005).**

[www.globalwarmingart.com/wiki/Image:1000_Year_Temperature_Comparison.png]

Climate Change during the Glacial Period

Information about current climate variability will improve as the duration of the instrumental record is increased with time. However limitations in the availability of past observations mean proxy data have been used to capture past climate variability. Sudden and short-lived warm events within the glacial period known as interstadials were first picked up as brief fluxes of warm climate plants and insects into northern Europe. These events are also recorded in the oxygen isotope record from Greenland

ice cores, where they are known as Dansgaard-Oeschger events (DO). It is now known that DO events occurred 24 times between 115,000 and 14,000 years ago [Bond et al., 1993; Dansgaard et al., 1993; Taylor et al., 1999; Mayewski et al., 1997; NGRIP members 2004].

Dansgaard-Oeschger climate oscillations are believed to be linked to orbital forcing and are especially prominent during periods of orbitally-mediated cooling and warming at the beginnings and ends of glacial stages [Alley 2001]. The temperature jumps from periods of extreme cold to periods of intermediate cold are observed in the ice core record as changes in temperature, dust and sea salt deposition in central Greenland and in the global methane record. Ice core evidence combined with ocean sediment data suggests that the warm and moist interstadials began and ended suddenly, occurring over a few decades or less with a duration varying from a few centuries to two thousand years [Mayewski et al., 1997]. Alley (2001) hypothesized that DO events are caused by interactions between weak solar periodicity and noise in the climate system and linked in part to North Atlantic processes. This noise in the climate system can be in the form of amplifiers, which can enhance the affect of a climate trigger. In the case of cold events the increase in sea ice may further shift the meridional overturning southward, causing the newly formed NADW to sink at shallower depths, further weakening the THC resulting in yet colder conditions. Another amplifier is the case of increased snow cover or extended sea ice during cold periods, which can cause temperatures to drop further as a result of increased solar radiation reflecting from the reflective surface. In some cases there may be a sufficient increase in snow fall that the thickness of an ice sheet can increase to a

point where the surface is high enough to prevent melting and maintain snow cover, hence maintaining the ice albedo effect.

In sharp contrast to the sudden warm interstadials are the sharp declines from background glacial climate to the most extreme glacial conditions. Such declines have been observed in a series of North Atlantic Ocean sediments cores, from sites stretching from the Hudson strait to the coast of France, as six layers dominated by ice rafted debris. These are known as Heinrich events [Heinrich et al., 1988; Bond et al., 1992; Grousset et al., 1993], and they occur on time intervals of approximately 7,000 years coinciding with massive ice rafting from North America. They are documented in the $\delta^{18}O$ values of planktonic foraminifera as decreased salinities in the North Atlantic, as a result of the melting ice armadas, sufficient to impact the conveyor circulation. Coinciding with the times of Heinrich events in the North Atlantic other palaeoclimate records give evidence for disruptions in THC with the greatest cooling observed in the Mediterranean Sea and cooling of the Atlantic ocean of the Iberian margin. In addition, sediment discharge events were recorded off eastern Brazil, and sharp weakening in the monsoons recorded from the Chinese, Hulu cave [Wang et al., 2001]. The last Heinrich event occurred after the last Glacial Maximum and marked extreme cold and aridity in many parts of the world 17,000- 15,000 years ago.

Younger-Dryas

The northern hemisphere ice sheets decayed rapidly at the termination of the last glaciation, producing a series of abrupt climate oscillations observed in the vegetation sequence from European terrestrial sediments as the Oldest Dryas/ Bølling/ Older Dryas/ Allerød and the Younger Dryas. In the Greenland ice core records the

transition from the last glacial period to the present warm Holocene was punctuated by a millennial-scale cold snap known as the Younger Dryas, which occurred between 11,000 and 10,000 ^{14}C years ago (11,703 years before 2000 (B2K) according to the GICC05 Greenland ice core chronology [Rasmussen et al., 2006]). The cold snap shows many similarities to the larger Dansgaard-Oeschger climate oscillations, however substantial paleoclimatic evidence suggest that this was a very different climate response, triggered by a catastrophic outburst of freshwater into the North Atlantic.

The trigger is believed to have come from the draining of Lake Agassiz, a large proglacial lake that covered the area now known as the Great Lakes in North America. Due to the relation between the glacially excavated topography and the position of the retreating ice sheet, the water was diverted from the Mississippi into the St Lawrence valley and ultimately the North Atlantic. The estimated release of freshwater was 9500km^3, which if released in just one year would equal the present day net flux of freshwater to the North Atlantic region north of 45°N [Broecker et al., 1999; Teller et al., 2002].

The Younger Dryas event is observed in the Greenland ice core record as a cooling (inferred from the $\delta^{18}O$ record), accompanied by a sharp decrease in snow accumulation and an increase in deposition of dust known to have originated from Asian deserts. The latter would suggest that a cooling in central Greenland was synchronous to an increase in aridity in Asia or an increase in frequency of intense storms. A decrease in atmospheric methane, observed from the trapped gas record of the Greenland ice cores, occurred at the onset of the Younger Drays, which is

consistent with a reduction in the extent of tropical wetlands, linking climate change in the tropics to that in northern latitudes.

This tropical link and the proposed role of THC in climate change was explored further by Clark (2001) who compared the changes in the melt-water history in the North Atlantic with a variety of palaeoclimate records. Using evidence from ice rafted debris (IRD) containing detrital carbonate lithologies; the detrended $\delta^{14}C_{atm}$ record from Lake Suigetsu, Japan; the $\delta^{18}O$ record from GISP2 [Grootes et al., 1993; Meese et al., 1997]; alkenone derived SSTs in North Atlantic, South Atlantic and tropical Atlantic cores [Bard, 1999]; the tropical Atlantic sediment record at Cariaco Bay, offshore Venezuela [Hughen et al., 1996] and the Byrd ice core from western Antarctica [Blunier and Brook, 2001] he was able to show strong similarities to climate events in North Atlantic regions.

Holocene

The presence of abrupt climate changes is not limited to glacial periods, even within the present Holocene, several severe and devastating climate changes have been observed [O'Brien et al., 1996; Mayewski et al., 1997]. The Younger Dryas to Holocene warming started approximately 11,500 years BP, and is estimated as an increase of 15°C occurring in a series of abrupt steps of a few decades or less [Severinghaus et al., 1998; Alley et al., 2000]. The event is associated with cold and widespread arid conditions over northernmost South America, eastern North America and much of North West Europe, North Africa and Southern Asia (involving the failure of summer monsoons) [Alley et al., 2000; Hughen et al., 1996; Von Grafenstein et al., 1998 & 1999; Gasse and Van Campo, 1994; Street-Perrott and

Roberts, 1983; Sirocko et al., 1993]. Following the sudden onset of the Holocene, a number of climate oscillations are seen in the palaeoclimate record, the most prominent occurring 8,200 years ago, the so-called 8.2 kyr BP event [Alley et al., 1997]. The widespread cool, dry conditions lasted approximately 200 years before rapidly returning to climates warmer and moister than the present. Observations from the stable isotope record in Greenland ice cores show that the event was approximately half as severe as the earlier Younger Dryas to Holocene warming.

Throughout the Holocene the palaeoclimate record reveals prominent periods of drought; desiccation of lakes in Africa, weakening Asian monsoon, hurricane frequency and changes is flood regimes. The Little Ice Age was a period of severe cold and dry conditions across northern Europe approximately 350 years ago, a period well documented in the ice core record and corroborated in historical accounts. Similar historically documented records have been compared with the palaeoclimate record to reveal multi-decadal droughts preceded the collapse of the Mayan civilization and multi-centennial droughts coincided with the collapse of the Akkadian empire. The timing of the climate change 8,200 years ago also coincides with widespread abandonment of villages in southwestern Asia, which marks the end of the Pre-Pottery Neolithic B (PPNB) interval, which began around 9,600 years BP.

The social and economic consequences of such rapid climate changes in the future in such densely populated areas would be substantial. Greater understanding of the forcing behind such changes and the global spatial coverage is required to understand the patterns and attempt to understand whether they could re-occur.

Chapter Two

Sample Collection and Analysis

Sample collection and analysis

2.1 Introduction

The main method of analysing ionic chemistry in ice cores has been ion chromatography (IC). Due to the need to analyse ice cores continuously at high resolution, the IC method has been supplemented in recent years by continuous flow analysis (CFA) [Fuhrer and others 1993]. In this method the central section of an ice core is passed over a melt head and the subsequent melt water stream is then split into several lines and led into different detectors. Several deep ice cores have been analysed in this way including the Greenland Ice core Project (GRIP) [Fuhrer et al 1993; 1999] and the North Greenland Ice core Project (NGRIP) [NGRIP members 2004]. The advantage of the new CFA method is that a continuous record of a range of ions and neutral chemicals can be obtained quickly and relatively easily in the field. However, despite the continuing increase in sensitivity of the CFA method [Rothlisberger et al, 2000] the current best resolution is to within a few millimetres although due to the process of mixing on the melt head the method has a practical resolution of 1-3 cm.

Sampling Strategy:

The sections of both GRIP and NGRIP were chosen based on the published isotopic data [Johnsen et al., 1992; GRIP Members et al., 1993; NGRIP members, 2004] and discussions with myself, Eric Wolff, Sigfus Johnsen and Jørgen Steffensen. For the 8.2 kyr event the section of ice chosen from GRIP was selected as the area surrounding the isotopic minimum as shown in figure i (page viii). The amount of ice available at the University of Copenhagen was limited because this section of ice had

been heavily sampled previously. For the study of DO-8 two sections were chosen from the dramatic increase in isotope values, which had been determined as the onset, and from the slower decrease in isotopic values, which was believed to indicate the termination.

There was not enough ice remaining from the GRIP ice core at the depth to study DO-8 and for this reason the NGRIP core was used. The new NGRIP core was not made available to us for the analysis of the 8.2 kyr event and therefore the two events are not sampled from the same core but instead different locations in Greenland.

The aim of this project is to analyse ice samples from a Greenland ice core at sub-seasonal levels. For the analysis of the 8.2 kyr event the expected annual layer thickness at the depths that I am studying is 11 cm per year, therefore a sample size of 1 cm has been chosen to give almost monthly resolution. This is below the resolution obtainable using CFA and instead discrete samples were cut.

For the analysis of the NGRIP ionic chemistry the annual layer thickness for DO–8 is 1-2 cm and therefore even the annual resolution is below the range for CFA. To obtain sub-seasonal resolution for this event a sampling resolution of 2 mm is required, which can only be achieved by cutting discrete samples. Ice samples of this thickness have not been previously achieved and a new cutting method had to be developed for this study. Such small samples yield a very low volume of liquid (< 1 ml), requiring the development of a new IC method.

2.2 Sample location

Two ice cores were used in this study, the European Greenland Ice core Project ice core (GRIP) and the more recently drilled European North Greenland Ice core Project (NGRIP). The GRIP core was drilled to bedrock at the top of the Greenland ice cap, Dome Summit (72° 34'N, 37° 37'W,) in the summer of 1992 at an elevation of 3200 meters above sea level. The GRIP core was drilled 28 km east of the parallel US Greenland ice sheet project 2 GISP2 that reached bedrock a year later [GRIP Project members, 1993; Mayewski et al., 1994].

The GRIP core was used in this thesis for the analysis of the 8.2-kyr event.
The NGRIP ice core was drilled at 75.1 °N, 42.3 °W with an elevation of 2,917 m and an ice thickness of 3,085 m. The drilling at this site started in 1996 and reached bedrock in July 2003 and provides the ice for analysis in this thesis of Dansgaard-Oeschger event 8. The locations and relevant information about the ice cores used in this thesis are shown in figure 2.1 and table 2.1.

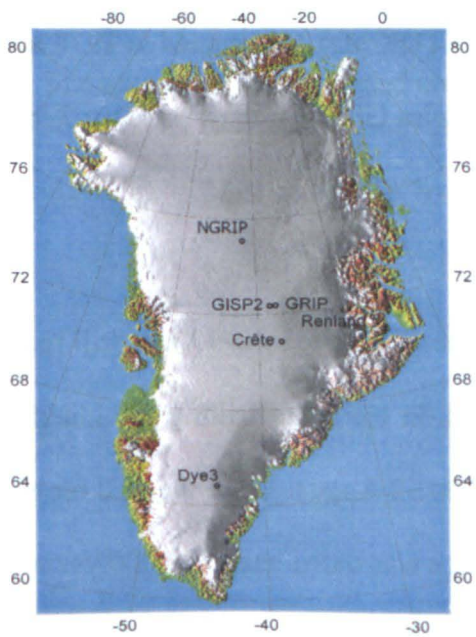

Figure 2.1. Map of Greenland showing the locations of the deep ice core drilling sites.

Drilling Site	Date of Collection	Location	Surface Elevation (m)	Accumulation Rate (m ice y^{-1})	Annual Mean Temperature °C
GRIP	1990-1992	72.5 °N, 37.3 °W	3,230	0.23	-32
GISP2	1990-1993	72.5 °N, 38.3 °W	3,200	0.24	-32
NGRIP	1996-2003	75.1 °N, 42.3 °W	2,917	0.19	-31.5
DYE 3	1981	65.2 °N, 43.8 °W	2,490	0.56	-20
RENLAND	1987	71.3 °N, 26.7 °W	2,350	0.50	-18
Camp Century	1966	77.2 °N, 61.1 °W	1,890	0.38	-24

Table 2.1. Locations of deep ice core drilling sites in Greenland.

2.3 Drilling

GRIP

The GRIP deep drill is an updated version of ISTUK (IS means ice in Danish, TUK means drill in Greenlandic). ISTUK was constructed in 1978 and used successfully under the American-Danish-Swiss GISP 1 program at Dye 3 in South Greenland where it hit bedrock at a depth of 2037 m in 1981.

In the first drilling season at the GRIP site in 1990, the drill reached a depth of 770 m where the ice is 3840 years old. In 1991, the drilling continued into 40,000 year old ice at a depth of 2521 m, and on 12 August 1992, the drill hit bedrock at 3029 m below the surface, where the ice was dated back 110,000 years with older stratigraphically disturbed ice at the bottom of the core [GRIP members, 1993; The Greenland Summit Ice Cores CD-ROM. 1997].

NGRIP

The NGRIP ice core was drilled using a drill based on a Japanese JARE drill, closely related to the European Project for Ice Coring in Antarctica (EPICA) drill. A 110 m deep hole was drilled with a shallow drill and the first 100 m cased to prevent loss of drill fluid. The 11 m long European electromechanical drill retrieves core sections with a diameter of 98 mm and up to 3.55 m long. The drilling commenced in 1996 reaching a depth of 300 m, but in 1997 the drill became stuck after retrieving 1,371.80 m of ice core. In 1999 the drilling started again from the surface, 25 m from the previous site, and at the end of the 2003 field season 3085 m of ice core had been recovered [NGRIP members 2004].

2.4 Method

The Cutting process:

The ice is drilled in lengths of up to 4-4.5 meters and subsequently cut into 55 cm lengths for transportation [Hvidberg, 2002; Dahl-Jensen, 2002]. These 55 cm cores, with a diameter of 98 mm, are logged as described by Hvidberg (2002) and divided up for archive and analysis. The section of the core used comes from the outer edge, as shown in figure 2.2.

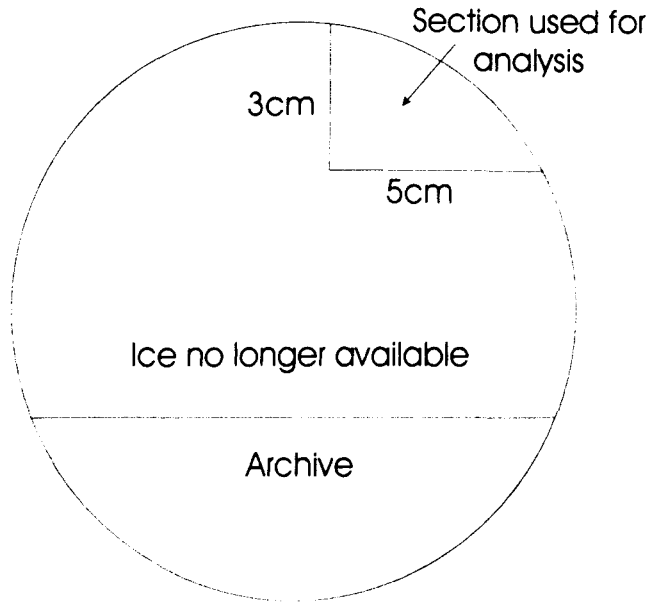

Figure 2.2. Diagram to show size and location of the ice section for analysis in both the GRIP and NGRIP cores (not to scale).

In October 2003 I travelled to Copenhagen, to collect and sub-sample the GRIP and NGRIP ice used in this thesis. In the -20°C cold-laboratory at the University of Copenhagen, I cut a 20-meter section of the GRIP core from 1320 m to 1340 m, corresponding to the 8.2 kyr event. Two sections of the NGRIP core were cut corresponding to the transition into and out off Dansgaard-Oeschger event 8, found at depths 2021.8 m and 2068.55 m. A total of 12.65 m was collected from the NGRIP core.

The cores were carefully packed in ice and cold packed insulated boxes for transportation and flown to the UK where they were stored in the -20°C cold-laboratory at Cambridge for the duration of the study.

A second cutting trip to Copenhagen was needed to extend the analysis of the 8.2 kyr event and in May 2005 a further 2.75 meters of GRIP ice was cut and returned to Cambridge.

Cleaning the core

Both cores from Greenland were drilled using a fluid-filled borehole and the outer edges of the cores were contaminated with the drilling fluid (Blended industrial organic solvent (Exxsol D60) and high density hydrochlorofluorocarbons (HCFC-141B) [Gundestrup et al., 2002]). For this reason the outer most edge of the core must be removed before analysis. This was done using a band saw in the cold laboratory removing a minimum of 0.5 cm from the outer edge, 0.2 cm from the inside edge and 0.2 cm from the bottom and top of the 55 cm core sections. Although the inside edge has been far enough away from the drilling fluid for contamination from this source to be minimized, contamination from handling is still possible so ice is removed from here too.

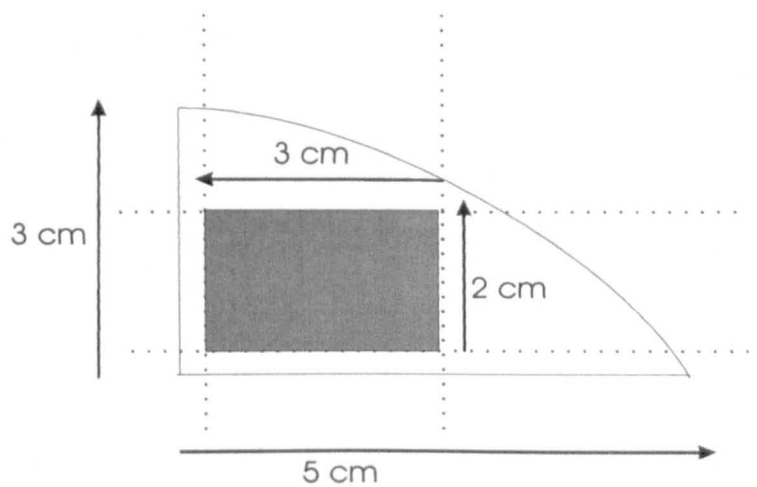

Figure 2.3. Diagram of cleaning procedure. Dotted lines indicate area cut from core to remove outer layers. Central grey rectangle is the size of the sample after outer ice and contamination have been removed.

The resulting ice from the centre of the core (coloured in grey in diagram 2.3) was a rectangle of 2 cm by 3 cm, which based on discussions with Eric Wolff and Robert Mulvaney (October 2003) and following established laboratory procedures was expected to be free of contamination from drilling fluid and handling.

To minimise the risk of contamination from fibres or dust particles, protective clean room clothing was worn over the insulated cold room clothing. Powder-free nitrile gloves were worn when handling the ice and clean metal tongs were used to handle the cleaned section.

Cutting into discrete samples

The 8.2 kyr event from GRIP

For the analysis of the 8.2 kyr event the GRIP core was cut into 1 cm samples using a band saw and stored in clean accuvettes. The waste ice from the outer edge of the core (shown in Figure 2.3) was also cut into 1 cm thick samples and subsequently used for oxygen isotope analysis (because contamination from drilling fluid and handling is not significant in the analysis of water isotopes). Additional isotope samples were cut from the waste into 10 cm samples for the analysis of ^{18}O and deuterium where a larger volume of sample was required.

Dansgaard-Oeschger event 8 from NGRIP

For the analysis of Dansgaard-Oeschger event 8 the NGRIP core was cut into 2 mm samples. A microtome device was used, since this leads to no loss of material at the cut as there is with the saw. The core was cleaned following the method described above and the contaminated outer sections of ice were cut into 2 cm samples for

isotope analysis. This is the minimum sample size to provide enough liquid for analysis using mass spectrometry.

The set-up of the microtome device is shown below (figure 2.4). The ice to be cut was placed in the vice and forced under the blade by pushing the handle and sliding the device forward. The mantle was automatically raised 40 μm with every forward stroke so that the exact size of sample can be determined. Once the ice has passed under the blade the ice section shaved from the top was brushed from the blade into a clean plastic accuvette using a spatula.

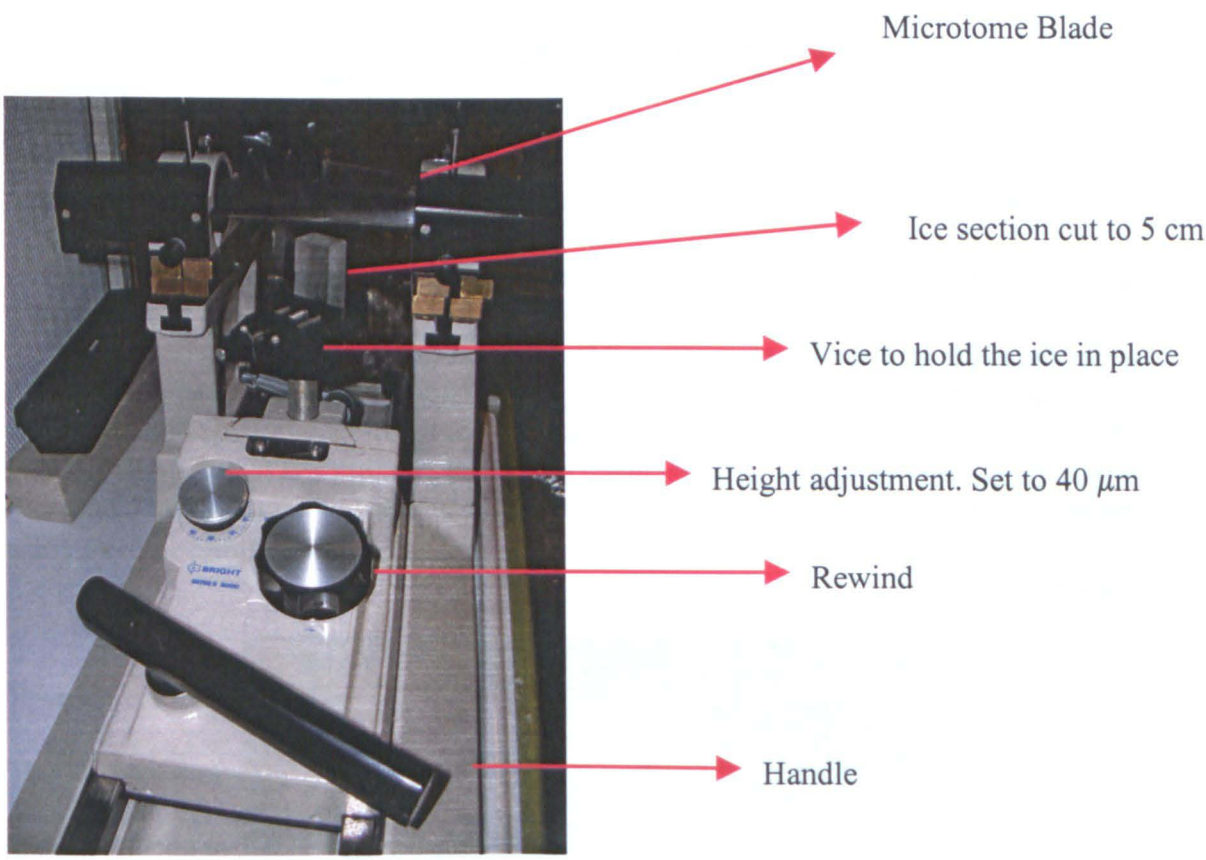

Figure 2.4. Set up of microtome system with key parts labelled

The blade holders were raised to allow a longer portion of ice to sit in the mantle. However, testing of this method determined that the optimum length of ice that could be cut in this way was 5 cm; any length greater than this risked breaking the ice as a result of too much pressure when the ice passed under the blade. Therefore the first step in the cutting method after cleaning with the band saw involved cutting the cleaned inner section of the core into 5 cm samples. The 5 cm sections were placed in plastic bags with the top clearly indicated until they could be cut using the microtome device.

There is an associated loss of material with every cut using the saw, which is unavoidable. Up to 1 mm of ice was lost at each cut and this was accounted for when determining the true depth when the samples were analysed.

Before each cutting session the blade and mantle were cleaned thoroughly to remove any dust. Several pre-frozen sections of Ultra High Purity (UHP) water were passed under the blade to clean it before using it to cut the ice core samples.
The 5 cm section to be cut was placed in a cleaned polyethylene tray, designed to hold the sections in place, while the outer layers were cleaned using a microtome blade (figure 2.5).

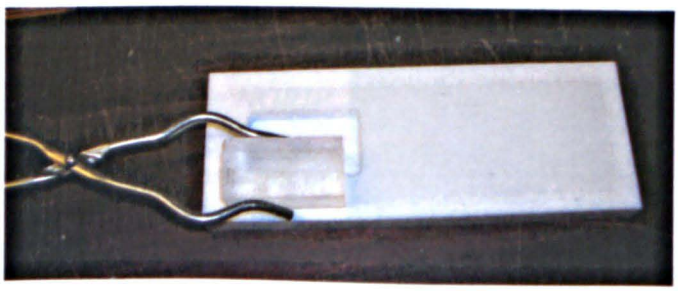

Figure 2.5. Demonstrating clean procedures using a clean polyethylene container and metal tongs to clean the outer layer from the NGRIP core.

Protective clothing and powder free nitrile gloves are worn throughout, and the cleaned sections handled only with metal tongs to prevent contamination.

The ice was then placed in the mantle and passed under the blade 50 times to give a sample size of 2 mm. The resulting ice was collected into a clean plastic accuvette and stored in the cold laboratory before being melted in a class-100 clean room.

Figure 2.6. Cutting process.

2.5 Chemical Analysis

The analysis of all samples was carried out in a class-100 clean room, which has less than 100 particles of 0.5 μm/ m^3. Full clean room clothing was worn throughout the analysis to minimise contamination.

Procedural Blanks

The ice was melted in sterile plastic accuvettes that had been tested for contamination and dust using ion chromatography. A full set of procedural blanks was analysed to test the cutting method of both events.

GRIP

Ion chromatography (IC) was used to determine five anions, chloride (Cl^-), fluoride (F^-), methansulphonate (MSA^-), nitrate (NO_3^-) and sulphate (SO_4^{2-}). The system used was a reagent-free Dionex ICS-2500 with a 2 mm column and a 250 μL sample loop. A potassium hydroxide eluent generator cartridge (EGC-OH) was used to reduce operational errors and contamination associated with eluent preparation. The flow was set to 0.25 mL min^{-1} with an isocratic elution of 23 mM KOH.

Four cations, calcium (Ca^{2+}), potassium (K^+), sodium (Na^+) and magnesium (Mg^+) were analysed using a reagent free Dionex IC-2000 3 mm column and 250 μL sample loop. The cation system is equipped with an MSA eluent generator cartridge and the method followed set the flow to 0.5 mL min^{-1} with an isocratic elution of 20 mM MSA^-.

At the start of each run the Ultra High Purity (UHP) water was topped up and the bottles spurged using helium gas. The pumps on both systems were primed and the autosampler flushed with UHP. The melted samples were then transferred to 1.5 ml sample vials that were placed in an AS50 autosampler using clean pipettes. Chromeleon 5 software was used throughout the analysis of the GRIP core and later updated to Chromeleon 6 for the analysis of the NGRIP core.

NGRIP

IC was also used to analyse the NGRIP core, but the method was adapted to allow for the exceptionally low sample volume obtained from cutting the samples to a resolution of just 2 mm. The ions analysed and the instruments used were the same as

for the GRIP core. However the systems were connected so that both could be run from the same sample vial in the AS50 autosampler, thus minimizing sample volume requisites.

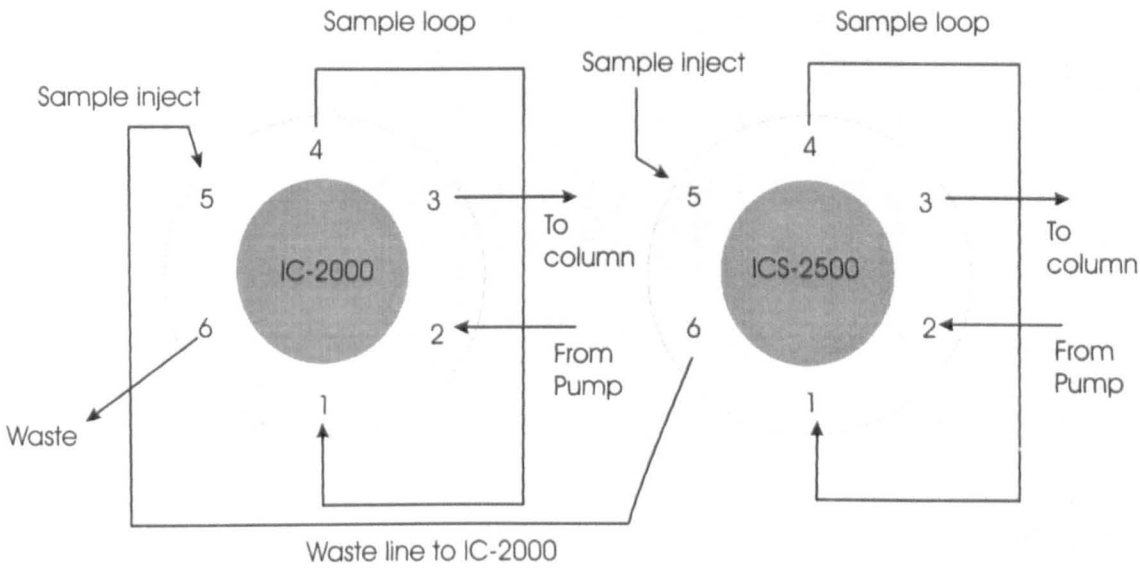

Figure 2.7. Injection valve flow schematic showing the flow from the ICS-2500 to the IC-2000 system.

The system is shown in figure 2.7. The 1 ml syringe is loaded with sample from a 1.5 ml vial in the Dionex AS50 autosampler. The sample is injected at position 5 on the ICS-2500 (right injection valve) where the anions are analysed using a 100 μL sample loop with a flow rate set to 0.25 mL min^{-1} and an isocratic elution of 20 mM KOH. After the sample has passed through the anion system it is directed to the waste valve at position 6 where a waste line has been connected to the sample inject (position 5) on the IC-2000 (left injection valve). The sample is then loaded into the IC-2000

cation system and analysed using a 250 μL loop with a flow rate of 0.50 mL min^{-1} and an isocratic elution of 20 mM MSA.

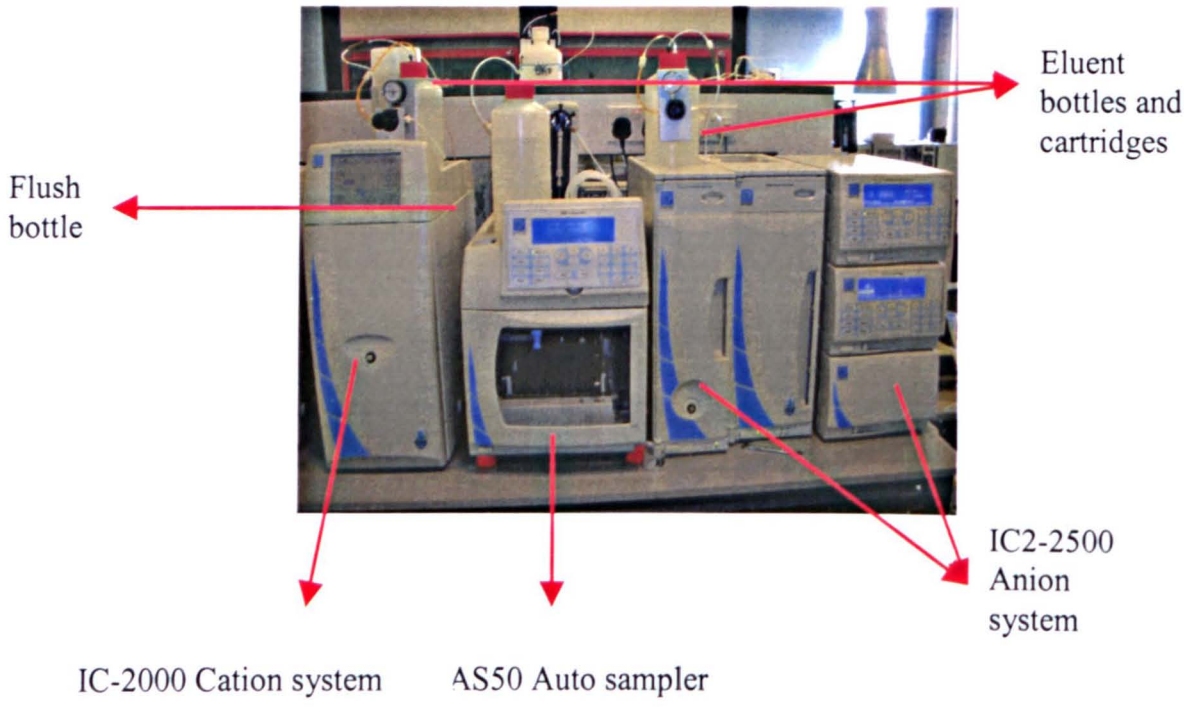

Figure 2.8. Set up of the IC systems for the sequential flow analysis of NGRIP samples

Using the sequential flow method (fig 2.7 and 2.8), both the sample and the anion eluent is passed from the ICS-2500 system into the IC-2000 system. This produced a minimal contamination (< 4 ppb) of potassium in the cation samples from the KOH used in the anion system. Considering the expected high concentrations of potassium in glacial ice from Greenland, this is acceptable; however it will reduce the validity of potassium during the analysis.

Standards

At the start of each run, laboratory seawater standards were made to known concentrations in the clean room. The standards were tested against external standards to ensure that the diluted standards were of the correct concentrations and that the

systems were properly calibrated. The figure below is an example of the calibration curves for the ICS-2000 cation system showing correlation coefficients of 0.99 for all four ions. The aim was to achieve a correlation coefficient greater than 0.99 for each ion before the samples were run. An example of the calibration curves and correlation coefficients for a sample run using cation standards is shown in figure 2.9 and table 2.2.

When calibrating the systems using the sequential flow method (described above), care had to be taken to prevent column damage by ensuring that the high concentration cation standards were not allowed to pass through the anion columns or the anions through the cation columns. A method was written using the Chromeleon software, which put a hold mode onto the injection valve of the system that was not being calibrated, preventing the standards from being passed into the columns, by sending it directly to waste.

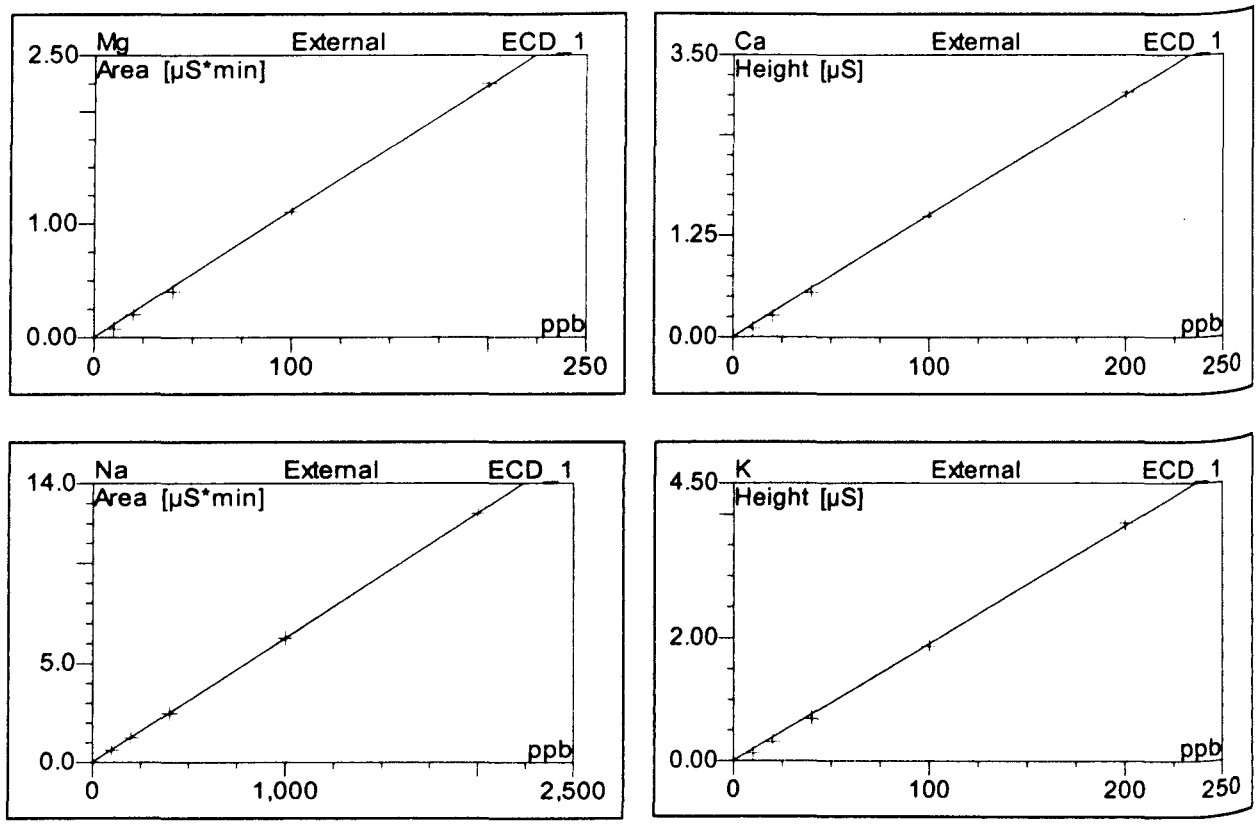

Figure 2.9. Sample calibration curves for cation standards. Graphs, top left sodium, top right potassium, bottom left magnesium, bottom right calcium.

No.	Peak Name	Calibration Type	Points	Correlation Coefficient	Slope
1	Na	Linear	5	0.9998	0.0062
2	K	Linear	5	0.9971	0.0191
3	Mg	Linear	5	0.9919	0.0112
4	Ca	Linear	5	0.9964	0.0151
Average:				0.9963	0.0129

Table 2.2. Sample calibration results for cation standards.

2.6 Isotope analysis

GRIP:

The 10 cm resolution oxygen and deuterium isotopes were measured at the National Isotope Geological Laboratory (NIGL) in Keyworth. The waters were equilibrated

with CO_2 using an Isoprep 18 device for oxygen analysis [Epstein & Mayeda, 1953] with mass spectrometry performed on a VG SIRA. For hydrogen analysis, an on-line Cr reduction method was used [Morrison et al, 2001] with a EuroPyrOH-3110 system coupled to a Micromass Isoprime mass spectrometer.

Isotopic ratios ($^{18}O/^{16}O$ and $^{2}H/^{1}H$) are expressed in delta units, $\delta^{18}O$ and δD (‰, parts per mil), and defined in relation to the international standard, VSMOW (Vienna Standard Mean Ocean Water). Analytical precision is typically ±0.05‰ for $\delta^{18}O$ and ±1.0‰ for δD. [www.bgs.ac.uk/nigl].

The 1 cm resolution GRIP samples were analysed for oxygen at the Department of Geophysics, University of Copenhagen where the accuracy is reported as ± 0.07 ‰ for $\delta^{18}O$ [Johnsen et al., 1997]. Despite the isotopic data being produced in different laboratories the data is highly comparable as shown later in figure 4.2 (chapter 4) with the same features observed in the 27 cm (University of Copenhagen [Johnsen et al., 1997]), the 10cm (NIGL) and the 1 cm resolution (University of Copenhagen).

NGRIP:

The 2 cm resolution oxygen and deuterium isotopes were measured at NIGL as described above.

GISP2:

A 1 m section of the GISP2 ice during the centre of the 8.2 kyr event was sampled at 1 cm resolution for comparison (as described later in the text). The oxygen and deuterium were measured at the Stable Isotope Laboratory, INSTAAR, Boulder,

Colorado using a SIRA series II dual-inlet mass spectrometer with an accuracy of ± 0.07 ‰ for $\delta^{18}O$ and ± 0.5 ‰ for δD [www.instaar.colorado.edu/sil/analyses].

2.7 Quality Control- GRIP analysis

Blanks:

Full procedural blanks were analysed prior to cutting any of the GRIP core in order to establish that the chosen technique was not susceptible to contamination.

Five samples of UHP ice were cut and analysed and the results are shown below.

	Concentration ppb							
Sample Number	**Na^+**	**K^+**	**Mg^{2+}**	**Ca^{2+}**	**F^-**	**Cl^-**	**NO_3^-**	**SO_4^{2-}**
1	0.0466	n.a.[1]	0.3397	0.3237	0.08	0.60	0.54	0.7767
2	0.0371	0.0185	0.0046	0.0440	0.41	0.59	0.17	0.2118
3	0.0586	0.0425	0.0053	0.0371	0.16	0.55	0.94	0.4334
4	0.1051	n.a.	0.2539	0.4028	0.12	0.57	0.34	0.9504
5	0.0425	n.a.	0.0054	0.0629	0.16	0.52	0.92	0.6740
Average	**0.0580**	**0.0305**	**0.1218**	**0.1741**	**0.1851**	**0.5643**	**0.5808**	**0.6093**
Expected values GISP2	6	1.5	2.1	9.2		14	85	43
Contamination as % of expected	1.0	2.0	5.8	1.9		4.0	0.7	1.4

Table 2.3. Results of ionic content found in procedural blanks analysed October 2003 showing the average, standard deviation and percentage of contamination relative to expected values from previously published low-resolution data of GISP2 [http://nsidc.org/data/gisp_grip/].

[1] The annotation (n.a.) indicates that the species below the detection limit of 0.001ppb.

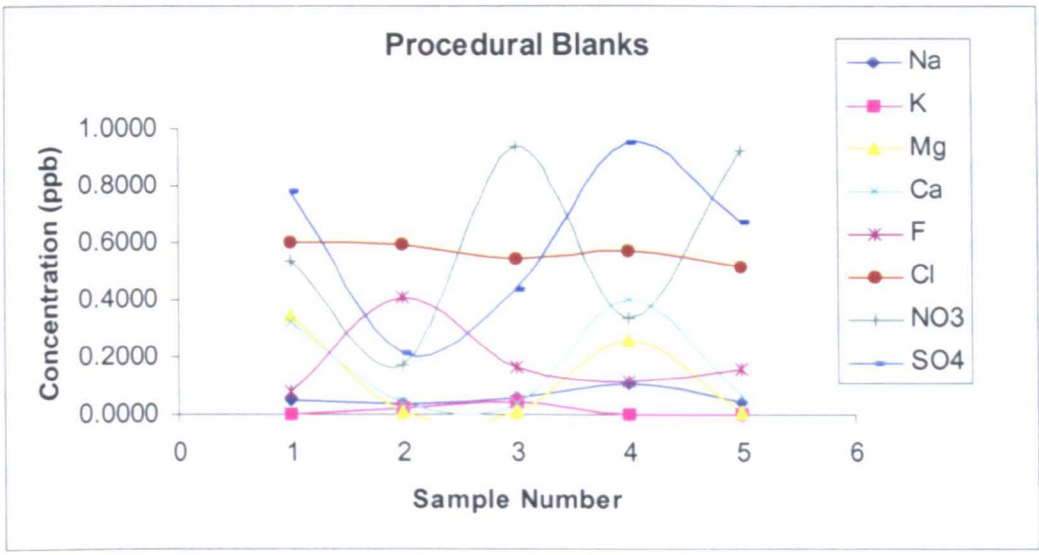

Figure 2.10. Procedural blanks for the 8.2 kyr cutting method.

The accepted level of contamination of each chemical species was set by determining the expected values for the GRIP samples using previously published low-resolution chemistry data from the GISP2 core and then setting the limit to less than 5% of this. The values of all chemical species in the blanks tested are below 1 ppb. The highest concentrations were found to be sulphate, with an average of 0.60 ppb and nitrate, with an average of 0.58 ppb. The values are only 1.4 and 0.7 % of the expected values respectively.

The highest percentage of contamination is from magnesium with concentrations in the procedural blanks of just 0.12 ppb but a percentage relative to the expected value of 5.8 %. Following these results the procedure was re-evaluated, however due to the low contamination of all other species this level of 5.8% was accepted but monitored.

With the level of accepted contamination set using the method above, blank samples were added at regular intervals in each of the IC runs during the two-year period of analysis. The sample concentrations of these continual blanks were tested against the

accepted level of contamination to check the cutting procedure and internal contamination of the IC systems throughout the course of the analysis. The results showed that the contamination in the cutting procedure remained below the accepted level throughout the analysis.

External Standards:

External standards from the Community Bureau of Reference (BCR) were used to test the IC systems. BCR 408 is simulated rainwater standard that was diluted by a factor of 10 (to fit within our calibration curve) and run throughout the period of data analysis in this thesis. Below is a selection of 5 such runs to show that the levels of each ion were close to the true value in all cases.

Sample Name	Amount					
	Na^+	Mg^{2+}	Ca^{2+}	Cl^-	NO_3^-	SO_4^{2-}
BCR 408 diluted by 10	93.1	14.6	31.0	239.5	125.1	99.9
BCR 408 diluted by 10	93.0	14.4	29.9	238.0	124.9	98.5
BCR 408 diluted by 10	93.1	14.8	32.6	239.3	126.7	101.8
BCR 408 diluted by 10	92.9	14.4	29.2	237.6	124.0	97.8
BCR 408 diluted by 10	93.1	14.6	31.0	238.8	126.4	98.9
Average	**93.1**	**14.6**	**30.7**	**238.6**	**125.4**	**99.4**
Actual Values	93.3	14.9	30.8	238.0	124.6	100.9
t (critical value for 4 degrees freedom = 2.78)	2.1	1.9	0.2	-1.6	-1.7	2.7

Table 2.4 Multiple analysis of external seawater standard.

The t test was used to decide if the true value (μ) was significantly different from the sample mean (x). If the value of t (regardless of its sign) exceeds the critical value then the null hypothesis is rejected. If the null hypothesis is true then it can be

considered that there is no significant difference between the observed and known values, other than that which can be attributed to random variation.

$$\mu = x \pm (ts/\sqrt{n}) \qquad \textbf{[Equation 2.1]}$$

$$t = (x - \mu) \sqrt{n}/s \qquad \textbf{[Equation 2.2]}$$

The significance level is chosen to be 0.05 (5%) and the critical value for 5 samples, therefore 4 degrees of freedom, is 2.78. All of the ions have critical values that are lower than this so the null hypothesis can be upheld.

Multi system analysis:

	IC-2000				DX-500			
Sample Name	**Amount (ppb)**				**Amount (ppb)**			
	Na^+	**K^+**	**Mg^{2+}**	**Ca^{2+}**	**Na^+**	**K^+**	**Mg^{2+}**	**Ca^{2+}**
MC20_231	34.5	3.4	4.7	38.5	35.5	4.9	3.0	38.1
MC20_234	45.4	7.3	6.5	48.7	45.2	8.9	5.4	41.5
MC20_237	14.4	2.2	3.3	13.1	15.5	2.5	0.8	14.4
MC20_238	12.7	2.6	3.3	12.5	16.8	4.0	0.9	19.4
MC20_239	9.3	3.8	3.1	18.9	9.7	3.0	0.1	18.3
MC20_91	22.6	4.8	4.2	20.5	24.0	4.6	3.3	27.3
MC20_93	56.2	4.3	6.6	47.3	54.7	5.7	7.6	36.5
MC20_94	9.0	3.3	3.4	41.9	11.9	4.3	1.1	43.2
MC20_95	34.9	4.7	6.0	46.7	34.3	5.1	4.5	41.5
MC20_97	19.8	2.9	3.7	22.3	16.6	6.7	1.3	27.8
MC20_99	67.6	4.0	7.1	17.0	66.1	4.7	8.2	18.0
MC20_100	32.0	3.6	4.4	17.2	29.8	0.9	5.0	7.7
Average	**29.9**	**3.9**	**4.7**	**28.7**	**30.0**	**4.6**	**3.4**	**27.8**
Standard Deviation	19.0	1.3	1.5	14.5	17.9	2.1	2.8	12.2

Table 2.5. Concentration of ions from an Antarctic core analysed on both the IC-2000 and DX-500 Dionex ion chromatographs.

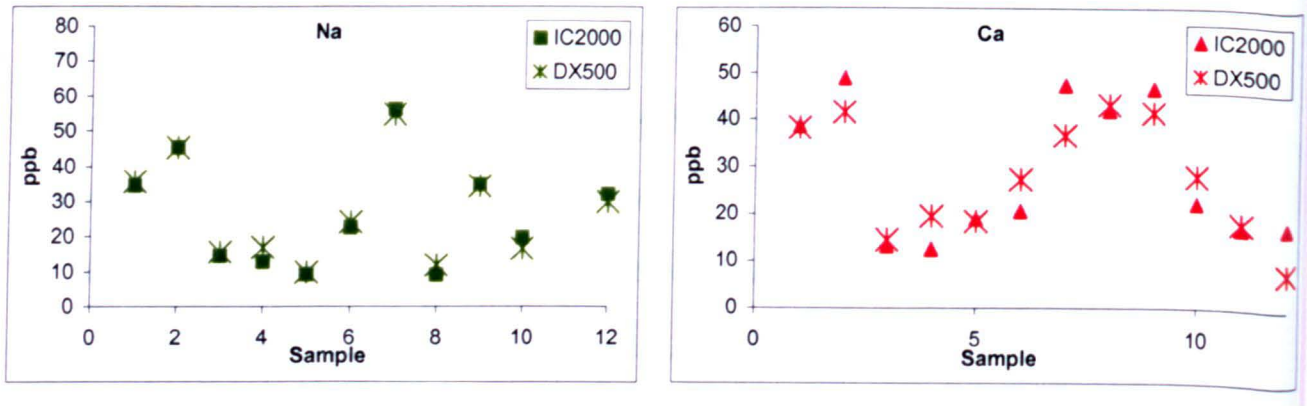

Figure 2.11 Graph showing Sodium and Calcium concentrations from Antarctic ice cores when analysed on the IC-2000 (Full shapes) and DX-500 (Crosses).

Another test of the IC systems was to test samples on more than one machine to see if the results were reproducible. We have the advantage that we have four Dionex ion chromatography systems in our clean laboratory, the IC-2000, ICS-2500 and two DX-500's for both anion and cation analysis. Due to the small volume of my samples I did not have enough for multiple analysis, however below is a table of results from the analysis of an Antarctic ice core that was available.

The table and the graphs show a very small range between the concentrations obtained from the IC-2000 and DX-500 system. This is shown by the average calculated for the ice samples, which is very close for all cation species.

Ideally I would have liked to do a similar test for the anions however this was not possible due to the lack of sample volume and the time available to use the DX-500 system.

2.8 Quality Control- NGRIP analysis

Procedural Blanks:

Full procedural blanks were analysed prior to cutting any of the NGRIP core in order to establish that the chosen technique was free of contamination.

Five samples of UHP ice were cut and analysed and the results are shown below.

	Concentration ppb							
Sample Number	**Na^+**	**K^+**	**Mg^{2+}**	**Ca^{2+}**	**F^-**	**Cl^-**	**NO_3^{2-}**	**SO_4^{2-}**
1	0.0288	3.23	0.1325	0.2247	0.08	0.52	0.71	0.64
2	0.0299	2.71	0.1368	0.1250	0.18	0.48	0.23	0.32
3	0.0172	2.33	0.0545	0.1186	0.13	0.61	0.48	0.35
4	0.0257	3.90	0.0295	0.0821	0.12	0.49	0.48	0.85
5	0.0657	2.36	0.1628	0.5961	0.14	0.51	0.62	0.57
Average	**0.09**	**2.96**	**0.16**	**0.29**	**0.19**	**0.58**	**0.56**	**0.61**
% Higher than GRIP method	36.59	98.97	24.45	39.40	1.54	2.71	-3.35	-0.53
Expected values CFA and IC	57.50	11	15.4	102.30	5.2	23.8	79.90	107.90
% Contamination relative to expected	0.16	26.94	1.05	0.28	3.62	2.44	0.70	0.56

Table 2.6. Results of ionic content found in procedural blanks analysed March 2005. Expected values are the average concentrations in the same section from NGRIP using IC (55 cm resolution) for potassium, magnesium, fluoride and chloride and CFA for sodium, calcium, nitrate and sulphate (Data curtsey of Matthias Bigler, University of Copenhagen). Percentage of contamination is relative to these average values.

With the exception of potassium, the average concentrations of all ions in the procedural blanks are below 1 ppb. The highest concentrations were found to be sulphate, with an average of 0.61 ppb, chloride with an average of 0.58 ppb and

nitrate, with an average of 0.56 ppb. These values are very similar to those found using the GRIP method and therefore can be concluded that no additional contamination was added for these ions in the NGRIP cutting method.

To determine whether the concentrations of each ion in the procedural blanks were acceptable, to within the 5 % level, the concentrations were compared with the expected sample concentration. This was done by comparing average concentrations from the same section of NGRIP ice analysed using CFA (for sodium, calcium, nitrate and sulphate) and IC (for potassium, magnesium, fluoride and chloride) [courtesy of Matthias Bigler at the University of Copenhagen]. With the exception of potassium, the concentrations of all ions in the procedural blanks are below 5 % of the expected sample concentration.

The concentrations of all anions in the NGRIP cutting method are very close to those during the GRIP cutting method. This is because the likely addition of these ions in the procedural blanks is from the water source and not the cutting method. The concentrations of the cations in the procedural blanks however are all higher in the NGRIP method than in the GRIP method. This suggests that the new cutting method is contaminating the sample with additional calcium, magnesium and sodium. This is expected in a method where handling has increased. In the GRIP method only the band saw was used, however for the NGRIP method the ice first comes into contact with the band-saw blade and then the microtome blade.

The increase in contamination from the GRIP and the NGRIP method is small. The concentrations of sodium, magnesium and calcium are still below 1 ppb, which is less

than 0.3 % of the expected sample concentrations for sodium and calcium, and only 1 % of the expected sample concentration for magnesium. Therefore I conclude that the levels of contamination for anions and cations (with the exception of potassium) are all within the accepted 5% limit.

The concentration of potassium in the procedural blanks tested for the NGRIP method is almost 100% greater than those determined using the GRIP method. This is because the new sequential flow method is contaminating the sample with potassium from the potassium hydroxide eluent used in the anion system (discussed in above). However, given the small sample volume obtained in this thesis it was decided that the method should still be used, regardless of the potassium contamination; which has an average of less than 3 ppb in the procedural blanks.

The percentage of potassium concentration, as determined by the expected sample concentration, is almost 25%, considerably greater than the 5 % level used to constrain the other ions. Because the source of the contamination is known and the concentration, as determined by the eluent concentration, is constant throughout the period of NGRIP analysis it can be assumed than the level of contamination also remains relatively constant. For the remainder of this thesis the results for potassium will be included however it is acknowledged that the samples are contaminated and that the results should be used with caution.

With the level of accepted contamination set at 5 % for all ions (except potassium), blank samples were added at regular intervals in each of the IC runs during the two-year period of analysis. The sample concentrations of these continual blanks could be

tested against the accepted level of contamination to check the cutting procedure and internal contamination of the IC systems. The concentrations remained below the accepted limit for the duration of the analysis.

Multiple Sample Analysis:

The sample volume of the NGRIP samples was so small that it was not possible to run multiple samples, however in some cases the ice was cut at a resolution lower than 2 mm and therefore there was enough sample volume for multiple analyses. Table 2.7 and figure 2.12 below show the multiple analysis of sample 3763_93, (which was the last sample in the section to be cut and therefore has a resolution of 5 mm) which was run three times for the anions but only twice for the cations. This is because the volume of the third sample was too small to completely fill the loop of both the anion and cation system.

Sample Name	Amount (ppb)								
	F^-	MSA	Cl^-	NO_3^-	SO_4^{2-}	Na^+	K^+	Mg^{2+}	Ca^{2+}
3763_93	1.3	15.0	92.6	61.0	109.7	159.1	55.3	8.5	110.4
3763_93	1.4	13.2	92.8	59.6	107.5	158.8	59.4	7.7	112.4
3763_93	1.8	13.6	92.9	63.8	108.0	n.a.[2]	n.a.	n.a.	n.a.
Average	1.5	13.9	92.8	61.5	107.8	159.0	57.4	8.1	111.4

Table 2.7. Results from multiple analysis of sample 3763_93. The cations could only be analysed twice because the volume of the third run was too small and an air bubble prevented the correct results.

[2] Notation (n.a.) means values were lower than the detectable limit of 0.01 ppb.

The results show very small standard deviations, which is shown as small error bars on the graph.

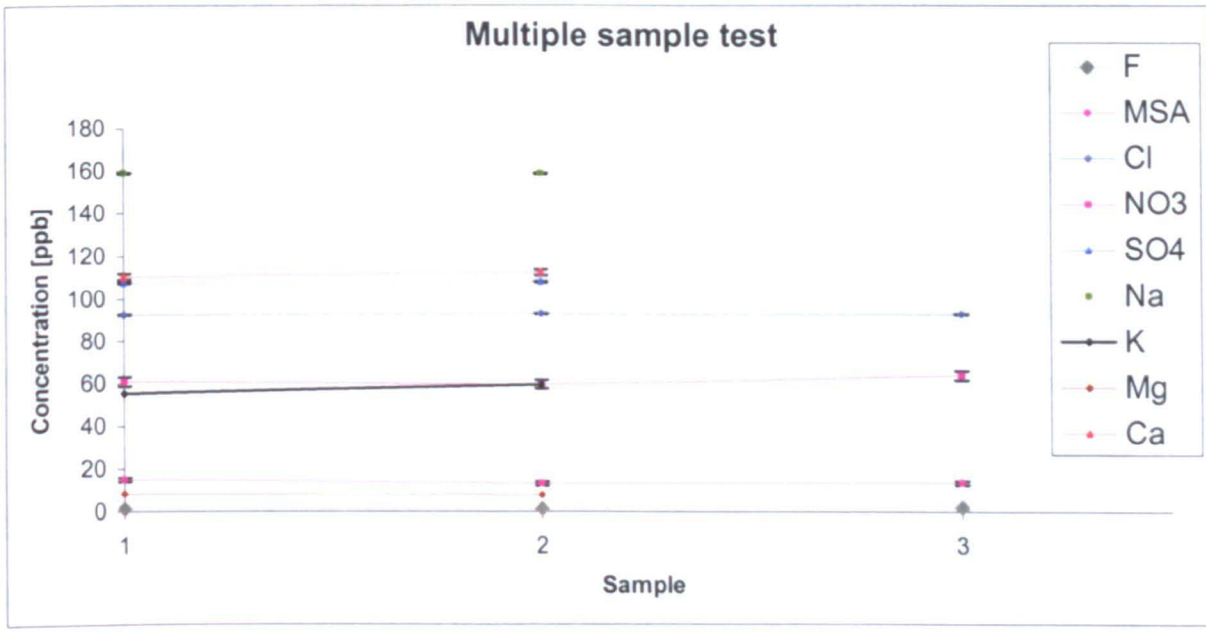

Figure 2.12. Graph of the multiple analysis of 3763_93.

The contamination detected in both the GRIP and NGRIP cutting methods was consistently below the 5 % level throughout the period of analysis, as shown in tables 2.3 and 2.6 and figures 2.10. External standards were used to confirm the calibration of the IC systems and (with the exception of potassium in the NGRIP method) revealed no significant contamination over the two-year period. As a further test, multiple samples were run to prove the results were reproducible on the same IC systems and on other IC systems, as shown in tables 2.5 and 2.7 and figures 2.11 and 2.12. It can therefore be concluded that the cutting and analysis method used in the collection of data for this thesis are free of external contamination and represent the true concentrations of ions within both ice cores.

2.9 Comparison with published data (GRIP)

Based on evidence that the cutting and analysis methods were free of external contamination, the GRIP samples were cut and analysed to produce the new high-resolution chemical record. The record is described in Chapter 5 however the following findings, from an investigation carried out in the summer of 2005, highlight contamination issues which need to be discussed before the record can be evaluated.

Previously published results by Alley et al., (1997) indicated significant increase in calcium, chloride and sodium during the 8.2 kyr event. The results were published as percentage increases 60% for all three ions and were compared to the depositional changes observed during the Younger Dryas.

	Event deviation from baseline	
Indicator	8.2 kyr event	Younger Dryas
Accumulation	-20	-50
Methane	-10	-30
Na^+	+ 60	+ 260
Cl^-	+ 60	+ 200
Mg^{2+}	+ 40	+ 370
Ca^{2+}	+ 60	+ 600
K^+	+ 110	+ 230
NO_3^{2-}	+ 20	+ 10
$\delta^{18}O_{[ice]}$	-2 ‰	-3.5 to -4 ‰

Table 2.8 Deposition change during the 8.2 kyr event and the Younger Drays reproduced from Alley et al (1997).

My findings (described in chapter 5) do show significant changes in deposition within the 20-meter section of ice analysed but attempts to provide percentage changes have yielded changes much lower than those proposed by Alley. The GISP2 data used by

Alley et al (1997; 2005) is available from the NSIDC website (http://nsidc.org/data/gisp_grip) and I was able to make comparisons with the chemistry record from GRIP.

The comparison between the average concentrations of ions from the 20 meter section of GRIP ice, produced in this thesis, and the same 20 meter section from GISP2, published by Mayewski et al (1997) revealed alarming differences. This led to a quality control assessment and further tests, which is described in the following section.

2.9.1 Contamination Tests

Following the analysis of the chemistry data from the GRIP core during the 8.2 kyr it became obvious that when the average values for each species were compared with the average values for the same section of the GISP2 core, large differences exist. Table 2.9 shows the average values across the 8.2 kyr event from both the GRIP core, measured in this thesis, the GISP2 core [Mayewski et al., 1997], and the continuous flow analysis (CFA) of Calcium [Fuhrer et al., 1999].

The values reported here are higher for all ions when compared to the GISP2 chemistry however most notable is calcium, chloride, sodium and potassium. Calcium is 4.3 times higher in the GRIP core, which I analysed, than in the GISP2 core and 3.8 times higher than the GRIP CFA. This is a very serious problem when using calcium as a proxy for dust during this section of ice and the 8.2 kyr event.

	GRIP [Fuhrer et al., 1999]	GISP2 [Mayewski et al., 1997]	GRIP [Thomas et al, 2006]	Difference	
Depth	1324.77-1340.12 m	1380-1400 m	1324.77-1340.12 m	GRIP (Thomas) /GISP2	GRIP (Thomas) /GRIP (Fuhrer)
Ion	Concentration (ppb)	Concentration (ppb)	Concentration (ppb)		
Na^+ 1σ		5.8 ± 2.3	16.9 ± 31.3	2.9	
K^+ 1σ		1.6 ± 2.0	7.5 ± 11.1	4.7	
Mg^{2+} 1σ		2.2 ± 0.6	2.4 ± 2.1	1.1	
Ca^{2+} 1σ	10.8 ± 5.7	9.5 ± 3.2	40.6 ± 33.8	4.3	3.8
Cl^- 1σ		14.3 ± 7.4	31.1 ± 27.2	2.2	
NO_3^{2-} 1σ		85.3 ± 12.1	108.0 ± 36.8	1.3	
SO_4^{2-} 1σ		41.7 ± 22.0	61.6 ± 52.6	1.5	

Table 2.9 Comparative concentrations of ions in the GRIP ice that I analysed, the GRIP CFA [Fuhrer et al., 1999] and the GISP2 core [Mayewski et al., 1997]. (σ = 1 standard deviation).

There is a high standard deviation for all species throughout this section due to the high resolution and inter-annual variability, which is not seen in the much lower resolution CFA and GISP2 chemistry (2 cm and 20 cm respectively), however even with this in mind the values are all consistently higher than those published for this section and we need to understand why.

The first thing was to re-evaluate the quality control procedures described earlier in this chapter. I am confident that there was no contamination from the cutting

procedure as demonstrated by the procedural blanks, which showed low concentration for all species.

The tests with the external standards and the cross analysis of the same standards on different IC's in the laboratory showed that there could be no problem with incorrect calibration or accumulated contamination within the IC's. For this reason it was decided that the high values observed were from the ice (and not an artefact of contamination or bad calibration) and therefore the only possible theory for the high values was that not enough of the contaminated outer layer of ice was removed.

To test this theory I devised an experiment to determine the extent of contamination from the outer layers of the ice, and to assess how much ice needed to be removed.

In order to measure how far the contamination had penetrated from the outer layers, thin layers of ice were cut from the outside towards the middle. The hypothesis was that the highest concentrations of each species would be found at the outermost layers, with the levels dropping sharply towards the middle of the core. The ice could be considered unaffected by contamination at the point at which the values remained constant.

2.9.2 Contamination method

I obtained an extra bag of GRIP ice from the University of Copenhagen in May 2005 from a section of core just before the 8.2 kyr event, at a depth of 1342 meters. This section was chosen because it was outside of the area of interest but close enough to

expect similar concentrations of the chemical species being investigated. The ice section had the same dimensions as all the other bags of GRIP ice used in the analysis of this thesis.

Experiment 1

A five cm section of the ice core was cut using a band saw from the 55 cm length of ice in bag number 2440. The ice section was then cut and cleaned following the clean method described earlier in Chapter 2.

Therefore the most convex section was removed, as was always the case with the ice analysed during the 8.2 kyr event and the ends (at the top and bottom of the ice) removed. Using the band saw, slices of ice were cut to a thickness of 0.4 cm from the outside edge of the ice section towards the inside edge, until no ice remained. The 0.4 cm thick ice sections were placed in a pre-cleaned accuvette and analysed using ion chromatography as described in the method section.

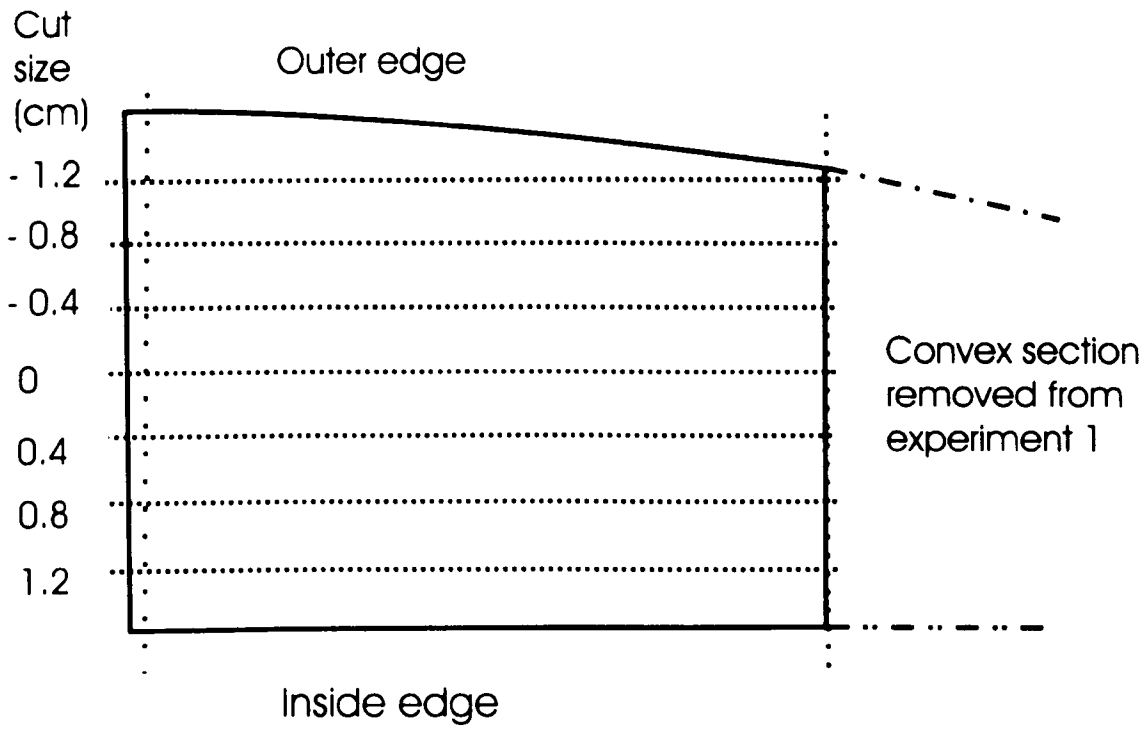

Figure 2.13 Diagram of ice section used in experiments 1 & 2. Cutting 0.4 cm of ice from the outside edge to the inside edge, as shown by the horizontal dashed lines. In experiment 1 the ends were cleaned, as shown by the vertical dotted lines.

The experiment was repeated by cutting another 5 cm section (section b) from bag 2440 and the procedure followed as above.

Experiment 2

This experiment was used to prove the hypothesis that the outermost edges of the ice core were the most contaminated. The most convex section of ice, which had been removed from experiment 1, was cut into layers with a thickness of 0.5 cm from the outside edge towards the middle.

The slices of ice were cut using a band saw and placed in a pre-cleaned accuvette for analysis using ion chromatography.

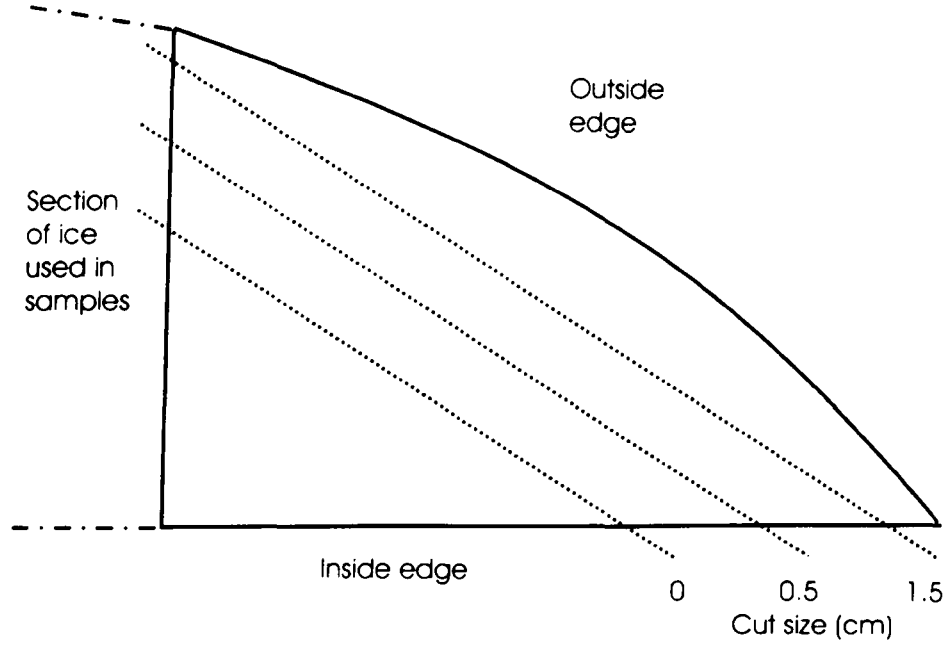

Figure 2.14 Diagram of the convex section of ice, normally removed from the sample ice for isotope analysis, used in experiment 2 section a.

2.9.3 Contamination results

The results for experiment 1 and 2 are shown in figures 2.15 to 2.18 below. In figure 2.15 the concentrations of seven ions from section (a) are plotted with relation to the distance from the centre. The centre is given as 0 with the negative numbers increasing towards the outer edge (shown on the left of the graph) and the positive numbers increasing towards the inner edge (shown on the right of the graph).

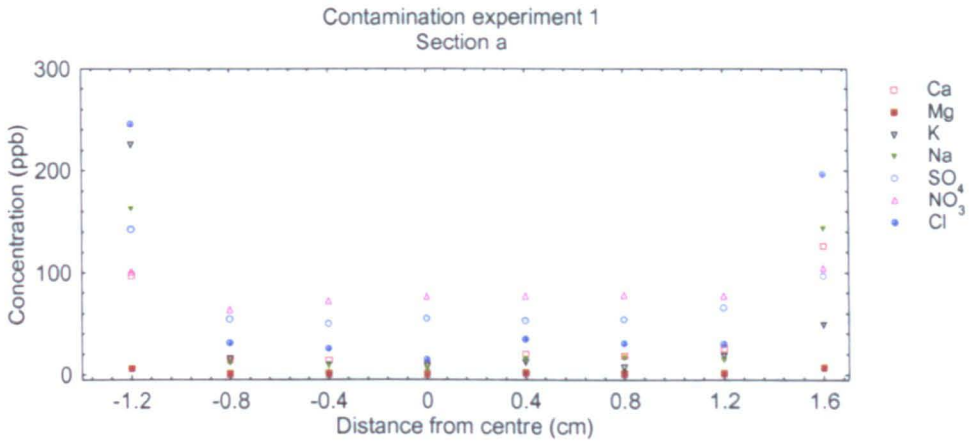

Figure 2.15 Contamination experiment 1 showing the concentrations of each ion found in section 1 with relation to the distance from the centre. The outer edge is on the left and the inner edge is on the right.

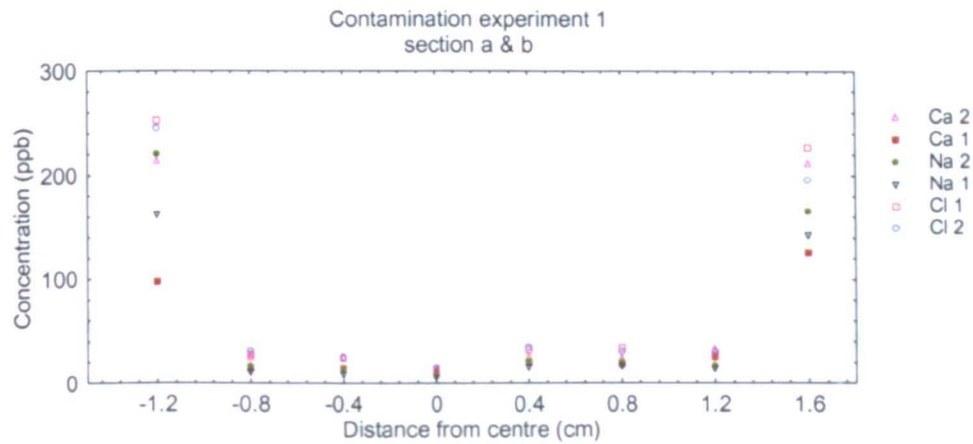

Figure 2.16 Contamination experiment 1 showing the concentration of Chloride, Sodium and Calcium found in both section a (filled data points) and section b (crosses) with relation to the distance from the centre. The outer edge is on the left and the inner edge is on the right.

Figure 2.16 (above) shows the concentrations of calcium, chloride and sodium from both section (a) and section (b) to show that the shape of the graph is reproducible throughout the different depths of the ice. The concentrations of each ion are slightly

different because they are from different depths within the ice core (section a is 5 cm shallower than section b).

Figures 2.15 & 2.16 show that the outer edges have the highest and the centre has the lowest concentrations of all ions measured. The difference in concentration from the outer and inner edge to the middle is shown in table 2.10.

Distance from centre (cm)	**Cl^-**	**NO_3^-**	**SO_4^{2-}**	**Na^+**	**K^+**	**Mg^{2+}**	**Ca^{2+}**
-1.2	269.2	98.8	142.1	190.7	111.3	9.2	121.2
-0.8	42.6	77.8	68.6	25.2	26.3	2.2	35.6
-0.4	59.3	73.3	51.2	38.0	28.0	2.5	33.2
0	29.5	77.4	51.1	14.3	19.8	1.3	23.4
0.4	85.8	95.4	70.9	42.4	25.9	2.1	31.1
0.8	51.0	78.0	54.7	30.8	24.7	1.9	33.8
1.2	198.0	104.1	113.6	141.3	78.4	7.3	145.7
Sample average	**56.4**	**81.0**	**57.0**	**31.4**	**24.6**	**2.0**	**30.4**
Standard deviation	23.28	9.84	9.44	12.37	3.49	0.46	4.78
Difference (sample average – centre)	26.88	3.60	5.85	17.10	4.82	0.61	6.96
	Enlargement factor						
Outer edge to sample average	4.77	1.22	2.49	6.07	4.52	4.61	3.99
Inner edge to sample average	3.51	1.28	1.99	4.50	3.19	3.65	4.79
Outer edge to centre	9.1	1.3	2.8	13.3	5.6	6.9	5.2
Inner edge to centre	6.7	1.3	2.2	9.9	4.0	5.4	6.2

Table 2.10 Concentration from experiment 1 section (a).

The average has been determined from the concentrations after the inside and outside edge has been removed. The enlargement factor was calculated when the concentrations were normalized to the average (with the ends removed) or the concentration in the centre.

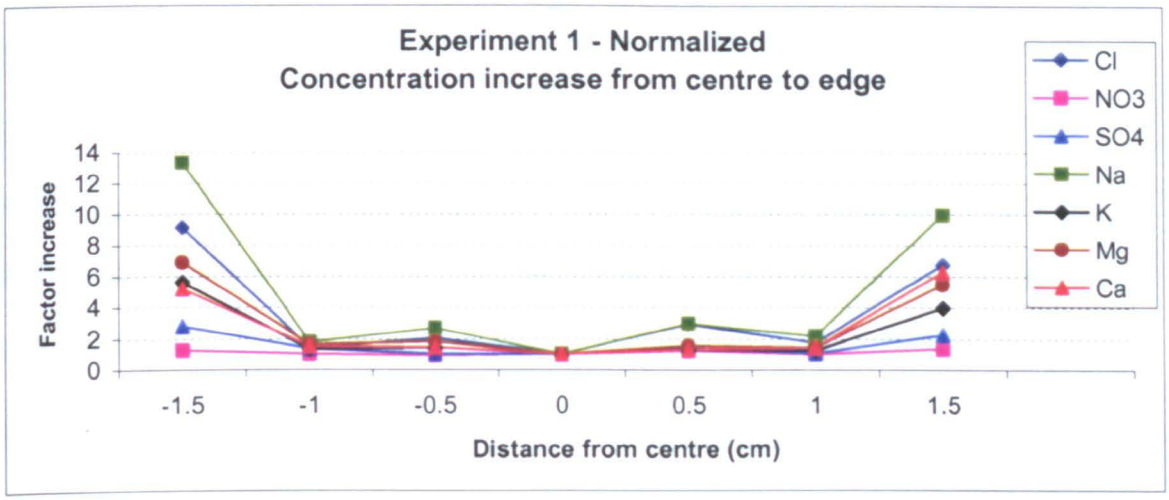

Figure 2.17 Experiment 1 section a, normalized to the central point of each ion to show the enlargement factors from the outside edge (left) and the inner edge (right) to the centre.

Figure 2.18 (below) shows the concentration of seven ions from experiment 2 (which was the convex section removed from experiment 1a) with respect to the distance from the centre. The outermost ice is shown on the left of the graph moving towards the centre at point 0.

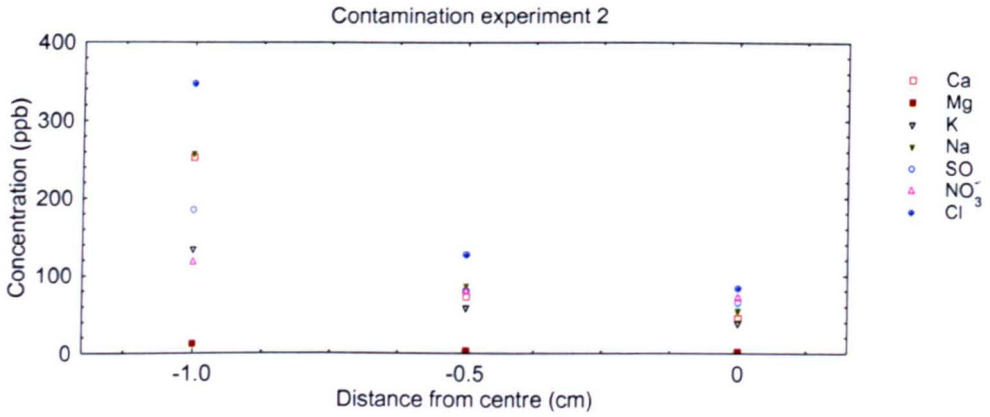

Figure 2.18 Contamination experiments 2 showing the concentration of all ions with relation to the distance from the centre. The outer edge is on the left.

2.9.4 Contamination Conclusions

Most contaminated section?

The first part of the hypothesis proved true, the most contaminated sections of the ice were the outer most sections. The central point (marked 0 in the graphs) has the lowest concentrations in all ions with the concentrations dropping sharply from the inner and outer edges towards the middle.

With the exception of calcium, all ions show the greatest concentration difference is from the outside edge to the centre, increasing by as much as 13 times for sodium and 9 times for chloride. The concentration of calcium is 6 times higher in the inner edge than the centre but only 4 times higher in the outer edge than the centre. All species show high concentrations on both the inner and outer edge, which is not expected. I had hypothesized that the outer edge of the ice would be much more contaminated, due to its contact with the drilling fluid, while the inner section should have had only

minimal contamination from handling and not have been in contact with the drilling fluid directly.

The contamination appears to have happened after the initial drilling. It must have come from either the bags that it was stored in whilst at the University of Copenhagen or from the bags it was transferred to, after cutting in October 2004. The bags used however, when I cut the ice and transported it to Cambridge, were cleaned and previously unopened lay flat tubing, commonly used in ice core storage. It is possible that the samples were packed initially in bags that were contaminated with drilling fluid, which was able to pass around the bag and affect all outer surfaces of the ice section.

Was enough ice removed?

In order to test whether enough ice was removed from either edge, during the cutting procedure, the experiments were devised to remove the same amount (or less) as described in the methods chapter. That is to say removing 0.5 cm from the inner edge and 1 cm from the outer edge.

The results are shown in table 5.7. We can assume that the centre concentration is the lowest obtainable concentration. Therefore by comparing the calculated average, (for the section of ice that would have been used in the sample analysis) with the lowest value, it is possible to determine the possible extent of contamination in that section.

The average concentrations of calcium, chloride, potassium and sodium in the section of ice used in the actual analysis are all significantly higher (greater than 1 standard deviation above the mean) than the central point.

The next step was to test how much ice needed to be removed in order to obtain a constant central value and therefore non-contaminated ice. This is shown in table 5.8 where 1 cm of ice was removed from both the inside and outside edge.

	Cl^-	NO_3^-	SO_4^{2-}	Na^+	K^+	Mg^{2+}	Ca^{2+}
Average with 1cm removed	58.25	82.05	57.73	31.58	24.58	1.97	29.23
Standard Deviation	28.16	11.79	11.41	15.14	4.28	0.57	5.15
Difference from centre point	28.70	4.61	6.60	17.29	4.78	0.62	5.82

Table 2.11 Average concentrations and standard deviation if 1cm of ice was removed from both the inside and outside edge.

The values show that removing more ice has not removed more contamination. With the exception of nitrate and sulphate, all ions show an average concentration that is still significantly higher than that of the centre. This shows that it would not have been beneficial to remove more ice from the inner layer because the level of contamination is unaffected.

The concentrations of the majority of the ions analysed were comparable with the GISP2 data, and can still be considered reliable proxies for environmental change. Calcium however is significantly greater than the expected values and is no longer reliable for calculating percentage change. The contamination appears to be from the

same source, either during the initial drilling process, from the drilling fluid or form the storage bags and therefore it is probable that any significant changes in deposition of calcium would still be visible above the background contamination.

Future work

The implication of this level of contamination in these cores is of great importance with respect to ice core storage. If the ice can become contaminated with storage to the point where chemical analysis of certain species is no longer possible then this is an area that requires consideration, especially by ice core curators.

To test this theory it would have been interesting to compare the same sections from the GISP2 core to see if it is possible to obtain the same concentrations as the originally published data. Of course this could be influenced by different factors in storage, however it would be valuable to know what is happening to the ice cores in long-term storage.

2.10 Comparison with Continuous Flow Analysis (NGRIP)

The GRIP ice, used to investigate the 8.2 kyr event was contaminated with respect to calcium, as discussed above. In order to determine if this contamination had also affected the NGRIP ice the concentration of calcium measured from the discrete 2 mm samples analysed using IC (results presented later in chapter 10) was compared with those measured using Continuous flow analysis (CFA).

The NGRIP core was analysed in the field using a CFA system developed by the University of Bern, Switzerland, to detect Ca, Na, NH_4, NO_3, SO_4, H_2O_2, and HCHO. The data were made available courtesy of Matthias Bigler, now working at the University of Copenhagen.

The high-resolution (2 mm) data from discrete samples analysed using IC are plotted in figure 2.19, showing a very high degree of inter annual variability. The data has been smoothed by a factor of 10, to compare with the 2 cm resolution for the CFA, and the mean concentrations of nitrate, calcium, sulphate and sodium compare well with the CFA record throughout the transition. The concentration of calcium determined from the two separate methods is shown in table 2.12 to reveal differences of just 0.3 %. Such a small difference would imply that there is no similar contamination in the ice from NGRIP that was observed in GRIP.

	CFA [ppb]	IC [ppb]	Difference [ppb]	%
Ca^{2+}				
Mean	102.3	102.7	**-0.3**	**-0.3**
Standard Deviation	76.7	61.1		
Variance	5882.7	3738.0		

Table 2.12. Comparison of average concentration of calcium measured using CFA and IC for transition 1.

There are differences in the features observed in the IC and CFA records with some periods of high concentrations measured using IC that are not observed in the CFA record. The quality control was checked and it was concluded that no external contamination was produced in the cutting and analysis methods.

The greatest differences are observed during the interstadial (2069.5 m for Ca and Na; 2069.3 m for SO_4) when concentrations are lowest. This could be the result of greater inter-annual variability in the 2mm resolution IC record which is dampened by the mixing in the CFA analysis or it could indicate that the levels are approaching the detection limit for the CFA system, however a larger study would be needed to conclude this. For the benefit of this thesis the levels are approximately comparable, indicating there has not been a similar contamination issue as experienced in the GRIP ice.

Interestingly, the sections of ice used from both GRIP and NGRIP were of comparable size and from the same outer section of the core (chapter 2 - methods). The ice was stored in the same way, at the same place and the same amount was cleaned from the core before analysis. The main difference appears to be the length of time that the ice was stored prior to analysis but possibly also the proximity of the ice to the brittle zone. Alternatively an additional cleaning method may have been implemented in the field to remove excess drilling fluid before storage.

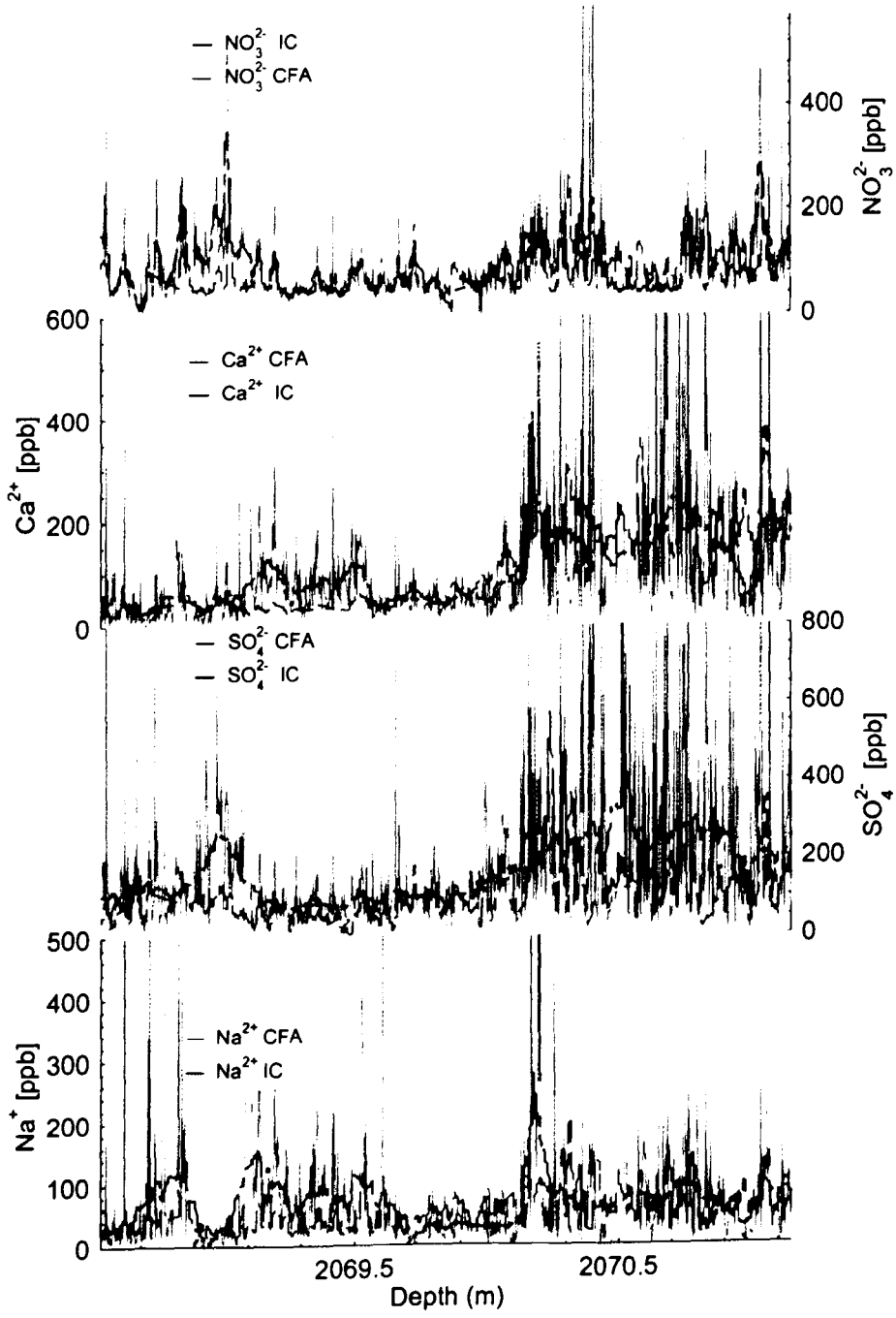

Figure 2.19. Comparison with CFA and discrete sample IC analysis for Nitrate, Calcium, Sulphate and Sodium. High-resolution IC data (grey) has been smoothed to 2 cm resolution (dashed black) to compare with the resolution of the CFA (blue).

Chapter three

Introduction to the 8.2 kyr event

Introduction to the 8.2 kyr event

3.1 The 8.2 kyr event in ice cores

The cold event 8,200 years ago (8.2 kyr event) was first observed in the stable isotope records from Greenland ice cores [Johnsen et al., 1992]. It is seen in both the Greenland Ice core Project (GRIP) and the Greenland Ice Sheet Project 2 (GISP2) ice cores as a sharp negative deviation from the baseline Holocene values (values near 8,000 and 8,400 years ago from a 50-year average). The drop of almost 2 ‰ is approximately half the amplitude of the Younger Dryas change and equates to a cooling of 6 ± 2 °C at Summit Greenland [Alley et al., 1997].

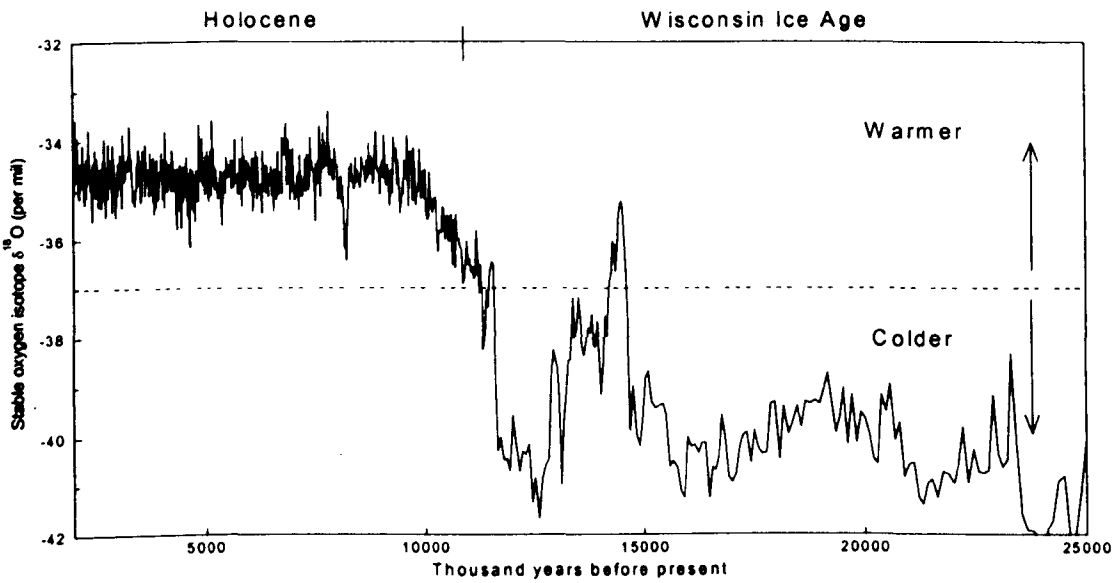

Figure 3.1 Stable Oxygen isotope, $\delta^{18}O$ data from GRIP. The Greenland Summit Ice Cores CD-ROM. 1997. Data provided by the National Snow and Ice Data Centre, University of Colorado at Boulder, and the WDC-A for Paleoclimatology, National Geophysical Data Centre, Boulder, Colorado [GRIP Members et al., 1993].

Dating the event

The exact timing and duration of the 8.2 kyr event differs between sources with varying degrees of error associated with the dating procedure. High accumulation rates of 0.24 meters ice/yr at GISP2 [Meese et al., 1997] provide a continuous stratigraphic record, showing only very occasional periods of minor melt occurring less than once a century [Alley and Anandakrishnan et al., 1995].

Comparison of the event in four deep cores from Greenland (Summit, Dye 3, Camp century and Renland) revealed a notable climate event in all cores corresponding to the 8.2 kyr BP[1] event. The largest deviations occurred between 8.4 and 8.0 kyr BP in most indicators with slight variations in the peak age between sites. Muscheler et al (2004) correlated tree-ring ^{14}C records with cosmogenic isotopes in the GRIP core to determine that the most extreme $\delta^{18}O$ values were observed at 8150 years BP.

The $\delta^{18}O$ minimum for the GRIP ice core is observed at a depth of 1334.50 m. It has been given a calendar date of 8.21 kyr BP with an estimated error of 30 years [Johnsen et al., 1992] at GRIP, compared to 8.23 kyr BP ± 50 years for Dye 3 [Dansgaard et al., 1985] and 8.25 kyr BP for GISP2 [Meese et al., 1997]. As part of the Carlsberg dating initiative at the University of Copenhagen a new Greenland ice core chronology 2005 (GICC05) was created using ECM reference horizons to match DYE-3, GRIP and NGRIP ice core records throughout the Holocene. By exploiting the high accumulation of the DYE-3 site, oxygen isotopes were used to count annual layers back to the 8.2 kyr event where the new calendar date for the 8.2 kyr event is

[1] BP denotes Before Present and in this thesis BP always refers to BP 1950, unless otherwise stated.

given as 8204 BP [Vinther in progress; Rasmussen et al., 2006; Copenhagen dating group, personal communication and the Carlsberg dating conference August 2005].

Snow accumulation

The snow accumulation rate has been calculated following Alley et al (1993) by counting the annual layer thickness and correcting for ice flow. Generally, accumulation rates are low during cold periods and high during warm periods. This is observed in the ice core data for the 8.2 kyr BP event as a rate decrease of 20% from the surrounding values (baseline defined by values near 8.0 and 8.4 kyr BP) [Alley et al., 1997].

Aerosols

Atmospheric loading is reflected by the chemical composition in Summit ice [O'Brien et al., 1995]. The marine input (determined from sodium and chloride concentrations) was previously believed to represents vigour of atmospheric circulation and location from oceanic sources. More recent studies in Antarctica however have determined that the sea salt component observed in the ice core record is derived from the seasonally variable frost flowers formed on the sea ice [Rankin et al., 2002]; the continental component (inferred by the concentrations of calcium) is indicative of long range atmospheric transport and dustiness in the Asian source [Biscaye et al., 1997; Svensson et al., 2000]. The calcium concentration found in GISP2 was shown to have increased by 60% from baseline values[2] during the 8.2 kyr BP event [Alley et al., 1997] indicating increased dryness and aridity in Asian sources, an increase in

[2] Baseline values defined by values near 8.0 and 8.4ka in 50 year average data from the GISP2 core [Alley 1997]

wind speed or a change in atmospheric circulation during this period (see chapter 5 for further discussion).

Trapped Gases

The method of gas-isotopic fractionation has been used by Leuenberger et al (1999) in the GRIP ice core to determine that the drop in Greenland temperature during the 8.2 kyr event was 5.4 to 11.7 °C, with a best estimate of 7.4 °C. A similar value has been determined from the GISP2 core by Kobashi et al., 2003 (abstract only) [Alley et al., 2005] where the temperature deviation at the 8.2 kyr event was found to be in the order of 5°C.

A sharp decrease in methane concentrations (725 to 600 p.p.b.v (parts per billion by volume)) is observed in the GRIP core at 8.2 kyr BP [Chappallez et al., 1993; Blunier et al., 1995] (Fig 3.2) reported by Alley (1995) as a decrease from surrounding values of 10-15 %. The methane oscillation, unlike the isotope signal that is regional in character, has its origins in sources far from Greenland, which indicate that the 8.2 kyr BP event had a significant effect throughout the northern hemisphere.

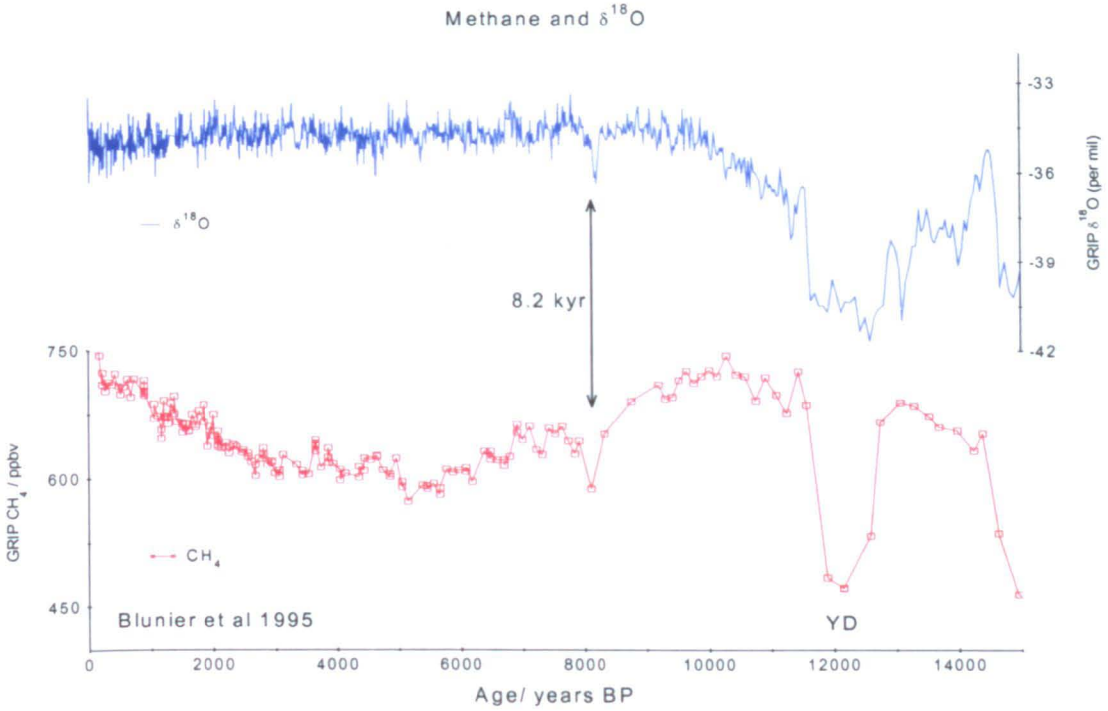

Figure 3.2. Stable Oxygen isotope, $\delta^{18}O$ data (blue curve) from GRIP and Methane concentration (red curve) from the GRIP core [Blunier et al., 1995].

The Greenland Summit Ice Cores CD-ROM. 1997. Data provided by the National Snow and Ice Data Centre, University of Colorado at Boulder, and the WDC-A for Paleoclimatology, National Geophysical Data Centre, Boulder, Colorado [GRIP Members et al., 1993].

Indeed, the 8.2 kyr BP minimum appears to coincide with episodes of severe drought in tropical Africa [Street-Perrott et al., 1983; 1990; Magaritz et al., 1993] and Tibet [Van Campo and Gasse, 1993] and is linked to changes in the evaporation rate over tropical Atlantic [Duplessy et al., 1992].

3.2 Global Evidence

The overall duration and speed at which the 8.2 kyr BP event occurred is often below the temporal resolution of many palaeoclimate records however the synchronicity of the ice core evidence with other global events can be seen. In a recent review of the literature by Rohling and Palike (2005) a collection of the best dated paleoclimate

records of the 8.2 kyr event were collected as shown in figure 3.3. The location of the different records is shown in figure 3.4 and described in the text.

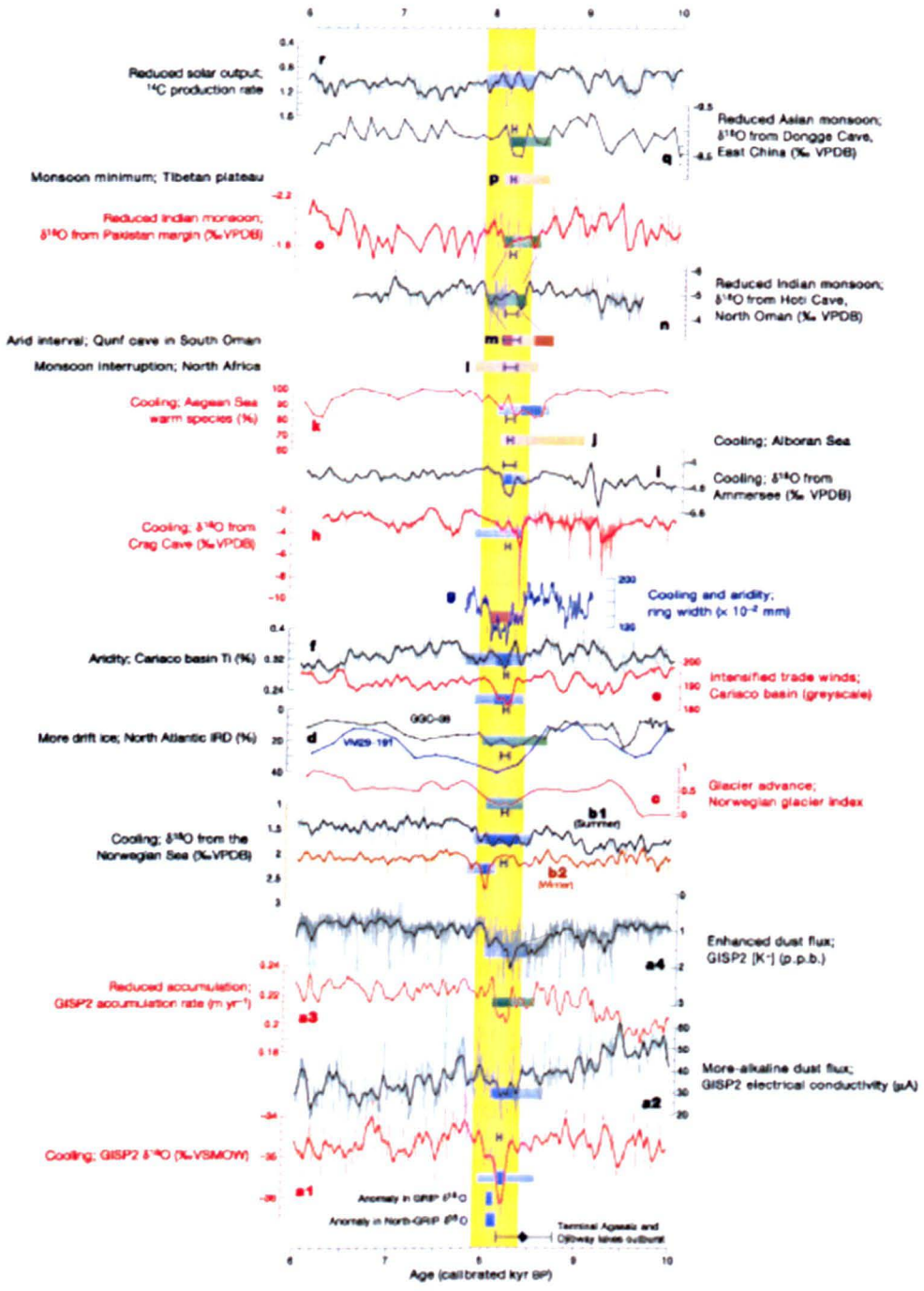

Figure 3.3 Collection of well dated climate proxy records, taken from Rohling and Palike (2005) figure 1. Location of all the records is shown in figure 3.4 and described in the text. (a1) GISP2 $\delta^{18}O$, (a2) GISP2 ECM, (a3) GISP2 accumulation rate, (a4) GISP2 dust flux K^+, [Grootes et al., 1993; Alley et al., 1997]. (b1& 2) $\delta^{18}O$ from ocean sediment core from the Norwegian Sea, [Risebrobakken et al., 2003]. (c) Glacier advance in Norway [Nesje and Dahl 2001]. (d) IRD in North Atlantic [Bond et al., 1997], (e) Greyscale and (f) acidity in the Cariaco basin [Hughen et al., 1996]. (g) Tree ring width in Germany [Spurk et al., 2002]. (h) $\delta^{18}O$ from Crag Cave

[McDermott et al., 2001]. (i) Lake Ammersee Germany [von Grafenstein et al., 1999]. (j) Arabian sea [Siroko et al., 1993]. (j) Alboran Sea, western Mediterranean and (k) Aegean Sea, northeastern Mediterranean [Cacho et al., 2002; Rholing et al., 2002]. (l) African monsoon maximum [Gasse 2000]. (m) $\delta^{18}O$ for Qunf Cave in South Oman [Fleitmann et al., 2003] and (n) Hoti Cave in North Oman [Neff et al., 2001]. (o) $\delta^{18}O$ of the surface-dwelling planktonic foraminifer *Globigerinoides ruber* in a laminated sediment core from Pakistan margin [Staubwasser et al., 2003]. (p) reduced monsoon activity identified from cellulose in a peat-bog section in East Tibet [Hong et al., 2003]. (q) stalagmite $\delta^{18}O$ for Dongge Cave, East China [Yuan et al., 2004]. (r) ^{14}C production rates [Muscheler et al., 2004].

Europe

The first comparative isotope record to confirm the transatlantic nature of the 8.2 kyr BP event was presented by von Grafenstein et al (1998 and 1999) from lake sediments in Ammersee, southern Germany. The excellent correlation between the $\delta^{18}O$ from deep-lake ostracods and the Greenland ice core records suggested that Europe was controlled by the same climate mechanism as Greenland. The negative $\delta^{18}O$ excursion of 1 ‰ (~8,200 yr BP) lasting approximately 180 years exhibits the same abrupt beginning and end with an inferred temperature drop of 1.7 °C [von Grafenstein et al., 1998; 1999].

McDermott et al (2001) correlated the isotope record from Greenland ice cores with speleothem $\delta^{18}O$ records from Crag Cave, southwest Ireland. Despite dating uncertainties, comparisons between the two sources show a similar sequence of events, especially for the prominent 8.2 kyr BP event. The subtle multi-century $\delta^{18}O$ variations surrounding the event are also strongly correlative indicating the variations in Greenland ice cores reflect regional North Atlantic margin climate signals rather than localised effects. The 37-year interval described by Baldini et al., 2002 and McDermott et al., 2001 was the most prominent $\delta^{18}O$ shift in calcite reported for this

event with a deviation of 8 per mil for the 8.2 kyr event. This evidence however has since been withdrawn as an analytical error in the speleothem analysis [McDermott and Fairchild personal communication Rapid annual meeting Swansea 2005; McDermott et al., 2005; Fairchild et al., Earth Science Review, in press]. The trace element analysis of this section of the speleothem does still remain significant and it is still believed that an 8.2 kyr signal is observed in the records from this area of Southern Ireland.

Across south eastern England Rousseau et al (1998) reports a cooling of approximately 1 °C, based on a low-resolution sub-fossil snail record. A short lived cold event was also observed in Wateringbury, Southern England from the geochemical analysis of tufa deposits and ostracod shells possibly correlating to the 8.2 kyr event [Garnett et al., 2004].

A range of palaeoclimatic records exist in Scandinavia of the 8.2 kyr event, known as the Finse event [Nesje and Dahl 2001]. Evidence for a sudden cold period are found in tree-line fluctuations and lake sediments that indicate short-term cold events in Sweden, glacier advances in central and southern Norway and the Austrian Alps [Von Grafenstein et al., 1998]. Pollen and diatom records from lakes in northern Finland [Seppä and Birks, 2001] and northern Sweden [Rosen et al., 2001] show a sharp cooling in inferred July temperature by roughly 1°C.

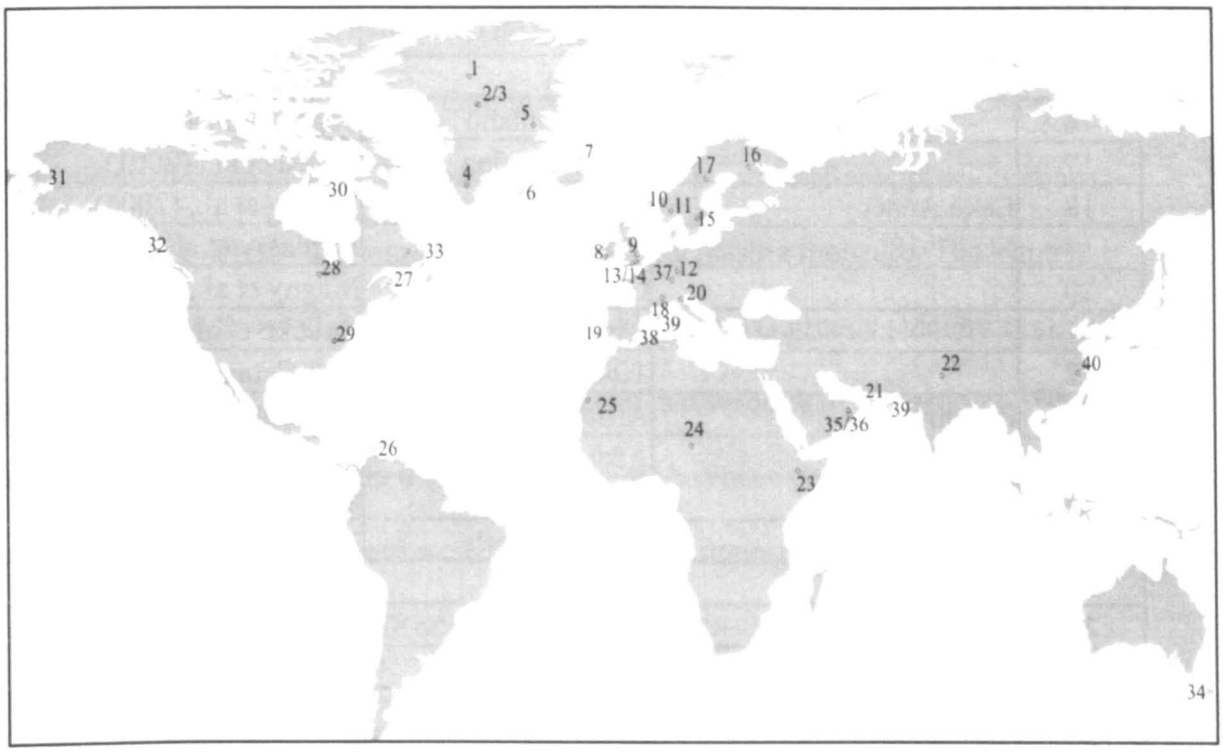

Figure 3.4 Locations of key sites where 8.2 kyr event is reported in the proxy record. Full list of site locations and references shown in table 3.1.

Number	Site	Area	Reference
1	NGRIP	Greenland	NGRIP members (2004)
2	GRIP	Greenland	Johnsen et al., (2001), Dansgaard et al., (1993)
3	GISP2	Greenland	Grootes et al., (1993), Alley et al., (1997)
4	Dye 3	Greenland	Johnsen et al., (2001),
5	Renland	Greenland	Johnsen et al., (2001),
6	VM29-191 & GGC-36	North Atlantic	Bond et al., (1997)
7		North Iceland	Knudsen et al (2004)
8	Crag Cave	Ireland	McDermot et al., (2001), Baldini et al., (2002)
9	Hawes Water	Northern England	Marshall et al., personal communication
10	Core 28-03	Northern North Sea	Klitgaard-Kristensen et al., (2004)
11	Fisktjorna, + five other glaciers	Norway	Nesje and Dahl (2001)
12	Lake Ammersee	Germany	Von Grafenstein et al., (1999)
13	Wateringbury	Southern England	Garnett et al., (2004)
14		South Eastern	Rousseau et al., (1998)

		England	
15		Sweden	Von Grafenstein et al., (1998)
16		North Finland	Seppa and Birks (2001)
17		North Sweden	Roseu et al., (2001)
18	Lake Annecy	Southern France	Magny et al., (2003)
19	SU 81-18	Off Portugal	Duplessy et al., (1992)
20		Central Italy	Magny et al., (2003)
21		Arabian Sea	Sirocko et al., (1993)
22		Tibet	Van Campo & Gasse (1993)
23	Ethiopia	Africa	Gasse and Van Campo (1994)
24	Chad Basin	Africa	Street-Perrot et al., (1983)
25	Western Sahara	Africa	Street-Perrot et al., (1983)
26	Cariaco Basin	Off Venezuela	Hughen et al (1996)
27	Nova Scotia	Canada	Spooner et al., (2002)
28	Ontario	Canada	Yu & Eicher (1998)
29	Massachusetts	North America	Shuman et al., (2002)
30	Hudsen Bay		Barber et al., (1999)
31		Alaska	Denton & Karlen (1977)
32	British Columbia	Canada	Menounos et al., (2004)
33	Newfoundland	Canada	Daley eprsonal communication
34	Tasmania	Australia	Xia et al., (2001)
35	Qunf Cave	South Oman	Fleitmann, et al. (2003)
36	Hoti Cave	North Oman	Neff et al., (2001)
36		Germany	Spurk et al., (2002)
37	Alboran Sea	Mediterranean	Cacho et al., (2002)
38	Aegean Sea	Mediterranean	Rohling et al., (2002)
39		Off Pakistan	Staubwasser et al., (2002)
40	Dongge Cave	East China	Yuan et al., (2001)

Table 3.1 List of palaeoclimate records where the 8.2 kyr event is reported. Locations shown in figure 3.4.

The drier conditions observed in sites of northern and southern Europe for the 8.2 kyr BP event correlate well with low lake levels and drought in Africa [van Campo and Gasse et al., 1993; 1994] however comparative evidence put forward by Magny et al (2003) suggest that this was not true for all of Europe. The 8.2 kyr BP event is characterized, from lake level and pollen data from lake Annecy, eastern France, by

two successive phases of higher lake level and increased annual precipitation. The cooling event determined to be a drop in summer mean annual temperature of ~2 °C is accompanied by an increase in the water budget (an increase of precipitation minus evaporation (P-E) of ~130 mm) corresponding to increasing moisture. The same is observed in the Swiss plateau, northern Central Italy and Germany [Magny et al., 2003 and references therein]. Changes in accelerated velocity of the Atlantic Westerly Jet in relation to variations in the thermal gradient has been used by Magny et al (2003) to explain the observed wetter zone in mid-European latitudes (between 50° and 43°) during the 8.2 kyr BP cooling event.

Africa and Asia

Sirocko et al (1993) reported a series of abrupt changes over Southeast Asia during the Holocene from the $\delta^{18}O$ record of surface dwelling foraminifera from the Arabian Sea. An abrupt transition was observed 7,300 ^{14}C yr BP (dating uncertainties exist) when a rapid influx of the dolomite, used as an indicator of weak southwest monsoons, interrupted an otherwise warm and humid period. The monsoonal pattern is greatly influenced by the Tibetan plateau whose summer heating and formation of low pressure over land surface draws the Indian monsoon cyclonic air inland. The probable cause of the weakening monsoons observed by Sirocko et al (1993) can thus be explained by the palaeoclimate record from western Tibet. Van Campo and Gasse (1994) concluded that the event between 8,000 and 7,000 years BP was caused by abrupt disequilibria in the climatic system. Pollen records from the Tibetan plateau reported a sharp drop in the ratio of steep pollen to desert pollen, synchronous with deceasing pollen concentrations, relating to a reduction in vegetation cover and a return of dry conditions for this period [Van Campo and Gasse et al., 1993 and 1994].

Shallow and slightly saline conditions, depicted from the diatom record of lake sediments, correlate with the increased aridity and can been seen in northwest India as a decrease in summer and winter rainfall.

Independent palaeoecological records have shown consistent transitions, from the generally moist and humid climate of the mid-Holocene, in the period between 8,000 and 7,700 year BP over much of the northern tropics of east Africa, the Western Sahara, the Sahel and subequatorial Africa. Gasse and van Campo (1994) have shown reduced lake levels and extreme aridity, demonstrated by reworked sediments and the corrosions of pollen grains, in Ethiopian lakes. This combined with the deficit in the hydrological balance, recorded by the percentage decrease in littoral diatoms and diatom inferred water conductivity, is also seen in lakes of the Chad basin [Street-Perrott et al., 1983] and palaeolakes of Western Sahara, where water depth and salinity were deduced from geomorphic and diatom evidence.

Americas

There is some evidence of the 8.2 kyr event in the Americas with the strongest revealed in the Grey-Scale record of the Cariaco bay, offshore Venezuela [Alley and Agustsdottir, 2005; Hughen et al., 1996]. Spooner et al (2002) reports a period of ecological change in central Nova Scotia while Yu and Eicher (1998) observe a shift in oxygen isotopes toward colder conditions from lake sediments in Ontario, Canada at the time of the 8.2 kyr event. Shuman (2002) collated evidence of centennial scale cooling around this period from pollen records in Massachusetts, Pennsylvania, Maine and Quebec.

Evidence of colder conditions in northern North America exists, with reduced melting in the lake Agassiz Ice cap, Ellesmere Island, Canada [Fisher et al., 1995], glacier advance in Alaska [Denton and Karlén, 1977] and the coast mountains of British Columbia, Canada [Menounos e al., 2004] and a scarcity of whale bones of the age of the 8.2 kyr event of the coast of the Canadian Arctic, suggesting an increase in sea ice during this period [Dyke et al., 1996].

3.3 Theories behind the cause of the event

Although the existence of a cold, dry event in North Atlantic regions is now documented, some doubt still remains over the cause of the 8.2 kyr BP event. Barber et al (1999) proposed that the pattern of cooling, observed as a 4-8 °C decrease in central Greenland and a 1.5-3 °C decrease in marine and terrestrial environments respectively, implies heat transfer from ocean to atmosphere was reduced in the North Atlantic. The influence of the North Atlantic thermohaline circulation (THC) on climate is an idea expressed by Broecker et al (1985) with the hypothesis that large and abrupt fluctuations in high-latitude climate invokes changes in the rate of formation of North Atlantic deep water (NADW) and therefore oceanic heat transport. Further studies by Boyle et al (1987) confirmed a marked nutrient depletion of intermediate waters is associated with a decrease in glacial north Atlantic deep-water flux, proposing that cold high-latitude sea surface temperature enhanced intermediate water formation at the expense of deepwater formation. An increase in freshwater flux would result in a decrease in the formation of deepwater and ultimately a cooling in high-latitudes [Clark, 2001]. This amplification in freshwater budget in the North Atlantic is generally attributed to the final stages of the deglaciation of the Laurentide and Scandinavian ice sheets. Figure 3.5 shows the ice margins of the Laurentide ice

sheet from the last glacial maximum to the 8.2 kyr event and the proposed drainage routes based on results from Barber et al., (1999) and Clarke (2001). The freshwater input from melting icebergs in the Nordic sea has been discounted by Bauch et al (2001) for lack of ice rafted debris.

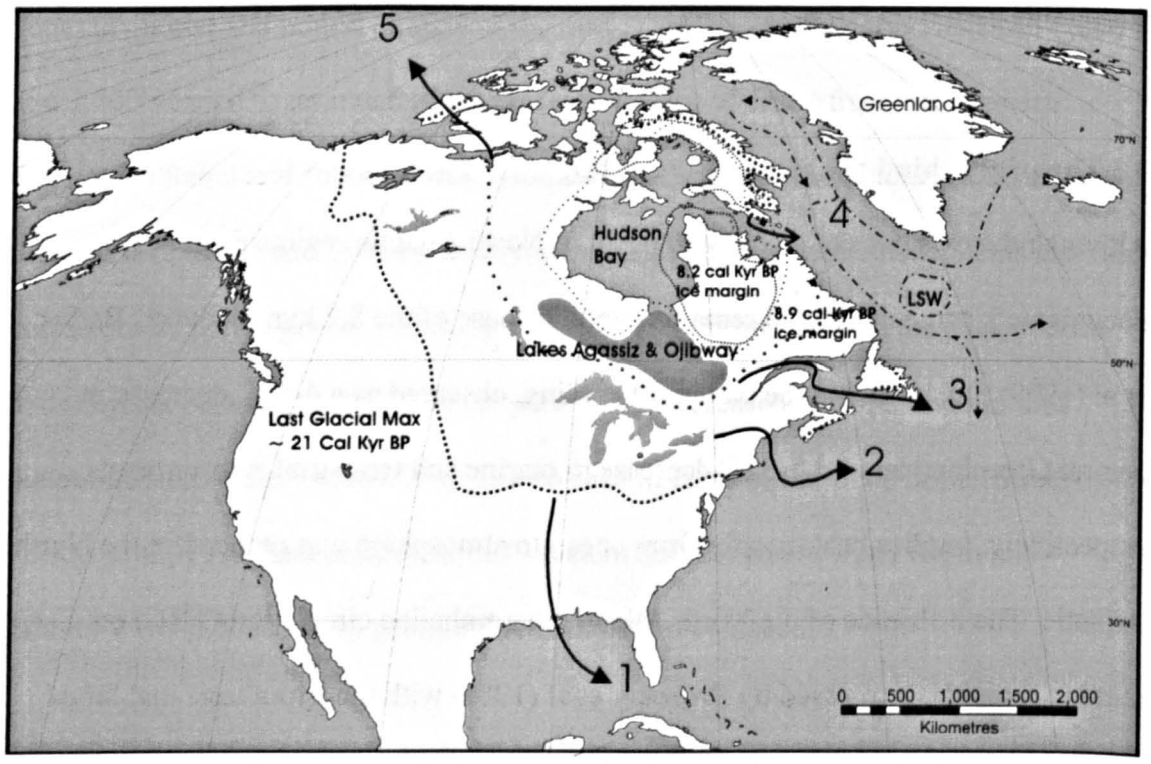

Figure 3.5 Map of proposed flooding of Lake Agassiz prior to the 8.2 kyr event. Dashed lines indicate ice margins at the last glacial maximum (~21 cal kyr BP), before the flooding (~8.9 cal kyr BP) and after the flooding (~ 8.2 cal kyr BP), based on estimates from Barber et al (1999) and Clark (2001). Dashed arrows represent ocean circulation of Labrador Sea surface water (LSW) and solid arrows represent proposed flood routes: 1, Mississippi River; 2, Hudson River; 3; St Lawrence River; 4, Hudson Strait; 5, Arctic Ocean.

Based on estimates of the marine ^{14}C reservoir for the Hudson Bay, Barber et al (1999) concluded that the massive outflow of freshwater required to reduce the formation of deepwater was from the glacial lakes of Agassiz and Ojibway,

northeastern Canada. The lakes, originally dammed by the Laurentide ice sheet (as shown in figure 3.5), located more than 175 m above sea level drained catastrophically 8,470 calendar years BP (~ 7,700 ^{14}C years BP) releasing 2 x 10^{14} m^3 of lake water over a period of 100 years [Barber et al., 1999; Clark, 2001]. Later investigation by Clarke (2004) proposed smaller water volume and a flood duration of just 0.5 years. Barber at al (1999) used the stratigraphy of the Hudson and James Bay lowland records to show the existence of glacial marine sediments directly above pro-glacial lake sediments. Cores from the Hudson Bay also show a layer of red coloured haematite-rich sediment, common within red glacial deposits in north-central Hudson Bay and the red brown glaciolacustrine sediments of the former Agassiz and Ojibway basins, traceable over 700 km. Barber et al (1999) proposed the degree of sediment transport required to create such a record as evidence of the catastrophic drainage. Correlative evidence exists throughout the Labrador Sea observed as lower sea surface salinities and increased water stratification [Knudsen et al., 2004].

Knudsen et al (2004) observed the 8.2 kyr BP event as a cooling of surface waters off North Iceland, a sensitive boundary region between warm, high-salinity Atlantic water and cold, low salinity surface water of the East Icelandic Current. The cold event is clearly expressed by a pronounced increase in the percentages of *N. pachyderma*,[3] corresponding to a temperature decrease of about 3 °C. The diatom record supports this with a pronounced peak in sea-ice species and cold species at this time. Knudsen et al (2004) suggest the presence of two distinct peaks in benthic species indicate a strongly stratified water column while the associated low epibenthic δ^{13}C has been used by Bauch et al (2001) to imply a decrease in ventilation in Nordic

[3] High percentages of sinistrally coiled *Neogloboquadrina pachyderma* show that Arctic or Polar surface waters did predominate [Knudsen et al., 2004]

seas. Values as low as 2.1–2.2 ‰ are reached from the planktonic oxygen isotope at this time and are assumed to indicate low-salinity surface waters.

Evidence of THC weakening

Ocean circulation models show that an excess of freshwater discharges of 0.06 – 0.12 Sv (1 Sv = 10^6 m^3 s^{-1}) can reduce the formation rates of the Labrador Sea intermediate water (LSW) and the North Atlantic deep water (NADW) [Rahmstorf et al., 1995]. The combined release of 2 x 10^{14}m of water from Agassiz and Ojibway would, according to numerical models, increase the freshwater flux to the Labrador Sea by as much as 6 Sv if the flux occurred over the predicted timescale of one year [Clarke et al., 2004], strongly affecting thermohaline circulation and heat transport.

The global sea-ice-ocean model used by Renssen et al (2001) to study the mechanism behind the 8.2 kyr BP event concluded that weakening of the thermohaline circulation, as a result of freshwater pulse associated with final stages of North American deglaciation, would indeed produce a model response of atmospheric cooling consistent with proxy data. Using a constant freshwater input of 4.67 x $10^{14}$$m^3$ and a flux of 0.75 Sv over 20 yrs the model returned to its pre-perturbed state of 17 Sv in a time of 320 years, a duration comparable to that of the 8.2 kyr BP event. Gradual release (0.03 Sv during a 500 year period) produced no significant weakening of the thermohaline circulation. However, predictions of a strong pulse (exceeding 1.5 Sv in a 10 year period) yielded significant THC weakening, in which the model did not recover to its pre-perturbed state, switching permanently (at least >1000 years).

Clarke et al (2004) estimated the magnitude of the flux to be ~5 Sv with a duration of ~0.5 yr but that the forcing may have been complex with more than one pulse, suggesting multiple floods. This supports some of the palaeoenvironmental evidence suggesting the event did not follow a simple pattern of deterioration and recovery but was two-pronged in character [Alley et al., 1997; von Grafenstein et al., 1998; Baldini et al., 2002].

The correlation between THC and aridity in Africa proposed by Street-Perrott and Perrott (1990), in a study of the 20-year sub Saharan drought between 1968 and 1988, concluded that a relationship existed between below average rainfall in the Sahel and a persistent pattern of global sea surface temperatures (SSTs). It was found that warmer than average waters in the Southern hemisphere mirrored cold conditions in the northern hemisphere as a result of declining northward heat transport. The tropical rain belt shifted southward and precipitation over West Africa and the North American tropics was reduced. It was found that a weakening of the THC not only produced colder SSTs in the North Atlantic but also to a lesser extent in the North Pacific. This evidence corroborates with findings by Menounos et al (2004) of a glacier advance in the coastal mountains of western Canada between 8630 and 8020 cal year BP suggesting a synchronous response to climate forcing between the two oceans, albeit on a much slower scale.

Synchronous evidence of the 8.2 kyr BP event as far south as Tasmania and South America [Xia et al., 2001; Hughen et al., 1996] put theories of solely northern hemisphere related changes into question with studies which proposed a global forcing mechanism to be responsible.

Sediment cores from the Cariaco Basin, off the northern coast of Venezuela have shown sub-decade to century-scale oscillations in surface-ocean biological productivity synchronous with climatic changes at high latitudes [Hughen et al., 1996]. The reduced greyscale values, formed by seasonal alteration in the sediment layers, indicate increased zonal wind speed due to high-latitude cooling and a southward shift in the inter tropical convergence zone (ITCZ). Xia et al (2001) reported similar abrupt climatic changes in stalagmite isotopic analysis from Northern Tasmania. Therefore the 8.2 kyr BP event can be seen as a dry episode, of slow-growing conditions and reduced organic contents, between two warm and wet periods. The transitions are abrupt with half the warming, inferred from $\delta^{18}O$, occurring in less than 100 years.

3.4 Conclusions

There is strong evidence of a rapid cold event 8,200 years ago from both the isotope and inferred temperature record from Greenland ice cores and a number of palaeoclimate proxies around the North Atlantic. The cold dry conditions implied by the decreased snow accumulation rate, increased continental component and decreased methane concentrations are synchronous with periods of drought in Africa, weakening monsoons in Asia and widespread cooling in northern Europe, but it is unclear if the same "event" is recorded in the distant regions.

The rapidity of the catastrophic release of freshwater from the Hudson Bay has been shown by models to produce a significant weakening of the thermohaline circulation and give a model response in terms of amplitude and duration equivalent to that of the 8.2 kyr event. It is worth noting that the model produced a complete shutdown of the

THC for timescales of less than 20 years, however palaeoclimate evidence suggests that the freshwater pulse was much faster. Indeed, evidence of the duration of the 8.2 kyr BP event is sometimes shorter than the models prediction of 320 years. Dating uncertainties and discrepancies between palaeoclimate evidence must be overcome to ensure accurate estimated of duration.

Whilst there is an abundance of corroborative evidence for the 8.2 kyr BP event, there are still many questions regarding the speed and sequence of change. The global response to future rapid climate change of the magnitude of the 8.2 kyr BP event would be immense, especially to the arid and semi-arid zone where changes in the water balance would severely impact densely populated areas such as north and central Africa and southwest USA where water is already scarce.

3.5 Aims

The literature regarding the 8.2 kyr event is vast but despite the large spatial coverage of the proxy records there are still a number of questions unanswered. Was the 8.2 kyr event a global phenomenon or were Rohling and Palike (2005) right to propose that the more abrupt climate changes around 8,200 years ago was superimposed on a background centennial cooling? Given that most anomalies in climate proxy records from locations around the globe are correlated with the sharp event observed in Greenland it is therefore important that ice core records are properly understood.

We need to define the event and determine the true rate of change, in the Greenland records, in order to determine the exact duration for the benefit of global proxy comparison and model parameters.

The aim of the next part of the thesis is to investigate the 8.2 kyr event in central Greenland using the GRIP ice core. A new continuous sub-seasonal record of chemical deposition to Greenland during the event has been produced along with a new high-resolution stable isotope record.

A total of 21.96 m of ice from the GRIP ice core has been cut into discrete samples of 1 cm resolution as described in the methods chapter (Chapter 2). More than 2,000 samples were analysed using ion chromatography (IC) to produce a sub-seasonal chemical record of deposition to Greenland during the 8.2 kyr event.

A new high-resolution (1 cm) oxygen isotope record was produced from GRIP ice core (analysed at the University of Copenhagen) and compared with the parallel GISP2 ice core during a central section of the 8.2 kyr event. In addition a near annual resolution (10 cm) oxygen and deuterium isotope record (analysed at the NERC National Isotope Geosciences Laboratory (NIGL) in Keyworth) has been produced and compared to three other deep ice cores drilled in Greenland, GISP2, NGRIP and Dye 3. The 8.2 kyr event has been defined statistically from the isotope records of the four cores.

The new sub-seasonal chemical record has been used to show the amount of deposition to Greenland during and to give the true duration of the 8.2 kyr event based on annual layer counting of nine chemical species. The new dating has been compared to independent ice core dating projects [GICC05; Rasmussen et al., 2006] and also to calculate the true accumulation rate based on the annual layer thickness.

Chapter four

The 8.2 yr event: Isotopes

The 8.2 kyr event: Isotopes

4.1 Introduction

Condensation and precipitation during air mass cooling preferentially removes the so-called "heavy" water (containing ^{18}O or ^{2}H), with its lower vapour pressure, compared to that of "ordinary water (containing ^{16}O or ^{1}H). The depletion in heavy water results in the air-mass precipitation becoming increasingly lighter. In general, the older the air mass, the lighter the precipitation it produces [Dansgaard et al., 1964]. The distribution of stable water isotopes HDO and $H_2{}^{18}O$ has been well documented to show the existence, in middle to high latitudes, of a linear relationship between mean annual isotope content of precipitation (δD and $\delta^{18}O$, expressed in per mil units with respect to standard mean ocean water (SMOW)) and the mean annual temperature at the precipitation site[6]. Research has shown that although the site temperature is the most important factor affecting isotopic composition [Jouzel et al., 1997], other factors must be considered when using the ice as a palaeothermometer.

The isotopic composition or the temperature of the ocean surface may change over time. So too could the path that the air mass follows, the seasonality of precipitation, the cooling process (adiabatic or isobaric), the degree of convective lifting and the offset between cloud and ground temperature. The conditions at the site could also alter the isotopic profile with the accumulated ice being sensitive to post-depositional sublimation or drifting, diffusion and ice-flow transport. Such uncertainties require that water isotope data be used with caution in the absence of reliable local calibrations.

---

[6] The relationship between $\delta^{18}O$ and temperature T, for time t, is assumed to be linear $\delta^{18}O(t) = aT(t) + b$ where a (the isotope/surface temperature slope, $d\delta/dT$) and b are coefficients that do not change with time [Cuffey et al., 1994]

Borehole palaeothermometry has proven especially valuable for Greenland utilizing the temperature of the ice itself to provide a depth temperature profile. For ice sheets, lacking abundant surface melt, the mean annual temperature primarily controls the temperature of near surface ice (~ 10m). Air temperature changes propagate into the ice by diffusive heat flow and ice flow producing a profile of temperatures through the ice that can be measured in a borehole [Cuffey et al., 1994]. The profile is then deconvoluted to give an estimate of past air temperatures. The thermal properties of heat diffusion are well understood and the remaining uncertainties that lie in the modifications caused by ice flow are reduced by the relatively stable nature of summit Greenland and provide accurate calculations for ice flow.

Fluid filled boreholes at GRIP and GISP2, which did not extend to the surface, were largely insensitive to changes in surface temperature during the drilling. The preferred calibration curves for the two sites were slightly different; a linear relationship between isotopic data and temperature with some time variations for GISP2 [Cuffey et al., 1995] compared to the GRIP site where the linear coefficients were kept constant but an additional term proportional to δ^2 was allowed [Johnsen et al., 1995]. Similar results from both methods concluded that isotopic ratios provide an excellent palaeothermometer and that the calibration for recent times is different to older times (~0.5 ‰ /°C and 0.6 ‰ /°C in $\delta^{18}O$ for GISP2 and GRIP respectively, in the last few centuries or millennia, compared to 0.33 ‰ /°C and 0.23 ‰ /°C for the glacial – interglacial transition).

The temperature records derived from the isotope profiles indicate an increase in temperature of up to 25 °C at Summit for the glacial maximum to the Holocene

transition, after the lapse rate effect of thickening associated with accumulation increase and the change in seawater $\delta^{18}O$ were accounted for.

The $\delta^{18}O$ records for the GRIP and GISP2 cores show a negative deviation from the baseline Holocene values (values near 8,000 and 8,400 years ago from a 50-year average) of –2 ‰ corresponding to the 8.2 kyr event, approximately half the amplitude of the Younger Dryas change. The Cuffey et al (1994: 1995) calibration has been used for the GISP2 core $\delta^{18}O$ to show a cooling of 6 ± 2°C occurred at Summit Greenland 8,200 years ago [Alley et al 1997].

4.2 Results

High-resolution analysis of $\delta^{18}O$ and δD (produced at NIGL, the University of Copenhagen and the University of Colorado for this thesis) has augmented previously published data for this event [Johnsen et al., 1992; GRIP members, 1993; Alley et al., 1997] (Figure 1) by increasing the resolution from 27.5 cm (half bag averages) to 1 cm resolution. The isotopic composition can be considered primarily to reflect the local temperature at summit but also alterations in the composition or source location.

The deuterium excess ($d = \delta D - 8\,\delta^{18}O$, [Dansgaard et al., 1964]) may be regarded as a residual that relates to the slight differences between D and ^{18}O, related to sea surface temperatures (SSTs) and sea surface humidity at the initial evaporation [Jouzel et al., 1984; Petit et al., 1991]. The combined errors associated with the measurement of both oxygen and deuterium measured at NIGL give an estimated error of ± 1.4 ‰ for deuterium excess.

Oxygen Isotopes

The oxygen isotopic data were analysed at 10 cm resolution to obtain an annual signal and at 1 cm resolution to obtain a sub-seasonal signal as described in the method chapter. The oxygen isotope data are shown in figure 4.1 below, using the low-resolution GRIP record from Johnsen et al., (1992) to zoom in from the whole Holocene (a) to the 8.2 kyr event (b) and the new 10 cm resolution 8.2 kyr record (c).

The 8.2 kyr event is characterized by a period of low isotope values that can be seen in the low-resolution isotope record from Johnsen et al (1992) (figure 4.1& 4.2). The new higher resolution records show that the isotopic values reached levels even lower than those observed in the low-resolution record. A core of very low values found between 1333.9 m and 1334.9 m can be seen in the 10 cm resolution record from GRIP (figures 4.1 & 4.2) with the 1 cm resolution record showing a very clear minimum at 1334.47 meters (figure 4.2). This corresponds to a decrease in $\delta^{18}O$ of almost 4 ‰ (± 0.05 ‰) from the Holocene average.

The 1 cm resolution data, despite being at much better than the annual resolution, do not appear to show an annual signal. Diffusion of the isotope annual signal has exceeded the layer thickness and so it cannot be used to date the core.

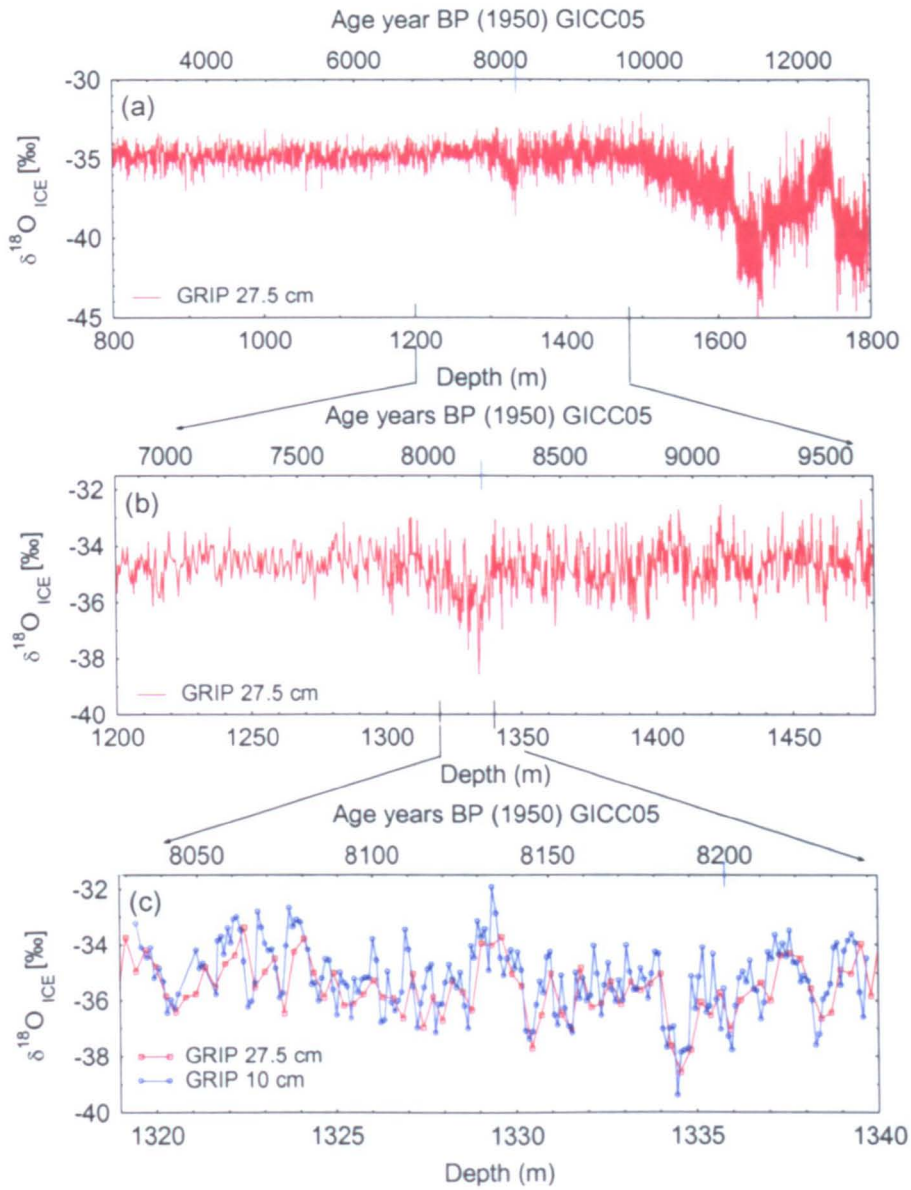

Figure 4.1 Oxygen isotope record from GRIP at 27.5 cm resolution (red) [Johnsen et al., 1992] and 10 cm resolution measured for this thesis. (a) The Holocene, 800 m to 1800 m; (b) 1200 m to 1480 m; (c) the 8.2 kyr event, 1319 m to 1340 m. All plotted on the GRIP depth scale and the GICC05 age scale [Rasmussen et al., 2006].

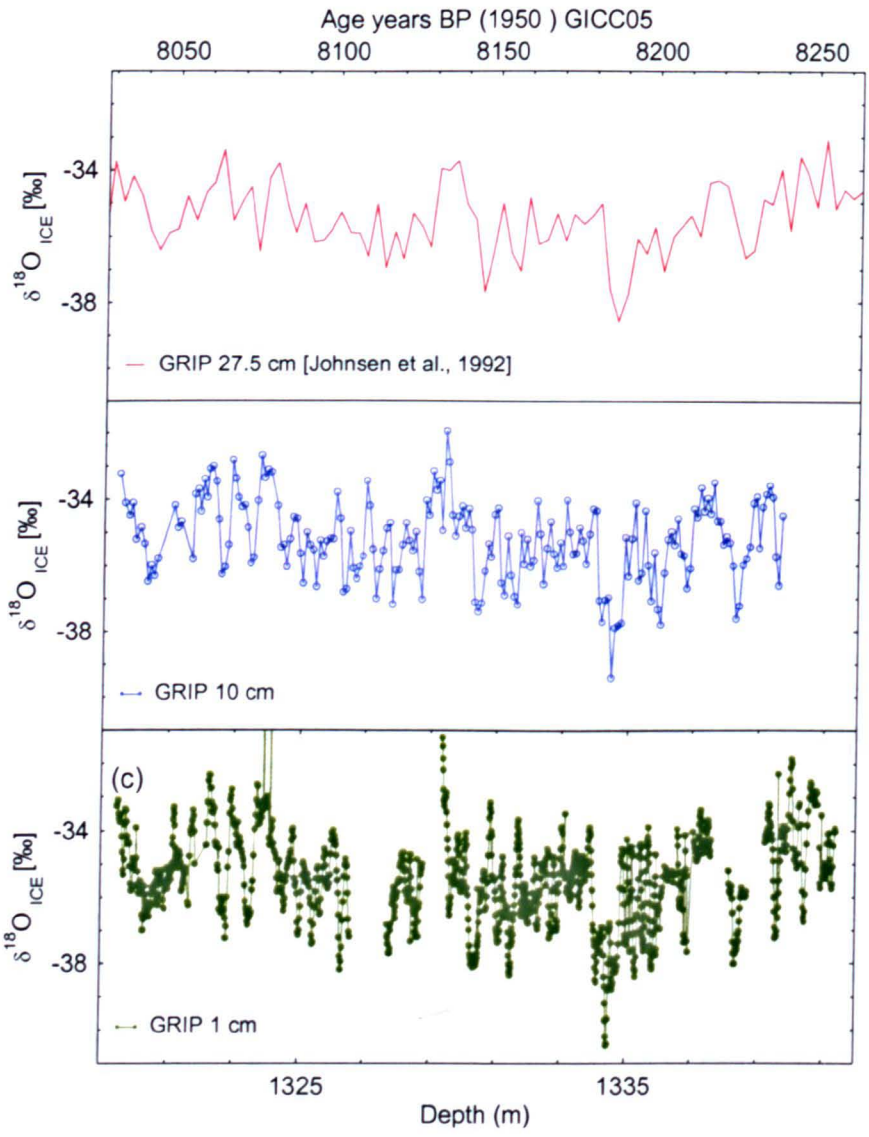

Figure 4.2 Oxygen isotope record from GRIP at 27.5 cm resolution (top red) [Johnsen et al., 1992], 10 cm resolution (middle blue) and 1 cm resolution (bottom green) for the entire period analyzed for the 8.2 kyr event.

The new resolution has improved upon previously published results to show that even greater extremes in isotopes, and therefore possibly temperature, were achieved throughout this period. Due to the high inter-annual variability of the high-resolution (1 cm) record the extreme values in the spike, with a maximum negative deviation observed at a depth of 1334.47 m, could be dismissed as outliers. The individual data

points have been added to figure 4.2 to show that during this section of ice the values were all consistently low making it unlikely that this is just a result of sampling error[7].

The presence of the 'spike' in both the 10 cm and the 1 cm resolution data (which were analysed at different laboratories, see methods Chapter 2) indicate that this is robust feature in the GRIP core, that embeds 1-3 years of very low values, typical of glacial ice. Such a sharp event, if real, might indicate an even more extreme temperature excursion, or could represent the signal of a change in freshwater content of the surface ocean, which might be expected if the ocean was really flooded with freshwater melt.

The availability of ice from the parallel US run GISP2 core gave us a unique opportunity to test whether this extreme 'spike' in the GRIP core was in fact a significant climate signal. High resolution (1 cm) samples from the American led GISP2 core were cut and analysed at Boulder, USA over the one-meter section, corresponding to the depth where the extreme low values from the GRIP core were observed. Differences in the isotope values between Greenland sites have been observed for the 8.2 kyr event and other isotope anomalies (as shown in section 4.2, defining the event) however the GRIP and GISP2 core are located only 30 km apart and should show very similar isotopic signals. To determine whether the extreme low values seen in GRIP show a real signal, oxygen and deuterium isotopes from the two cores have been compared.

[7] The statistical analysis of the isotope record is explored further in subsequent sections of this thesis (see 'Defining the Event' chapter).

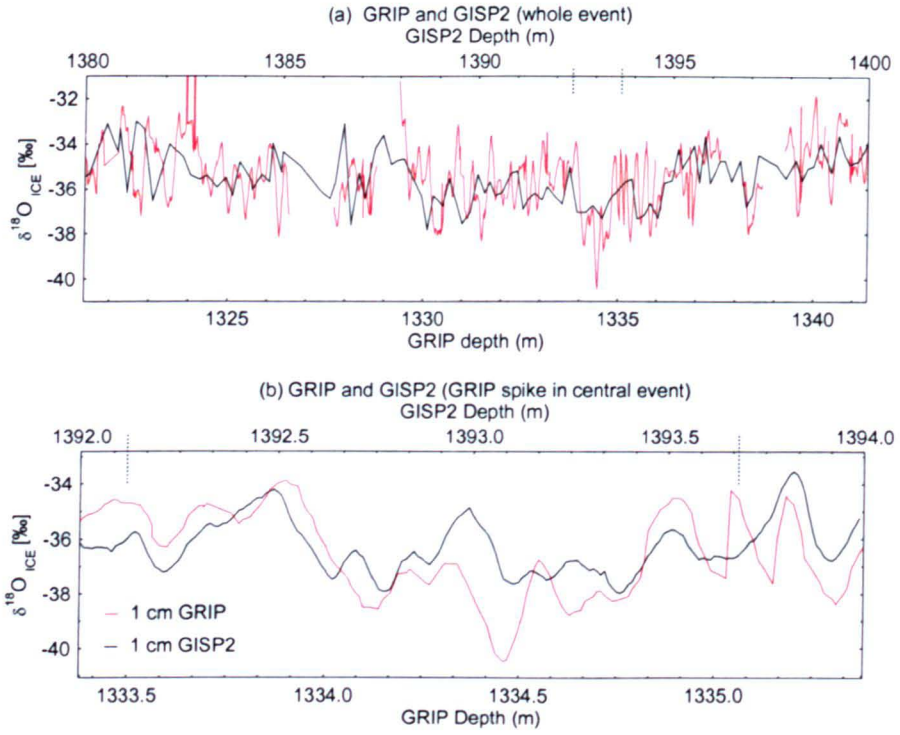

Figure 4.3 Comparison of $\delta^{18}O$ for GRIP (red) and GISP2 (black) for the whole event (graph a), 1 cm resolution for GRIP and 5 cm resolution for GISP2; and the central spike (graph b), 1 cm resolution for both GRIP and GISP2.

The isotopic signal for the two cores has been plotted on both the GRIP and the GISP2 depth scale. Slight differences in the accumulation rate at each site have led to slightly different depths at which the 8.2 kyr event appears in each core. Distinctive ECM peaks, which represent discrete volcanic eruptions, have been used to match up the isotope record from both cores. The section above was easy to match because a clear volcanic peak, in the form of an ECM triplet, occurs within the 8.2 kyr event at a depth of 1334.04 m in the GRIP core. The same peak is observed in the GISP2 core at a depth of 1392.66 m.

In figure 4.3 the 1 cm GRIP record has been compared with the 5 cm GISP2 record across the whole of the 8.2 kyr event (top of figure 4.3). The records show very

similar results for the duration of the 8.2 kyr event as expected however the new 1 cm resolution record from GRIP and GISP2 (compared in the bottom of figure 4.3) is quite different, especially between depths 1392.5 m and 1393.5 m (GISP2 depth) corresponding to the central spike of very low values in the GRIP core. The surrounding values appear to be similar in both cores however when the GRIP record shows a sharp extreme 'spike', the GISP2 record shows much less negative values. This obvious discrepancy between the two cores could suggest that the isotopic anomaly in the GRIP core was not a period of extremely cold winters but more likely an artefact of a build up of winter snowdrift.

In any case, there is no similar decadal scale event in the GISP2 or either of the other cores (Dye 3 or NGRIP), and we do not explore this any further. Rather the event should be seen as the somewhat broader signal around it.

Temperature derived from Oxygen Isotopes

Studies have shown a relationship between the seasonal variations of the water isotope signal of snow on the ice sheet at Summit with that of observed temperatures on the east coast of Greenland and the ice surface temperatures [Dansgaard et al., 1964; Johnsen et al., 1989; 1992; 1995; Cuffey et al., 1994].

According to Johnsen et al., (1989) a linear relationship exists in Greenland between the ice sheet surface temperature, T_s (°C), and present mean annual values of precipitation δ (‰), represented by the following equation;

$$T_s = 1.50\delta + 20.3 \qquad \textbf{[Equation 4.1]}$$

It was suggested that this equation can be used for temporal changes if the sensitivity, $dT_s / d\delta$, was slightly higher than 1.50 °C per ‰. Cuffey et al., (1994) determined the sensitivity to be in the range 1.52 to 2.22 °C per ‰ based on comparison of the seasonal δ variations in the snow on the Greenland ice sheet with that of the observed temperature, using the upper part of the GISP2 core.

The temporal relationship between δ and T_s can be used to convert the palaeoclimate record, after it has been corrected for changes in the surface elevation and isotopic composition of seawater. Over the Greenland ice-sheet at the present time the mean annual $\delta^{18}O$ of snow is related to surface temperature by the following equation from Johnsen et al (1989; 1997):

$$\delta^{18}O = 0.67 \times T - 13.7‰ \qquad \textbf{[Equation 4.2]}$$

The above relationship however does not hold true for the isotope changes along the GRIP core, this can only be achieved by modelling the borehole temperature profile, using parameters from instrumental measurements [Johnsen et al., 1997] and the new relationship is assumed to be;

$$T = \alpha + \beta \times \delta^{18}O + \gamma \times (\delta^{18}O)^2 \qquad \textbf{[Equation 4.3]}$$

The values of α, β and γ are constants determined from the modelled and measured temperature profile described in Johnsen et al., (1997) with values of α = -211.4°C, β = -11.88 °C/ ‰, γ = -0.1925 °C/ (‰)^2.

The temperature profile has been plotted in figure 4.4 (below) showing the difference in temperature during the 8.2 kyr event from present-day values at Summit Greenland.

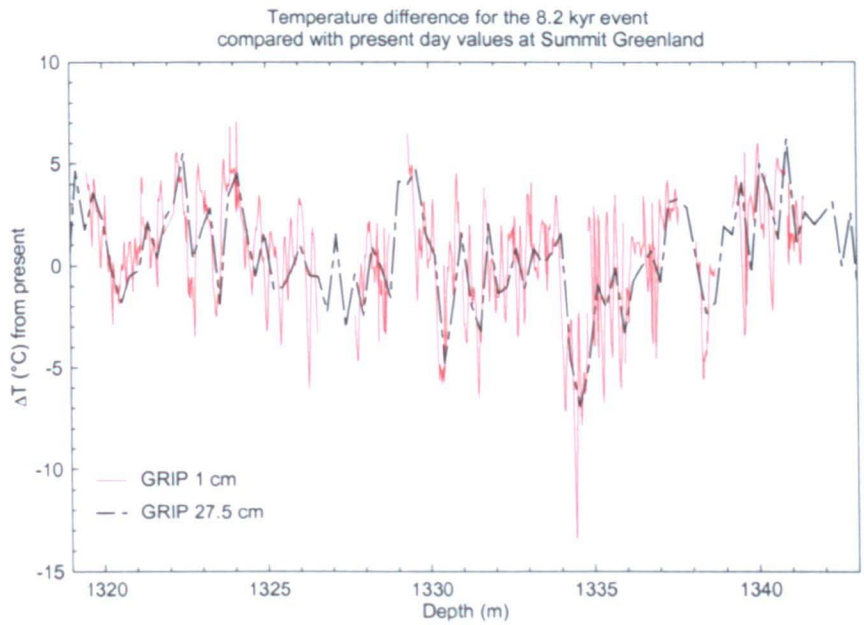

Figure 4.4 Temperature difference from present day values at Summit, Greenland during the 8.2 kyr event, derived from the oxygen isotope record, from the GRIP core at 27.5 cm resolution [Johnsen et al., 1992] and 1 cm resolution for the 8.2 kyr event.

In figure 4.4, the new 1 cm resolution data collected for this thesis are shown overlain on the previous best resolution data (27.5 cm) from the GRIP core.

Deuterium

The deuterium isotopic ratio was also analysed at 10 cm resolution as described in the methods chapter. Figure 4.5 below shows the deuterium and oxygen both at 10 cm resolution for the whole event. As expected there is a strong covariance of the two isotopes.

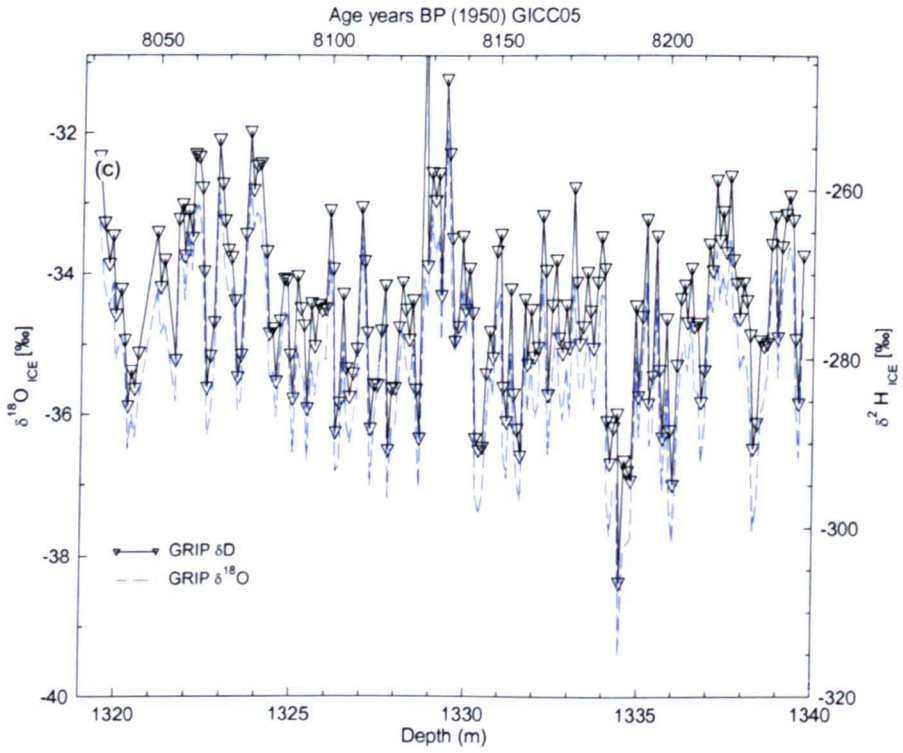

Figure 4.5 Oxygen and Deuterium isotopes from the GRIP core at 10 cm resolution.

Deuterium Excess

The deuterium excess can be calculated for the whole event using the 10 cm resolution oxygen and deuterium samples following the equation below.

$$d\ (‰) = \delta^{2}H - 8\ (\delta^{18}O) \qquad \textbf{[Equation 4.4]}$$

d is a measure of the relative proportions of ^{18}O and ^{2}H contained in water and can be visually depicted as an index of deviation from the global meteoric water line (MWL: d= 10) in $\delta^{18}O$ versus $\delta^{2}H$.

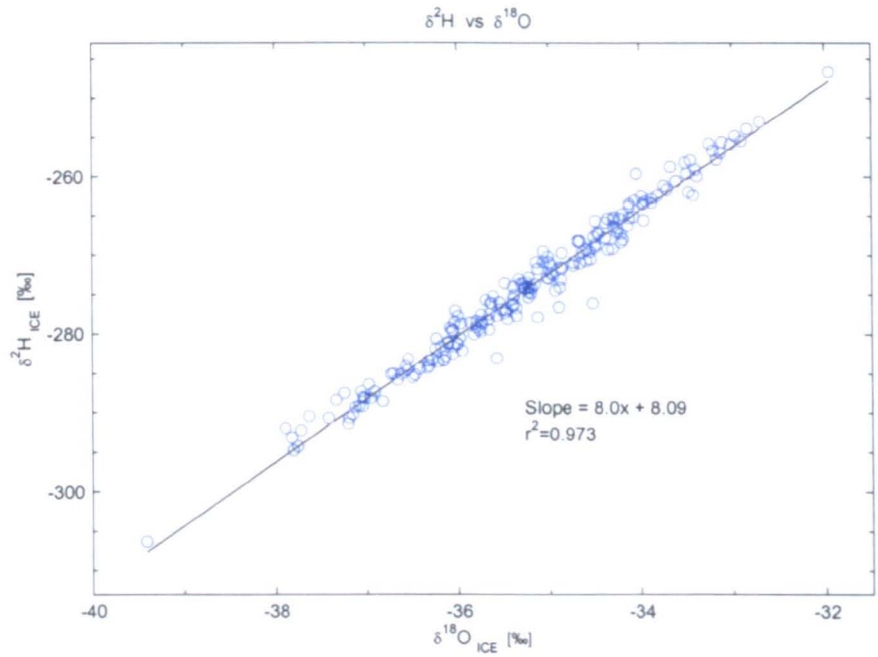

Figure 4.6 $\delta^{18}O$ versus $\delta^{2}H$ from the 20-meter section of GRIP ice core showing a slope of 8.0 and a correlation coefficient of 0.97.

The deuterium excess was calculated for a 20-meter section of GRIP ice at 10 cm resolution. The average deuterium excess over this section is shown in table 4.1, along with the average values from GISP2, which were measured at 1 cm resolution. The deuterium excess from GRIP during the most extreme negative values in the record increases by 0.44 ‰ compared to the average of all the ice analysed, this equates to an increase of 6 %. This increase is small, and within the standard deviation for this section of ice, however it could still be significant. In order to determine statistically whether there is an increase in the deuterium excess at this time a much larger data record would be needed. A background value from a long section of ice outside of the event would be needed to make a comparison; unfortunately this is not available at this time.

The absence of a large change in the deuterium excess puts some limits on possible composition or temperature of the source water, and also offers some constraints to model reconstructions of the isotopic composition of Greenland ice.

	Average Deuterium excess		
	GRIP 10 cm	GISP2 (smoothed to) 10 cm	GISP2 1 cm
All ice (1319 – 1340.12m)	**8.09**		
Standard Deviation	1.497		
1333.39 - 1335.38 m	**8.33**	**9.08**	**9.29**
Standard Deviation	1.366	0.923	1.57

Table 4.1 Average and standard deviation of deuterium excess from GRIP, for all ice analysed, and both GRIP and GISP2 during the central "spike" of negative values.

The deuterium excess for the GISP2 core was measured at Boulder at 1 cm resolution, for a 2-meter section within the central event, which has an average value of 9.29. The GISP2 data was smoothed to 10 cm resolution and compares well to the GRIP data as shown in figure 4.7. The values for d-excess in GISP2 appear higher than those in the GRIP core however that is due to the discrepancies in the isotope record in both cores at this period, where the GRIP core shows a negative 'spike', and is therefore to be expected.

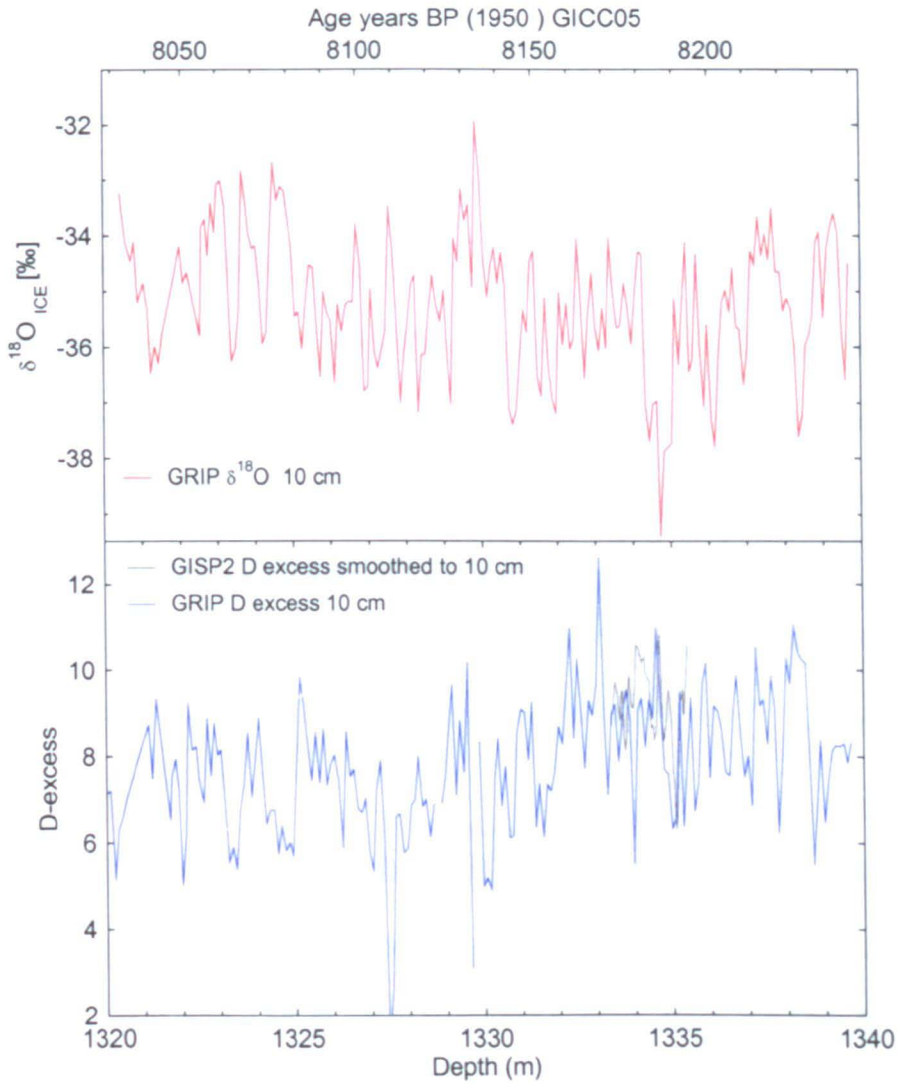

Figure 4.7 $\delta^{18}O$ from the GRIP core at 10 cm resolution (top red) and deuterium excess from the GRIP core at 10 cm resolution (bottom blue) and GISP2 (bottom grey) which has been smoothed to 10 cm resolution.

The water isotope records analysed for the GRIP and GISP2 cores will be used in the remainder of this thesis to define the 8.2 kyr event and compare with changes in the chemistry during this period.

4.3 Defining the Event

In order to determine the true rate of change and duration of this event the event itself must first be defined. Discrepancies in the dating between different palaeoclimate records and ice core records from different sites have made this difficult. The extent of the 8.2 kyr event has been discussed in recent papers [Rohling and Palike, 2005] and in chapter 3 of this thesis, indicating that the event has been reported globally in time scales ranging from a few decades to several centuries. In this thesis I do not attempt to define the 8.2 kyr event as observed globally, instead I will define the event as observed in Greenland only. I will do this by comparing the isotope records from the deep ice cores GRIP, GISP2, NGRIP and Dye 3 drilled in different locations across Greenland.

The different geographical locations and accumulation rates of the four deep ice core sites means that the depth-scales, between the four cores, differs greatly (as shown in figure 4.8). A uniform depth-scale is produced using ECM horizons to compare the oxygen isotope records of the four cores during the 8.2 kyr event.

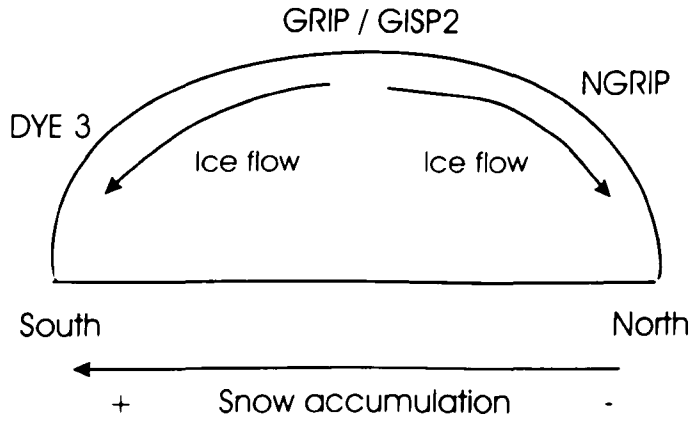

Figure 4.8 Cross section of Greenland ice sheet showing the increase in snow accumulation from south to north and the direction of the ice flow.

Matching the cores

The matching up the different isotope records has been done using the Electrical Conductivity Measurement (ECM) peaks, which represent discrete volcanic signals and therefore create a recognisable signature between the cores regardless of geographical location. For the period surrounding the 8.2 kyr event, distinctive peaks have been matched and are shown below.

The ECM record for both the GRIP and GISP2 cores has been matched in several places over a large period during the early Holocene between depths 1200 – 1400 meters in the GRIP core. Distinctive comparable ECM peaks were determined in figure 4.9 & 4.10 with the depths marked in the table below.

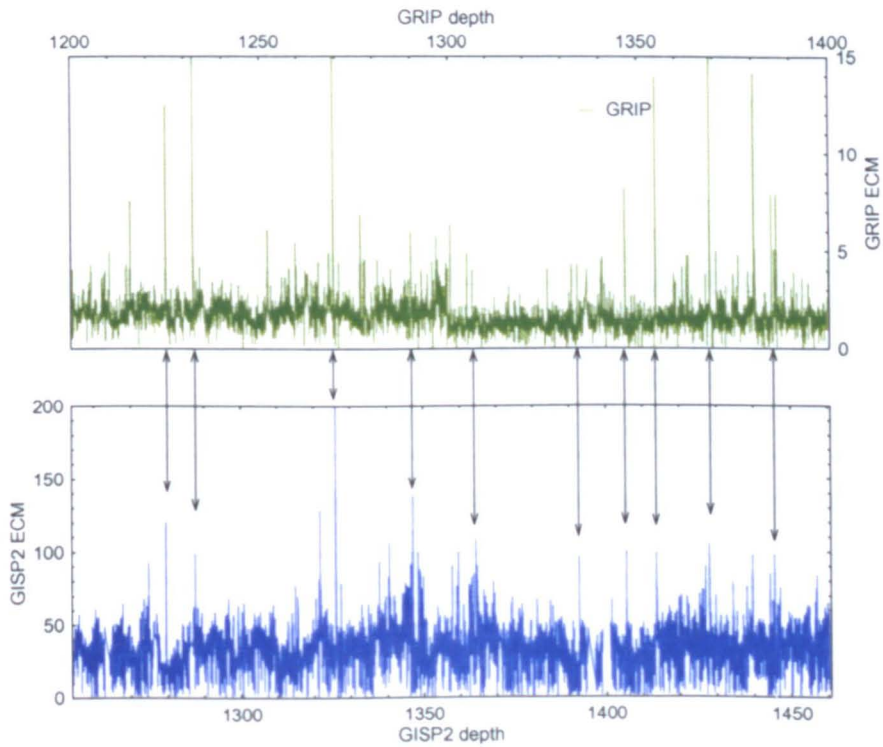

Figure 4.9 ECM match for GRIP (top green) and GISP2 (bottom blue) between GRIP depths 1200 – 1400 m.

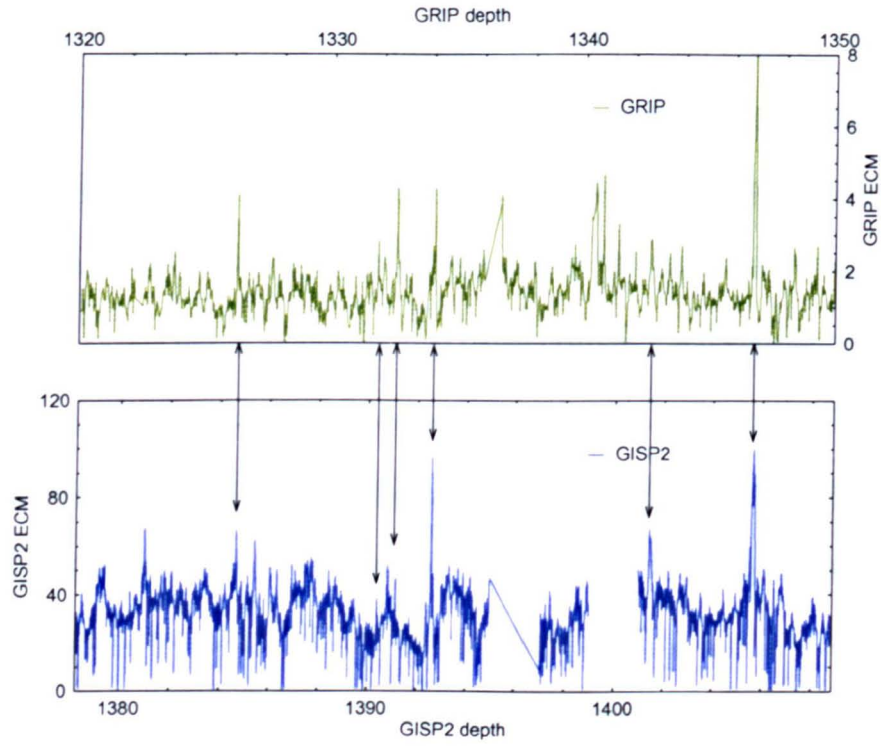

Figure 4.10 ECM match for GRIP (top green) and GISP2 (bottom blue) between GRIP depths 1320-1350

GRIP depth (m)	GISP2 depth (m)
1225	1279.58
1232.29	1287.66
1269.53	1325.89
1290.1	1347.16
1332.68	1391.13
1334.04	1392.66
1346.61	1405.64
1354.69	1413.66
1369.01	1428.2

Table 4.2 Comparative depths of distinctive ECM peaks in the GRIP and GISP2 cores

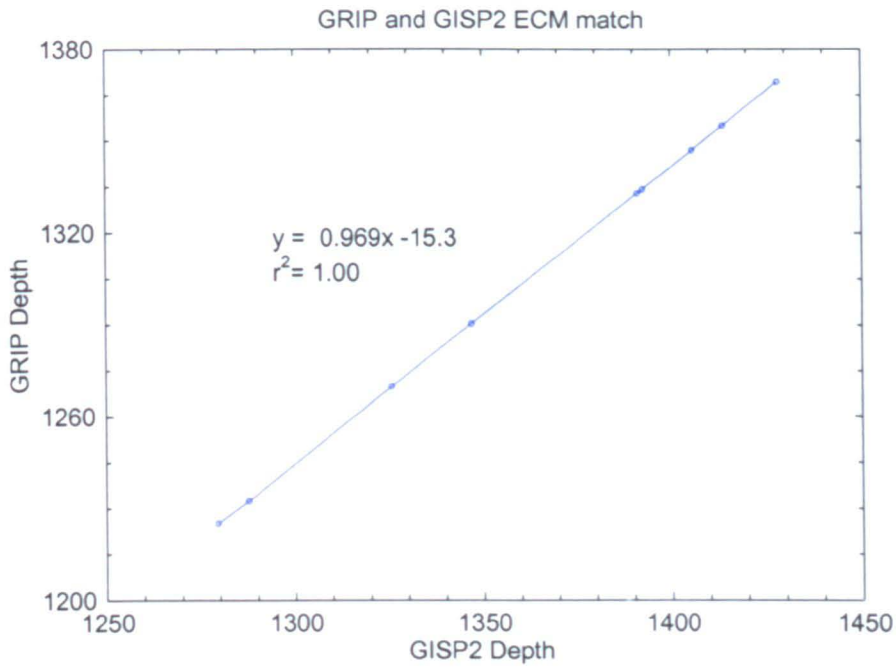

Figure 4.11 Correlation between GRIP and GISP2 depth scales based on comparative ECM tie points.

The excellent correlation between ECM tie points is shown in the graph with the R^2 value equal to 0.99. The slope of the graph is determined to be 1.032 x + 15.773. Equation 4.5 will be used to convert the GRIP depth scale to a GISP2 depth scale and equation 4.6 used to convert GISP2 to a GRIP scale, to enable comparison of isotopes and climate proxies from the two cores.

GRIP Depth (m) = 0.969 x GISP2 Depth (m) – 15.3 **[Equation 4.5]**

GISP2 Depth (m) = 1.032 x GRIP Depth (m) + 15.773 **[Equation 4.6]**

NGRIP Depth (m)	GRIP Depth (m)	DYE 3 Depth (m)
1223.16	1328.55	1689.03
1228.67	1334.04	1691.075
1235.14	1340.79	1693.622
1240.94	1346.68	1695.895
1248.51	1354.56	1698.941

Table 4.3 ECM reference depths for NGRIP, GRIP and Dye 3.

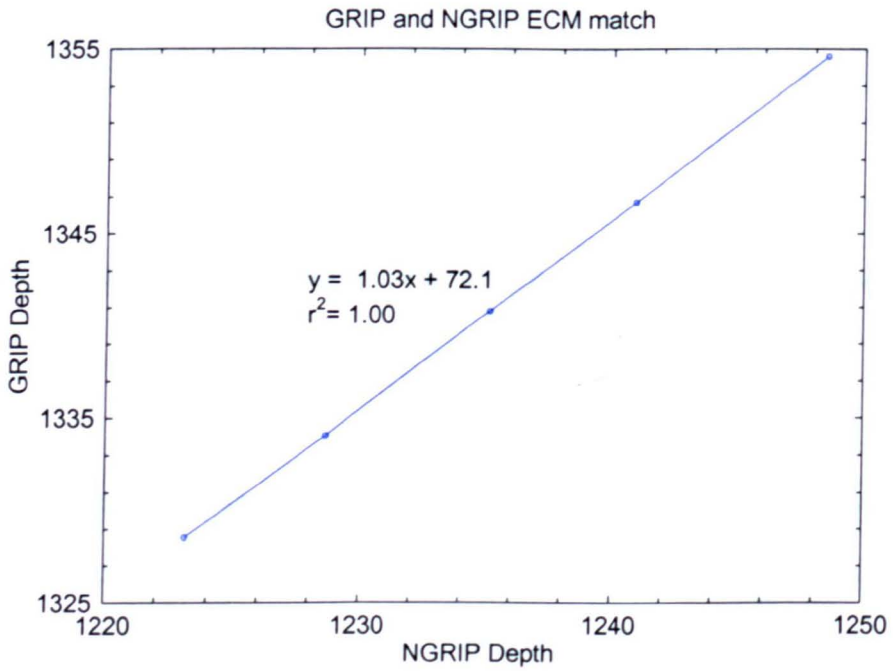

Figure 4.12 Correlation between GRIP and NGRIP depth scales based on comparative ECM tie points

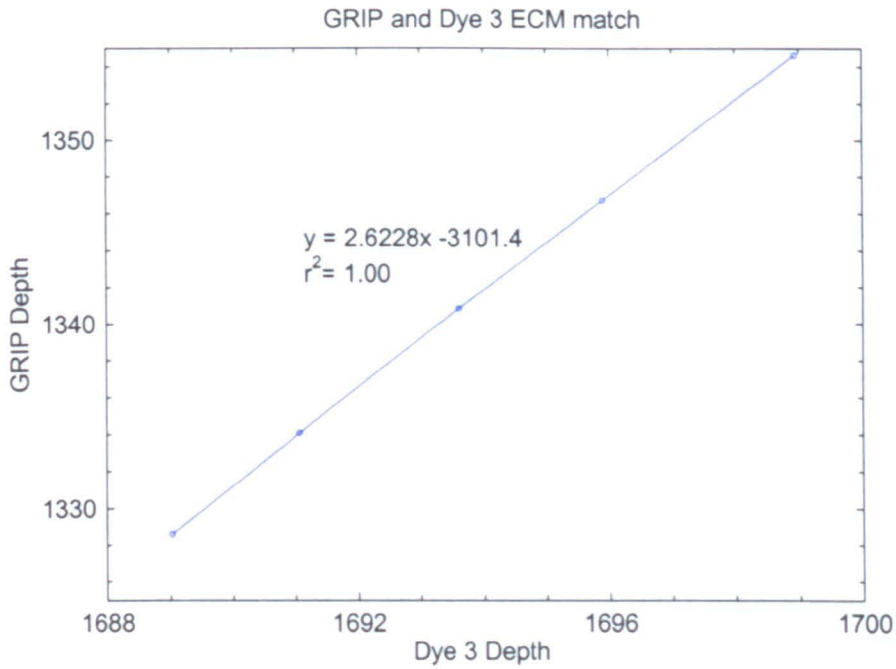

Figure 4.13 Correlation between GRIP and Dye 3 depth scales based on comparative ECM tie points

Figure 4.12 shows the correlation between GRIP and NGRIP and Figure 4.13 shows the correlation between GRIP and Dye 3 based on the ECM reference horizons for a 30 meter section of the GRIP core, as shown in table 4.3. Equations 4.5 and 4.6 are equated from the slope of the graphs and are used to convert DYE 3 and NGRIP depths to a common GRIP depth scale.

GRIP Depth (m) = 2.6228 x Dye 3 Depth (m) -3101.4 **[Equation 4.7]**

GRIP Depth (m) = 1.0272 x NGRIP Depth (m) + 72.081 **[Equation 4.8]**

In Figure 4.14, the oxygen isotope data from GRIP, NGRIP, GISP2 and Dye 3, smoothed to approximate 20-year resolution (using a sliding data window of the average Holocene annual layer thickness of each site), have been compared for the period between the Younger Dryas transition and the mid Holocene. The 8.2 kyr event is shown more clearly in figure 4.15 for the period between 7950 to 8325 years BP. The age scale used is GICC05 [Rasmussen et al., 2006; discussed in chapter 6]

In each case, the cores have been synchronised to the same GRIP depth scale using ECM spikes, with confidence that the depths are matched to within a few cm. In Fig 4.14, the event at 8.2 kyr BP is clearly seen as the extreme event of the Holocene in all 4 cores. The general shape and duration of the event is similar in all 4 cores, although there are substantial differences in detail at decadal and shorter timescales. This has been explored further in the previous section (see 4.1 Isotopes).

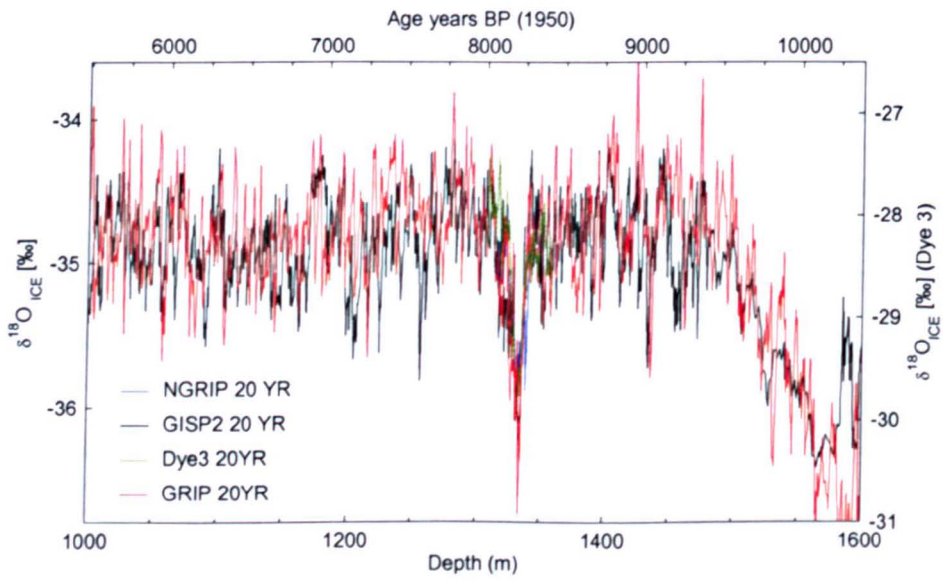

Figure 4.14 Oxygen isotope record from GRIP (red), GISP2 (black), Dye 3 (green) and NGRIP (blue) between GRIP depth 1000 – 1600 m. The data have been smoothed to depth intervals roughly equivalent to 20 years.

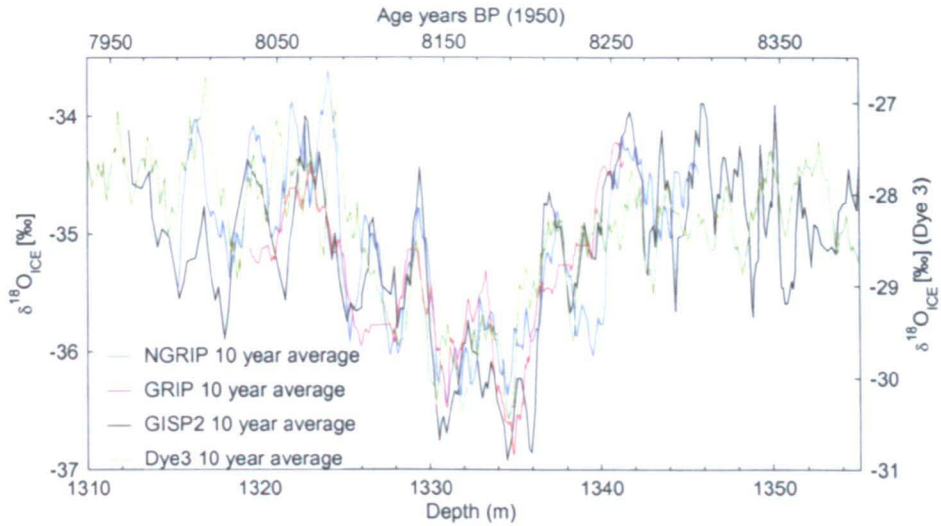

Figure 4.15 Oxygen isotope record from GRIP (red), GISP2 (black), Dye 3 (green) and NGRIP (blue) between GRIP depth 1310 -1355 m.

Method

The stable oxygen isotope records from four cores from Greenland were compared to determine the onset, termination and duration of the 8.2 kyr event. The oxygen isotope record exhibits a normal (Gaussian) distribution (figure 4.16) with approximately 68% of values within one standard deviation, 95% within two standard deviations and 99.7% within 3 standard deviations. Therefore, a statistical significance test was applied to all four records using the following method:

1. The point at which the oxygen isotope record is considered to be outside of the norm of values, is the point at which the oxygen isotope values in all cores consistently exceed one standard deviation from the isotope mean.

The records available to determine the event are summarized in table 4.4. The highest resolution data available in GRIP and GISP2 is not used because of the high inter-annual variability, which has been shown to give different isotopic signals at the two

sites on a sub-decadal scale. Thus the 27.5 cm resolution GRIP record and the 5 cm GISP2 records were used.

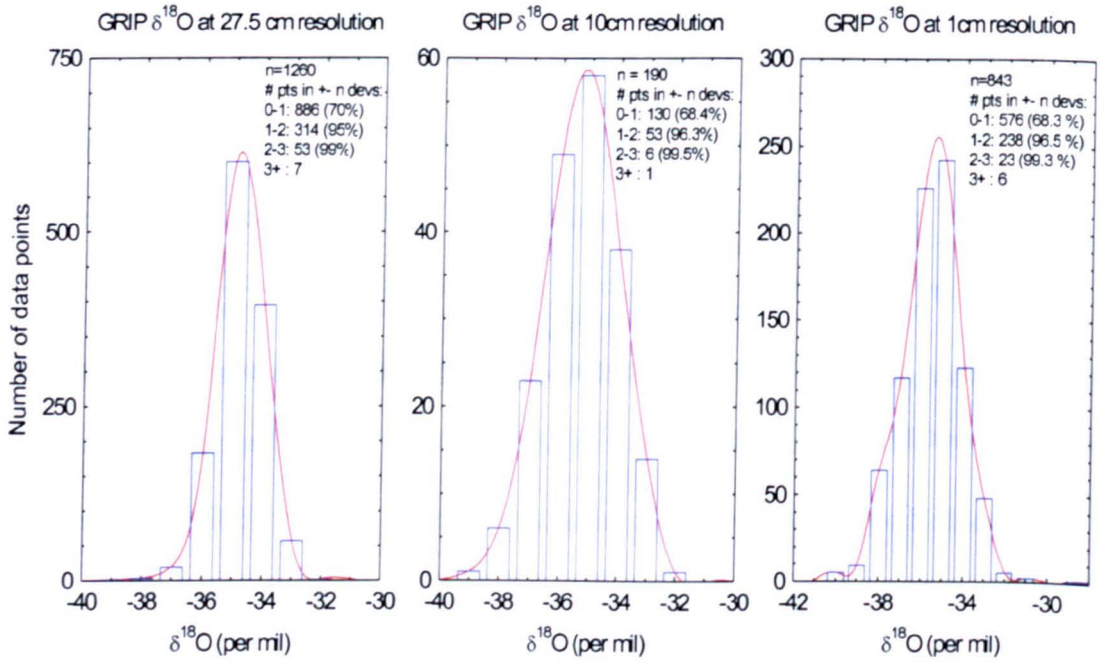

Figure 4.16 Distribution of the GRIP $\delta^{18}O$ (‰) record at 27.5cm (1000 to 1500 m), 10cm (1320 to 1340 m) and 1cm (1320 to 1340m) resolution.

Core	GRIP			GISP2		NGRIP	DYE 3
Resolution	27.5 cm	10 cm	1 cm	5 cm	1 cm	5 cm	5 cm
Reference	Johnsen et al., 1992	Thomas et al., 2006	Thomas et al., 2006	Alley et al., 1997	Thomas et al., 2006	NGRIP members 2004; Rasmussen et al., 2006	Vinther et al., in prep; Rasmussen et al., 2006
Annual layer thickness	11	11	11	10.5 cm	10.5 cm	10 cm	3.8 cm

Table 4.4 Available isotope data for the 8.2 kyr event.

Figure 4.17 shows the shape of the 8.2 kyr event as observed at the different sites in Greenland. The shape appears to correlate; however the length of the records and the site characteristics varies. Therefore, it is not possible to obtain an isotope average and standard deviation based on the same parameters for each site (see table 4.5). In

fact, the averages and standard deviations shown in figure 4.17 are calculated for each record between 1312.5m – 1355m, therefore including the event itself.

To overcome this, a composite record was produced whereby data from the event for each of the sites was averaged and compared statistically to a longer record. The previous best record from GRIP is the obvious choice because it has a resolution of 27.5 cm, which is approximately 2.5 years, spanning the whole of the Holocene.

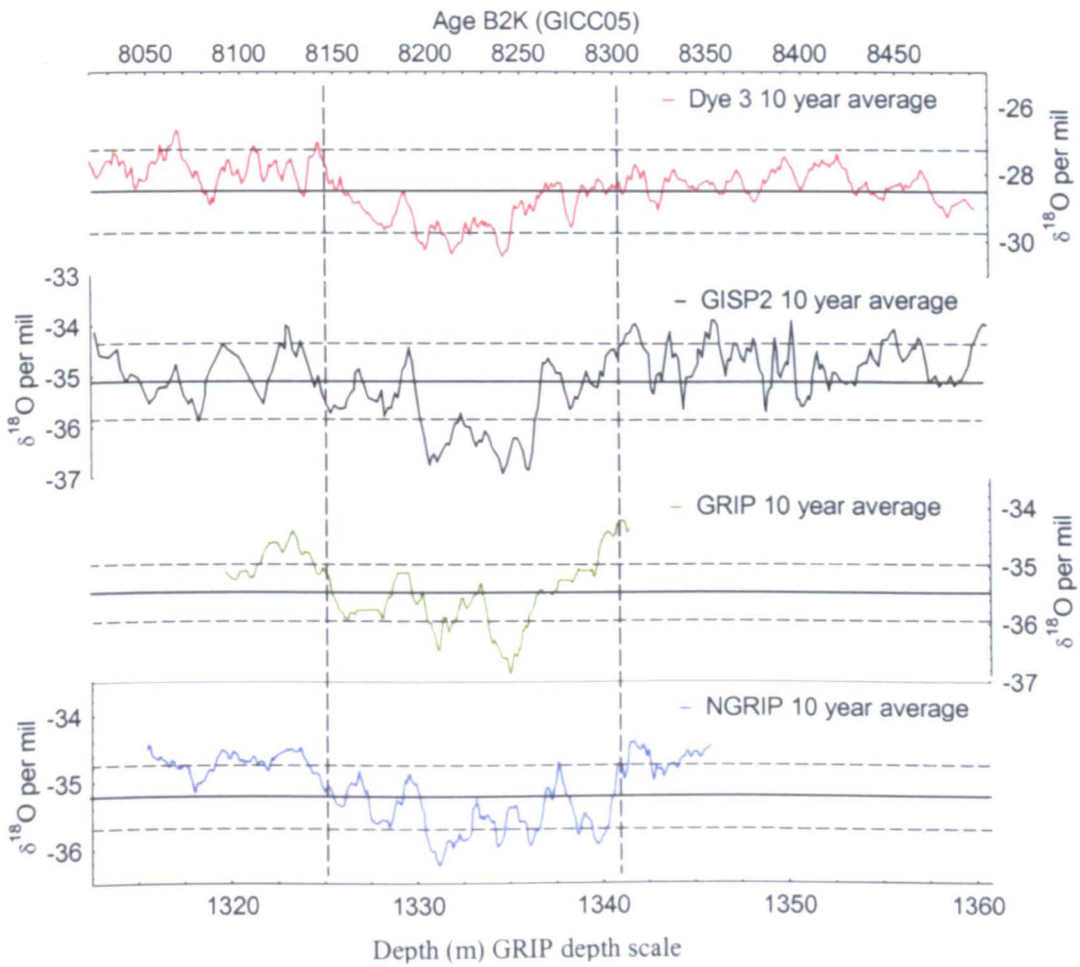

Figure 4.17 Individual oxygen isotope records from Dye 3 (red), GISP2 (black), GRIP (green) and NGRIP (blue) with the average (solid horizontal lines) and standard deviation (dashed horizontal lines) determined for each record between GRIP depth 1312.5 -1355 m (or the total length of record for GRIP and NGRIP). All data smoothed by a factor of 10 (running average), vertical dashed lines mark onset and termination of event as defined later in text.

Creating a normalized record

The data were first plotted on the GRIP depth scale, as described above and smoothed to 27.5 cm on the GRIP scale. Each data point had to be normalized to GRIP by first calculating the difference between the site data point, X_{SITE} and the site average, $Mean_{SITE}$. This value is divided by the standard deviation at that site, σ_{SITE}, to show how many standard deviations that data point is from the mean. The difference can then be multiplied by the Standard deviation at GRIP, σ_{GRIP}, and added to the mean at GRIP, $Mean_{GRIP}$, to give the normalized value of that data point.

$$\text{Normalized value} = + \frac{(X_{SITE} - Mean_{SITE})}{\sigma_{SITE}} * \sigma_{GRIP} + Mean_{GRIP} \qquad \textbf{[Equation 4.9]}$$

The new composite record is formed from the average of the new normalized data points from each site. The record is shown by the grey curve in figure 4.18 and then a decadal smoothing (red curve) was applied to better see the onset and termination.

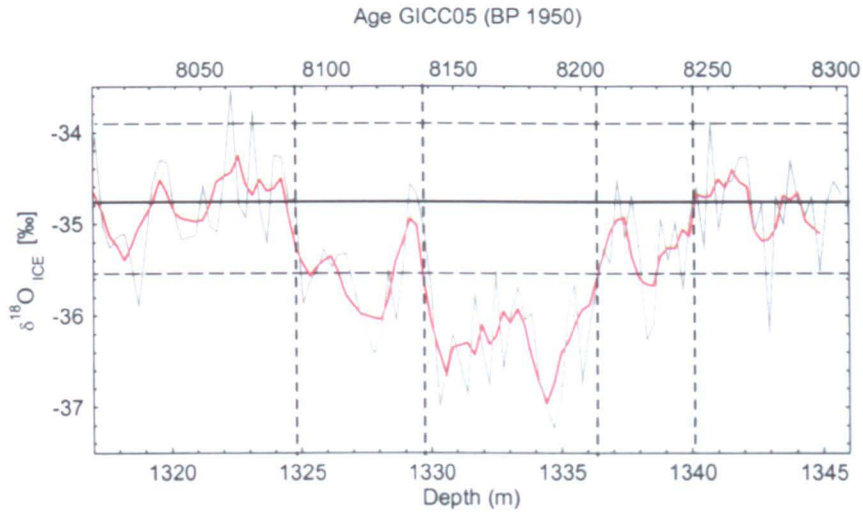

Figure 4.18 Composite of the oxygen isotope record (calculated from all sites and normalized to GRIP) at 27.5 cm resolution (grey) and decadal smoothing (red). Horizontal lines indicate the 27.5 cm composite average (solid line) and 1σ above and below it (dashed lines) from the previous 1000 years (9300 – 8300, based on the GICC05 age-scale [Rasmussen et al., 2006]). Vertical lines indicate the onset and termination of the whole and central event as defined later in the text.

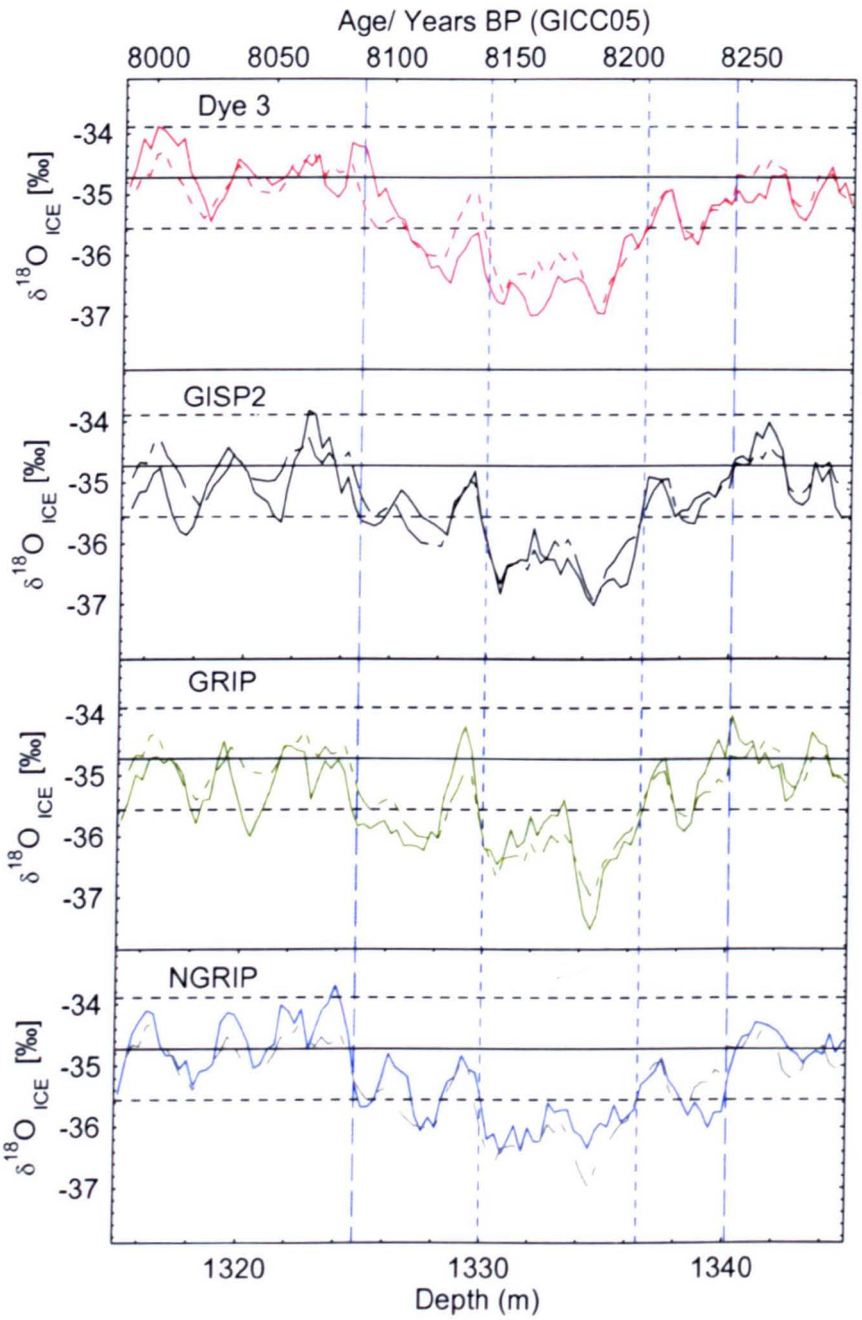

Figure 4.19 Normalized decadal records from NGRIP, GRIP, GISP2 and Dye 3 compared to the composite record (dashed curves). Horizontal lines indicate the 27.5 cm composite average (solid line) and 1σ above and below (dashed lines) calculated from the period between 9300-8300 years BP (based on GICC05 [Rasmussen et al., 2006]). Vertical dashed blue lines indicate the onset and termination of the whole and the central event.

Core Site	Record Mean	Record Standard deviation
GRIP	-35.12	0.96
GISP2	-35.07	0.94
NGRIP	-35.11	0.97
DYE 3	-28.42	0.85
Average (except Dye 3)	-35.10	0.93
Composite record	**-34.72**	**0.83**

Table 4.5 Comparison of the individual mean and standard deviations from each site between 1312.5m-1355m, compared with the mean and standard deviation from the composite value, calculated between 1345.8 – 1432.125m (9300 – 8300 years BP).

The average $\delta^{18}O$ and the standard deviation obtained from the individual records have been compared with the values calculated from the composite record. Both methods provide similar values for the average isotope value during this section, providing Dye 3 is not used (this is due to the warmer temperatures at the more southern site resulting in less negative $\delta^{18}O$ values). When plotted graphically the composite curve replicates the normalized records at each site, indicating that the composite is robust enough to represent all sites in Greenland.

In order to determine the significance of the negative deviation in $\delta^{18}O$ during the 8.2 kyr event, a much larger record is required to test against. The advantage of the composite record is that the mean and standard deviation from GRIP can be extended for the 1,000 years surrounding the event and is relevant because this is what all the sites records have been normalized to.

Calculating the onset and termination depths

The isotope average was determined from the GRIP record, between 8300 – 9300 kyr BP (1345.8 – 1432.15 m), to be –34.72 ± 0.83. This value was used to determine the onset and termination of the event. The decadally averaged $\delta^{18}O$ values remain greater than one standard deviation lower than the mean for a total of 6.49 meters (GRIP depth). This is to be termed the "Central event" which begins at 1336.45 m and terminates at 1329.96 m.

When looking at the $\delta^{18}O$ record it is obvious that although the 6.49 meters of the "central event" is obviously significant, the values surrounding this are below the norm too. The values drop below the average at a depth of 1340.12 m and do not return to normal until 1324.77 m. The "central event" appears within this section but the greater background appears to represent a longer climate event.

Therefore the 15.35 m section of consistently lower than average values is to be termed the "Whole event" which begins at 1340.12 m and ends at 1324.77 m. The estimated ages at which the whole and the central event began and ended are given in table 4.6, based on the new GICC05 age scale [Rasmussen et al., 2006]. A new duration will be determined from the annual layer counting of chemical species in later chapters of this thesis.

Event	Depth (GRIP m)	Age (GICC05 yrs BP)	Age (GICC05 yrs b2k*)
Start	1340.12	8246	8296
Start central event	1336.45	8211	8261
End central event	1329.96	8141	8191
End	1324.77	8087	8137
Duration of central event	70 years		
Duration of whole event	159 years		

Table 4.6 Onset and termination depths for the Whole and the Central event and the ages in years according to the GICC05 age scale [Rasmussen et al., 2006]. *b2k means before 2000 AD.

4.4 Summary of isotopes during the 8.2 kyr event

The 8.2 kyr event is observed as a period of negative anomalies in isotope values, comparable on the decadal scale in the records from four deep ice cores (GRIP, GISP2, NGRIP and Dye 3) drilled across Greenland. Analysis of GRIP and GISP2, drilled 30 km apart, revealed differences at higher resolution, with a sharp spike observed during the event at GRIP but not GISP2.

A composite isotope record was produced from the four Greenland ice cores to define the 8.2 kyr event. The whole event was determined as the period in which isotope values were consistently below the Holocene average, with a central period defined in which decadal-average isotope values fell consistently greater than one standard deviation below the average.

Defining the 8.2 kyr event and determining its duration is important for future research, especially to set the parameters for model experiments. Rohling and Palike 2005 collated a large amount of paleoclimate proxy data published about the 8.2 kyr event, which showed climatic anomalies from across the globe with durations ranging from a few decades to several hundred years. As described in the introduction chapter, a wide range of evidence exists to suggest that the 8.2 kyr event was a worldwide anomaly with records from as far a field as Tasmania (speleothem record from Lynds cave [Xia et al., 2001]) and the southern pacific (Corals from Alor, Indionesia, [Gagan et al., 2002]). The further from the North Atlantic, the proposed source of the anomaly, the records become weaker in amplitude and longer in duration. It is evident that a wider climatic regime change was occurring at about this time but the fact that the Greenland records and other proxy records from across northern Europe show a distinct, short and sharp signals within this background shift gives weight to the theory that two distinct events were happening at the same time.

It is therefore important to separate the two and name them accordingly, in order to avoid confusion and potential "wiggle matching" with other paleoclimate proxies, further confusing the literature.

Chapter five

The 8.2 kyr event: Chemistry

5.1 Chemistry Introduction

Airborne particles and chemical compounds of marine, continental, biological, atmospheric, extraterrestrial and volcanic origin can be transported large distances before being removed by clouds, precipitation and dry deposition to ice sheets. Analysis of chemical compounds related to primary continental and marine aerosols found in ice cores can therefore be considered tracers of atmospheric content [de Angelis et al., 1997; Barrie et al., 1995].

Ice sheets are remote from local soil sources and therefore wind blown dust found at Summit can be assumed to be from distant sources [Barrie et al 1996]. The high altitude of Summit (3150 m a.b.s.l) suggests the site is more influenced by the upper troposphere and stratosphere as sources of chemical constituents than low altitude coastal sites with lower troposphere air masses tending to be deflected by coastal topographic barriers [Putnins., 1970]. The close proximity of North America and Eurasia however, impacts the aerosol composition and concentration to the ice cap with such events as dust storms and forest fires.

Atmospheric loading is reflected by the chemical composition in Summit ice [O'Brien et al., 1995]. The marine input (determined from Na and Cl concentrations) represents vigour of atmospheric circulation and location from oceanic sources while the continental component (inferred by the concentrations of Ca) is indicative of long range atmospheric loading and dustiness [Biscaye et al., 1997; Svensson et al., 2000].

Marine Input

Geochemical analysis of the GISP2 core showed that 99% of Na^+ is of sea salt origin during the Holocene [O'Brien 1997] making it a good conservative tracer for sea-salt aerosol. The marine aerosol at source areas is mainly made up of marine spray with a composition close to that of seawater. The marine aerosols to reach Summit are chloride depleted and sulphate enriched with respect to seawater composition due to sea salt reactions with SO_2 and H_2SO_4 [Legrand and Delmas, 1988]. Therefore, sodium has been used as the primary tracer of sea salt activity.

Sea salt ions were previously thought to have been from the open ocean, reaching the ice caps via atmospheric loading from bubble bursting. More recent studies have shown that a more plausible source of the marine ions, from Antarctic ice cores, is from the sea ice itself [Rankin et al., 2002] as observed in the ice core record with greater concentrations of sodium during the glacial period; however the situation in Greenland remains unclear. The sea salt ions are primarily sodium and chloride but also potassium and magnesium. Alley et al (1997) reported a combined increase in marine aerosols during the 8.2 kyr event, with both sodium and chloride, primarily from sea salt, increasing by 60% from baseline values[8].

MSA is an atmospheric oxidation product of dimethyl sulphide (DMS) and is used in ice core studies as an indicator of biological activity. It is observed in the ice core record as a peak in the spring when the sea ice retreats allowing algal bloom. It has therefore been used as a proxy for sea ice extent (SIE) with an increased sea ice cover observed in the ice core record as an increase in MSA the following spring. The mechanism by which MSA reaches a glacier is complex; dependent on among others,

primary production, plankton species, conditions at source and conditions at the glacier. Therefore the relationship between MSA and SIE is hard to constrain.

In Antarctica, a positive correlation between SIE and MSA was observed from a core near the Ross Sea [Welch et al., 1993] however a negative correlation was observed on the Antarctic Peninsula [Pasteur et al., 2000]. In the Arctic a positive correlation with North Atlantic SSTs is observed in a south Greenland ice core [Whung et al., 1994] and at the GRIP site a negative correlation between MSA and SIE has been found [Legrand et al., 1997]. Ice cores from Svalbard, have shown an increase in MSA with increasing SSTs and reduced SIE in the Barents Sea; a greater correlation is observed if a 3 year delay is used for the SSTs [O'Dwyer et al., 2000]. Migration of MSA in the firn layer introduces some difficulty for its use and it should be used with caution.

Continental Input

Comparison of clay mineralogy and Sr, Nd and Pb isotopic composition of dust in ice at Summit determined the probable source of terrestrial dust to be Asian [Biscaye et al 1997, Svensson et al 2000]. Calcium is a valid indicator of continental input providing its marine component has been removed. Calcium from continental dust gives a signal of dust availability, dryness and transport vigour. The calcium concentration found in GISP2 was reported to have increased by 60% from baseline values[8] during the 8.2 kyr event [Alley et al., 1997] indicating increased dustiness and dryness in Asian sources and an increase in wind speed during this period.

[8] Baseline values defined by values near 8.0 and 8.4ka in 50 year average data from the GISP2 core [Alley 1997]

If the continental component of Na^+ is neglected, assuming Na^+ is completely of marine origin, [O'Brien et al 1995] the continental input of calcium (Ca_t) can be calculated from the total Calcium by subtracting the marine input, Ca_m using standard seawater compositions [DeAngelis, et al 1997, Handbook of marine science (table 2.4-3 p.80)].

$$Ca_t = Ca^{2+} - (0.038 * Na^+)_{seawater} \quad \textbf{[Equation 5.1]}$$

Mg^{++} has a continental component (Mg_t) of 65% [O'Brien et al., 1995] during the Holocene and has been used as a secondary tracer for atmospheric loading.

$$Mg_t = Mg^{2+} - (0.12 * Na^+)_{seawater} \quad \textbf{[Equation 5.2]}$$

Volcanic Input

Unlike the continentally isolated Antarctic ice cores, local eruptions are revealed in Greenland and not just the large equatorial eruptions. These equatorial eruptions have to be large enough to propel debris and gases into the stratosphere and from there it is transported to the poles and deposited on the ice sheets via precipitation. It is these large eruptions that act as tie points linking ice cores from both hemispheres such as the Tambora eruption of 1815 which is clearly seen in both Antarctic and Greenland cores [Langway et al., 1995].

The geographical location of Greenland close to active volcanism in the 50-60°N latitudinal band, with neighbouring source locations such as Iceland, means Greenland ice cores record large numbers of volcanic eruptions. The eruptions show up in the ice core record as peaks in the ECM record, which indicate increased acidity, as a result of sulphur compounds emitted from explosive volcanoes. Visually

too, eruptions may be seen in the ice core as orange or brown ash layers, where volcanic debris has been deposited on the ice sheet.

5.2 Chemistry Results

Over two thousand discrete samples were taken from the GRIP core at a depth of 1320 – 1339.8 meters to investigate the 8.2 kyr event. The samples were cut as described in the method section and analysed using ion chromatography. A total of nine ions were analysed from the GRIP core at 1 cm resolution.

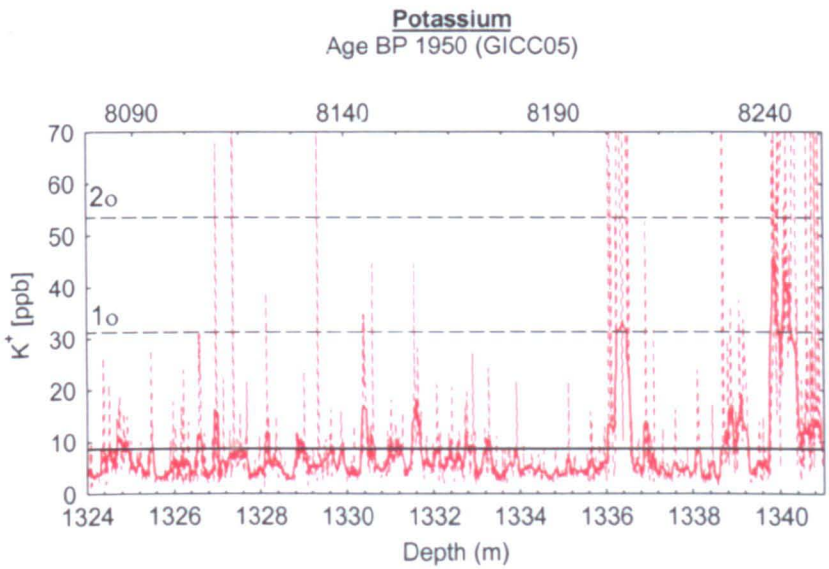

Figure 5.1 Potassium from GRIP at 1 cm resolution (dashed) and annual average (solid), showing the average for all samples (solid horizontal line) and the standard deviation indicated by σ (dashed horizontal lines).

The 1 cm resolution data and the annual average (using a sliding data window and an average annual layer thickness of 9.8 cm, see chapter 6) from each ion have been plotted in figures 5.1 to 5.9, on the GRIP depth scale and the new GICC05 age-scale [Rasmussen et al., 2006]. The average concentration of all samples has been shown (horizontal solid line on the graphs) along with the level of one and two standard

deviations above this (horizontal dashed lines on the graphs). A combination of eight ions has been plotted in Figure 5.10 to compare the changes in different species during the 8.2 kyr event.

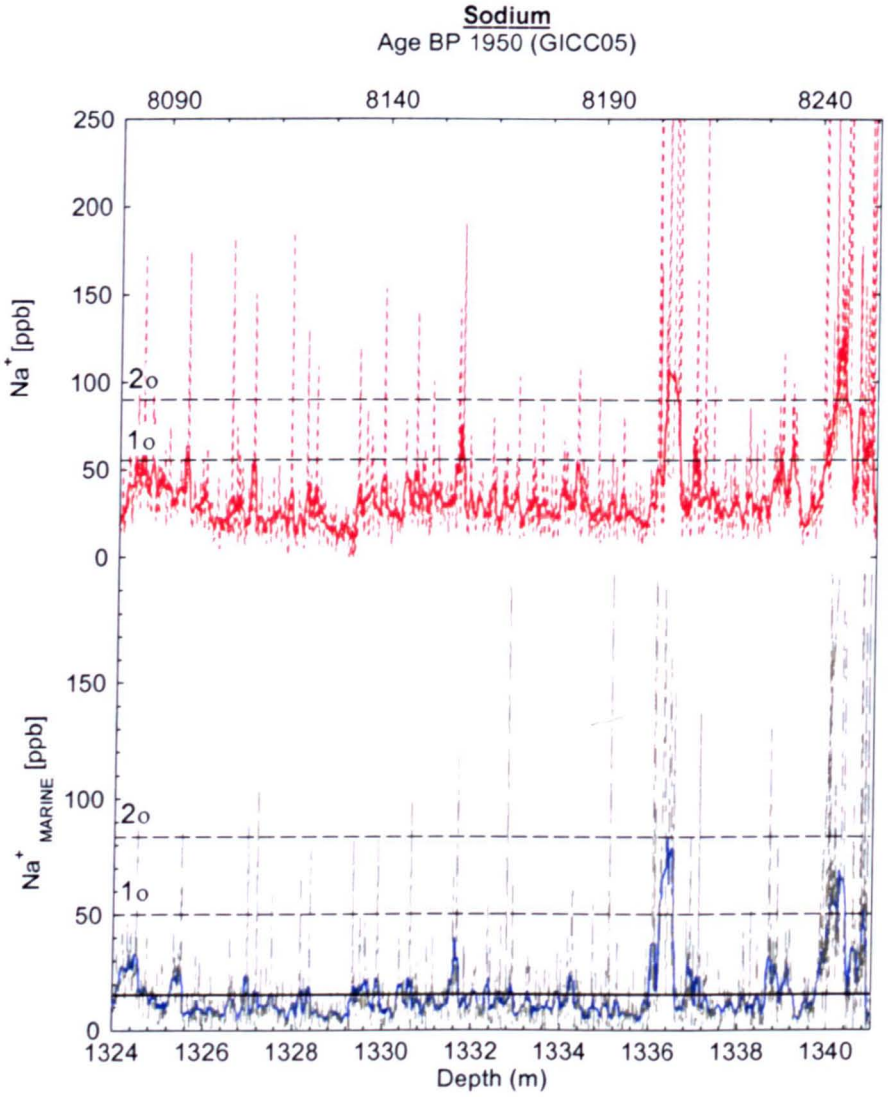

Figure 5.2 Sodium (top) and marine sodium (bottom) from GRIP at 1 cm resolution (dashed) and annual average (solid), showing the average for all samples (solid horizontal line) and the standard deviation indicated by σ (dashed horizontal lines).

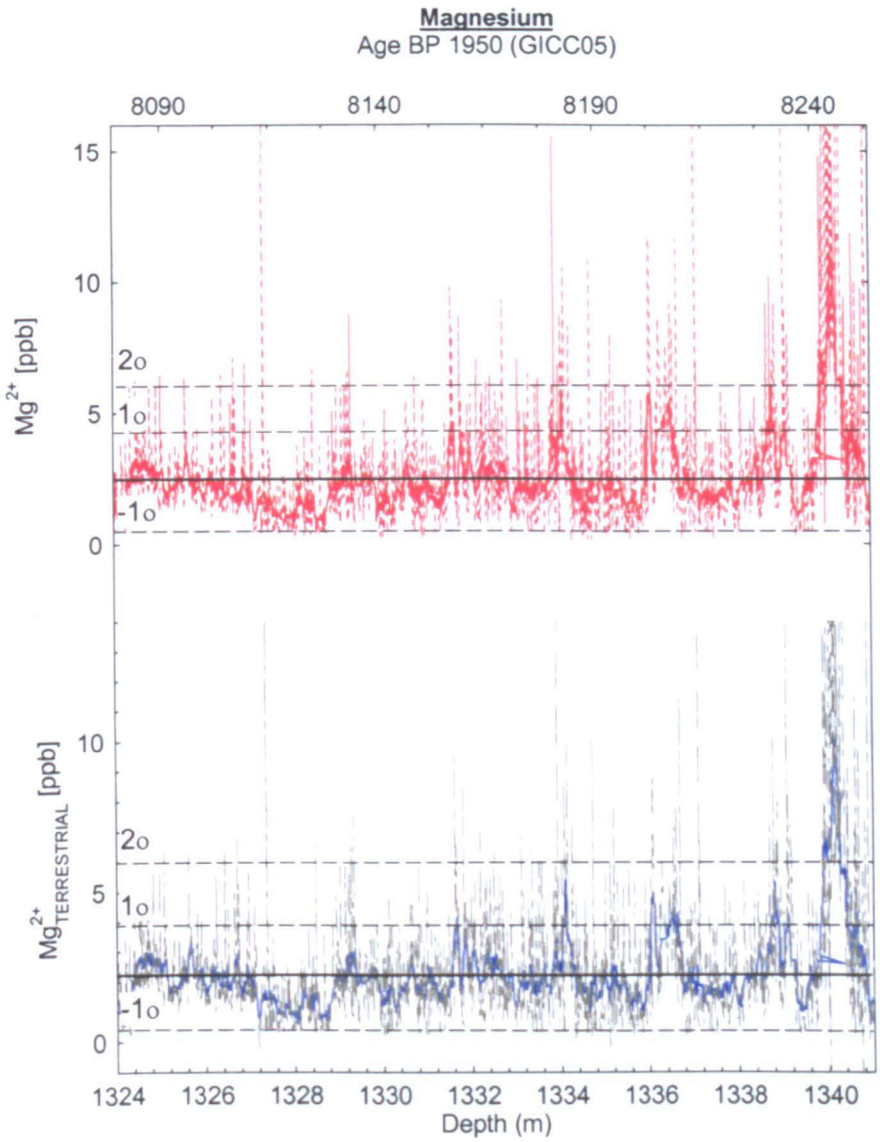

Figure 5.3 Magnesium (top) and Terrestrial Magnesium (bottom) from GRIP at 1 cm resolution (dashed) and annual average (solid), showing the average for all samples (solid horizontal line) and the standard deviation indicated by σ (dashed horizontal lines).

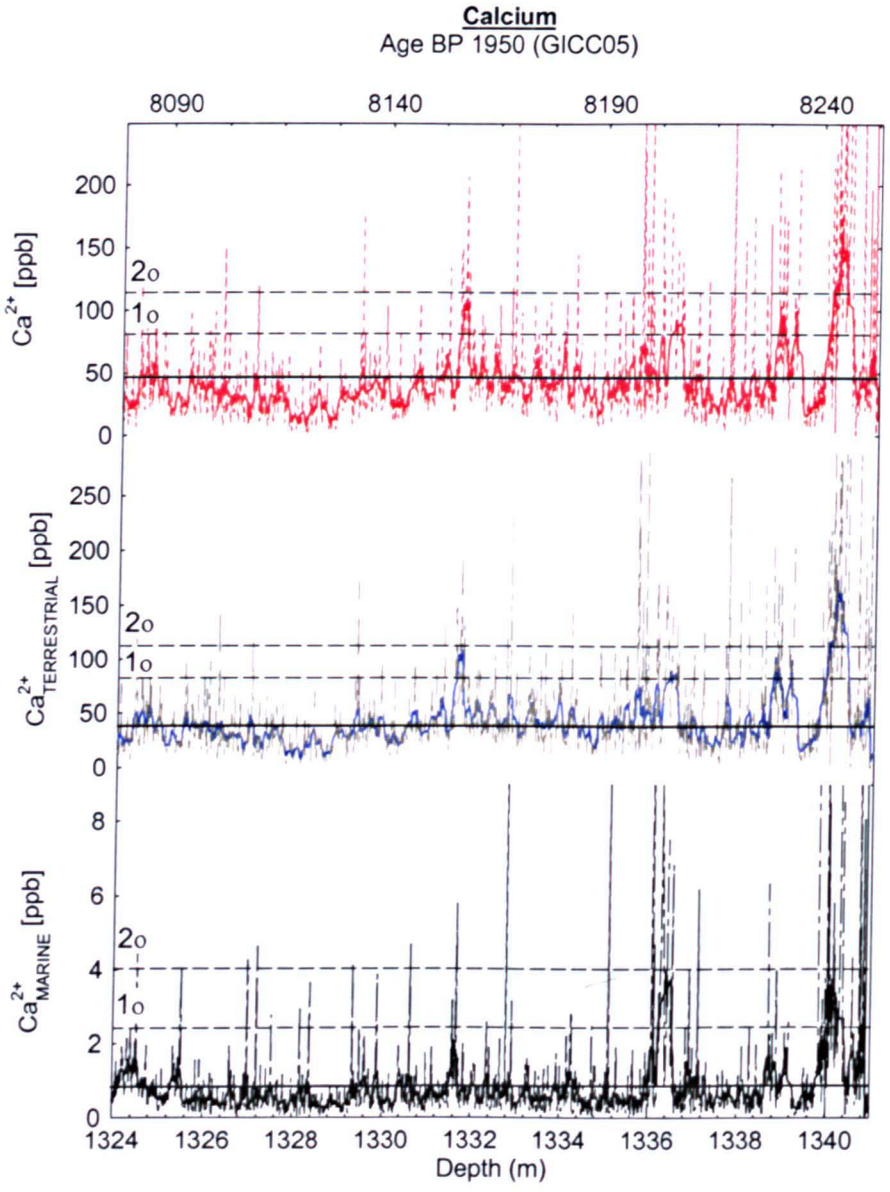

Figure 5.4 Calcium (top), Terrestrial Calcium (middle) and Marine Calcium (bottom) from GRIP at 1 cm resolution (dashed) and annual average (solid), showing the average for all samples (solid horizontal line) and the standard deviation indicated by σ (dashed horizontal lines).

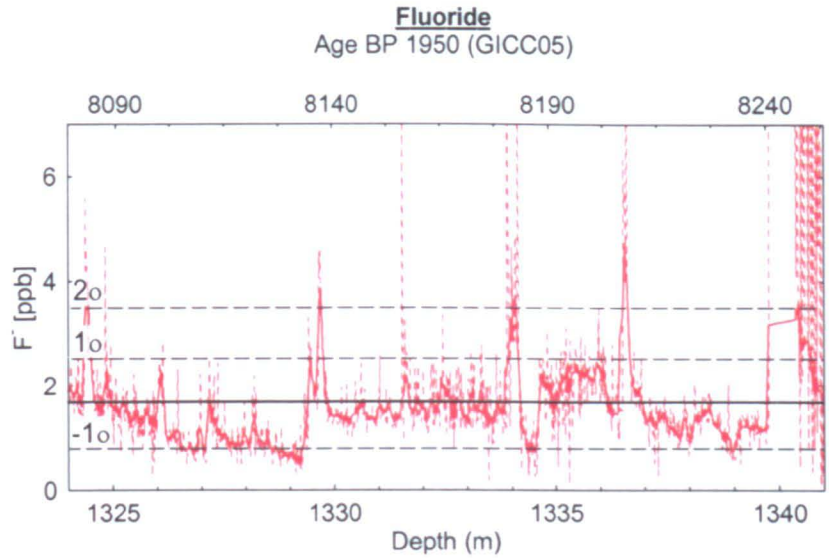

Figure 5.5 Fluoride from GRIP at 1 cm resolution (dashed) and annual average (solid), showing the average for all samples (solid horizontal line) and the standard deviation indicated by σ (dashed horizontal lines).

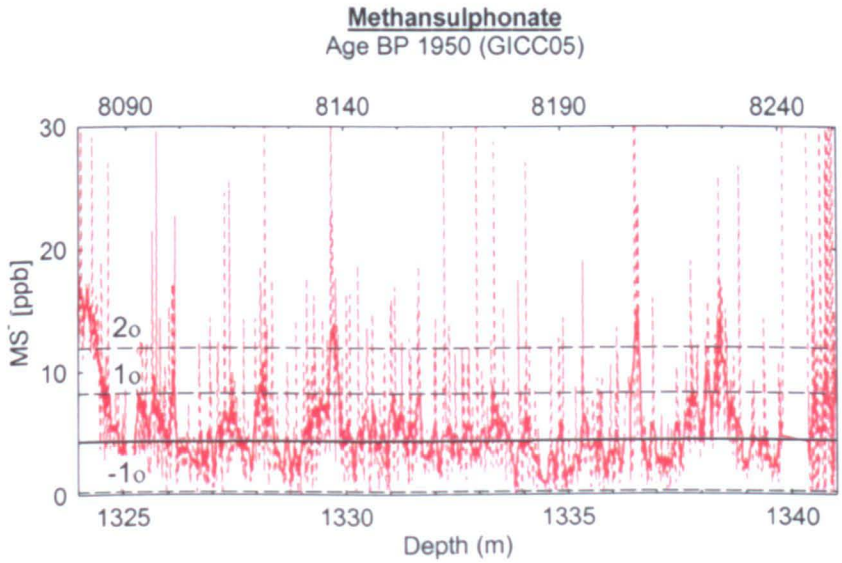

Figure 5.6 Methansulphonate from GRIP at 1 cm resolution (dashed) and annual average (solid), showing the average for all samples (solid horizontal line) and the standard deviation indicated by σ (dashed horizontal lines).

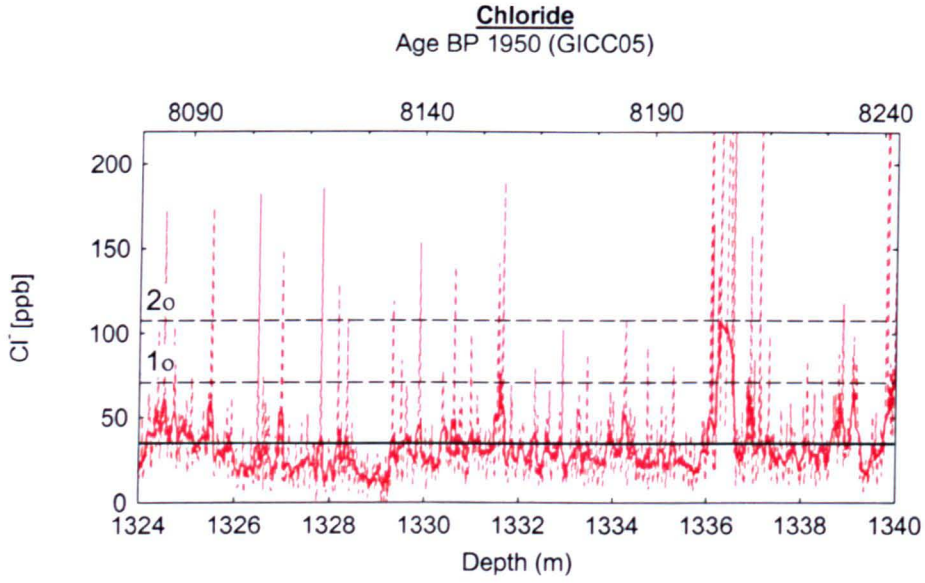

Figure 5.7 Chloride from GRIP at 1 cm resolution (dashed) and annual average (solid), showing the average for all samples (solid horizontal line) and the standard deviation indicated by σ (dashed horizontal lines).

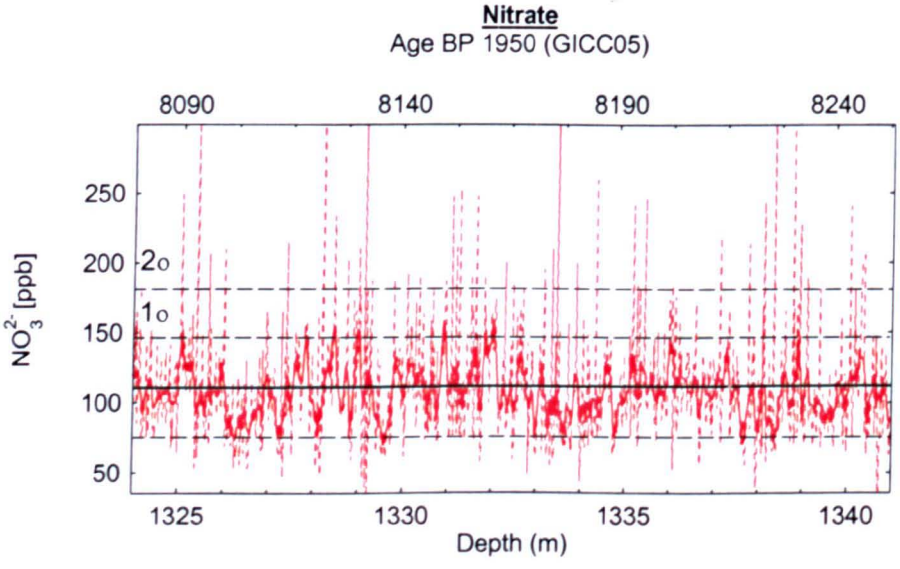

Figure 5.8 Nitrate from GRIP at 1 cm resolution (dashed) and annual average (solid), showing the average for all samples (solid horizontal line) and the standard deviation indicated by σ (dashed horizontal lines).

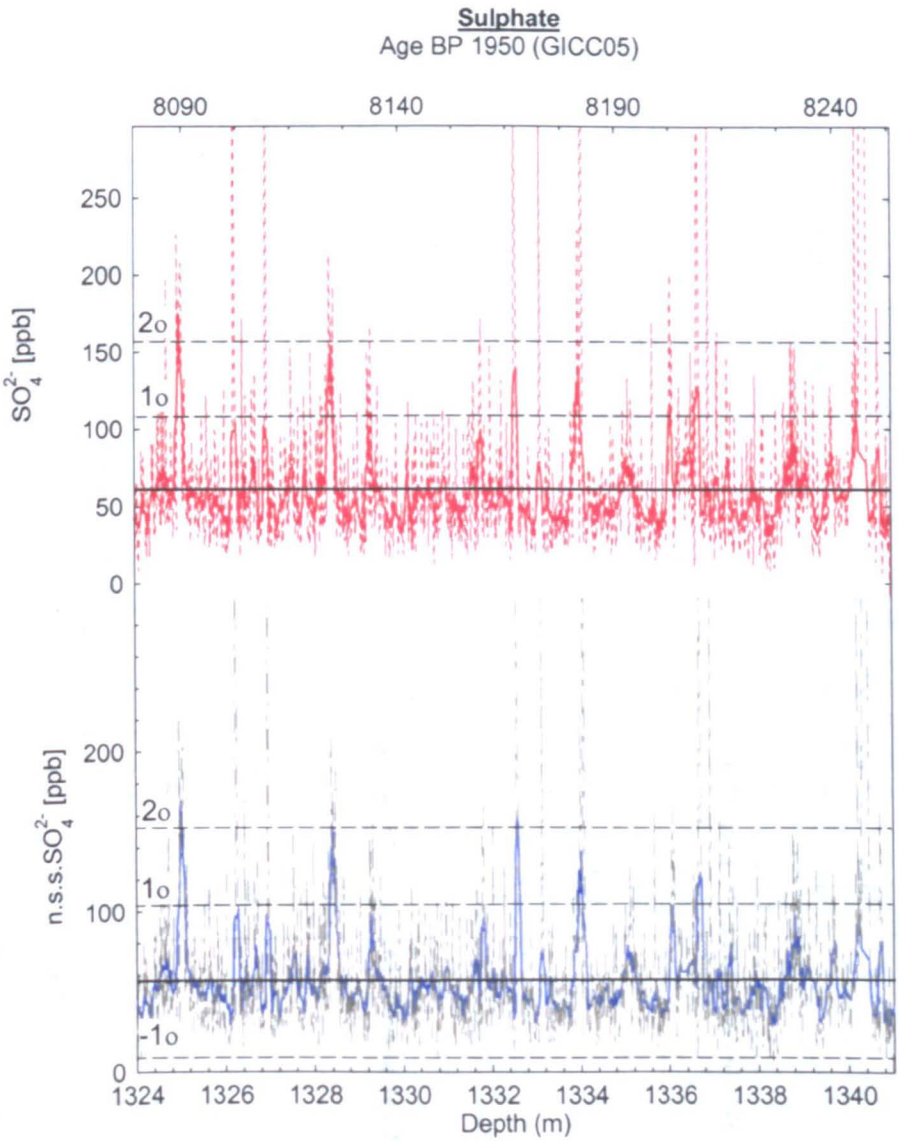

Figure 5.9 Sulphate (top) and non-sea salt sulphate (bottom) from GRIP at 1 cm resolution (dashed) and annual average (solid), showing the average for all samples (solid horizontal line) and the standard deviation indicated by σ (dashed horizontal lines).

The 8.2 kyr event has been defined in the previous chapter (chapter 4.2 – Defining the event). The average concentration and standard deviation for each ion has been calculated for all data (1319.47 – 1341.44m), the whole event (1324.77 – 1340.12m) and the central event (1329.96 – 1336.45m). This is shown in table 5.1.

Concentration (ppb)														
	Na^+	Na^+_{marine}	K^+	Mg^{2+}	$Mg^{2+}{}_t$	Ca^{2+}	Ca^{2+}_{marine}	$Ca^{2+}{}_t$	F^-	MS^-	Cl^-	NO_3^{2-}	SO_4^{2-}	n.s.s. SO_4^{2-}
All samples 1319.47 - 1341.44 m														
Average	26.4	23.6	10.8	2.5	2.2	40.7	1.2	39.6	2.4	9.4	43.2	106.4	63.6	59.2
Standard Deviation	54.9	54.0	40.9	2.6	2.4	38.3	2.4	37.4	4.5	30.4	82.7	36.0	54.4	52.9
Average with outliers removed	15.0	13.2	7.2	2.1	1.9	36.6	0.7	35.8	1.5	4.1	30.7	104.1	55.0	51.5
Standard Deviation	11.9	12.0	7.0	1.3	1.2	21.6	0.6	21.4	0.6	2.8	11.2	26.5	28.4	27.6
Whole event 1324.77 - 1240.12 m														
Average	17.8	15.0	8.6	2.4	2.2	41.3	0.8	40.5	1.9	6.1	33.5	108.4	62.1	58.7
Standard Deviation	32.9	31.9	17.8	2.2	2.0	34.4	1.4	33.8	2.7	9.1	33.7	36.8	52.4	51.6
Average with outliers removed	16.9	14.1	7.5	2.4	2.2	40.6	0.7	44.6	1.9	6.2	31.7	108.0	61.6	58.4
Standard Deviation	31.3	30.5	11.1	2.1	2.0	33.8	1.4	32.7	2.7	9.2	27.2	36.8	52.6	52.0
% Difference from total ice	-32.5	-36.6	-20.0	-3.7	0.8	1.3	-32.5	2.3	-20.8	-34.9	-22.5	1.8	-2.4	-0.9
% Difference from total ice (With outliers removed)	18.5	13.7	20.3	16.3	16.5	12.7	11.1	13.2	29.7	49.6	9.0	4.1	13.0	13.9
Central event 1329.96 - 1336.45 m														
Average	18.4	15.2	8.8	2.4	2.2	46.6	0.8	45.8	1.7	4.3	34.3	110.8	60.3	56.7
Standard Deviation	35.5	34.4	22.2	1.9	1.8	34.4	1.6	33.7	0.9	4.1	36.5	34.8	48.3	47.4
Average with outliers removed	15.0	12.4	6.4	2.2	2.0	38.2	0.7	37.6	1.5	4.8	28.8	109.0	61.7	58.7
Standard Deviation	25.1	24.4	7.5	1.7	1.6	28.9	1.1	28.4	0.8	4.5	20.7	36.7	53.2	52.7
% Difference from whole event	3.5	1.7	2.5	-1.8	-2.3	12.9	3.5	13.1	-7.4	-30.3	2.5	2.2	-2.9	-3.3
% Difference from total ice	-30.2	-35.5	-18.0	-5.4	-1.5	14.4	-30.2	15.7	-26.6	-54.6	-20.5	4.1	-5.3	-4.2
% Difference from total ice (With outliers removed)	22.7	15.7	23.3	14.2	13.9	27.2	15.1	28.1	20.2	4.3	11.7	6.4	9.7	10.2

Table 5.1 Average, standard deviations and deposition change for all ions during the whole event and the central event.

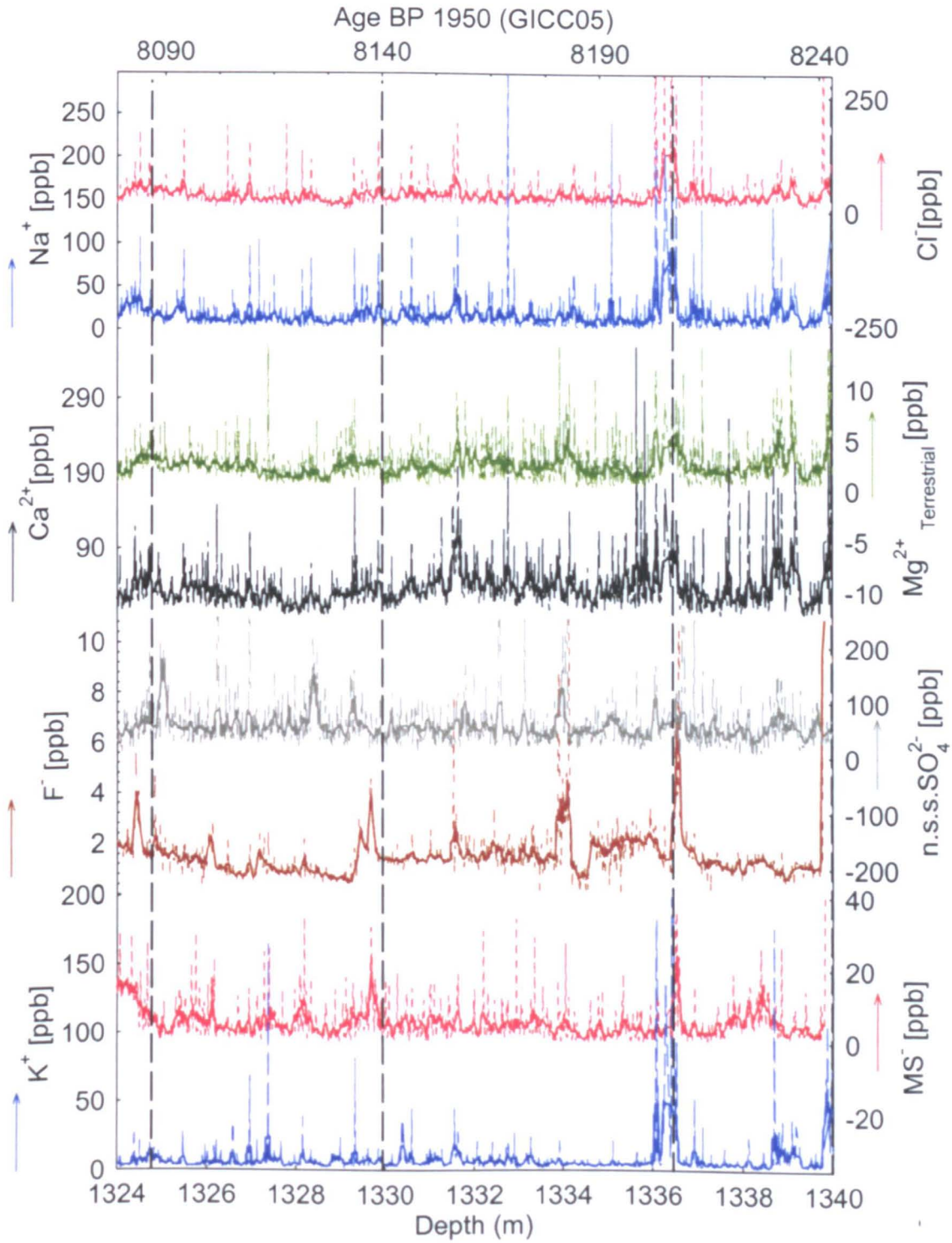

Figure 5.10 Chemical deposition during the 8.2 kyr event at 1cm (dashed curves) and annual (solid curves) resolution. Vertical dashed lines indicate the onset and termination of the whole and central event.

The chemical record shows a large degree of variability with some periods of significantly increased deposition, in particular at the onset of the central event (fig 5.10). In order to determine the probable source of these significant events, molar equivalents can be used to compare with known seawater ratios. Molar equivalents can be calculated according to the following equation:

$$\text{Molar equivalent} = \text{Concentration (ppb)} / \text{Molar Mass} \qquad \textbf{[Equation 5.6]}$$

The ratios in seawater are compared with the ratios found in the ice samples during these significant events in the table 5.2.

	Cl^-/Na^+	Mg^{2+}/Cl^-	K^+/Cl^-
Standard Seawater	1.16	5.12	53.48
Ice samples	1.47	5.67	13.56
Standard deviation	0.18	0.14	0.16

Table 5.2 Comparison of bulk seawater ratios (from the handbook of marine sciences) with ratios found in ice samples during the significant increase observed at the onset of the central event.

The ratio of Cl^-/Na^+ is equal to 1.1647 in standard seawater which is close to the value of 1.47 (+/- 0.18) found in the ice samples at the onset of the central event. The ratio of Mg^{2+}/Cl^- is also close to seawater ratios however the K^+/Cl^- ratio is much lower in the ice samples than the seawater ratio, implying that potassium is not a marine tracer in this instance. These comparative ratios do however imply that

sodium, chloride and magnesium, deposition during this period, are probably of sea salt origin.

The increase in marine components at the onset of the central event has been determined to be of seawater ratio, indicating a possible increase in sea ice at this time, increasing the amount of sea salt aerosols reaching summit. However, the onset and termination of the whole and central event is only based on the statistics used in this thesis, if different parameters were set their location would be different.

Calcium also increases during the onset of the whole and the central event. An increase in continental deposition to Summit could indicate an increase in atmospheric loading or an enlargement of the source area. In the time scales that we are looking at, lasting no more that a few years, the latter is unlikely. An increase in vigour or a shift in atmospheric circulation during this period is more feasible, and would also explain the increase in marine species. These affects have previously been attributed to this event, however a much larger record is required in order to determine if these changes in deposition are significant within the Holocene: not just in a 20 meter section lasting only 200 years within it.

5.3 Re-analysis of previously published data

The new GRIP high-resolution chemical record was compared with the previously published GISP2 record in the methods chapter (chapter 2) and the subsequent contamination investigated. The following section re-evaluates the GISP2 record in terms of the reported increases in chemical deposition during the 8.2 kyr event.

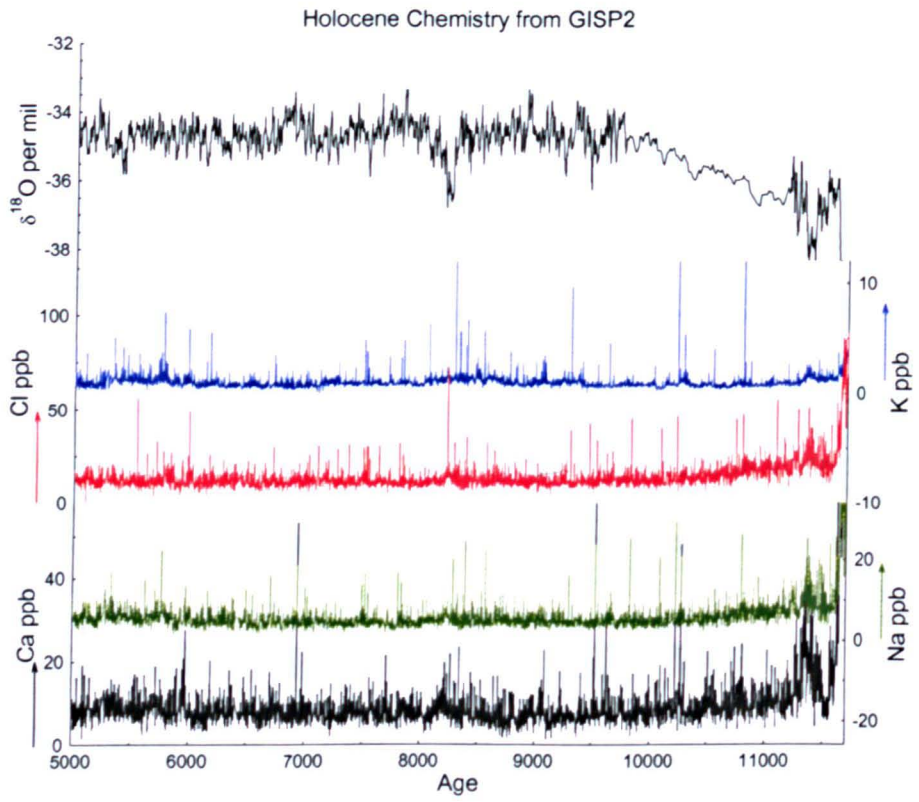

Figure 5.11 GISP2 [hhtp://nsidc.org/data/gisp_grip/] chemistry and $\delta^{18}O$ between 5,000 – 11,500 years BP

The GISP2 geochemical record and the oxygen isotope record for the Holocene are shown in figure 5.11. On initial observation the change in deposition during the Holocene is not obvious, with many similar geochemical changes observed at other time periods that are not accompanied by an isotopic change. Certainly the periods of

significance reported in the 20 meter section of ice analysed in this thesis are not significant within the wider Holocene record.

By obtaining a background Holocene average for each species the percentage increase during the 8.2 kyr central event can be calculated. The values show considerably lower increases for all species but especially for chloride, calcium and sodium, which are 9.1%, 17.9% and 10% respectively. This is much smaller than the previously published values of 60%.

	Concentration (ppb)						
	Na^+	K^+	Mg^{2+}	Ca^{2+}	Cl-	NO_3^{2-}	SO_4^{2-}
	Background (5,000 to 10,000 years)						
Average	5.2	1.1	1.9	8.1	12.4	81.1	46.4
Standard Deviation	2.1	0.7	0.6	3.6	4.2	11.9	41.3
	Central Event						
Average	5.8	1.6	2.2	9.5	13.6	85.3	41.7
Standard Deviation	2.3	2.0	0.6	3.2	7.4	12.1	22.0
% Difference from background	10.0	44.7	18.9	17.9	9.1	5.2	-10.1

Table 5.3 Average concentrations and standard deviations for the early Holocene (5,000 to 10, 000 years ago) and central event from GISP2 [hhtp://nsidc.org/data/gisp_grip/] and the percentage of deposition change.

Following the recent review of the 8.2 kyr event by Alley and Agustsdottir (2005) examination of the more detailed data suggest that the averaging of single extreme points, especially for chloride, influenced these percentage increases. The method of calculating the increase was based on the difference between the maximum value at

the peak of the event and the values just outside the event. This is shown in figure 5.12 below, taken from the review paper by Alley and Agustsdottir.

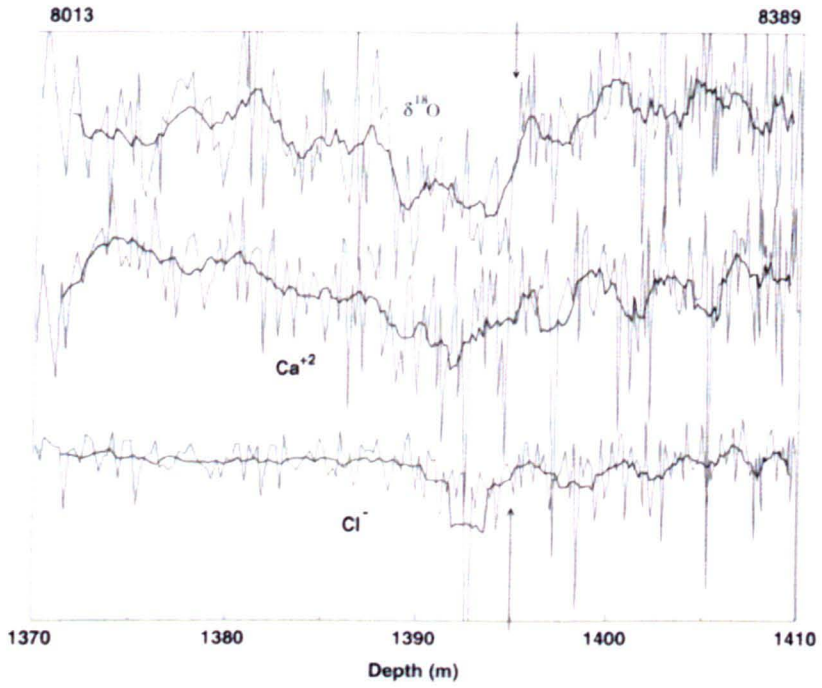

Figure 5.12 Taken from Alley and Agustsdottir (2005) (Figure 3). Data shown are $\delta^{18}O_{ice}$ [Stuiver et al., 1995; Grooted and Stuiver, 1997] with temperature increasing upward, Ca^{+2} and Cl^- [O'Brien et al., 1995] from the GISP2 core, with concentration increasing downward. Approximate ages are given at top. Samples are approximately biyearly, and a 10-sample (hence ≈20 year) running average is shown as well as the raw data. The onset of the event, as picked from the $\delta^{18}O_{ice}$ record, is shown by arrow.

The single extreme data point for chloride, with a value of 72 ppb, is not supported by similar values of other sea salt ions and therefore does not represent an enhancement of marine input. By removing the single anomalous chloride data point the record was re-plotted for chloride and calcium on the GRIP depth scale (for comparison with earlier figures in this thesis), and included vertical lines representing the duration of the 8.2 kyr event. In order to clarify the presentation we have plotted only 1.1 m

averages (approximately decadal), and also approximately 67-year averages (the length of the central event see "Dating and Duration" 4.2).

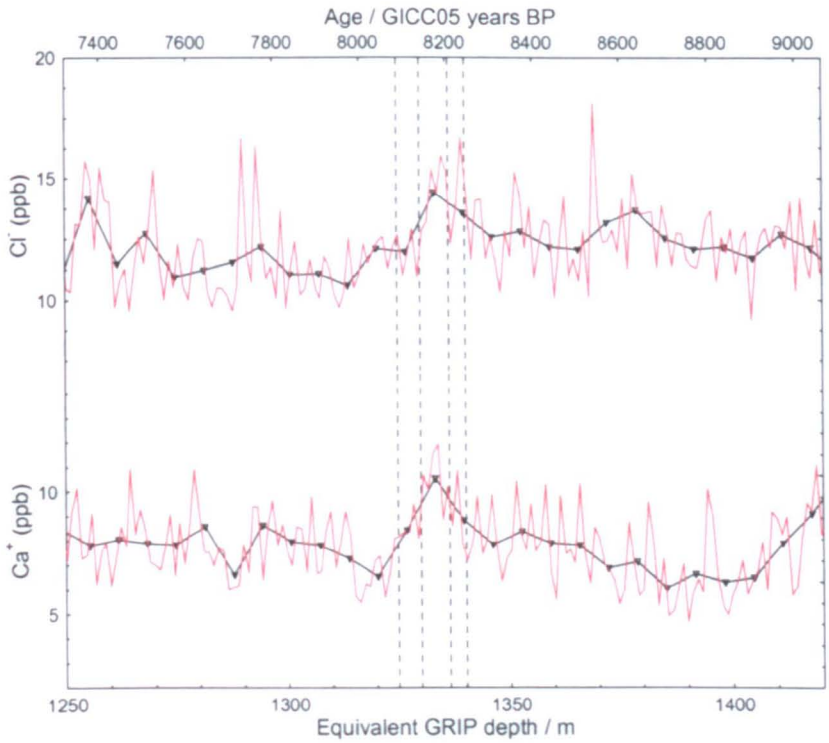

Figure 5.13 Chloride and calcium from GISP2. 1.1m running averages (red) and approximate 67 year averages (black) plotted on a GRIP depth scale and GICC05 age scale. Vertical dotted lines represent the onset and termination of the whole and central event.

It is immediately obvious that the enhancements, when seen in the context of the data from the centuries surrounding the event, are relatively small. For chloride, neither decadal nor 70-year average values are the highest of the section shown.

For calcium, there is a clear increase in concentration across the event, although only for the period of the central event is it unusual compared to the surrounding period. Specifically, the average value in the central event is elevated about 35% compared to

the average for the 1000 years surrounding (but excluding) it. High values are sustained in the decadal values throughout the central event.

An additional calcium record is available from GRIP, produced by CFA analysis. [Fuhrer et al., 1993]. In this record the 67-year central event has an average concentration of 8.4 ppb that is higher, but without statistical significance, than the average concentration of the 10 sections, each about 67 years long, which preceded it (7.1 +/- 1.3 ppb). Thus it has been shown that statistically significant increase in calcium and chloride occurred during the central event but they are smaller than have been reported previously. The relatively small changes compared to the normal variability prevent further analysis of the phasing of chemical and isotopic changes.

5.4 Summary: The 8.2 kyr event chemistry

The chemical deposition during the 8.2 kyr event has been investigated in the analysis of the concentrations of nine major ions in the GRIP ice core. The record was too short to make any statistically significant estimates of percentage deposition change however there were small periods of significance found within the 20-meter record. This contradicts previously published results of large increases (60 % increases in calcium, chloride and sodium [Alley et al., 1997; 2005]) during the event. Re-analysis of previously published GISP2 data exposed statistical bias; where-by single extreme data points were used to determine the percentage changes. This, combined with the re-analysis of previously published data, allow us to conclude that the changes in deposition during the 8.2 kyr event were small and unlikely to be indicative of large atmospheric changes.

Chapter six

The 8.2 kyr event: Annual layer counting

The 8.2 kyr event: Annual layer counting

6.1 Introduction

The reported timing and duration of the 8.2 kyr event differs between sources with varying degrees of error associated with the dating procedure. High accumulation rates of 0.24 meters ice/yr at GISP2 [Meese et al., 1997] provide a continuous record with stratigraphy records showing only very occasional periods of minor melt occurring less than once a century [Alley and Anandakrishnan, 1995]. The favourable conditions have provided a good and comparable depth-age scale in both GISP2 and GRIP based on methods primarily of visual stratigraphy, electrical conductivity measurements ECM, and laser light scattering from dust LLS. The use of oxygen isotope ratios to determine seasonality is restricted to the top 300 meters of the core; below this the effects of diffusion rapidly alter the seasonal cycle. Volcanic aerosols (H_2SO_4) and tephra have been used to correlate with known and dated volcanic eruptions, the oldest and largest of which is Vesuvius, A.D.79. However they are of little use for ice core dating prior to date-recorded history.

The estimated error at GISP2 has been given as 2 % for ice at depths where the 8.2 kyr event may be observed [Alley et al 1997]. Due to its location within the brittle zone, where relaxation stresses exceed the tensile strength, resulting fractures have interfered with ECM and LLS; however good visual stratigraphy was maintained throughout. Assessing the error of a multi-parameter depth-age scale is difficult due to the lack of comparative sources, the closest are deep-sea cores or corals where ^{14}C dating is quite precise but the 8.2 kyr event is not well defined.

A better method for determining the exact date of the ice core record would be to extend the annual layer counting for oxygen isotopes, which unfortunately diffusivity within the core below a depth of about 300 metres prevents. It was possible using the Dye 3 core; however oxygen isotopes are not the only readable tracer for an annual signal. The chemical composition of ice cores and snow-pits is dependent on both atmospheric and precipitation chemistry. It is possible to relate changes in the concentrations of ions in the ice to changes in the atmospheric composition such as different transport pathways or source areas at different times of the year. Analysing the ions at a sub-seasonal scale enables us to observe these alterations in concentration throughout the year to pick up a seasonal signal.

Dating

Using the layer counting described above the location of the spring peak for all years has been recorded. The depths have been recorded as shown in table 6.1 below. The years have been added, counting out from year 8,204 b2k (before the year 2000) as selected by Rasmussen et al (2006) in the GICC05 age-scale. Ice core dating uncertainties have been described previously in this thesis and I do not intend to produce a new dating record as part of my PhD but instead use an existing age scale to anchor my counting, which will be used only to determine the duration of the event.

The absolute minimum in the oxygen isotope record from the GRIP core appears at a depth of 1334.50 m that according to the GICC05 age scale has a calendar date of 8,190 years BP (8,204 years B2K (years before 2000)), with a counting uncertainty given as 47 years [Rasmussen et al., 2006; Vinther at al., in press]. For the benefit of

this thesis I will use this date as the marker for the layer counting with the understanding that there is an uncertainty of 47 years.

6.2 Annual layer counting method

Whitlow et al., 1992 in a comparative study of seasonal concentrations of major chemical species determined their locality within an idealized $\delta^{18}O$ curve for pre-1900 summit Greenland. Based on this evidence the annual peaks for all species could be matched up to determine the true annual signal over the 20 m section of the GRIP core.

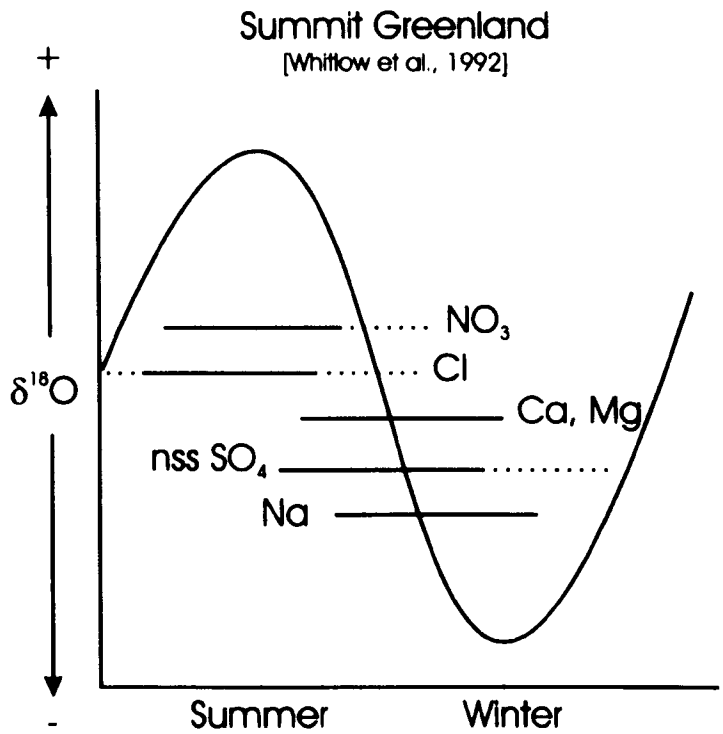

Figure 6.1 Summary of seasonal timing at pre-1900 Summit, Greenland, superimposed on an idealized $\delta^{18}O$ curve. Based on diagram from Whitlow et al., 1992 (Figure 2).

By convention the term winter when applied to a snow-pit corresponds to the portion of the year with light (more negative) $\delta^{18}O$ values while summer is dominated with heavy values.

The event duration, ice layer thickness and accumulation were all determined by layer counting using chemical species analysed in the GRIP core as described in the methods chapter. The parameters set for the counting are described below and the location of the peaks in different species followed according to the observed, but not process derived, locations of the peaks from Whitlow et al., 1992.

The annual layers were counted using all nine species with the best reproducible results from sulphate, nitrate, sodium and chloride as shown in figure 6.2. The different ions peak at different times during the year [Whitlow et al., 1992], as such the layers were determined as a peak in sodium and chloride followed by a peak in nitrate and sulphate approximately 6 months later.

From the 20 m section of ice used, the idealized locations of the peaks in each ion have been determined, based on the observed locations, and shown below (figure 6.3).

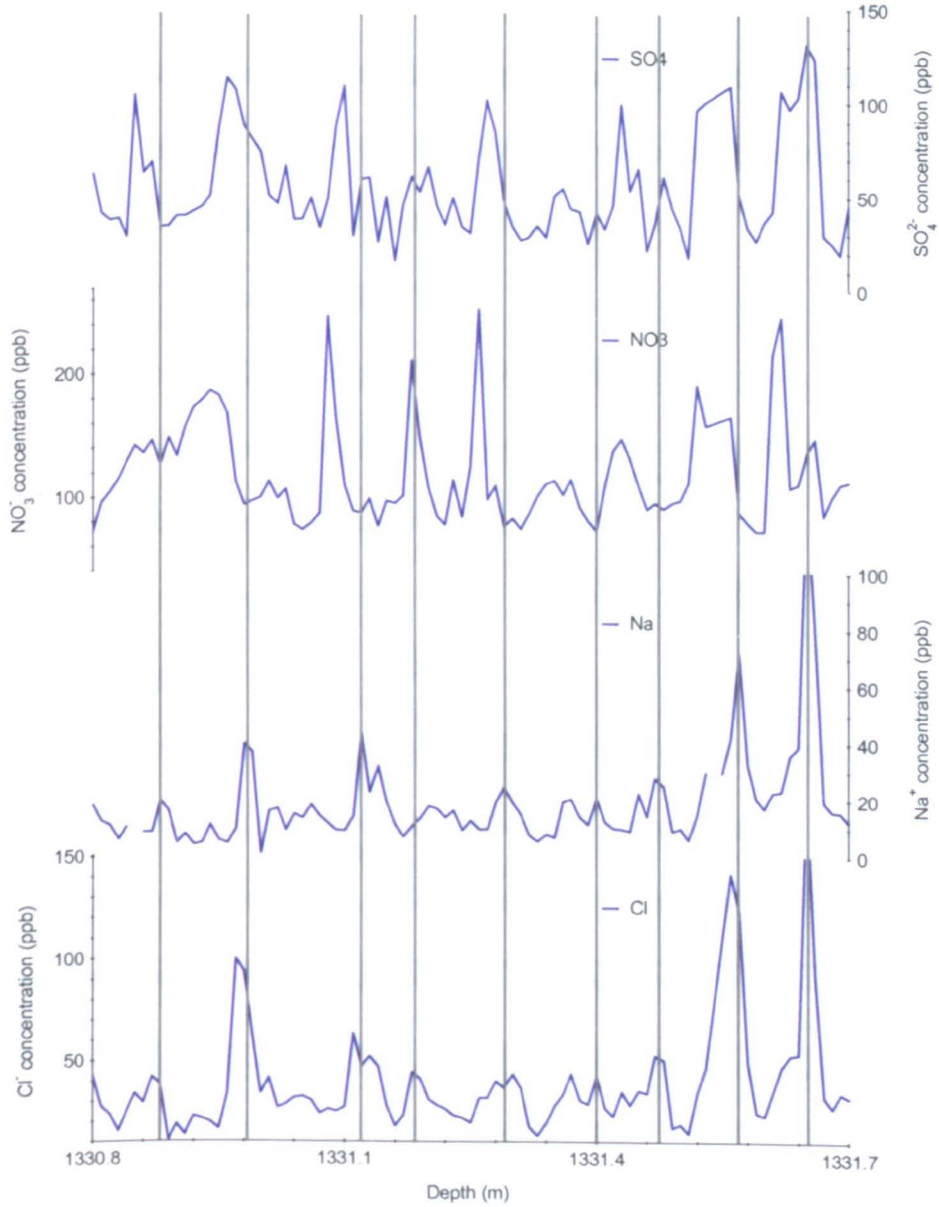

Figure 6.2 Seasonal cycles for sulphate (Top), nitrate, sodium and chloride (bottom) over a 90 cm section of the GRIP core. The grey lines indicate annual layers.

The contamination of the GRIP ice is described in chapter 2. Despite higher concentrations of some ions, compared to previously published data, I am confident that the species used in this section provide reliable seasonal variations and countable annual layers. Calcium showed the largest degree of contamination and is therefore not used in the annual layer counting; instead, sulphate, nitrate, chloride and sodium are used. Sulphate and nitrate showed only minimal contamination while sodium and

chloride, despite some contamination, show a seasonal range of typically 20 ppb compared to a contamination of around 10 ppb, therefore showing suitability for annual layer counting and indicating relatively uniform contamination.

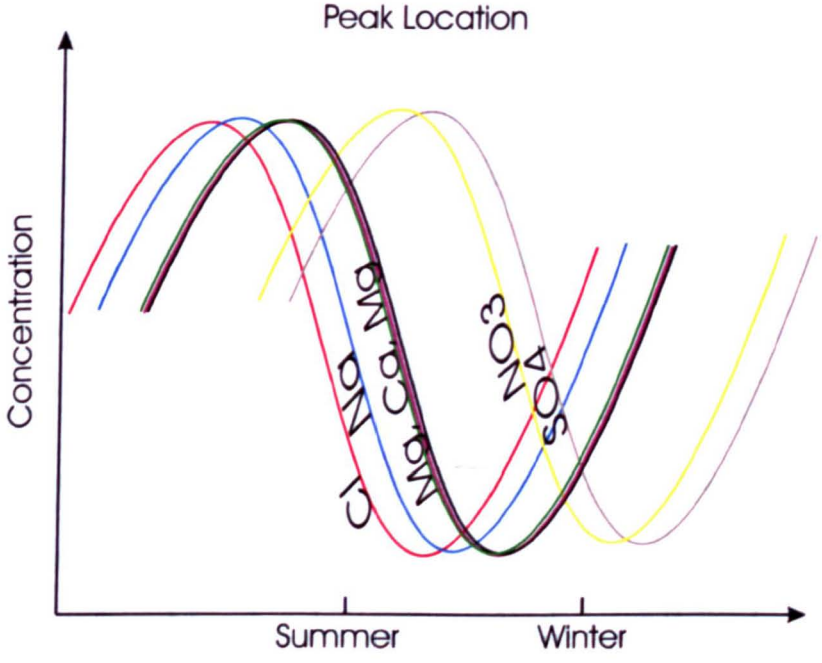

Figure 6.3 Idealized diagram of the location of the different ions during the year.

The following parameters were set for layer counting:

1. Each year must show a spring peak in sodium and chloride
2. Each year must show a summer peak in nitrate and sulphate
3. Annual layers will be marked with a line indicating a spring peak
4. Annual layers where not all parameters are met will be marked with a dashed line indicating a possible spring peak
5. Annual layers cannot be counted where chemical data are not present
    a. In such cases suspected spring peaks will be marked with a dashed line

b. The depth will be recorded as the counter's best guess

6. Three counters will be used to mark annual layers for the whole event
    a. First counter, Elizabeth Thomas
    b. Second counter, Robert Mulvaney
    c. Third counter, Eric Wolff
7. The depth of the spring peak will be recorded
    a. In cases where the depth of the spring peak differs between counters the average depth will be used.

6.3 Event Duration

The event has been defined in section 1 of the results chapter (Chapter 4.2, figures 4.18 & 4.19) based on the significance testing of oxygen isotope from a composite of the four cores at GRIP, GISP2, NGRIP and Dye 3. The whole event was determined to occur between depths 1324.77 m and 1340.12 m in the GRIP core. An average of 155 spring peaks were confidently marked during this depth period with an average of 11 spring peaks marked with dashed lines, where not all parameters were met or where data was missing. Assuming that half of the uncertain years represent true annual layers (in the same method used by GICC05 [Rasmussen et al., 2006]) then this equates to 160.5 ± 5.5 years.

The central event was determined to occur between depths 1329.96 m and 1336.45 m in the GRIP core. An average of 67 spring peaks were confidently marked during this section with an average of 3.6 dashed lines, where not all the parameters were met. The total duration of the central event, following the GICC05 error method, is 69 ± 2 years.

Comparison with independent method

The total number of years counted using the annual layer counting of nine chemical species can be compared to the totally independent dating, using the oxygen isotope annual signal, carried out to produce the GICC05 age scale [Rasmussen et al., 2006]. Through my counting method we found 155 years during the central event with 11 uncertain years. This compares well to the GICC05 scale that reported 159 years with an estimated error of 2%, therefore approximately 3 years.

For the central event, my method counted 67 years with less than 4 uncertain years, compared to the GICC05 scale that found a total of 70 years with an error of approximately 2 years.

Both sets of values compare well with each other and are within the estimated uncertainty reported for each method. The method that I used should however be independent and, unlike the GICC05 scale, it was dependent on more than one parameter.

The table below shows that annual layer counting is very operator dependent. To overcome this, the average number of certain and uncertain years was used. Therefore the onset and termination dates for the whole event and the central event could be determined from the GICC05 age scale, as shown below in table 6.2, using only the certain years.

Event name[9]	Depth (m)	Operator	Whole lines	Dashed lines	Overall Average Duration (years)	Average Uncertain years	% Uncertain years	Number of years (GICC05)	Number of years reported with GICC05 error
Whole event	1324.77 to 1340.12	ET	159	7	155	11	7	159	160.5 ± 5.5
		RM	150	12					
		EW	156	12					
Central event	1329.96 to 1336.45	ET	69	3	67	3.6	5	70	69 ± 2
		RM	67	4					
		EW	65	4					

Table 6.1 Table of results for the annual layer counting using chemical species.

Event	Depth (GRIP m)	Age (GICC05 yrs BP)	Age (GICC05 yrs b2k)
Onset	1340.12	8246	8296
Onset central event	1336.45	8211	8261
Termination central event	1329.96	8141	8191
Termination	1324.77	8087	8137

Table 6.2 Age markers for the 8.2 kyr event based on the GICC05 age scale [Rasmussen et al., 2006]

6.4 Accumulation Rate

The accumulation rate can be calculated from the thickness determined by the annual layers of the chemical species, providing ice thinning is accounted for. The annual layers are gradually stretched and thinned under the vertical compression and longitudinal stress from the ice and firn.

[9] A determined from the 'Event definition' Chapter

The Dansgaard-Johnsen type model assumes thinning is proportional to burial and that the upper 3% or less of the ice depth consists of compressible firn [Johnsen et al., 1992; Johnsen et al., 1995]. If ice deforms in a plane strain and the density-depth relation does not vary along the flow line [Schott et al., 1992] then the shear stresses at depths below 100 meters should be accurately represented.

With these assumptions in mind the percentage of ice thinning is therefore determined from the ice core depth divided by the ice sheet thickness, providing the firn compaction removed.

Ice thinning % = (Ice core depth / Ice sheet thickness) * 100 **[Equation 6.1]**

If the layer thickness and percentage of ice thinning is known then the accumulation rate can be calculated.

Accumulation rate = Layer thickness / 1-(Ice thinning/ 100) **[Equation 6.2]**

Twenty-four meters was subtracted from the surface elevation to correct for the low densities in the upper layers giving a corrected ice thickness of 3004 meters [Schott et al., 1992]. The ice thinning range, for the 20 m of GRIP ice analysed, is 44.24 – 44.47%. The mean accumulation rate for the 67-year central event (1329.96 to 1336.45 m) is thus calculated as 0.16 m ice/yr, a decrease of 31 % from the mean Holocene value[3].

The decrease in the accumulation rate during the whole event, shown in figure 6.5, is slightly lagging the decrease observed in the isotopes. The accumulation rate profile from GRIP exhibits approximate Gaussian distribution (fig 6.4); therefore

significance testing of the accumulation rate was carried out to determine if the alterations in accumulation during the event were statistically significant.

Event name[10]	Depth (m)	Layer Thickness (m)	Accumulation Rate (m/ ice/ year)	Difference from Holocene average[10]
Whole event	1322.92 - 1341.12	0.098	0.17	- 24 %
Central event	1329.96 - 1336.45	0.088	0.16	- 31 %

Table 6.3 Average layer thickness and Accumulation rates for the whole event and the central event.

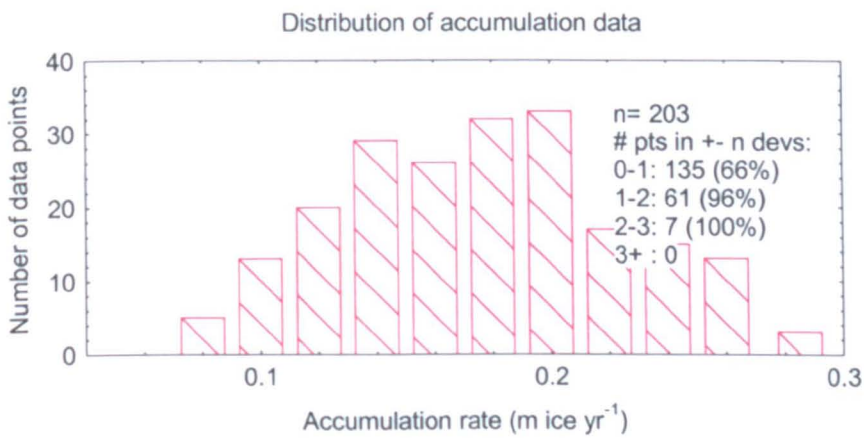

Figure 6.4 Gaussian distribution of accumulation data from GRIP.

The mean surface accumulation (μ) for the Holocene is 0.23 meters of ice per year with a population standard deviation (σ) of 0.056. It is expected that approximately 65% of values will be within the range $\mu \pm \sigma$, the accepted inter-annual variability. Samples outside of this range with accumulation rates greater than $\mu \pm \sigma$ can be considered outside of the accepted inter-annual variability and therefore statistically significant.

[10] Holocene average 0.23 m ice / year [GRIP 1993]

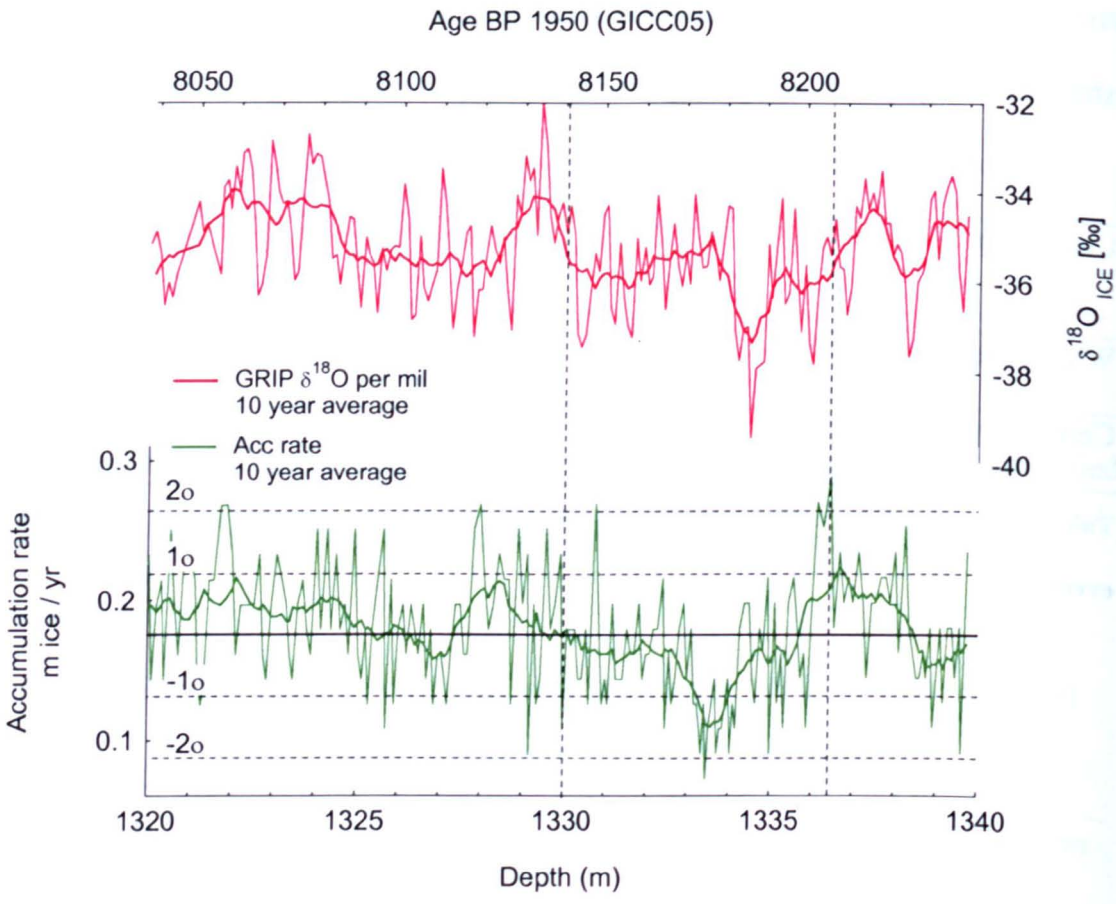

Figure 6.5 Top: $\delta^{18}O$ (per mil) at 1.5 cm resolution (thin red curve) and 10-year average (thick red line) and Bottom: Accumulation rate (m /ice /yr) derived from the average annual layer thickness from nine species corrected for ice thinning. Solid horizontal line indicates average accumulation rate for the 20-meter record and horizontal dashed lines indicate 1 and 2 standard deviations above and below this. Vertical dashed lines indicate the onset and termination of the central event. Age scale derived from GICC05 [Rasmussen et al., 2006]

The largest significant change in accumulation, in the decadally smoothed accumulation record (thick green line in figure 6.5, smoothed using a sliding data window based on an average layer thickness of 9.8 cm), is observed between depths 1333 m and 1334 m. This decrease, lower than one standard deviation below the mean, is outside of the accepted inter-annual variation and corresponds to the central event observed in the isotopes (Figure 4.18 and 4.19, p.115 and 116).

Accumulation derived from Oxygen isotopes

An ice deformation model was formulated by Johnsen and Dansgaard, (1992) which found that there was a relationship between the surface accumulation rate (λ) and the isotopic ratio of precipitation, δ in Greenland. This enables the surface accumulation rate to be calculated from the isotopic record using the following equation [Johnsen and Dansgaard, 1992; Johnsen et al., 1995].

$$\lambda(\delta) = 0.23 \exp(-10.09 - 0.653\,\delta - 0.01042\,\delta^2) \qquad \textbf{[Equation 6.3]}$$

Using the 1 cm oxygen isotope record, the above equation was used to calculate the annual layer thickness during the 8.2 kyr event. The results are shown in figure 6.6 along with the comparison of the annual layer thickness derived from the annual layer counting described above. The average layer thickness and the standard deviation of the two methods have been compared in table 6.4.

The results show that in general the model works well to simulate layer thickness from the oxygen isotope record. The average for the 8.2 kyr section is however slightly lower than that derived from the method of annual layer counting described above. It appears that the model underestimates the variation in layer thickness and many of the key features shown in the annual layer counted accumulation profile (fig 6.5) are not present. This is because the model derived accumulation rate is dependent on the $\delta^{18}O$ values (representing several years) that are influenced by more than just temperature and accumulation and does not account for anomalies in the $\delta^{18}O$, such as the spike described in chapter 4.

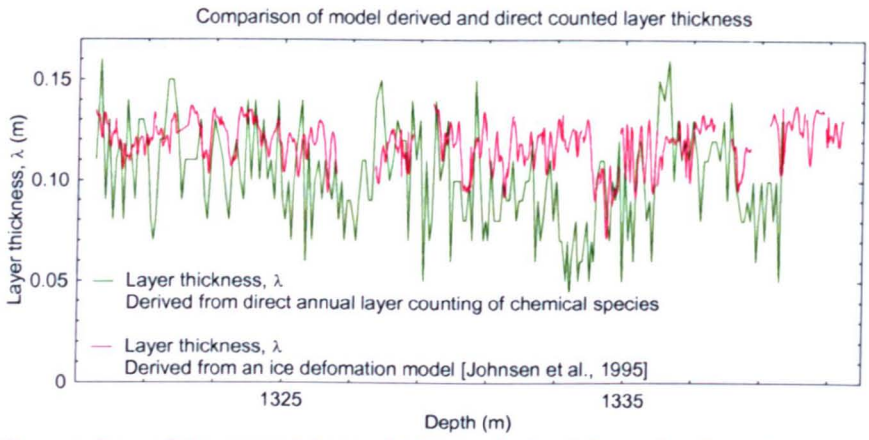

Figure 6.5 Comparison of the annual layer thickness derived from the direct layer counting of chemical species (green) and the layer thickness derived from an ice deformation model (red) [Johnsen et al., 1995]

	Derived from annual layer counting	Derived from ice deformation model [Johnsen et al., 1995]
Average annual layer thickness	0.098	0.118
Standard Deviation	0.025	0.011

Table 6.4 Comparison of the average annual layer thickness derived from annual layer counting and from an ice deformation model.

6.5 Summary of 8.2 kyr event: Annual layer counting and accumulation rate

The duration of the whole and central 8.2 kyr event has been determined as 160.5 ± 5.5 years and 69 ± 2 years respectively, based on annual layer counting. This compares well with the independently dated GICC05 age-scale and therefore confirms that the ions used were suitable for layer counting and not affected by contamination issues discussed in chapter 5. The accumulation rate was determined from the exact layer thickness (after ice flow had been accounted for) to show a decrease from the Holocene average of 25 % for the whole event and 32 % for the central event.

Chapter seven

The 8.2 kyr event: Discussion

The 8.2 kyr event: Discussion

Isotopes

The 8.2 kyr event is clearly observed in the ice core record as a negative deviation in the isotopes of four deep ice cores drilled in Greenland, GRIP, GISP2, NGRIP and Dye 3. The new higher resolution records obtained from GRIP and GISP2 as part of this thesis have augmented previously published results and enabled a comparison of all four deep cores on a decadal scale.

The new sub-seasonal resolution oxygen isotopes from GRIP show a significant amount of inter-annual variability in the isotopes. However, due to diffusion and ice compression at this depth, the seasonal signal is no longer present and therefore could not be used in the annual layer counting of this section. The new 1 cm oxygen isotope record produced from the GISP2 core was compared with the GRIP record to reveal differences on the sub-annual scale with the prominent "spike" observed in GRIP, absent in GISP2. Such a dramatic difference in the isotope record was unexpected from two ice cores drilled just 30 km apart, affected by the same climate regime. A possible explanation for the differences, on the sub-annual and sub-decadal scale, is post-depositional alterations at the two locations; such as wind induced snow ablation at the GISP2 site or excessive winter accumulation from snow drift at the GRIP site. The more ^{18}O-depleted winter build-up would explain the extreme negative values in the GRIP record however this would also be seen in the chemical record with a loss of seasonal signal or an increase in layer thickness. The annual layers for this section of the core are shown in figure 7.1; they have been confidently marked by three people, based on the parameters discussed in section 6.3, and show no loss of signal. In

addition, the number of years counted for the whole section of ice compares well to the independently calculated age scale from GICC05 (produced from the Dye 3 isotope record), which would not be the case if extra years were calculated in a section where the signal had been lost.

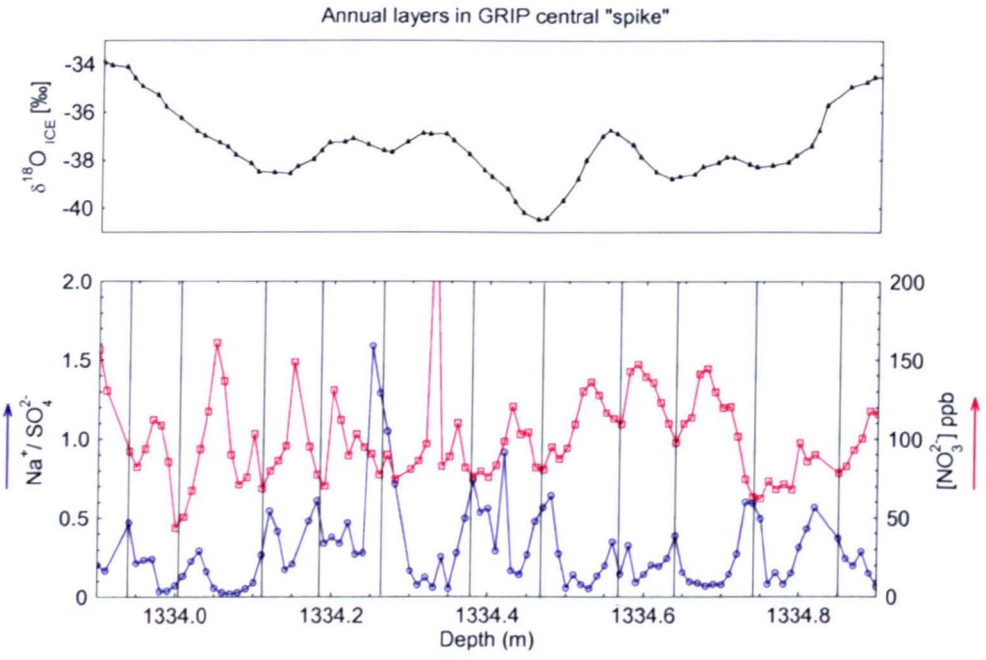

Figure 7.1 Annual layer counting of NO_3^{2-} (red) and Na^+/SO_4^{2-} (blue) (commonly used dating parameter [Joe McConnell personal communication May 2004]) between 1333.9 and 1334.9 meters where the GRIP "spike" is seen, as shown by the high-resolution isotope record (top black).

Possible snow ablation at the GISP2 site could still be the cause, but the general conclusion from this comparative research is that isotopic records on a sub-annual scale are not robust enough to be used in climate reconstructions. When comparing isotope records from ice cores at different sites, even those influenced by the same climate regime, it is best to use a decadal scale smoothing.

Defining the Event

The oxygen isotope records for the four deep ice cores (GRIP, GISP2, NGRIP and Dye 3) were decadally smoothed and compared, using a uniform depth scale. Due to the different lengths of the records, a composite of the four sites was derived using the 27.5 cm resolution GRIP record. The Holocene average (-34.73 ‰) and standard deviation (0.83 ‰) could then be calculated from the proceeding 1000 years; between 9300 to 8300 years BP. Using the composite record, the onset of the whole event was determined as the point at which the oxygen isotope record fell consistently below the Holocene average. This was found to occur at a depth of 1340.12 m. The termination was determined as the point in which values returned to a normal range, found to occur at a depth of 1324.77 m. For the more extreme central event, the onset was determined as the point at which values fell below the statistically significant level of one standard deviation below the mean, and the termination was the point at which values returned above this. This put the central event between depths 1336.45 m and 1329.96 m.

The event definition is important in order to avoid confusion and potential "wiggle matching" with other paleoclimate proxies, further confusing the literature. The Greenland records and other proxy records from across northern Europe show a distinct, short and sharp signal within the background climatic shift and it is therefore important to separate the two and name them accordingly.

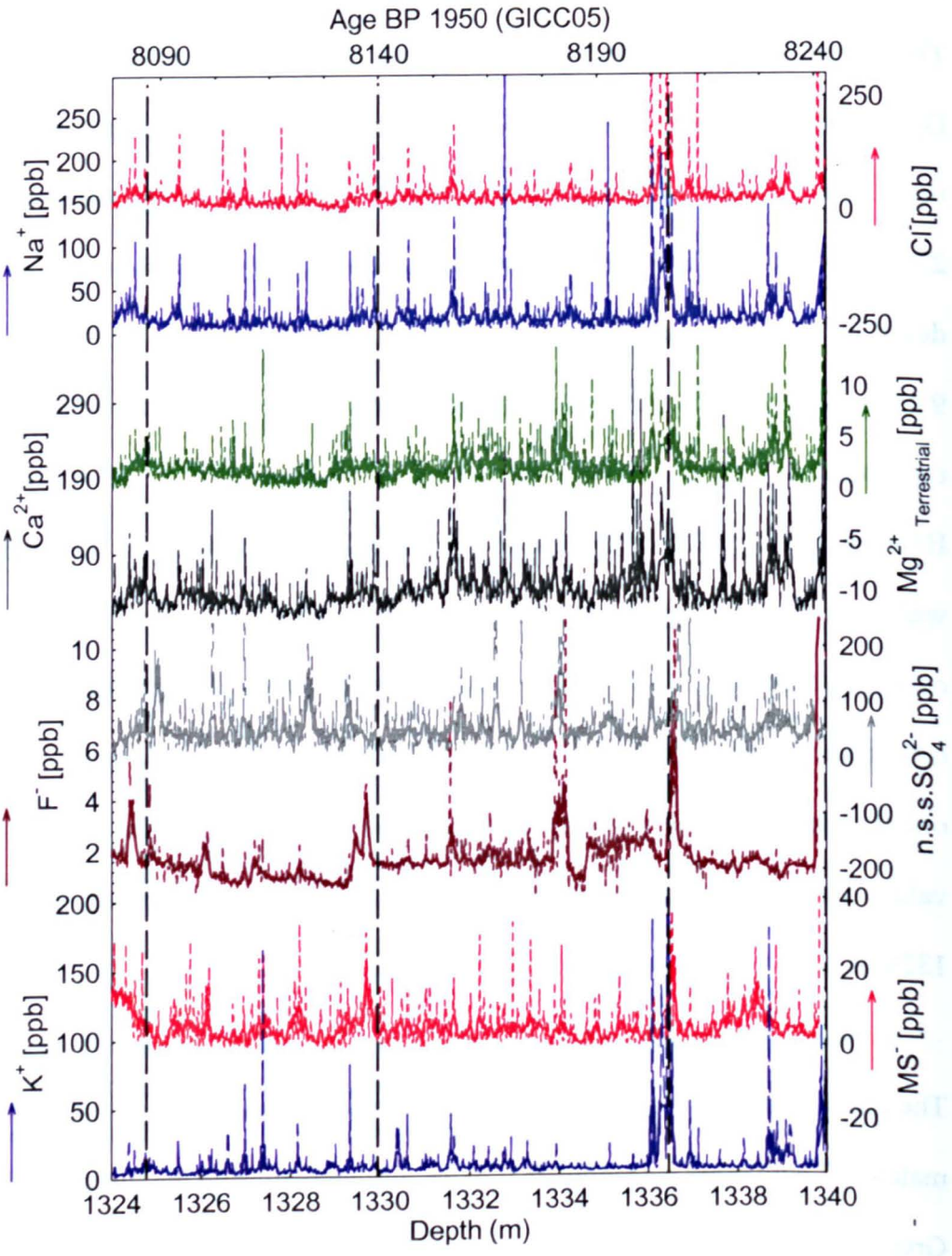

Figure 7.2. (also fig 5.10) Chemistry of eight ions from the GRIP core analyzed at 1 cm resolution (dashed lines) and 1 year averaged (solid lines), Ca from CFA [Fuhurer et al 1999]. Vertical dashed lines indicate the onset and termination of the whole event and the central event as defined in chapter 4.

Chemical Record

A sub-seasonal record of chemical deposition in Greenland during the 8.2 kyr event was produced for nine ions. Over two thousand discrete samples were prepared and analysed using ion chromatography as described in the methods chapter (Chapter 2), to give a continuous record of chemical deposition for over 200 years covering the 8.2 kyr event. The 1 cm chemistry has been smoothed to give an annual record of deposition during this period in figure 7.2 below; the calcium values have been replaced by data obtained by Fuhrer et al (1999) due to the contamination discussed in chapter 2.

The chemical record from GRIP does show that large increases in all ions occurred at the onset of the whole event, the onset of the central event and to a lesser extent, at the termination of both events. This is an interesting result, indicating an alteration in the chemical deposition at summit, Greenland accompanied the initial cooling into both of these events, and indeed it appears to precede the isotopic anomaly. The marine ions, sodium and chloride, during these sections are close to the seawater ratios (Cl^- /Na^+), therefore confirming that both ions are of marine origin. The increases could therefore be indicative of a shift in oceanic conditions possibly reflecting greater sea ice extent or increased storminess. A shift in atmospheric circulation and vigour would also explain the observed increases in continental and non-marine ions (Ca, Mg, n.s.s.SO_4, K).

The increases do appear to be significant within the 20 m record, however it is important to remember that the 8.2 kyr event has been statistically defined and therefore the location of the onset and the termination is dependent on the statistics

used in this thesis. And as seen in the GISP2 record, similar or even larger depositional changes exist throughout the Holocene. Many of these are not associated with an isotopic anomaly or a significant climate event. Therefore it cannot be concluded that these changes during the 8.2 kyr event indicate any significant alterations in atmospheric circulation, as previously proposed. Certainly no comparison can be made with the much larger glacial events, or the Younger Dryas, which saw increases of 600 % for continental and sea salt species [Alley et al., 1997; 1995; 2005].

With the exception of a significant increase in all species (found to be of sea salt origin), at the onset of the central event, the results show very little alteration during the 8.2 kyr event. This contradicts what has previously been published by Alley et al (1997; 2005) who reported 60% increases in calcium, chloride and sodium, indicating a large atmospheric circulation shift accompanied this event.

Comparison with other records

The obvious discrepancies in the record produced in this thesis and the previously published deposition changes, led to a re-evaluation of the results by comparing the average values in all ions with those measured in the GISP2 core. Disappointingly the findings revealed that my samples contained significantly higher concentrations of calcium and slightly higher concentrations for chloride and sodium. Re-analysis of the quality control section determined that contamination was not a result of bad laboratory procedures but that it came from the ice itself. An experiment was devised, using an extra section of the GRIP ice core, whereby layers of ice were cut from the outside toward the middle. The results showed the highest concentrations in all ions

were found in the ice from the outermost layers of the GRIP ice core section, as expected (and therefore removed in the initial cleaning process), but that the middle section never fell to a sufficiently low concentration. It was therefore concluded that the contamination had penetrated through the ice and that removal of a greater amount of ice in the cleaning process would still have resulted in elevated concentrations.

The contamination was regrettable but due to the small section of ice available in the GRIP archives, it was unavoidable. Despite the contamination, the annual signal for all seasonally deposited ions, including calcium is apparent throughout this section of ice. This can only imply that the results are in fact true representations of deposition or that the contamination was uniformly consistent. Several ions were affected by the contamination, especially calcium, which is significantly higher than previously published Holocene levels, making it unsuitable as a paleoclimate proxy. The other ions show only slightly elevated concentrations and are therefore still considered suitable proxies to be used in determining atmospheric response and for annual layer counting during the 8.2 kyr event.

The conclusions drawn from the contamination experiment are interesting for the larger subject of ice core storage and archiving. The GRIP ice core was stored for nearly 20 years in a -20°C storage freezer at the University of Copenhagen before sections of it were moved to Cambridge, for use in this thesis. Clean conditions were maintained thought storage and subsequent analysis (as demonstrated in the quality control results, Chapter 2); therefore the calcium contamination must have been from the ice itself, possibly from the bags it was stored in. Another possibility is that the drilling fluid was not properly removed from the ice before storage and has somehow

contaminated further into the ice than was previously thought possible. Small sections of the ice was damaged, resulting in missing data in the chemical and isotope records, suggesting that the ice could have been from the brittle zone. If this was the case small cracks and fractures at the time of drilling could have enabled the fluid to penetrate the ice. These are interesting factors that need to be considered for the future ice storage.

Despite the contamination problems, which were discovered during this thesis, the results from the remaining eight chemical species still provide a valid indicator of atmospheric circulation patterns during the 8.2 kyr event. The discrepancy in the previously published 60% increases in continental and sea salt species [Alley et al., 1997; 2005] cannot be explained by the contamination differences alone. Even with contamination effects, a 60% increase in any species would still be visible above this. Re-examination of more detailed GISP2 data published about this event [Alley et al., 1997; Alley and Agustsdottir, 2005] suggests that the averaging of single extreme points, especially for chloride, influenced these percentage increases. The method of calculating the increase was based on the difference between the maximum value at the peak of the event, and the minimum values just outside the event. One extreme chloride value was not accompanied by a similar change in sodium and cannot therefore be considered of sea salt origin. The single data point was removed and the new levels from GISP2 during this section were calculated (using a background from the surrounding 5000 years), giving an increase of 9 % for chloride, 18 % for calcium and 10 % for sodium.

Duration

The event has been defined from the composite isotope record from all four sites as a cold central event lasting 67 years with four uncertain years, within a larger "whole" event lasting 155 years with 11 uncertain years. The later compares well with previously published estimates from GISP2 of 200 years [Alley et al., 1997; 2005], and from lake sediments at Ammersee, Germany [von Grafenstein et al., 1998]. The short sharp signal lasting 67 years is compatible with peat bogs records from Newfoundland [Tim Daley; personal communication 2005] that has an estimated duration of 60 years and speleothem records in northern England [Jim Marshall, Pipikin Pot], which all report a similar shape, amplitude and duration. The new central event appears to be only visible in other paleoclimate sites within close proximity to Greenland, and the North Atlantic. A much shorter duration of isotopic anomaly was previously reported in a speleothem record from Ireland [Baldini et al., 2002], however this has recently been identified as an analytical artefact (Fairchild et al, In Press).

The new GICC05 age scale [Rasmussen et al., 2006] gives an estimated calendar age of 8,190 ± 47 years BP, for the most negative central oxygen isotope value observed at a depth of 1334.50 meters, which is exceptionally close to that of the Newfoundland peat bogs that have an estimated age of 8,190 ± 85 years (based on ^{14}C markers) [Tim Daley, personal communication 2005].

Accumulation

The accumulation rate, determined from annual layer counting (Chapter 6, p.154), was 31% lower than the Holocene average during the whole event. Values were 24%

lower than the Holocene average during the central event with a nine year period (1333.99m – 1333.18m) in the middle of significantly lower values (< 2σ). This nine-year minimum slightly lags the minimum values observed in the $\delta^{18}O$ record (see fig 6.5 p.158) indicating that accumulation changes lagged the temperature, assuming $\delta^{18}O$ is truly representing temperature.

The annual layer derived accumulation rate was compared to the model derived accumulation profile [Johnsen et al., 1995], showing differences in the features and mean values. Due to its dependence on $\delta^{18}O$, the model-derived method produces an earlier accumulation minimum, associated with the minimum in $\delta^{18}O$. The overestimation of the model derived accumulation rate and the underestimation of the variability suggests that the relationship between $\delta^{18}O$ and accumulation is not constant.

Comparison with Model results

The 8.2 kyr event has been attributed to the final stage of the collapse of the Laurentide ice sheet, which melted rapidly during the early Holocene to produce huge proglacial lakes, with the remnants of the LIS forming a massive ice dam. The timing of the collapse of the ice dam and the subsequent draining of the Laurentide Lake is estimated at 8,470 calendar years BP [Barber et al., 1999]. Discrepancies in the timing have been attributed to dating uncertainties, and many investigators have concluded that this outburst flooding coincided with the 8.2 kyr event [Klitgaard-Kristensen et al., 1998 von Grafenstein et al, 1998; Barber et al., 1999].

The mechanism proposed is a slow down of the Meridional Overturning Circulation (MOC), preventing dense water from sinking in the North Atlantic and therefore reducing heat transport to the North Atlantic region. This mechanism has been investigated extensively by the modelling community in which the North Atlantic is perturbed by freshwater. The estimates of the volume of the freshwater flux have been debated, so too has the duration of the floods and the possible drainage routes [Leverington et al., 2002; Clarke et al., 2004]. Model predictions [Renssen et al., 2002; Wiersma and Renssen, 2006] based on a 20-year pulse of freshwater to the North Atlantic appear to replicate temperature changes observed in the proxy record. When introducing a volume of 1.63×10^{14} m^3, the estimated volume of the Laurentide Lakes [Leverington et al., 2002], the maximum simulated duration of the weakening of the MOC is ~160 years. Simulations of the 8.2 kyr event by LeGrande et al (2006) provided evidence that reductions in NADW production by about 50 % are consistent with multiple paleoclimate proxies.

Improving our understanding of the 8.2 kyr event is therefore of great importance to the modelling community. Despite different initial conditions (primarily the existence of the Laurentide ice sheet in North America), it is a good scenario for testing model parameters of THC slowdown and future climate change. The response to a freshening of the north Atlantic is especially relevant following recent evidence that the meridional overturning circulation (MOC) has shown a 30 % decline in recent decades [Bryden et al., 2005]. It is therefore beneficial for future research that the event in Greenland has been defined and the duration confidently determined. The comparison of the isotope record in Greenland from all sites and the new deposition

increases will better constrain model parameters of ocean and atmospheric circulation patterns.

Chapter eight

Introduction to

Dansgaard-Oeschger event 8

Introduction to Dansgaard-Oeschger event 8

8.1 Background

Evidence from a wide range of paleoclimate proxies has shown that the Earth's climate has been far from stable, with ice core records from Antarctica recording eight glacial cycles over the past 750,000 years [EPICA community members 2004]. The presence of large temperature variations is clearly observed in the ice core record, with large and abrupt changes appearing frequently during the last glacial period. Sudden and short-lived warm events known as interstadials were first picked up as brief fluxes of warm climate plants and insects from northern European lake sediments and are also recorded in the Greenland ice core oxygen isotope record (where they are known as Dansgaard-Oeschger events) as warm events that occurred 24 times between 115,000 and 14,000 years ago [Bond et al., 1993; Dansgaard et al., 1993; Grootes et al., 1993; Taylor et al., 1993; Mayewski et al., 1997, NGRIP members, 2004].

The oxygen isotope record from Greenland was used by Johnsen et al (1995) to conclude that the temperature dropped by more than 20° C, compared to present day temperatures, several times during the last glacial with the absolute minima (25°C colder than present) observed 21,500 and 71,000 years BP. These Dansgaard-Oeschger events (DO) were jumps between periods of extreme cold to a period of intermediate cold with a magnitude ranging from 9 °C to 16 °C, based on the isotopes from enclosed air [Lang et al., 1999; Severinghaus and Brook, 1999]. Recent work by Ahn (2004), using the combined analysis of water isotopes and $\delta^{15}N$ measurements in trapped air, revealed that the jumps between DO events and intervening cold stadials,

were much larger than those reconstructed using water isotopes alone. Ice core evidence combined with ocean sediment records suggest that the warm interstadials began and ended suddenly, within the transition occurring over a few decades or less with a duration varying from a few centuries to two thousand years [Mayewski et al., 1997].

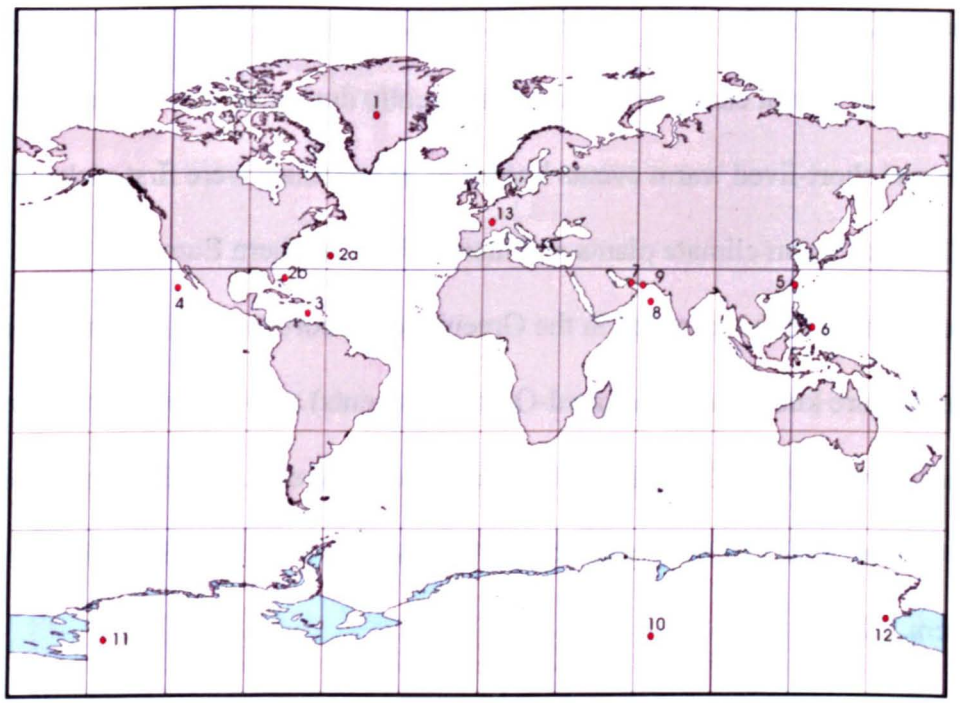

Figure 8.1. Locations of key sites referred to in the text. (1) GRIP/GISP2 ice cores. (2a &2b) marine sediment cores GPC-5 Bermudan Rise and GPC-9 Bahaman outer ridge [Keigwin and Jones. 1994]. (3) Cariaco Basin marine core [Hughen et al., 1996]. (4) Santa Barbara Basin, Californian margin marine core [Hendy and Kennett 1999]. (5) Hulu cave, south China [Wang et al., 2001]. (6) MD98-2181 marine core from edge of Indonesian archipelago [Stott et al., 2002]. (7) Marine cores from the Arabian Sea [Shultz et al., 1998]. (8) Marine sediment cores, the Persian Gulf [Altabet et al., 2002]. (9) Speleothem from Socotra Island, Yemen [Burns et al., 2003]. (10) Vostok ice core East Antarctica. (11) Byrd ice core Western Antarctica. (12) Taylor Dome, Western Ross Sea, East Antarctica. (13) Stalagmites from southwest France [Genty et al., 2003]

Analysis of the GRIP and GISP2 ((1) in Fig 8.1) ice cores has shown that millennial scale changes in the atmospheric composition of greenhouse gases such as N_2O and methane accompanied DO events [Brook et al., 1996]. Combined with the alterations in the deposition of dust and sea salt from the GISP2 geochemical series, which provides a sensitive record of change in the atmospheric circulation systems affecting Greenland [Mayewski et al., 1994b], the implications are that DO events are larger than just local Greenland temperature events.

North Atlantic

The abrupt warming events are replicated in North Atlantic sediment cores, as alterations in the sea surface temperatures (SSTs) at high and low latitudes [Bond et al., 1993; Curry and Oppo, 1997; Hendy and Kennett, 1999] and in the geochemical records of deep-water ventilation [Keigwin and Jones, 1994]. Reconstructions of SSTs based on alkenone unsaturation ratios in sediments from the Bermudan Rise ((2a) in Fig 8.1), in the subtropical North Atlantic, during marine isotope stage (MIS) 3 (between 30 and 60 ka) show the largest temperature excursions. Abrupt cold reversals of 3-5 °C, lasting less than 250 years, occurred at interstadials 8 and 12 and are confirmed by additional sediment cores in the southern Sargasso Sea [Sachs and Lehman, 1999].

The Bermudan Rise records (Fig 8.2) show clear correlation in sediment lightness (a proxy for $CaCO_3$) with temperatures observed in Greenland. Sedimentation rates (plotted as a log scale in figure 8.2) at Bermudan Rise increase when SST's sink to a minimum. This indicates that these transitions are associated with increasing melt water and iceberg delivery of sediments to the North Atlantic basin during Heinrich

events (defined as periods of massive ice rafting); especially during Heinrich events 5 & 4.

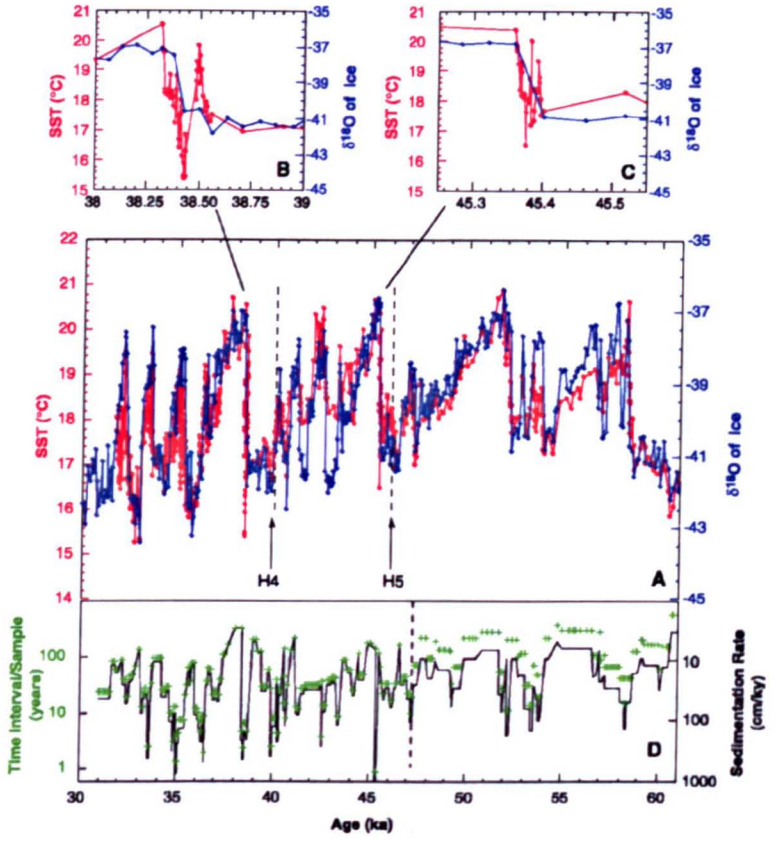

Figure 8.2 (A) Bermuda Rise SSTs (red) and central Greenland $^{18}O_{ice}$ (blue) for MIS 3 on the GISP2 ice core time scale. IRD peaks associated with Heinrich events 4 and 5 (dashed vertical lines). (B) IS-8 and (C) IS-12. (D) High instantaneous rates of sedimentation (black line) of 100 to 1000 cm/ky characterize cold stadial periods and the transitions into interstadials, and interstadial periods are characterized by lower sedimentation rates of 3 to 10 cm/ky. Figure 3 in Sachs and Lehman, 1999.

Tropical Atlantic

The sediment record from the Cariaco Basin ((3) in Fig 8.1), in the Western tropical Atlantic, off the coast of Venezuela, shows shifts in the Atlantic Intertropical Convergence Zone (ITCZ) coincident with Greenland temperature fluctuations [Hughen et al., 1996]. The increased productivity (inferred from the sediment colour,

as shown in figure 8.3) is believed to have resulted from increased upwelling in the region during cold periods, when North Atlantic SST's cooled relative to the South Atlantic. The resulting pressure increase between the North and South Atlantic forced the ITCZ southward.

An alternative interpretation by Peterson et al (2000) related the observed increase in productivity during interstadials to an increased supply of river-borne nutrients to coastal waters, based on an increased iron and titanium component in the sediments. They concluded that increased precipitation, and therefore river discharge, is closely linked to the warm interstadials observed in Greenland.

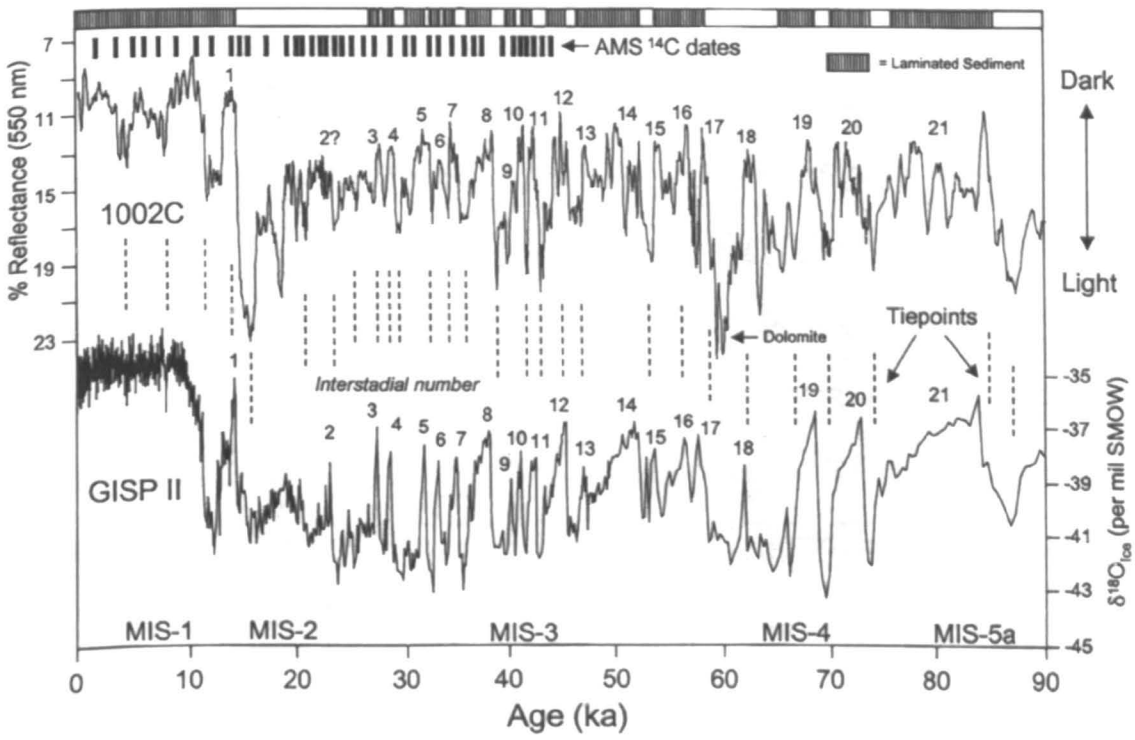

Figure 8.3. Comparison of measured reflectance in sediments in the Cariaco basin with $\delta^{18}O$ in GISP2. Figure 1 from Peterson et al., 2000. DO-8 is seen as a rapid change from light to dark sediments analogous with the Greenland temperature increase.

Pacific

In the Pacific, fluctuations in surface and intermediate waters in the Santa Barbara Basin on the Californian margin, have been linked to the abrupt changes in the atmospheric circulation over the North Pacific ((4) in Fig 8.1). These changes appear to be correlated with the temperature in Greenland [Hendy and Kennet, 1999] so too do the monsoons, with analogous shifts in summer intensity in the South China Sea ((5) in Fig 8.1). The stable isotope record (from calcite) from Hulu cave stalagmites, China, records the ratio of summer to winter precipitation, which reflects the intensity of the East Asian summer monsoon. The record indicates weak summer monsoons during cold periods (stadials) and increased summer monsoons during warm periods (interstadials) in Greenland as shown in figure 8.4 [Wang et al., 2001].

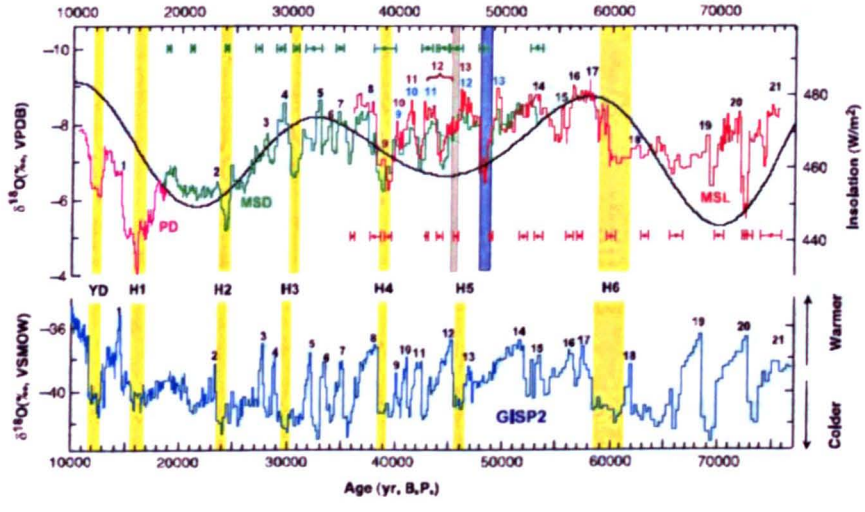

Figure 8.4. $\delta^{18}O$ of stalagmites from Hulu cave, near Nanjing (purple, green and red) and the GISP2 $\delta^{18}O$ (blue) for the last glacial period. Black curve indicates insolation at 33°N. Figure 1 from Wang et al., 2001. Overlap of two stalagmites during DO8 show an increase of almost 2‰ following Heinrich event 4.

In the western tropical Pacific ((6) in Fig 8.1) salinity changes appear to correlate with DO events, as observed from the change in $\delta^{18}O$ from planktonic foraminifera. Increased tropical salinities coincided with cold stadial periods while interstadials are associated with a salinity decrease. The magnitude of variability during DO events was in the order of 0.5 – 1 ‰, equivalent to a salinity change of 1-2 ‰ [Stott et al., 2002].

Indian Ocean

High-resolution marine sediment cores from the northwest Indian Ocean ((7) in Fig 8.1) show a strong correlation between Arabian Sea monsoon events and interstadial events observed in Greenland. The fluctuation between bioturbated intervals in the Arabian Sea sediment record (coinciding with Heinrich events, H1-6) and the dark coloured Total Organic Carbon (TOC) rich sediments (coinciding with interstadials), indicate changes in the summer monsoonal intensity, also reflected in the stable isotope record of near surface dwelling foraminifera [Shultz et al., 1998]. In Oman too, the denitrification record from $\delta^{15}N$ in marine cores from the mouth of the Persian Gulf, has been tied to the intensity of summer upwelling, associated with the Indian monsoon ((8) in Fig 8.1). Nitrification is shown to decrease during stadials in Greenland and increase, reflecting an increased summer upwelling intensity, during warm interstadials [Altabet et al., 2002]. These rapid millennial and centennial fluctuations in the intensity of the southeast monsoonal circulation, point to large scale ocean-atmosphere interactions between high and low latitudes.

Speleothem records from Socotra Island, Yemen in the Indian Ocean ((9) in Fig 8.1), an area dominated by the east African-Indian monsoon, have been used to reconstruct

changes in monsoon precipitation during DO events. In tropical settings the isotopic ratio of precipitation (from calcite) is strongly anti-correlated to the amount of rainfall. Thus in the Socotra Island stalagmites, the oxygen isotope record reflects changes in the amount of rainfall and to a lesser extent, the cave temperature. The record shows high latitude cooling corresponds to a decrease in low latitude precipitation. The rapid high latitude warming during DO12 (similar in magnitude to DO 8) is seen as a sudden increase in the precipitation with the transition from dry to wet conditions taking place in just 25 years [Burns et al., 2003].

The Southern Ocean and Antarctica

The Southern Ocean and Antarctica does not appear to have played a role creating these large climate oscillations with most of the 24 interstadial events observed in Greenland, uncorrelated with changes in the Antarctic climate. Only the largest oscillations, of greatest magnitude and lasting longer than two thousand years, may be associated with warmer periods in East Antarctica [Bender et al., 1994], only eight of which are inferred from the Vostok isotopic record [Jouzel et al., 1987]. Blunier and Brook (2001) related seven warm events from the Byrd ice core record from West Antarctica (figure 8.5 labelled A1 – A7) with DO events 8, 12, 14, 16/17, 19, 20 and 21. As observed in the Antarctic isotope and methane records from the Byrd ice core, the warmings appear to precede DO events in Greenland by 1500 to 3000 years [Blunier and Brook, 2001] with the onset of the DO events leading to a cooling in Antarctica. Variations in the isotopic composition of calcium carbonate of foraminifera in deep-sea sediments have been used to infer diminished global ice volume during these Antarctic warm periods [Shackledton and Pisias, 1985]. However in general an anti-phase relationship exists between the northern and

southern hemisphere known as the "bipolar see-saw" where Antarctic temperatures gradually increased when Greenland temperatures decreased [Broecker, 1998; Blunier and Brook, 2001].

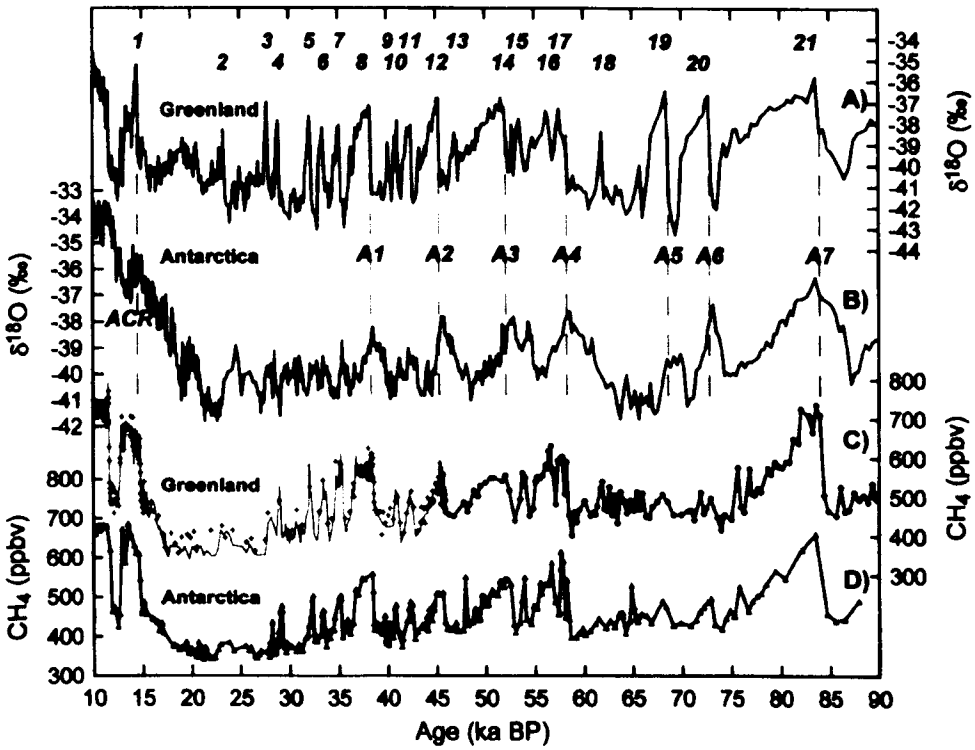

Figure 8.5 Isotopic and CH_4 data from Greenland and Antarctica on the GISP2 time scale. Fig 1 in Blunier and Brook (2001). Dashed lines indicate the onset of major D-O events. (A) $^{18}O_{ice}$ from GISP2, Greenland. (B) $^{18}O_{ice}$ from Byrd station, West Antarctica. (C) CH_4 data from GISP2 and GRIP. Crosses and dots are from GISP2; the solid gray line is from GRIP. The solid line runs through the data used for the synchronization: GISP2 (black line) up to 45.5 ka and GRIP data (gray line) from 45.5 ka to the Holocene. (D) CH_4 data from Byrd station.

Stocker and Johnsen (2003; 2005) applied a simple, purely thermodynamic, thermal bipolar sea-saw model to the stable isotope records from the GRIP and Byrd ice core. It is suggested that strong inter-hemispheric coupling can explain much of the variation observed in the Antarctic cores, with not just the prominent DO events represented. The characteristic timescales on which thermal dampening occurs

showed greatest correlation for 1,000 to 1,500 years, suggesting a long adjustment period in the Southern Ocean or an additional heat reservoir during the last glacial such as additional changes in the northern and southern terrestrial ice sheet extent and associated sea- level rise [Stocker and Johnsen, 2003; corrected 2005].

Taylor Dome in East Antarctica is the exception, apparently showing contrasting results to those of Vostok (Vostok station, 1000 km from South Pole in central East Antarctica, (10) in Fig 8.1) and Byrd (Byrd station West Antarctica, (11) in Fig 8.1). The rapid warming at the end of the last glacial period and the Bølling-Allerød to Younger Dryas transition at Taylor Domes ((12) in Fig 8.1) near coastal site from the western Ross Sea, East Antarctica, appears synchronous with changes in the Northern Hemisphere. Large fluctuations in the geochemical record during the last glacial-interglacial transition at Taylor Dome are reminiscent of those in Greenland with a similar magnitude of warming inferred from the isotope record. Other Antarctic ice cores do not record the abrupt warming into the Holocene seen in Greenland, but instead show a gradual warming known as the Antarctic Cold Reversal (ACR), which preceded the Younger Dryas in Greenland by at least 1,000 years. Dating uncertainties in the Taylor Dome core have been questioned by Mulvaney et al (2000) (based on the calcium record from Dome C) suggesting that the main warming at the near-coastal site of Taylor Dome was slower than reported previously, and similar to that of central Antarctica.

Theories behind Dansgaard-Oeschger events

The high heat capacity of the oceans relative to the surrounding land modulates the Earth's daily, seasonal, and inter-annual temperature fluctuations. The oceans act as a

conveyor transporting heat from the equator toward the poles by a process known as Thermohaline Circulation (THC). The strength of THC is primarily controlled by density, which is a function of temperature and salinity, and the wind curl stress. [See Chapter 1, Role of the oceans]. The meridional overturning in the north Atlantic is dominated by freshwater forcing from the Nordic seas, and subsequent North Atlantic Deep Water (NADW) formation. During Heinrich events, characterized by massive ice rafting, the associated influx of freshwater to the North Atlantic resulted in a reduction of NADW and THC shutdown. The resulting cooling of the ocean and atmosphere has been simulated in a range of models from those of reduced complexity to fully coupled, three-dimensional AOGCMs [Stocker et al., 1992; Schiller et al., 1997; Ganopolski and Rahmstorf, 2001].

Intensified formation of NADW and THC following Heinrich events has been used to explain the onset of DO events in Greenland. Due to the expansion of sea ice during glacial periods the formation of NADW was shifted southwards and was generally slow. If the formation of NADW increased, the effect on the Greenland climate and landmasses adjacent to the North Atlantic would be extreme and rapid [Broecker, 1985; 1987].

The role of the Tropics

The combined records from the tropical Atlantic (Fig 8.3) [Hughen et al., 1996; Peterson et al., 2000], the tropical Pacific [Bard et al., 1997; Stott et al., 2002], the Indian ocean [Burns et al., 2003] and Asia [Wang et al., 2001] support the theory that these large scale abrupt climate oscillations, observed in the Greenland ice core record may have involved the tropics. The abrupt warming of the tropical deep basin water is

attributed to the strengthening of the THC northerlies indicating a tropical precursor to DO events and maybe even a tropical trigger [Hendy et al., 2002; Broecker., 2003; Denton et al., 2005]. The tropics can certainly also act as an amplifier for climate change because the most important atmospheric greenhouse gas is water vapour, the majority of which comes from the tropical ocean.

Dansgaard-Oeschger event 8

Dansgaard-Oeschger event 8 is one of the prominent interstadials of the last glacial period observed during Marine Isotope Stage 3 (MIS 3), an interval characterized in the Northern Hemisphere by intermediate ice sheet size, radiation receipt and atmospheric CO_2 concentrations. It is observed approximately 35 kyr ago according to the GRIP dating (ss09 timescale) [Johnsen et al., 2001] and 38 kyr ago according to the GISP2 dating [Meese et al., 1997]] however large dating uncertainties exist at this depth. The new GICC05 dating initiative has given an earlier onset of 38.4 kyr B2K (before 2000, 38.35 kyr BP 1950) [Andersen et al, submitted] based on annual layer counting, however the error is still ± 1460 years at this depth. It has been suggested by $^{234}U/^{230}Th$ dating of ocean sediments that an error of more that 3,000 years exists in both the GRIP and GISP2 timescales by 42 kyr BP [Burns et al., 2003; 2004]; however the new GICC05 age-scale has been matched to ^{10}Be at 41 kyr BP [Andersen et al., submitted]. Stalagmites from southwest France ((13) in Fig 8.1) also dated using $^{234}U/^{230}Th$, show a regular decrease in $\delta^{13}C$ corresponding to DO-8 between 39.4 to 36.2 kyr BP [Genty et al., 2003].

In the ice core records at the start of DO-8 the climate appears to have shifted approximately 16°C from a period of extreme cold to a more moderate glacial

temperature where it remained latched for several thousand years. Analogous decreases in calcium, which is a proxy for dust, and sea salt species, imply a dramatic alteration in the atmospheric circulation [Mayewski et al., 1994] while the increased atmospheric composition of greenhouse gases N_2O and methane indicates a global response to the temperature change. The geochemical record has been extended in the more recent NGRIP core [NGRIP members, 2004] and is being used to improve the glacial ice chronology.

DO-8 follows Heinrich event 4 (H4), which was a period of massive ice rafting observed as a period of extreme cold in the Greenland ice core records and as decreases in SSTs in ocean sediment records. SSTs in the subtropical North Atlantic rose by as much as 2-2.5°C following Heinrich event 4 into DO-8 (Fig 8.2) [Sachs and Lehman, 1999], close to the reconstructed difference between the glacial and present day [Sachs and Lehman, 1999; CLIMAP members, 1981]. Along with changes during DO-12, this is the largest fluctuation observed during MIS 3.

8.2 Aims

The aim of this part of the thesis is to obtain a new high-resolution chemical record from the NGRIP ice core at the onset and termination of interstadial 8 (DO-8). The current best resolution geochemical record of glacial events is in the order of 2 cm from the CFA of the NGRIP core. The annual layer thickness at these depths is approximately 1-2 cm; therefore a sub-annual resolution is only possible by obtaining discrete samples more closely spaced than this. A new cutting method has been developed to produce discrete samples of 2 mm resolution. This ice was analysed

using ion chromatography using a novel sequential flow technique developed in this thesis, to enable the detection of five major anions and four major cations from a sample volume of less than 1 ml. The new methods are described in the Methods Chapter (Chapter 2).

The new record is used to show the rate of change of chemical deposition over Greenland during these large and abrupt transitions. Annual layer counting of the new high-resolution record is used to determine the duration of the transitions, and possible seasonality change.

In addition, a new high-resolution (2 cm) oxygen and deuterium isotope record was measured at NIGL Keyworth, from the NGRIP ice core into and out of DO-8. The record is used to determine the deuterium excess over the transitions, thus improving our understanding of possible moisture source changes during these rapid warmings.

A total of 10 meters of ice from the NGRIP core has been selected between 2021-2028 meters to investigate the cooling, and between 2068.5- 2073 meters to investigate the warming, shown in figure 8.6.

For ease of reference the different sections of ice analysed in both the warming and cooling transitions have been assigned a letter, which will be referred to throughout the following chapters. The warming transition consists of two distinct parts (as described above); the section before the warming and the section after warming. The ice from before the warming (2069.95 – 2073 m) is the oldest and has therefore been

defined as section A. The ice after the warming (2068 – 2069.95 m) has been defined as section B.

In the cooling transition, two sections of ice were taken from the total ice available. The oldest ice of this section (2026.2 – 2028.2 m) is referred to as section C and the youngest section D (2021.2-2022.9 m). The locations of the four sections are shown in figure 8.7, using the oxygen isotope records from NGRIP [NGRIP members 2004] during DO-8.

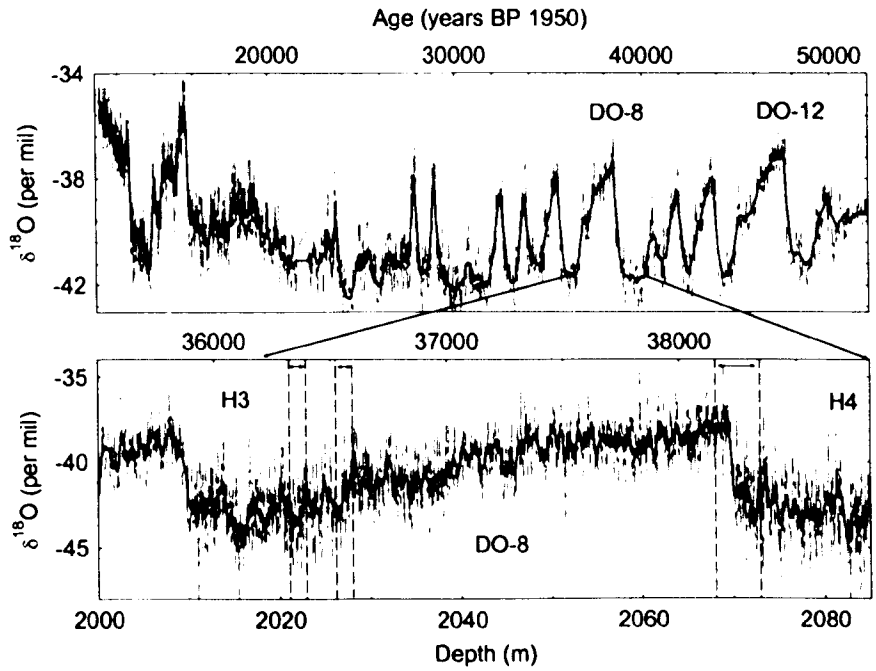

Figure 8.6 Oxygen isotope record from NGRIP between 10,000 and 50,000 years BP (top) and during DO-8 (Bottom) on the GICC05 age-scale [Andersen et al., 2006] bag averages (grey) and smoothed by a factor of 10 (running average) (blue) [NGRIP members, 2004]. Dashed vertical lines and red arrows on bottom graph indicate the sections of ice analysed in this thesis.

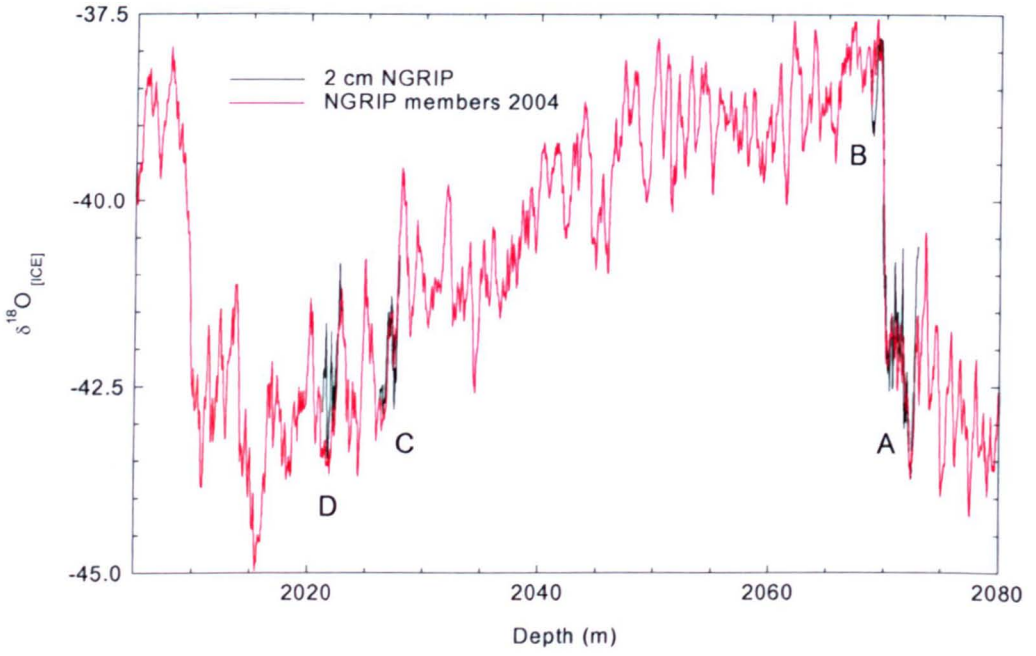

Figure 8.7. Locations of ice sections described in this thesis. NGRIP oxygen isotope record (red) with the 2 cm resolution oxygen isotopes from this thesis overlaid (black) smoothed to approximately 20 cm resolution.

Chapter nine

DO-8: Isotopes

DO- 8: Isotopes

9.1 Introduction

The distribution of stable water isotopes HDO and $H_2{}^{18}O$ and the linear relationship between mean annual isotope content of precipitation and mean annual temperature at the precipitation site has been described in chapter 4. The isotope record from Greenland has been used to derive temperatures during the glacial, and show the existence of the large-scale temperature jumps associated with Dansgaard-Oeschger events.

9.2 Warming transition

The warming transition at the start of DO-8 is seen as an abrupt temperature increase from extreme glacial temperatures to intermediate warm temperatures. The new isotope record (measured at NIGL as described in chapter 2) has improved upon previously published data of this period with a 2 cm resolution record corresponding to approximately 1-2 years (based on an average layer thickness of 1.8cm, see chapter 11). Deuterium, $\delta^{18}O$ and deuterium excess have all been measured, with reported errors of ± 1.0 ‰ for δd, ± 0.05 ‰ for $\delta^{18}O$ and ± 1.4 ‰ for deuterium excess.

At the resolution shown in figure 9.1, oxygen and deuterium show a gradual increase from extreme negative values to less negative values; starting around 2070.10 m (indicated by the vertical dashed lines in fig 9.1). Values do not appear to level off in this warmer state until after 2069.6 m (marked as (1) on figure 9.1)(approximately 20-25 years from the start of the warming, according layer counting). This appears to be

the most robust change in the isotope record, as values remain latched in this state for many hundred years, however there are several large fluctuations occurring in the record prior to the warming transition.

Oxygen and deuterium

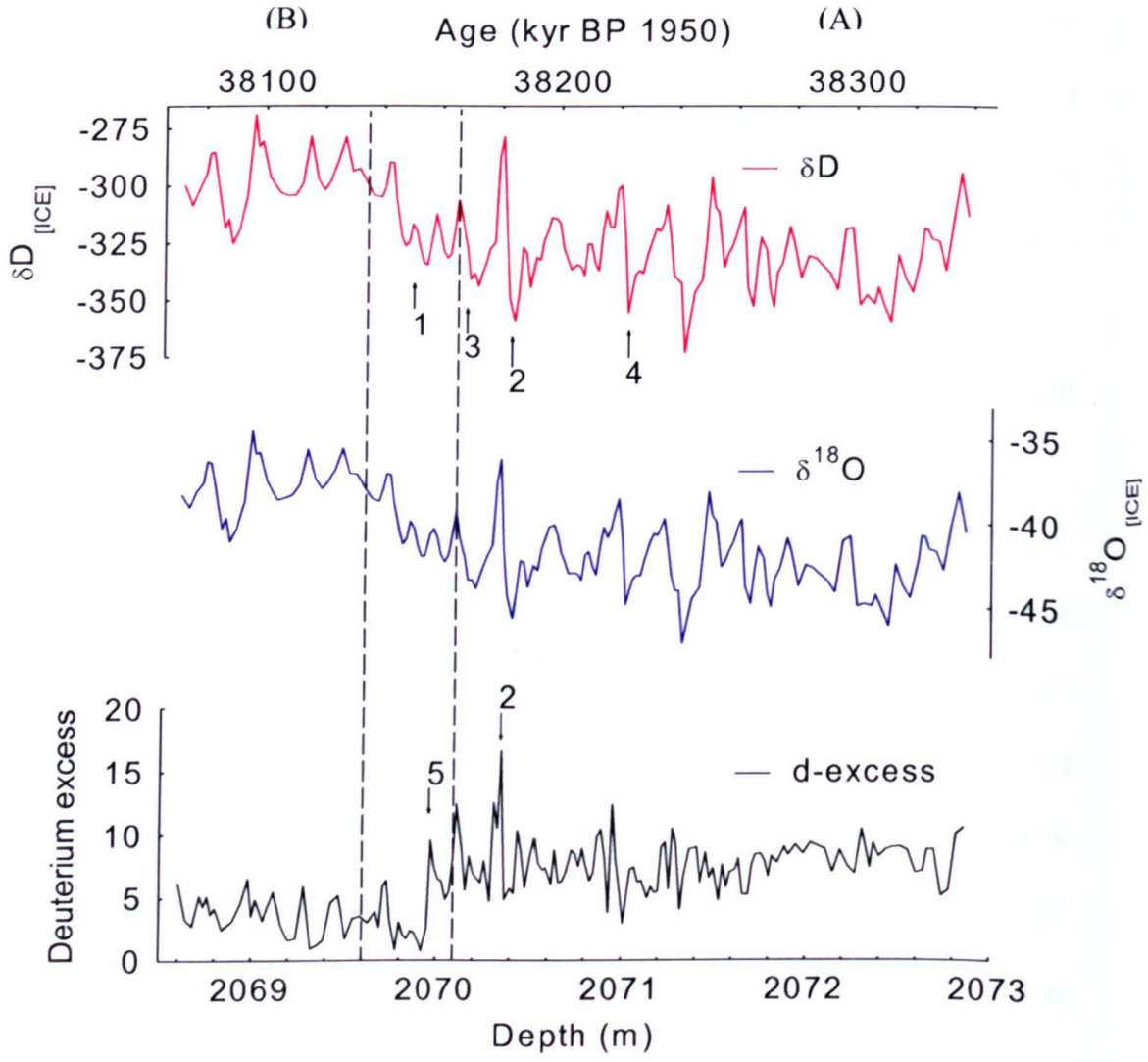

Figure 9.1. Isotopic composition during the warming transition at NGRIP, δD (red), δ ^{18}O (blue) and deuterium excess (black) all at 2 cm resolution between depths 2068.6 – 2073 m and on the GICC05 age-scale. Vertical dashed lines and numbers 1-6 indicate depths of interest referred to in the text. A and B refer to locations of ice shown in figure 8.7 (p.190) and referred to in the text.

Large fluctuations in the $\delta^{18}O$ and δd are observed in the period prior to the onset of the warming transition. Between 2070.33 – 2070.4m ((2) in fig 9.1), $\delta^{18}O$ and δd increase from among the lowest values in the record ($\delta^{18}O$, 45.6 ± 0.05 ‰) to almost the highest ($\delta^{18}O$, 36.1 ± 0.05 ‰). It is unlikely that this truly reflects a temperature change because this would equate to an increase of 28.3 °C[12], to temperatures that are just 0.84 °C colder than present day temperatures at Summit in just four years. These jumps are rapid and in some cases represent just 2-3 data points however, if real they could possibly be an indication of changes in the source or source location resulting in a shift in the relationship between temperature and $\delta^{18}O$.

After this point, levels return to within the expected range prior to this but only briefly before rising again slowly. This section could possibly be described as the onset of the warming and is certainly a significant event in the record but it is only after this that values rise steadily, as demonstrated by the lack of extreme negative values.

The transition at the onset of DO-8 can be observed graphically (Fig 9.1), however in order to determine the exact point of change a more robust method using running means and random variation was used.

Method

The population from which the δd, $\delta^{18}O$ and deuterium excess data arise have a distribution that is approximately "normal" (or Gaussian), as shown in figure 9.2 $\delta^{18}O$. Therefore the standard deviation provides a useful basis for interpreting the data in terms of probability. A range covered by one standard deviation above the mean

[12] Using a glacial calibration 0.33‰ /°C [Cuffey et al., 1994]

and one standard deviation below it ($x \pm 1\sigma$) includes about 68 % of the observations; a range of two standard deviations above and two below ($x \pm 2\sigma$) about 95 % of the observations; and of three standard deviations above and three below ($x \pm 3\sigma$) about 99.7 % of the observations.

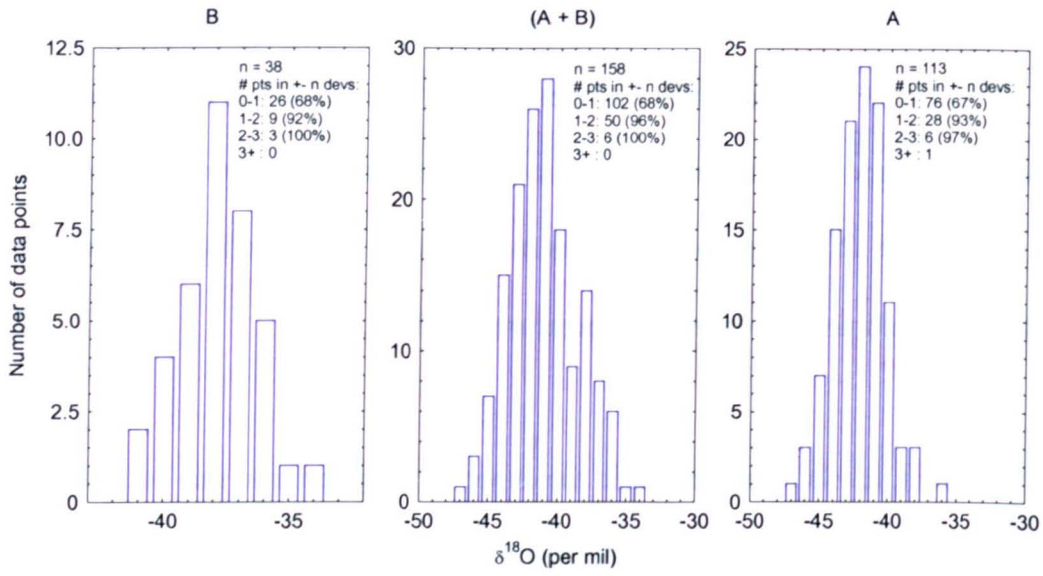

Figure 9.2 Gaussian distribution of $\delta^{18}O$ after the warming (B), during the whole transition (A+B) and before the warming (A).

The δd, $\delta^{18}O$ and deuterium excess records were tested, (figure 9.2 for $\delta^{18}O$) to show that all three records follow a normal (Gaussian) distribution, with 68.4 %, 65.8% and 68.4% of observations from δd, $\delta^{18}O$ and deuterium excess respectively found in the range less than or equal to one standard deviation[11].

The record was divided into 50 cm segments and the average and standard deviation calculated (figure 9.3). The point at which the average of one segment is no longer within the assigned limit ($\geq 1\ \sigma$) of its neighbour is deemed significant, and marked as a transition.

[11] Determined statistically form each record where n=158 and the number of observations in the range $\pm 1\sigma$ is 107, 104 and 108 for δd, $\delta^{18}O$ and deuterium excess respectively.

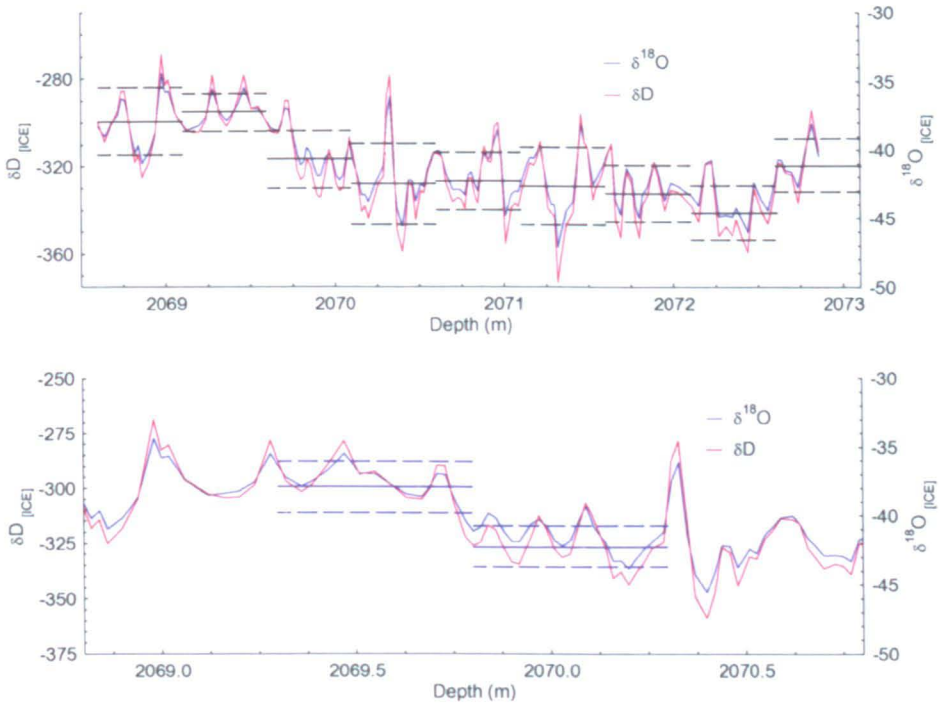

Figure 9.3. Oxygen (blue) and deuterium (red) for the whole warming transition (top) and just the transition step (bottom). Running averages indicated by solid horizontal lines, and ± one standard deviation indicated by horizontal dashed lines, for each 50 cm section.

The segments were shifted by 5 cm throughout the record in order to determine the greatest separation between segments and therefore the most robust transition point. As shown in figure 9.1, the transition does not occur in one single jump thus the onset and termination of the warming has been determined using the running average method.

Onset of the warming transition:

The segment between 2069.65-2070.15 m is significantly higher ($\geq 1\ \sigma$) than its neighbouring segment, between 2070.15- 2070.65 m (although to a lesser degree than the termination of the transition) and is assigned as the onset of the warming transition.

Termination of the warming transition:

The termination transition occurs at 2069.8 m with a jump so large that the standard deviation of both segments is no longer within the standard deviation of its neighbour (fig 9.3). After this point values remain relatively constant and is considered the termination of the warming transition.

The warming transition has been defined as starting at depth 2070.15 m and terminating at 2069.80 m. During this period the values of $\delta^{18}O$ (and δd) increase from a background average of 42.2 ‰ (329.6 ‰ deuterium) to an average of 37.7 ‰ (297.9 ‰ deuterium), which if reliably calibrated to temperature equates to an increase of 15 °C in less than 16 years[13].

Deuterium excess

Deuterium excess is a measure of the relative proportions of ^{18}O and ^{2}H contained in water and can be visually depicted as an index of deviation from the global meteoric water line (MWL: d= 10) in $\delta^{18}O$ versus $\delta^{2}H$, (see Chapter 4).

The deuterium excess was determined for the warming transition and is shown in figure 9.4. Unlike the oxygen and deuterium record, the warming transition is observed in the excess as a single large jump at 2069.95 m ((5) fig 9.1). Before this, there are several large and abrupt jumps, coincident and in phase with the $\delta^{18}O$ and δd record, such as at 2071.0 m ((4) fig 9.1), where there is a single large jump increasing 9.5 ‰. An even larger jump occurs at 2070.35 m ((2) fig 9.1), where values reach an

[13] Based on annual layer counting described in chapter eleven.

absolute maximum of 16.6 ‰; an increase of 11.8 ‰ from previous levels in just 2 cm (~1-2 years[13]).

A similar jump is also observed in the section defined as the onset of the warming for oxygen and deuterium but the transition that defines the change from cold to warm conditions is seen as at a depth of 2069.95 m, when the deuterium excess abruptly drops by 7 ‰. After this period the deuterium excess remains low with values averaging 3.4 ‰.

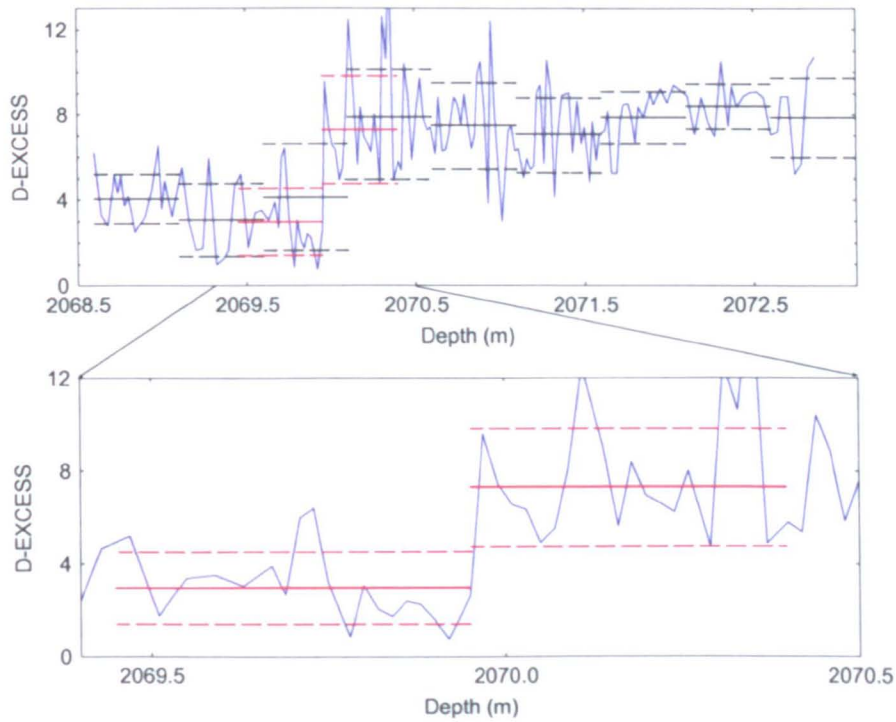

Figure 9.4. Locating the warming transition in deuterium excess using running averages.

The deuterium excess is shown in figure 9.5, $\delta^{18}O$ versus $\delta^{2}H$ for the period before warming (red squares) and the period after warming (blue circles). The period before warming is shown as a shift away from the global meteoric water line (MWL = 10), to a state of enhanced evaporation. This decrease in deuterium excess is indicative of a

change in the source location or conditions to colder waters, which is unexpected at a time when the temperatures (as inferred from the $\delta^{18}O$) in Greenland are increasing.

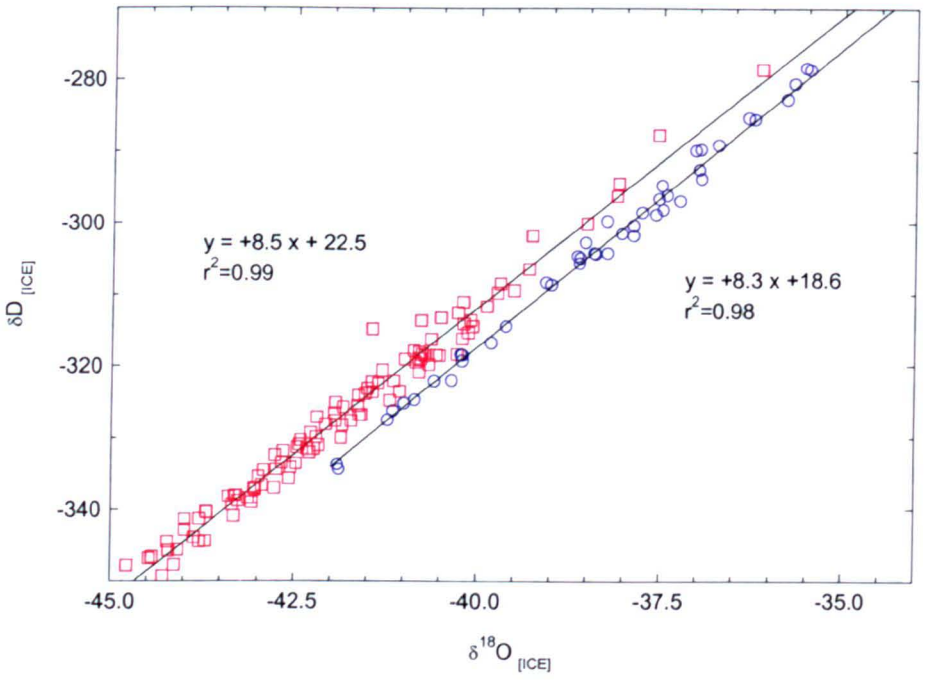

Figure 9.5. The deuterium excess as depicted by $\delta^{18}O$ versus δD, for the period prior to warming (red squares) and the period after warming (blue circles). Both significant at <1% level.

	Depth (m)		Change	
	Onset	Termination	‰	T (°C)
Oxygen	2070.15	2069.80	+ 4.5 ± 0.05	+ 15
Deuterium	2070.15	2069.80	+ 31.7 ± 1	
D-excess	2069.95		- 7 ± 1.4	

Table 9.1 Locations of the onset and termination of warming transitions (determined using running averages) in the $\delta^{18}O$, δD and deuterium excess (D-excess) records and the changes in ‰ (with analytical error) and temperature[12].

9.3 Cooling transition

Deuterium, $\delta^{18}O$ and deuterium excess were measured from two sections during the cooling transition; the first, between 2026.2-2028.2 m and the second between 2021.2 -2022.9 m (section C and D in fig 8.7).

Deuterium, $\delta^{18}O$ and deuterium excess for both sections of the cooling transition are shown in figure 9.6. There is little variation in isotopic composition or stability between both sections of ice during the cooling transition. This is shown by average $\delta^{18}O$ values in C, which are just 1.15 ‰ less negative than D and standard deviations of 1.78 and 1.80 respectively. There is a large amount of deviation during both sections (due to the decreased layer thickness in the colder ice); however none exceed the upper limit of its neighbour when using the running average method.

As seen in figure 8.7, the lower resolution record from NGRIP [NGRIP members 2004], the cooling appears gradual with a series of large jumps lasting several hundred years until a minimum is achieved. There are no abrupt jumps of the magnitude observed during the warming transition; certainly no significant changes appear during the sections of ice chosen for analysis.

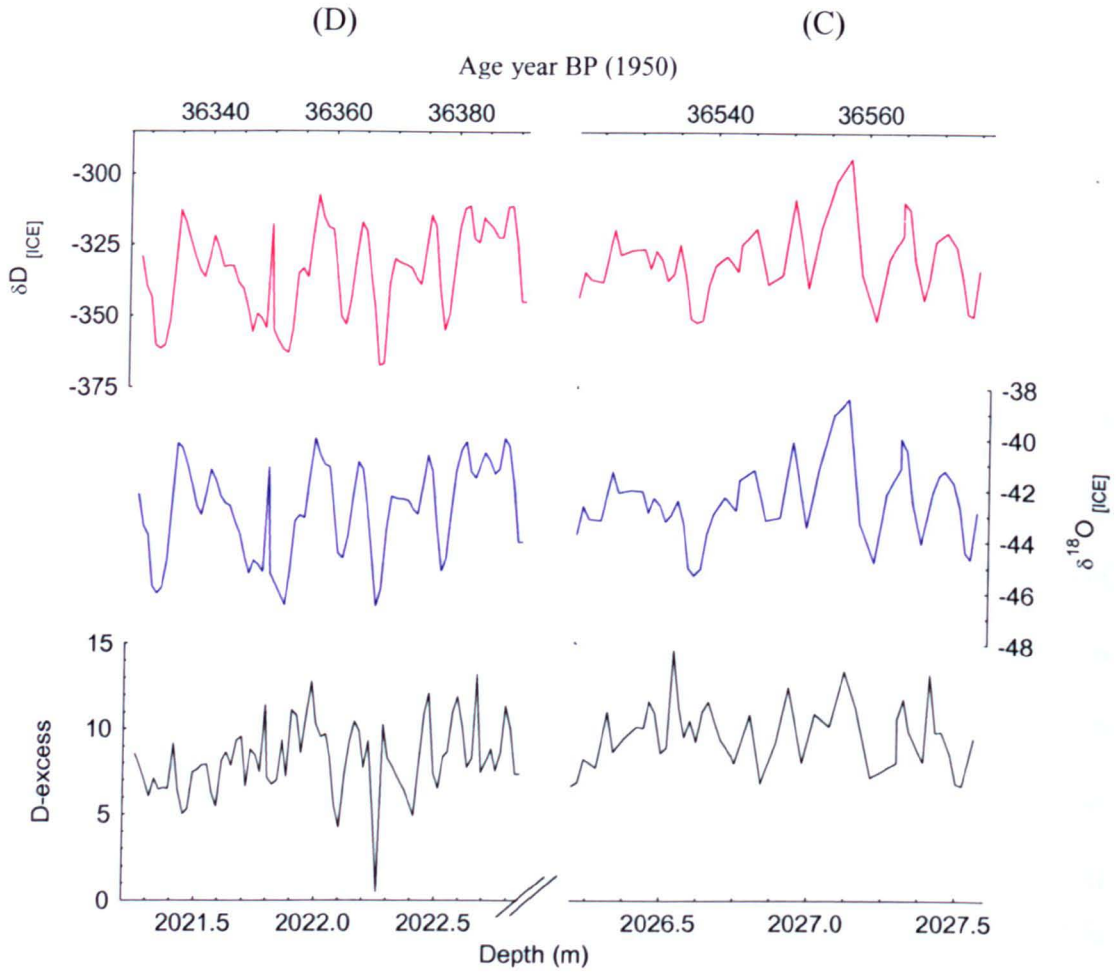

Figure 9.6. Deuterium (red), $\delta^{18}O$ (blue) and deuterium excess (black) at 2 cm resolution during the cooling transition on the NGRIP depth and GICC05 age-scale. D and C refers to locations of ice shown in figure 8.7 (p.190) and referred to in the text.

9.4 Comparison between warming and cooling

The isotopic composition and temperature difference from present values at Summit Greenland (ΔT) for each of the sections are shown in table 9.2. The results from NGRIP during DO-8 show a huge temperature range (if the $\delta^{18}O$ is assumed to be a reliable indicator of temperature) from a minimum of 46 °C colder than present day temperatures at Summit to just 0.85 °C colder.

	$\delta^{18}0$ (‰)	δD (‰)	D-excess	ΔT (°C)
	Section A			
Average	-42.1	-329.2	7.73	-20.5
Standard Deviation	1.9	15.7	2.0	7.9
	Section B			
Average	-38.3	-303.4	3.4	-7.0
Standard Deviation	1.8	15.7	1.6	5.5
	Section C			
Average	-41.7	-324.9	8.7	-20.4
Standard Deviation	1.8	14.5	2.2	17.5
	Section D			
Average	-42.8	-334.6	8.2	-23.6
Standard Deviation	1.8	15.6	2.1	8.4

Table 9.2. Average and standard deviation for oxygen, deuterium, deuterium excess and temperature[12] difference from present day summit values (-35.2°C) for all four sections of ice shown on figure 8.7 (p.190).

Ice section	A	B	C	D
A		-13.5	-0.1	3.2
B	13.5		13.3	16.6
C	0.1	-13.3		3.3
D	-3.2	-16.6	-3.3	

Table 9.3. Difference in temperature (°C) between the different sections of ice. Ice sections shown in figure 8.7 (P.190).

9.5 Summary of DO-8 Isotopes

The isotope record from NGRIP at the onset of DO-8 shows an abrupt change in $\delta^{18}O$ and deuterium, from extreme cold glacial temperatures to relatively warm temperatures, lasting approximately 16 years. If correctly representing temperature this equates to a change of almost 15 °C. The change in deuterium excess is much more rapid occurring in a single step of less than 2 years, during the middle of the $\delta^{18}O$ and deuterium transition. The shift from higher to lower values at the transition indicates a move to a cooler source location, with decreased evaporation.

The cooling transition, as observed from the lower resolution NGRIP record, is more gradual than the onset of DO-8 with small decreases in the isotope values but not of the magnitude of the warming transition.

Chapter ten

DO-8: Chemistry

DO-8: Chemistry

10.1 Introduction

The chemical deposition observed in Greenland was described in chapter 5. The sources of airborne particles and chemical compounds of marine, continental, biological, atmospheric, extraterrestrial and volcanic origin were assumed to be essentially the same during the last glacial as during the Holocene. The more northerly location of NGRIP compared to the Summit cores, GRIP and GISP2, has been shown to give different deuterium excess signals [Masson-Delmotte et al., 2005], attributed to alternative moisture sources or differences in advection toward Greenland. The NGRIP site is believed to receive a larger portion of moisture from remote sources, which may alter the isotope signal in NGRIP, compared to the more southern ice core sites. However, the majority of continental deposition at Summit and NGRIP is from long-range sources; believed to be transported from Asia, at several kilometres altitude, by the westerly jet stream [Fuhrer et al., 1999]. The source of marine aerosols is more local to Greenland and possible differences may arise between the amount to reach GRIP and NGRIP however the location can still be considered the same. Therefore analysis of chemical compounds related to primary continental and marine aerosols found in NGRIP have been considered tracers of atmospheric content [De Angelis et al., 1997; Barrie et al., 1996] in the same way as they were in GRIP.

The changes in chemical deposition, which accompanied Dansgaard-Oeschger events during the glacial period, are much greater than during the Holocene, as shown by the calcium records from GRIP (figure 10.1) [Fuhrer et al., 1999].

The large changes in calcium deposition, which are correlated to the abrupt temperature jumps, seen in the isotope record (red curve in figure 10.1), have been attributed to changes in the source strength, transport and residence time of continental aerosols [Fuhrer et al., 1999]. Changes in snow accumulation during Dansgaard-Oeschger oscillations suggest that rapid changes in the position of storm tracks occurred, which may have resulted from a possible shift in the jet stream [Dansgaard et al., 1993; Johnsen et al., 1995]. Changes in the conditions at the source location (Asia) are also required to explain the near simultaneous changes with temperature. As described in Chapter 7, a review of the literature, large changes in monsoon intensity appear correlated with DO events observed in Greenland. The alterations in local wind conditions in Asia could be responsible for increased mobilization and uplift of continental aerosols.

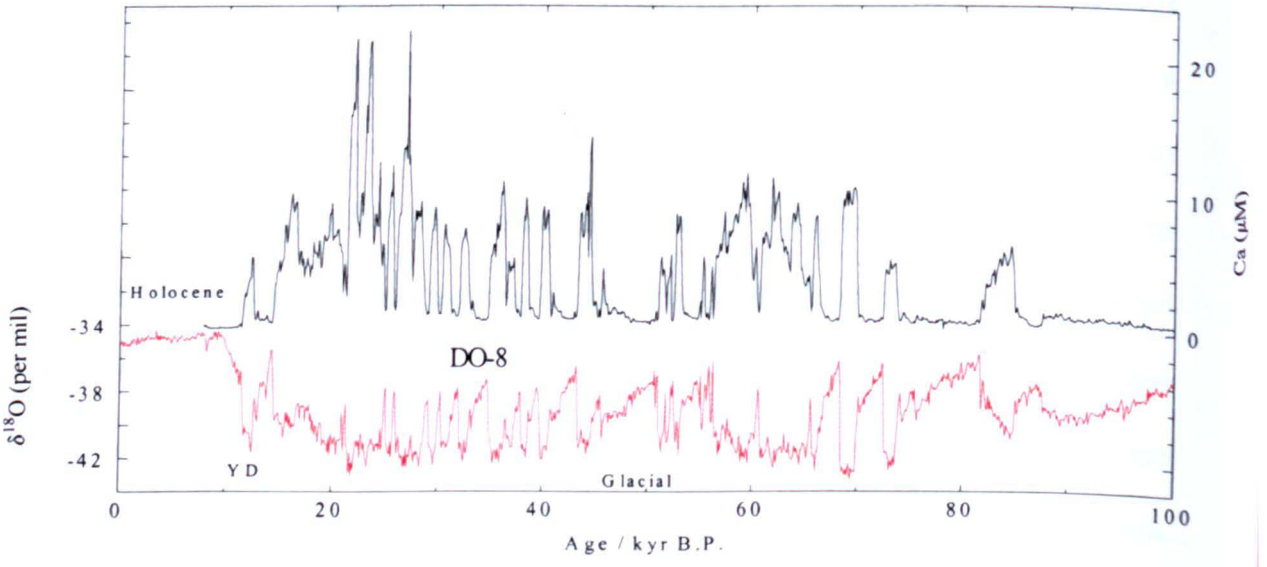

Figure 10.1. Calcium and $\delta^{18}O$ from GRIP during the last glacial period. Fuhrer et al., 1999 (figure 1)

Investigation into primary aerosols during the last climatic cycle by de Angelis et al., (1997) concluded that the marine component of sodium, Na_m, is a good primary tracer

of sea-salt aerosol. It was shown to exhibit a similar inverse relationship with $\delta^{18}O$, as found in calcium. The chloride to marine sodium weight ratios was shown to increase with temperature and is expected to be much closer to bulk seawater during the glacial than was observed during the Holocene.

10.2 Chemistry results – Warming Transition

In this project, almost three thousand discrete samples were taken from the NGRIP core between depths of 2021.25-2022.9 m (D), 2026.2 – 2027.5 m (C) and 2068.55 – 2071.3 m (A+B). The samples were cut as described in the method section (Chapter 2) and analysed using ion chromatography. The resulting high-resolution chemical record from NGRIP has been used to investigate alterations in concentrations and therefore amount of deposition to Greenland during the warming transition into DO-8 and the cooling transition after it. The continental and marine components are compared, during the transition, so too are the weight ratios with bulk seawater.

The depth at which the warming transition is observed in the chemical record is determined and compared with that found in the isotopes. The duration of the transition is calculated for the first time using annual layer counting of the chemical record, described later in chapter 11.

The combined chemistry data shows a clear transition from high concentrations with large inter-annual variability to a period of lower concentrations and a decreased variability. The chemistry has been compared to the oxygen, deuterium and deuterium excess to show that the highest concentrations in all species occur when the isotopic composition is most negative, indicating colder conditions. The rapid warming,

indicated by the isotopic record corresponds to a decrease in concentration of all species.

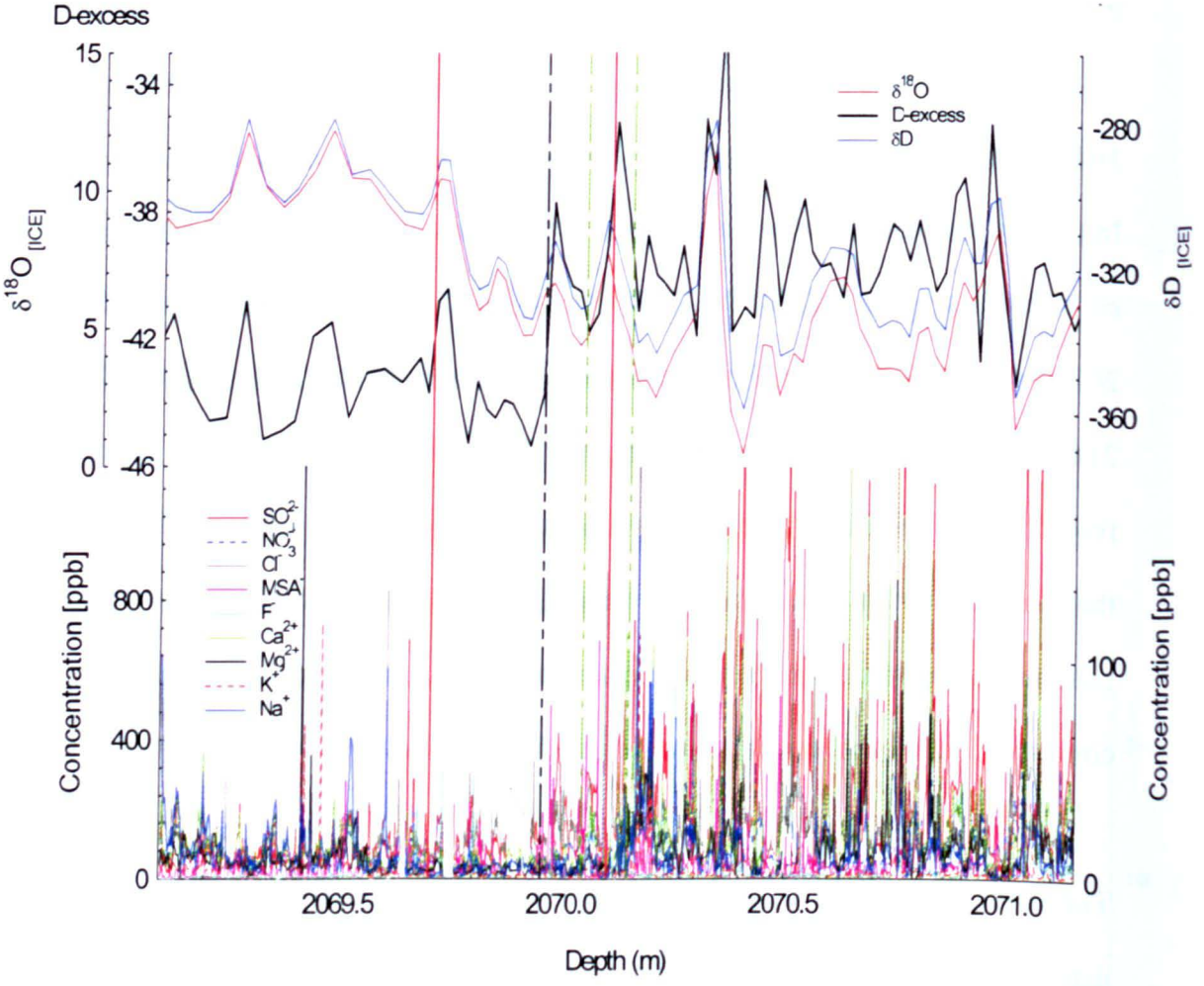

Figure 10.2. Top; Oxygen (red), deuterium (blue) and deuterium excess (black) at 2 cm resolution. Bottom; total chemistry at 2 mm resolution. Vertical lines indicate the onset and termination as determined in $\delta^{18}O$, and deuterium (red solid lines), the chemistry (dashed green) and the onset of the deuterium excess (single dashed black line), discussed in this chapter.

During the warming transition, chemical deposition changes in rapid steps reminiscent of the isotope record. However the point at which the transition terminates and constant interstadial concentrations are achieved is considerably earlier than the point at which temperatures stabilize. This is shown in figure 10.2 and 10.3,

for the total chemical record with the deuterium excess transition marked as a vertical dashed line at 2069.95 m.

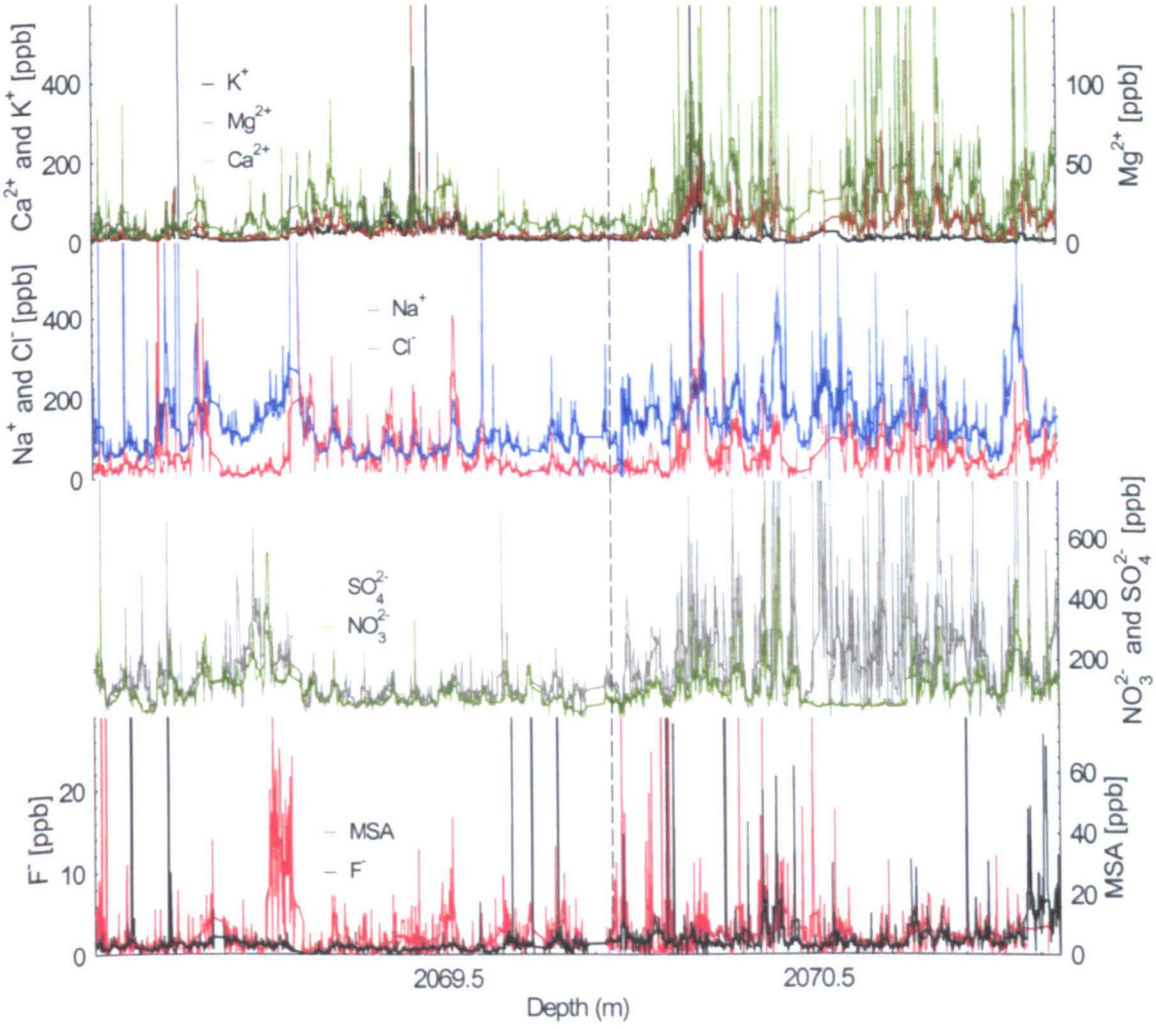

Figure 10.3. Chemical deposition in Greenland during the warming transition. Top: continental deposition, calcium (green), magnesium (brown) and potassium (black). Second from top; Marine deposition, sodium (red) and chloride (blue). Second from bottom: Sulphate (grey) and nitrate (green). Bottom: methylsulphonate (red) and fluoride (black). All data are shown in ppb at 2 mm resolution (thin coloured lines) and smoothed to annual resolution (thick coloured lines, based on an average annual layer thickness of 1.18 cm). Vertical dashed line indicates the transition (onset) in deuterium excess.

Continental component

Calcium is a proxy for dust and may be considered a primary tracer for continental deposition to Greenland [O'Brien et al., 1995; Chapter 5 this thesis]. The terrestrial component of calcium and magnesium (considered a secondary continental tracer) can be calculated, providing the marine component has been accounted for (following equations 5.1& 5.2). The difference between the marine and continental components of calcium is shown in figure 10.4 and compared with magnesium in table 10.1. The average values across the whole warming transition show that 98% of the total calcium and 92% of the total magnesium is of terrestrial origin, which confirms that calcium and magnesium may be considered primary tracers of continental deposition.

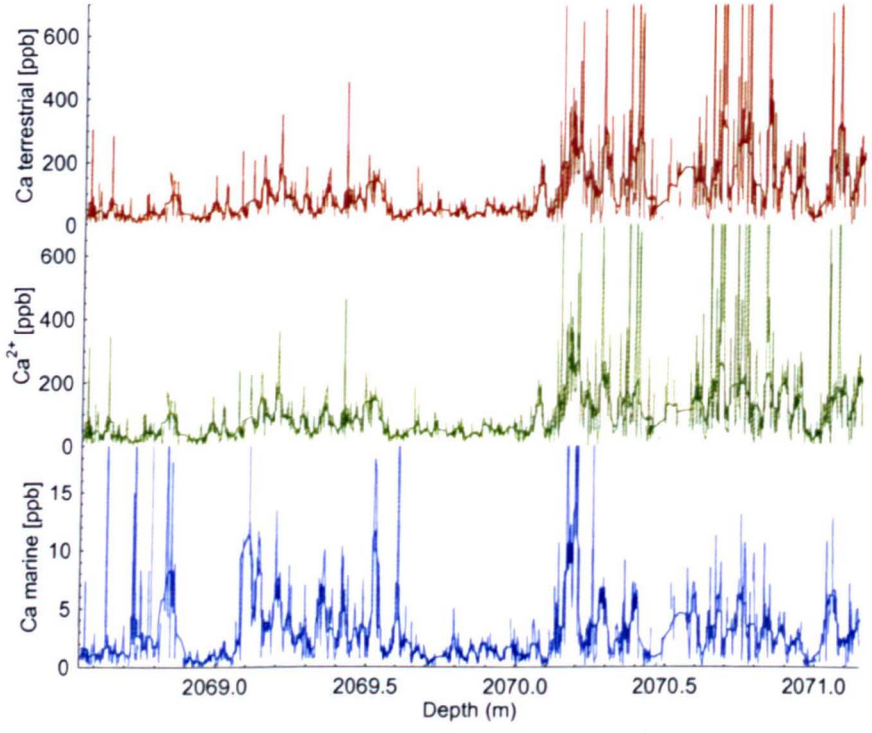

Figure 10.4. Terrestrial calcium (brown), total calcium (green) and marine calcium (blue) for transition 1.

	Ca^{2+}	Ca^{2+} Terrestrial	Mg^{2+}	Mg^{2+} Terrestrial
Average	112.5	110.2	10.5	9.7
Standard Deviation	146.0	144.7	13.2	12.8
% of total		98.0		91.9

Table 10.1. Terrestrial and marine component of calcium during the warming transition.

Marine component

Geochemical analysis of the GISP2 core determined that 99% of Na^+ is of sea salt origin during the Holocene [O'Brien 1997] making it a good conservative tracer for sea-salt aerosol. During DO-8 however the percentage has dropped to 89%, (based on the calculated values of non-sea salt Na^+ to sea salt Na^+[14] [DeAngelis et al., 1997]). The marine aerosols to reach Summit are chloride-depleted and sulphate-enriched with respect to seawater composition due to sea salt reactions with SO_2 and H_2SO_4 [Legrand and Delmas, 1988]. For this reason sodium, despite having a reduced marine component is still used as the primary marine tracer in this section.

Sea salt ratios

Molar equivalents were described in Chapter 5 (equation 5.6) to compare ions to known seawater ratios. The ratio of chloride to sodium has been calculated for the warming transition and is plotted in figure 10.8 (p 217); with red squares indicating values higher than the expected seawater ratio of chloride to sodium (1.165) and blue circles indicating values lower than this.

[14] $Na_m = Na^* - 0.036Ca_t$ [DeAngelis et al., 1997]

Throughout the warming transition (2070.15 – 2069.8 m based on the isotope transition) the values of Cl^-/Na^+ are within one standard deviation of the expected seawater ratio, indicating that sodium and chloride are of marine origin. However there appears to be some very high ratios, indicating excess chloride, during the glacial. The closest ratio to the expected seawater ratio is during the period after the warming transition, between 2069.5 – 2069.1 m.

Point of deposition change

The changes in all species at the onset of DO-8 appear synchronous with changes in the isotope record. Running averages (as described in chapter 9), of 5 cm and 10 cm moving segments, are used to determine robust transitions in the calcium and sulphate record, figure 10.5 and 10.6.

Calcium:

Three distinct steps are observed calcium record. The first occurs at 2070.35 m, when concentrations drop below the lower limit of the preceding segment for 5 cm before returning to pre-interstadial levels. The second is observed at 2070.15 m; where concentrations drop from exceptionally high to low values, (close to those observed after the final warming step) for a short period (~1-2 years[15]) before returning to concentrations approximately half what they were in the previous step. After 5 cm (~ 2-3 years[15]) the concentrations drop for a final time in a third step at 2070.05 m, to interstadial concentrations where they stay until a depth of 2069.5 m, where they appear to rise again.

[15] Based on annual layer counting in chapter 11.

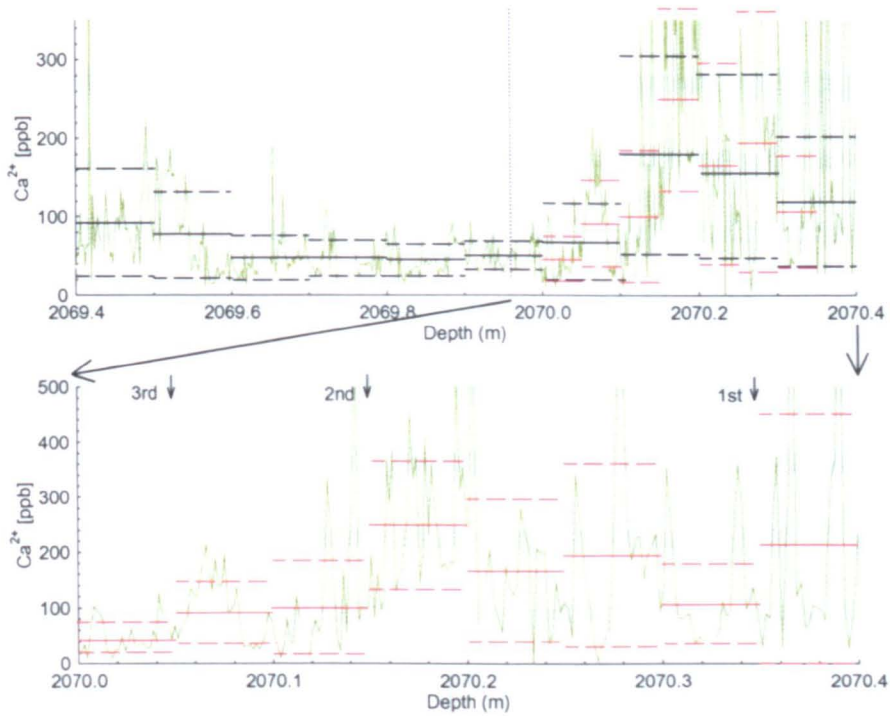

Figure 10.5. Determining the transition steps of calcium deposition using 5 cm (red) & 10 cm (black) running averages for the whole warming transition (top) and the point of change (bottom). Vertical dashed line on top graph indicates location of deuterium excess transition.

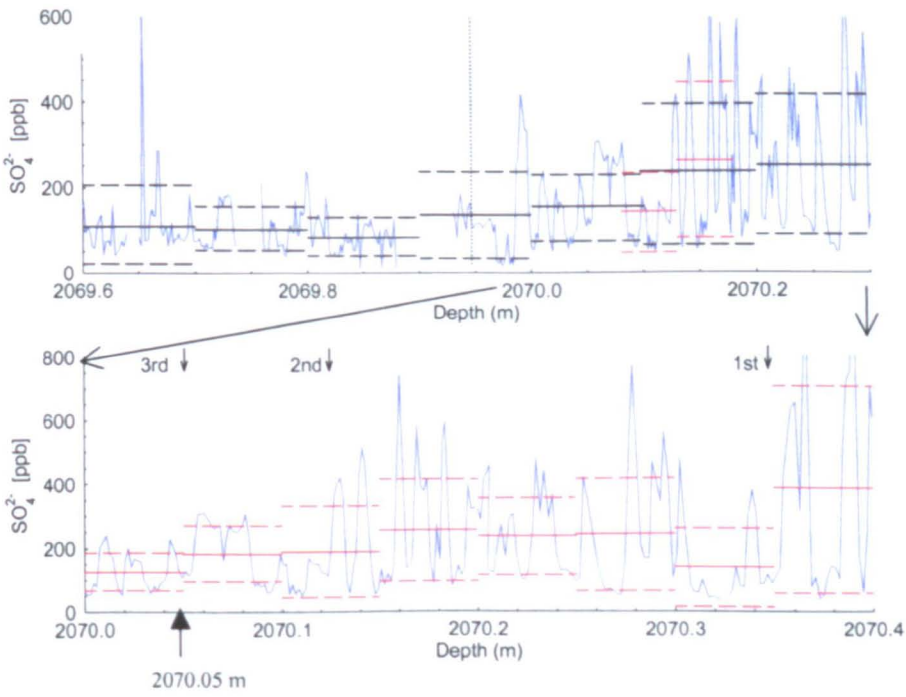

Figure 10.6. Determining the transition steps of sulphate using 5 cm (red) & 10 cm (black) running averages. Vertical dashed line on top graph indicates location of deuterium excess transition.

Sulphate:

Sulphate (fig 10.6) behaves in the same way as calcium (fig 10.5), with three major steps at the warming transition. The first step occurs at 2070.35m, the second at 2070.15 m and the third after 2070.05 m, but the variability in sulphate remains high and as such the final transition in sulphate is not as clear to calcium.For the benefit of calculating deposition change, the final transition step at 2070.05 m is chosen to represent the onset of DO-8. This is compared to $\delta^{18}O$, which terminates at 2069.80 m (as shown in fig 10.2), approximately 11 years later.

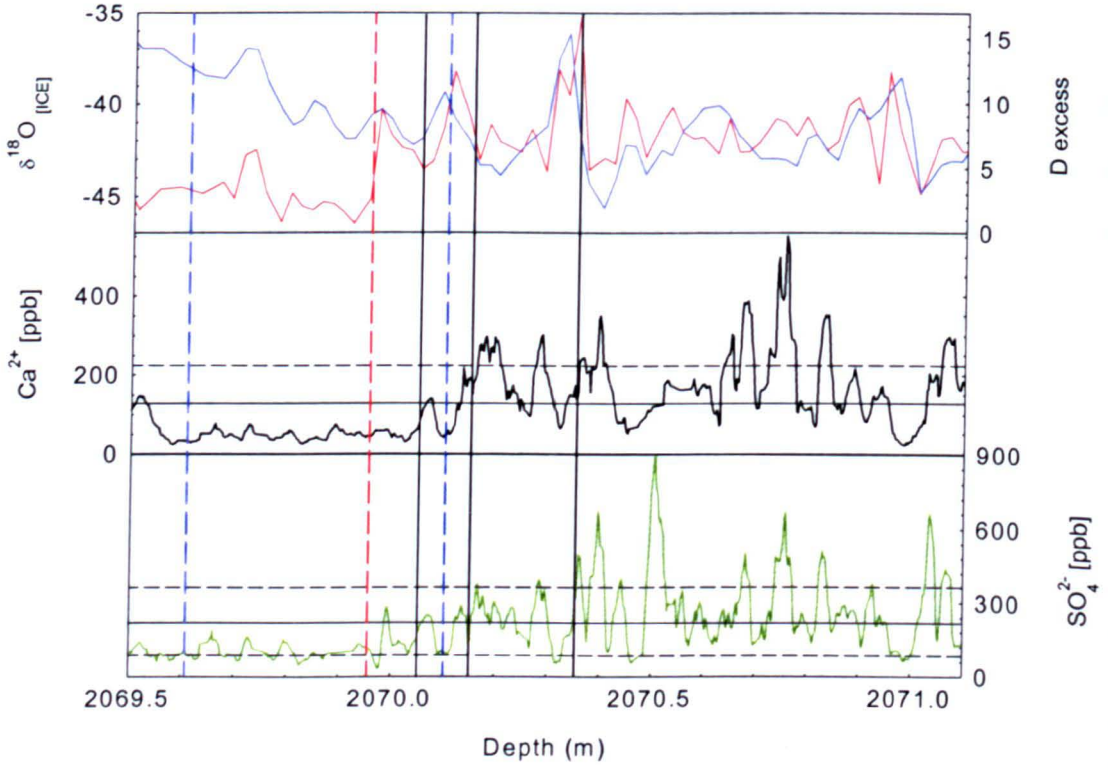

Figure 10.7 Top: $\delta^{18}O$ (blue) and deuterium excess (red). Middle and bottom: Calcium and sulphate at approximate annual resolution (based on average annual layer thickness of 1.8 cm, discussed later) with average (solid horizontal lines) and ± one standard deviation (dashed horizontal lines). Vertical lines indicate transition in deuterium excess (dashed red), the onset and termination in $\delta^{18}O$ and deuterium (dashed blue) and the three transition steps determined from calcium and sulphate (solid black).

The transition steps determined from the calcium and sulphate is shown along with the transition from deuterium excess and the onset and termination transitions from $\delta^{18}O$ and deuterium in figure 10.7.

Changes in marine species

The concentration of marine species decreases significantly after the warming transition however there are large changes in deposition of marine species prior to this. There is a significant increase in sodium concentrations in the period prior to the final warming transition (as defined by deuterium excess at 2069.95 m), shown in figure 10.8 as an abrupt jump to concentrations outside of the expected values ($\geq 1\sigma$). The increase begins at a depth of 2070.2 m ((1) on fig 10.8), coincident with an increase in calcium, and concentrations remain high until 2070.1 m, where they drop suddenly to levels considerably lower and may be considered the transition. The ratio of Cl^-/ Na^+ during this period of high concentrations is close to the expected seawater ratio and is therefore considered of sea salt origin.

Chloride and MSA (fig 10.8) also show a small increase during this period, although the amplitude of the change is not as great as the sodium increase nor is it the most significant of either the chloride or the MSA records. The largest changes in the chloride record occur at 2071.1 m ((2) on fig 10.8) and 2070.4 m ((3) on fig 10.8), synchronous with periods of significantly negative $\delta^{18}O$, deuterium and deuterium excess values. Following the first major increase at 2071.1 m the chloride concentrations appear to increase to values consistently greater than the average (of the whole warming transition), reaching a maximum at 2070.4 m. Values drop again

after 2070.4 m to background concentrations until 2070.0 m when the concentrations fall consistently below the background and are considered the interstadial.

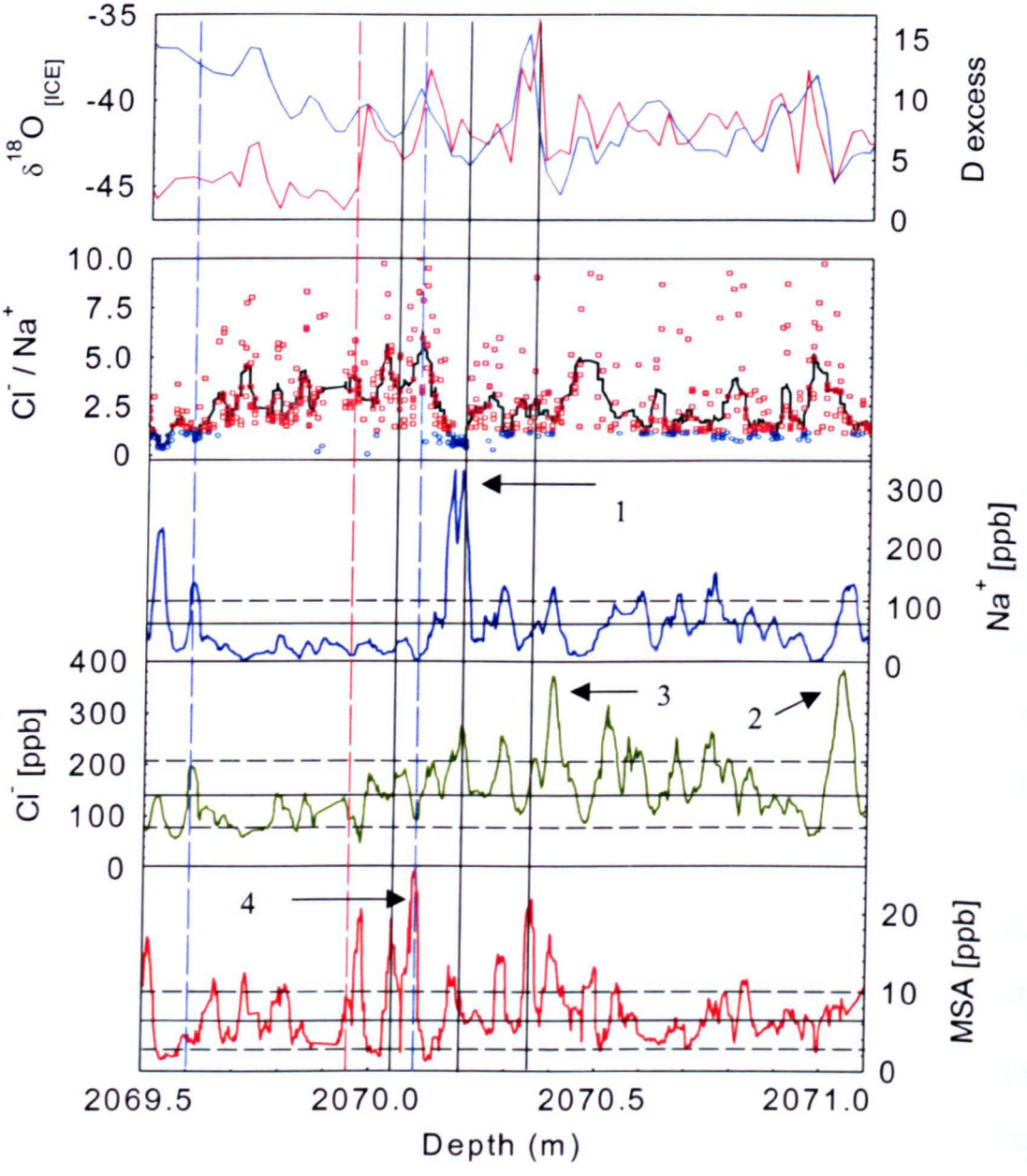

Figure 10.8. Top: Oxygen (blue) and deuterium excess (red). Second from top: Cl^-/Na^+, at 2 mm resolution (red squares indicate greater than and blue circles indicate less than seawater ratio), and approximate annual average (black curve, based on average annual layer thickness of 1.8 cm). Bottom three: Sodium (blue), chloride (green) and MSA (red) smoothed to approximately annual resolution (based on average annual layer thickness of 1.8 cm). Numbers and arrows indicate depths referred to in the text.

There are several significant changes in the concentration of MSA during the warming transition, however there is no distinct transition point. Prior to the warming (A) the concentrations of MSA are relatively constant and close to the background average until a depth of 2070.5 m ((4) on fig 10.8) when they increase in a series of abrupt jumps above expected values ($\geq 1\text{-}2\sigma$). This change occurs prior to the significant deuterium excess event (2070.35 m, fig 9.1) described previously with abrupt increases in MSA coincident with decreasing deuterium excess.

The largest increase in MSA is observed at 2070.1 m ((4) fig 10.8), corresponding to the onset of the warming transition determined in the deuterium excess record. During this period several significant increases are observed, which no longer appear correlated with sodium and chloride. The final significant increase is observed at 2070.0 m, dropping again suddenly at 2069.95 m; the transition point in the deuterium excess record. After this depth the concentration of MSA returns to background levels where it remains until 2069.5 m when the concentrations of all marine species show an increase.

The abrupt fluctuations in all marine species could be important with regard to the ocean circulation during the warming transition. The point at which they reach interstadial levels occurs prior to the end of the warming transition determined from the deuterium excess. This is interesting for MSA, which has been used in recent studies in Antarctica and the Arctic to show a correlation with sea ice extent [Curran et al., 2003] and SST's [O'Dwyer et al., 2000].

Correlation with temperature

The concentrations of all ions appear to decrease proportionally with increasing temperature during the warming transition, however the correlation before and after the transition is different. This is shown in figure 10.9, a-d for calcium, chloride, sodium and sulphate versus $\delta^{18}O$ (therefore temperature).

Calcium and sulphate show the strongest inverse relationship with temperature (significant at the 1% level) during the whole transition, with slopes of -21.6 ppb/ ‰ and -27.6 ppb/ ‰ respectively. The relationship is weaker in the marine aerosols, chloride and sodium, with slopes of -11.8 ($r^2 = 0.19$, n = 108) and 4.6 ($r^2 = 0.05$, n = 108) respectively.

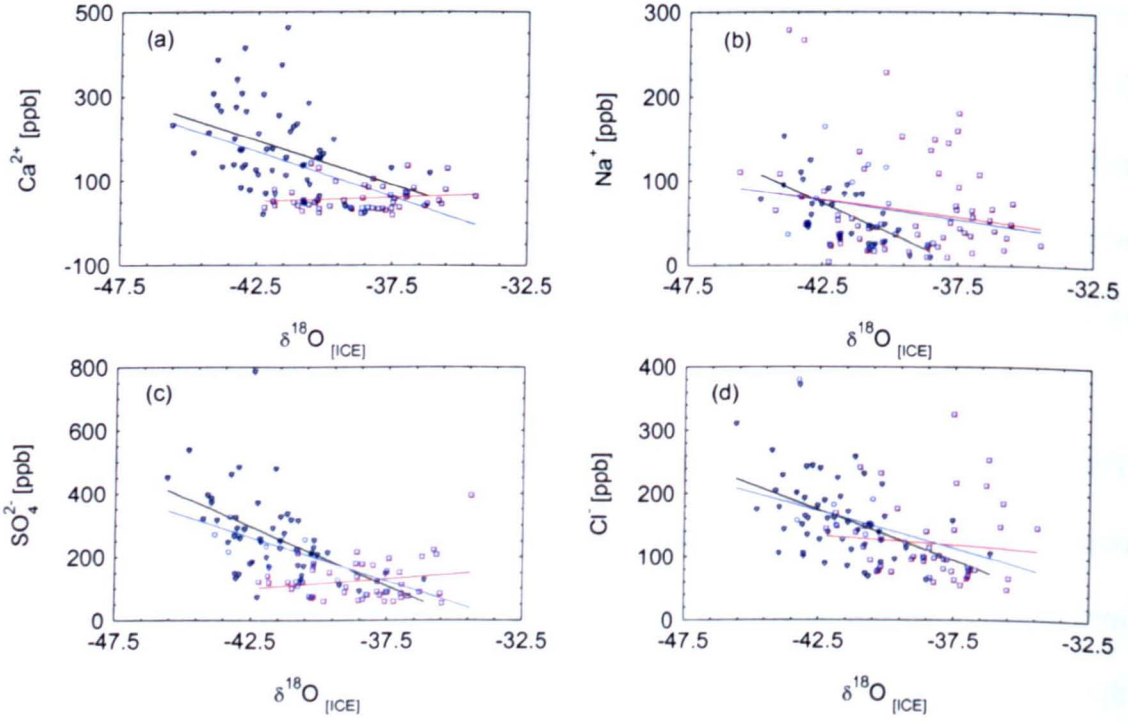

Figure 10.9. (a) Calcium, (b) sodium, (c) sulphate and (d) chloride, averaged to 2 cm resolution, versus $\delta^{18}O$ across the warming transition. Blue circles, blue curve fit; total data across the transition. Red square, red curve fit; values after the warming (during the interstadial). Black triangles, black curve fit; values prior to warming (glacial).

A much weaker relationship with temperature is observed during the interstadial, as shown in table 10.2, with an inverse relationship observed for calcium, sulphate, magnesium and nitrate significant at the >5% level.

Ion		Total Transition (n = 108)	Before warming (n = 48)	After warming (n = 53)
Ca^{2+}	slope	-21.60	-20.90	1.90
	R^2	0.30	0.13	0.02
Cl^-	slope	-11.80	-15.90	-2.90
	R^2	0.19	0.20	0.01
Na^+	slope	-4.60	-14.00	-4.20
	R^2	0.05	0.40	0.30
SO_4^{2-}	slope	-27.60	-37.50	6.20
	R^2	0.30	0.30	0.04

Table 10.2. Relationship between calcium, chloride, nitrate, sodium and sulphate and temperature, during the whole transition, before the transition and after the transition. Negative values indicate an inverse relationship with temperature. R^2 significant at <1% level for the total transition and before the warming.

10.3 Concentration changes at the warming transition

All species show a significant decrease during the transition from cold conditions to relatively warm conditions as shown in table 10.3. The largest changes are observed in magnesium and calcium with drops of as much as 70 %. The next highest change is observed in sulphate, which decreased by 57 % with a 59 % decrease in sulphate defined as non-sea-salt in origin. The marine species show a less dramatic decrease

with sodium dropping by 47 % (43 % for Na marine), while chloride was just 34 % lower during the interstadial.

The change in continental species is large and abrupt, while the changes in marine species are lower in magnitude and show a more gradual response. The onset and termination of the oxygen and deuterium transition, from colder to warmer temperatures, has been determined in the isotopes chapter. The onset of the deuterium excess transition is earlier than the oxygen and deuterium record, and it appears that the chemical deposition changes even before this.

10.4 Cooling

The cooling out of DO-8, where temperatures drop back to extremely cold values, took several hundred years. This time period equates to a large amount (see figure 8.7, p.190) of ice in the NGRIP core and consequently only a small section could be analyzed. Ice was available between depths of 2021.2 to 2028.95 m (D + C), which in itself was only a small section of the cooling transition. The labour intensive cutting method meant that I had to prioritize which ice to cut and as such I chose to split this ice section in two. I decided to analyse the coldest ice in this section, starting at 2021.2 to 2022.9 m (section D), and the warmest ice, between 2026.2 to 2028.2 m (section C), in order to capture the greatest transitions in the isotopes (determined from the lower resolution NGRIP $\delta^{18}O$ record [NGRIP members 2004]) and to give a comparative deposition change.

Concentration [ppb]													
	Na^+	Na^+ marine	K^+	Mg^{2+}	Mg^{2+} terrestrial	Ca^{2+}	Ca^{2+} terrestrial	F^-	MS^-	Cl^-	NO_3^{2-}	SO_4^{2-}	n.s.s. SO_4^{2-}
Average before warming (A)	78.8	65.9	19.8	16.7	15.8	183.6	183.0	3.2	11.7	173.1	106.0	273.5	255.7
Standard deviation	85.9	80.4	44.2	15.1	14.5	196.9	195.5	5.4	51.2	132.6	83.1	256.1	251.1
Average after warming (B)	41.6	37.8	13.5	5.1	4.5	55.9	54.1	2.5	7.6	113.6	67.7	117.3	105.6
Standard deviation	59.8	59.0	12.7	3.7	3.7	39.5	38.5	9.3	13.2	68.8	35.8	79.1	76.7
Change after warming [ppb] (B-A)	37.2	28.2	6.3	11.7	11.3	127.7	128.9	0.8	4.1	59.4	38.4	156.2	150.1
% concentration decrease after warming	47.2	42.8	31.8	70.1	71.5	69.6	70.4	25.0	35.0	34.3	36.2	57.1	58.7

Table 10.3 Changes in chemical deposition before and after warming into IS-8.

The chemical record for the ice during the cooling transition is shown in figures 10.10 for section C and 10.11 for section D. The total chemistry in all of the ice analysed is plotted against the oxygen isotope record in figure 10.12.

The change in isotopic composition between section D and section C is small (1.15 ‰ for oxygen), equal to a drop in the average temperature of 3.3 °C. It is therefore not expected that a large difference in the concentrations between the two depths will exist. Despite a gradual increase in deposition (figures 10.10 – 10.12) during the cooling and a large amount of interannual variability, there is no distinct transition point in either section C or D, such as that seen during the warming transition (between sections A and B).

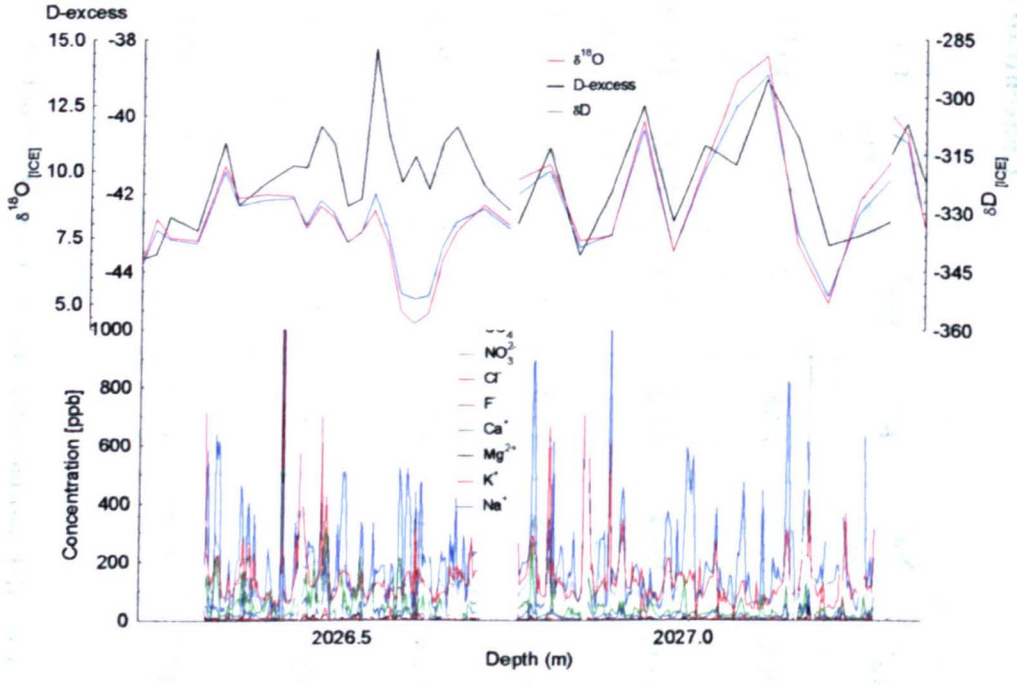

Figure 10.10 Oxygen (top red curve), deuterium (top graph blue curve) and deuterium excess (top graph black curve) all at 2 cm resolution, and total chemistry (bottom graph) at 2 mm resolution during section C, between 2026.2 m and 2028.2 m

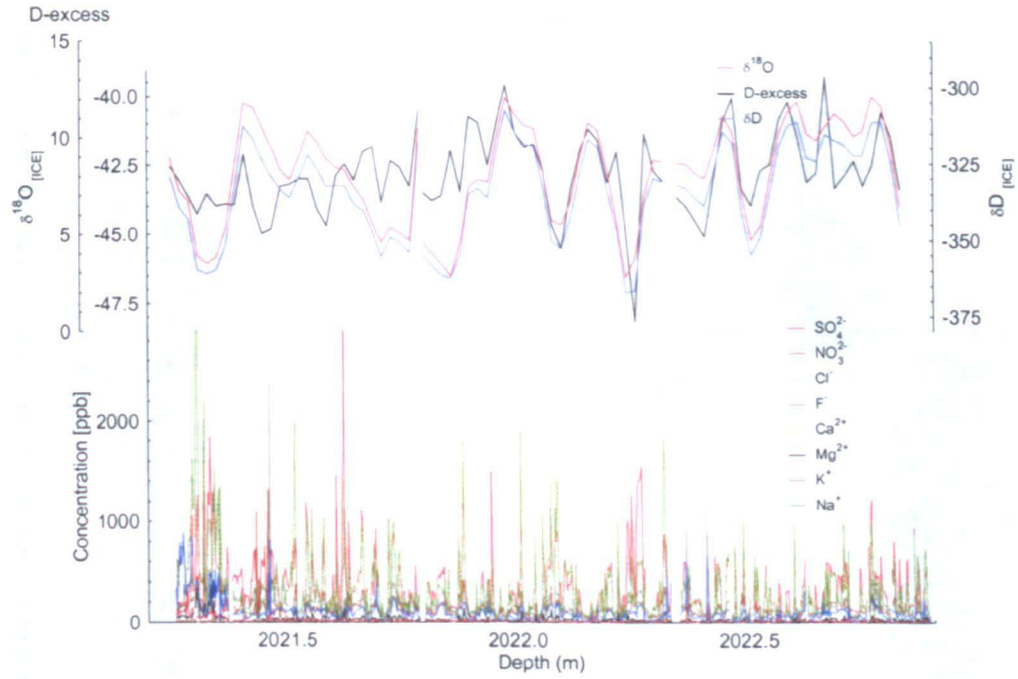

Figure 10.11 Oxygen (top red curve), deuterium (top graph blue curve) and deuterium excess (top graph black curve) all at 2 cm resolution, and total chemistry (bottom graph) at 2 mm resolution during section D, between 2021.3 m and 2022.6 m

With the exception of MSA, the concentrations of all ions in section D are significantly higher than those in section C, despite only a relatively small difference in isotopic composition between the two sections. The concentrations of calcium and magnesium increase by 328 % and 299 % respectively from section C to D, with a smaller but still significant increase in sodium and chloride of 176 % and 108 %. MSA is the only ion to show a decrease with decreasing temperatures, dropping from an average of 10.3 ppb in section C to 4.2 ppb in section D.

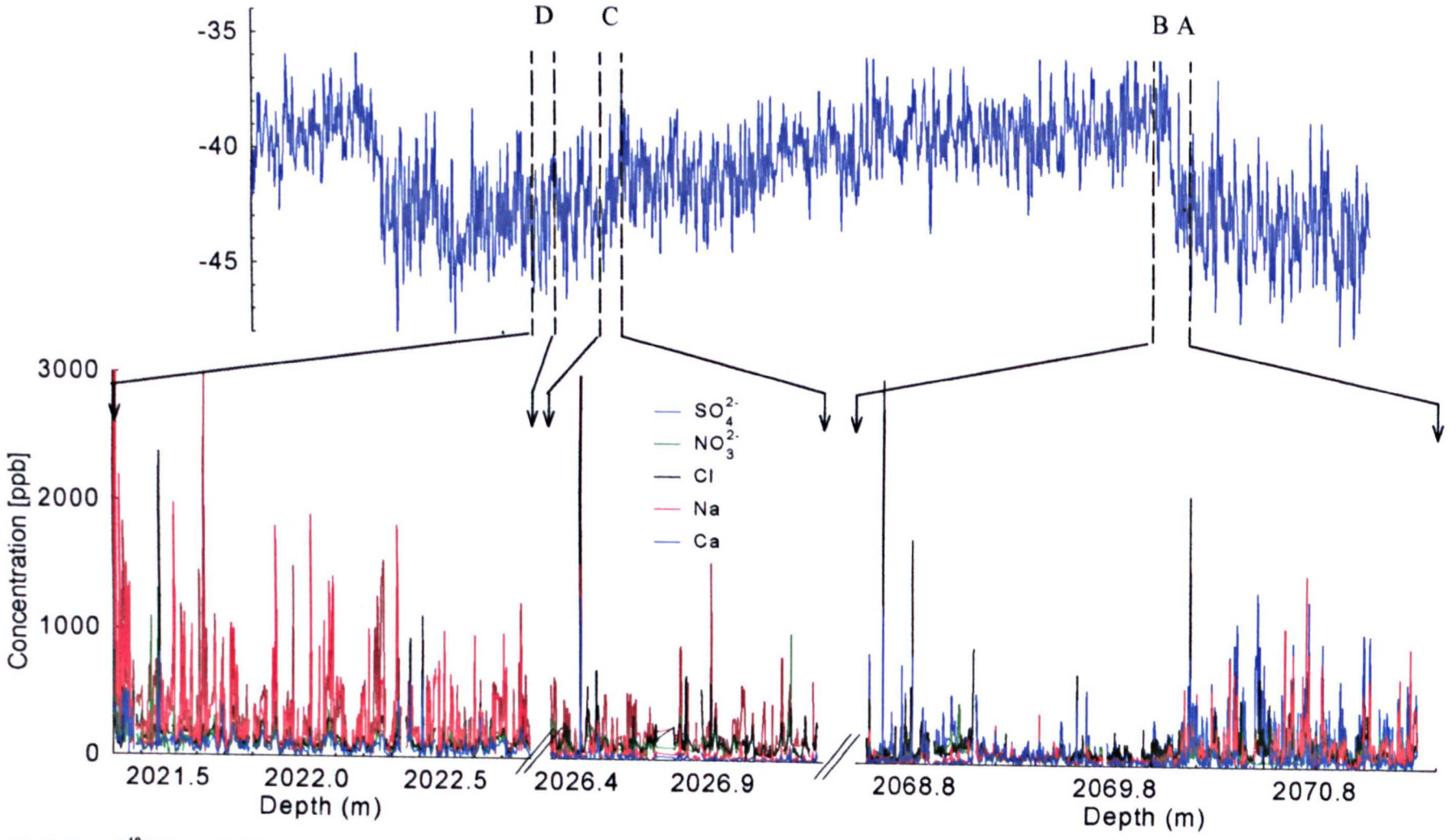

Figure 10.12 Top: $\delta^{18}O$ from NGRIP at 2 cm resolution [NGRIP members, 2004]. Bottom: Chemistry (sulphate, nitrate, chloride, sodium and calcium) at 2mm resolution during the warming and cooling transitions.

10.5 Comparing the warming and cooling transitions

The isotope comparison (see chapter 9) revealed that the highest temperatures were observed in section B, after the warming transition. The coldest ice was found in section D, after the cooling transition. It is expected that, if deposition follows the same pattern as temperature, the lowest concentrations of ions will be seen when the temperature is warmest (section B) and the highest concentrations will be observed in the coldest section of ice (section D).

Average Concentration [ppb]										
Section	Na^+	K^+	Mg^{2+}	Ca^{2+}	F^-	MS^-	Cl^-	NO_3^-	SO_4^{2-}	$\delta^{18}O$ (‰)
A	78.8	19.8	16.7	183.6	3.2	11.7	173.1	106.0	273.5	-42.1
B (Warmest)	41.6	13.5	5.1	55.9	2.5	7.6	113.6	67.7	117.3	-38.3
C	57.1	17.4	9.4	97.4	3.3	10.3	147.6	99.9	206.1	-41.7
D (Coldest|)	100.7	20.1	28.0	320.0	8.0	4.2	160.0	120.1	340.3	-42.8
Increase from warmest to coldest ice (B-D)	59	7	23	264	6	-3	46	52	223	4.5
% Increase (B-D)	242	149	549	572	319	-181*	141	177	290	10.5

Table 10.4 Comparison of average ion concentrations in all of the ice sections (A – D) analysed and the difference in concentration between the warmest (B) and the coldest (D) ice. * MS^- shows a decrease from B-D. Compared with the average isotopic ratio ($\delta^{18}O$ per mil) for the same sections.

The total chemical record for the warming transition and the cooling transition is shown in figure 10.12 along with the oxygen isotopes record (top blue curve). Comparison of the average concentrations from all ions in each of the sections analysed is shown in table 10.4.

With the exception of MSA, all ions follow the temperature trend, showing significant increases in concentration with decreasing temperatures, B-D. The terrestrial concentrations show the highest percentage change with calcium increasing by 572 % and magnesium 550 % from the warmest to the coldest ice.

Continental and marine components

The percentage of each ion considered of continental or marine origin can be calculated and the differences between cold and warmer temperatures determined. It appears that a slight trend exists between the percentage of continental calcium and magnesium with respect to temperature. The average percentage of continental calcium is higher during the coldest periods than the warmest periods, 99.7% compared to 96.8%. The difference for calcium is small but for magnesium the change is more apparent with 88.2% of terrestrial origin during cold periods increasing to 94.6% during warm periods. Sodium behaves in the same way, with a decrease in the percentage of marine component from warm periods to cold periods. The decrease from 90.9% to 84% indicates an increased terrestrial source as the temperature gets colder.

Rate of change

The fastest rate of chemical deposition (ppb yr^{-1}) is observed during the warming transition (A+B) where calcium and sulphate increase by 11 ppb yr^{-1} and with a slower rate observed in the marine ions sodium and chloride (Table 10.5). This was calculated from the onset of the chemical transition to the termination of the $\delta^{18}O$ transition, 2070.35 – 2069.80 m (number of years determined from annual layer counting discussed in chapter 11).

There have been no transitions determined during the cooling, however both sections (C and D) show a steady increase in chemical deposition that is not proportional to the increase in $\delta^{18}O$. The rate is doubled between section C and D for calcium, chloride and sulphate, and quadrupled for sodium, despite a rate decrease in the $\delta^{18}O$ from 0.02 ‰yr^{-1} to just 0.01 ‰ yr^{-1}.

		Rate of change				
		[ppb] yr^{-1}				‰ yr^{-1}
Ice location	Duration (yrs)	Ca	Na	Cl	SO_4	$\delta^{18}O$
Warming transition (A+B)	27	11	6	5.7	11	0.1
Section C	75	0.68	0.17	0.19	0.47	- 0.02
Section D	108	1.49	0.71	0.44	1.02	- 0.01
Increase C to D		2.2	4.2	2.3	2.2	0.5
Increase C to A+B		16.2	35.3	30.0	23.4	- 5.0
Increase D to A+B		7.4	8.5	13.0	10.8	- 10.0

Table 10.5 Rate of increase in chemical deposition and $\delta^{18}O$, during the warming (A+B) and cooling (C and D) and a comparison between sections. The warming transition is constrained as the period from the onset in the chemical record to the termination in $\delta^{18}O$. The number of years is from annual layer counting described in chapter 11.

10.6 Summary of DO-8 chemistry

The concentration of all species decreased significantly following the warming transition at the onset of DO-8. Continental ions (calcium and magnesium) showed the largest decreases with a lesser but still significant decrease for the marine ions (sodium and chloride).

The transition point for the chemistry was determined in the same way as the isotopes, using running averages. It was found that the transition occurs in three distinct steps starting at a depth of 2070.35 m and terminating at a depth of 2070.05 m, after which concentrations remain low during the interstadial. The transition in the terrestrial chemistry occurs several years earlier than the transition in $\delta^{18}O$, deuterium or deuterium excess, as shown in figures 10.2 (p.210) and 10.7 (p.216). It is almost a decade after the chemical concentrations have reached interstadial levels that the isotopes (and therefore temperature) begin to stabilize.

There were no distinct transitions observed during the cooling (section C and D), instead chemical deposition increases gradually as temperatures decrease but at a rate that is no longer proportional to $\delta^{18}O$.

Chapter eleven

DO-8: Annual layer counting

DO-8: Annual layer counting

11.1 Introduction

The seasonality of deposition in Greenland is described in Chapter 4. The distinct annual cycles in the chemical record can be counted using the peaks and troughs of each ion. Ice compression, at the depths investigated in this thesis, resulted in exceptionally thin annual layers of less than 2 cm (an average of 1.6 cm during the stadial and 3 cm during the interstadial based on the GICC05 dating). The new 2 mm resolution analysis provided a sub-seasonal record, of up to 10 samples per year, with clear seasonal cycles in all ions. This is the first time this kind of resolution has been achieved over several meters of deep ice.

The annual layers were counted for 2.7 meters of ice analysed over the warming transition, between depths 2068.6 to 2071.3 m, and between 2021.25 to 2022.85 m during the cooling transition. The duration of the transition, based on both the chemical and isotope records, is determined and the difference in the seasonal signal both before and after the transition investigated. The annual layer counting is also compared to the independent GICC05 layer counting [Andersen et al., submitted].

Dating

There is a large degree of uncertainty as to the age of DO-8. It is observed approximately 35 kyr ago according to the model derived GRIP dating (ss09 timescale) [Johnsen et al., 2001] and 38 kyr ago according to the GISP2 layer counted age scale [Meese et al., 1997]. The new GICC05 dating initiative has replaced the ss09 age with an onset of 38.4 kyr B2K (before 2000, 38.35 kyr BP 1950) [Andersen et al, submitted], however there is still an estimated error of ± 1460 years at this

depth. The GICC05 method is based on annual layer counting using CFA, visual stratigraphy and ECM which has provided a new age that is approximately comparable with the GISP2 layer counted method. However, it is worth noting that there are large discrepancies in the two methods, which appear to have reached the same age but via very different routes. The most notable difference is the onset of the Younger Dryas (YD), which is considerably older in the GISP2 method indicating either an underestimate in the GISP2 layer counting prior to the YD [Meese et al., 1997] or an over estimate on the GICC05 method [Rasmussen et al., 2006].

Despite the comparable date from the two ice core methods, it has been suggested by $^{234}U/^{230}Th$ dating of ocean sediments that an error of more that 3,000 years exists in both the GRIP and GISP2 timescales by 42 kyr BP [Burns et al., 2004]; however the new GICC05 age-scale has been correctly correlated to ^{10}Be at this depth. Stalagmites from southwest France also dated using $^{234}U/^{230}Th$, show a regular decrease in $\delta^{13}C$ corresponding to DO8 between 39.4 to 36.2 kyr BP [Genty et al., 2003].

For the benefit of this thesis, the new GICC05 age-scale has been used to provide a reference date, for the annual layer counting. The first peak in the high-resolution chemical record, which has been defined as the first year, occurs at a depth of 2070.05 m. Using the new GICC05 age-scale, the age of this peak has been given as 38,170 kyr BP.

11.2 Counting method

The counting method during the glacial was essentially the same as during the Holocene; years were counted based on the spring peaks in each ion. The locations of each ion in the annual cycle were determined by Whitlow et al (1992), as shown in figure 11.1.

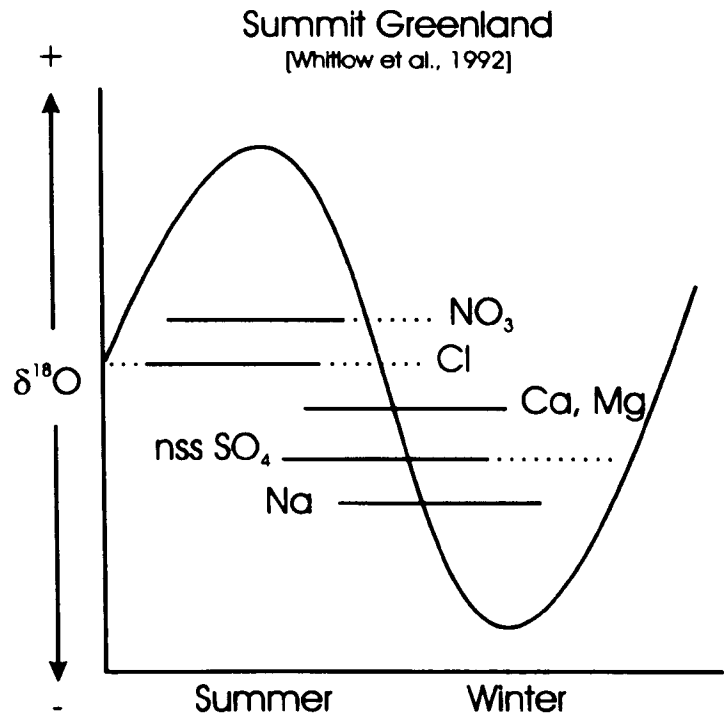

Figure 11.1. Summary of seasonal timing at pre-1900 Summit, Greenland, superimposed on an idealized $\delta^{18}O$ curve. Based on figure 2 from Whitlow et al., 1992.

The clearest cycles were observed in calcium, chloride, nitrate, sodium and sulphate as shown in figure 11.2 however, the seasonal signal during the stadial, in the section of ice prior to warming, differs considerably to that of the interstadial ice. The two sections have been compared in figure 11.2.

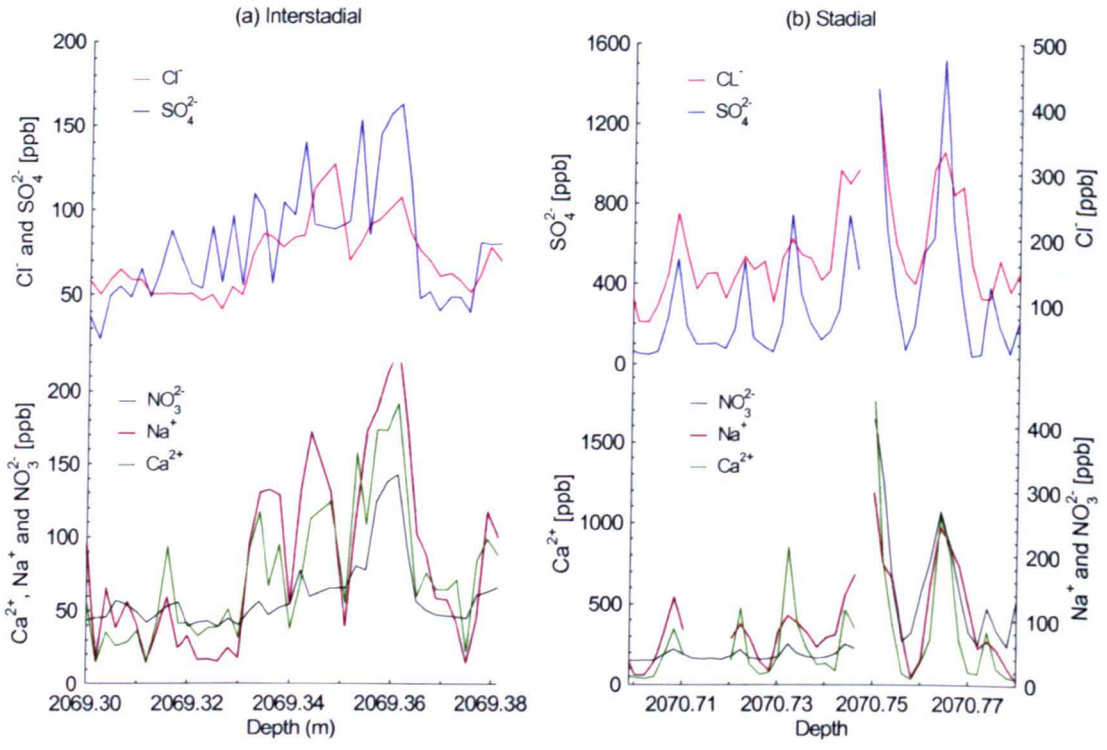

Figure 11.2. Comparison of annual layer. (a) After the warming, during the interstadial and (b) before the warming, during the stadial.

Stadial ice

In the stadial ice, the peaks of all five ions are located at the same point within the annual layer. The deposition does not appear to follow that described by Whitlow et al (1992) (figure 11.1), but instead a single synchronous (spring) peak is observed. Due to the increased chemical deposition to Greenland during these periods of exceptional cold (fig 10.2, p.210), the amplitude of these synchronous spring peaks is considerably greater than that of the Holocene record and the interstadial ice. Therefore, despite the thin annual layers during the coldest glacial period (as a result of the exceptionally cold temperatures reducing snow accumulation and layer thickness with depth), annual layer counting in this section was relatively easy.

The same rules of counting applied as for the counting of the Holocene ice surrounding the 8.2 kyr event (Chapter 6). Each annual layer was determined by locating the single spring peak in calcium, chloride, nitrate, sodium and sulphate as shown in figures 11.3 to 11.5 for the glacial section D and figures 11.6 to 11.10 for the warming transition (sections A & B). Peaks that are confidently assigned are marked with a solid vertical line. In sections where there was missing data, either as a result of damaged ice or insufficient liquid sample for analysis, a dashed vertical line has been added. This also applies to sections of ice where the annual signal is obscured or some doubt exists as to the location of the spring peak.

Annual layer counting of section D – 2021.8 m to 2022.9 m:

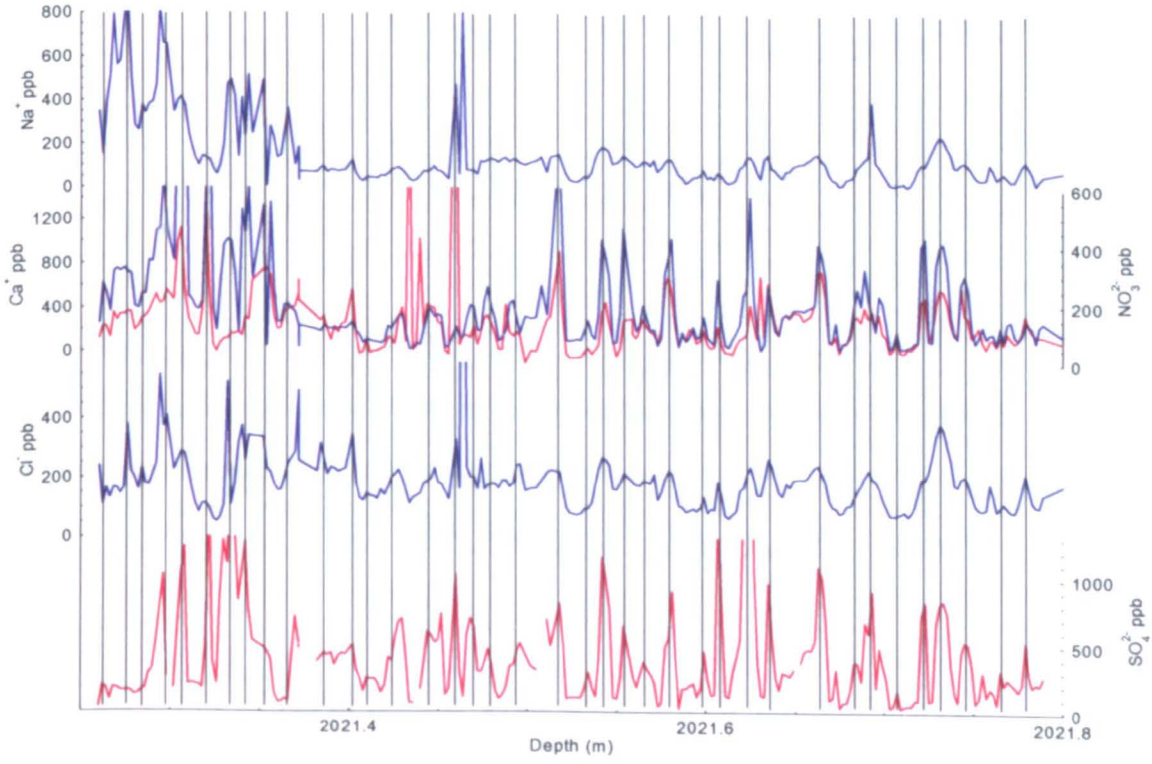

Figure 11.3. Annual layer counting of (top to bottom) sodium, calcium (red), nitrate (blue), chloride and sulphate between depths 2021.25 to 2021.8 m.

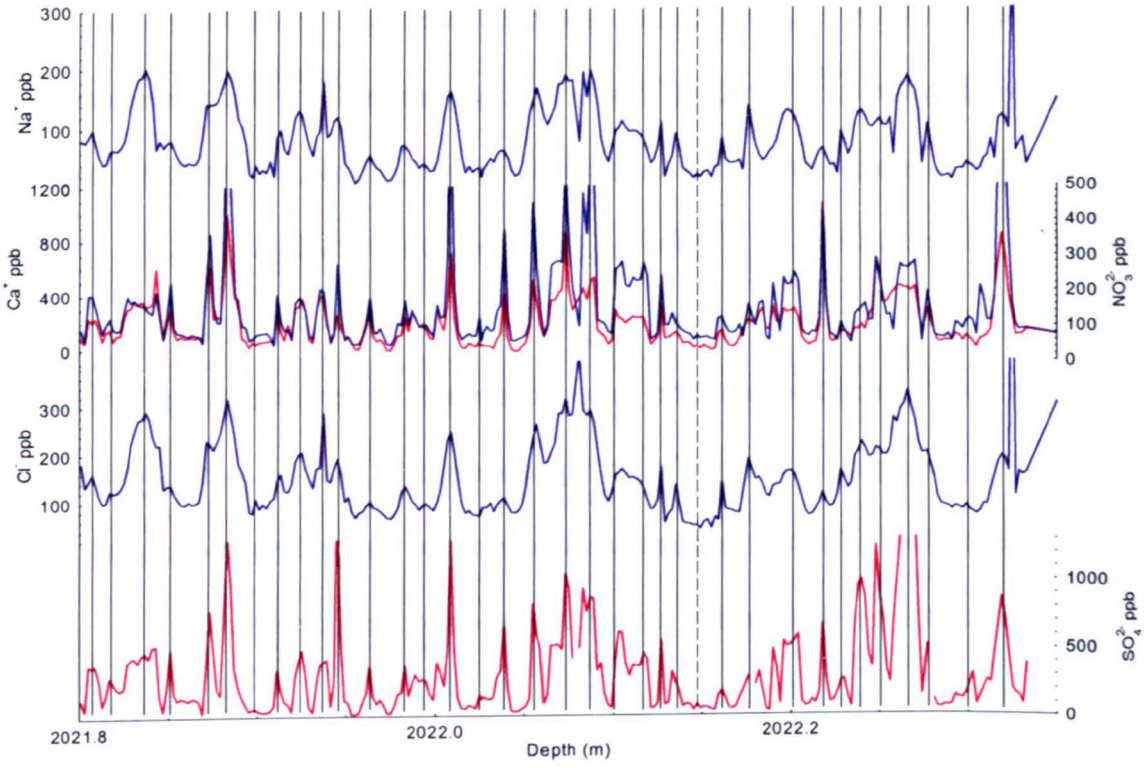

Figure 11.4. Annual layer counting of (top to bottom) sodium, calcium (red), nitrate (blue), chloride and sulphate between depths 2021.75 to 2022.3 m.

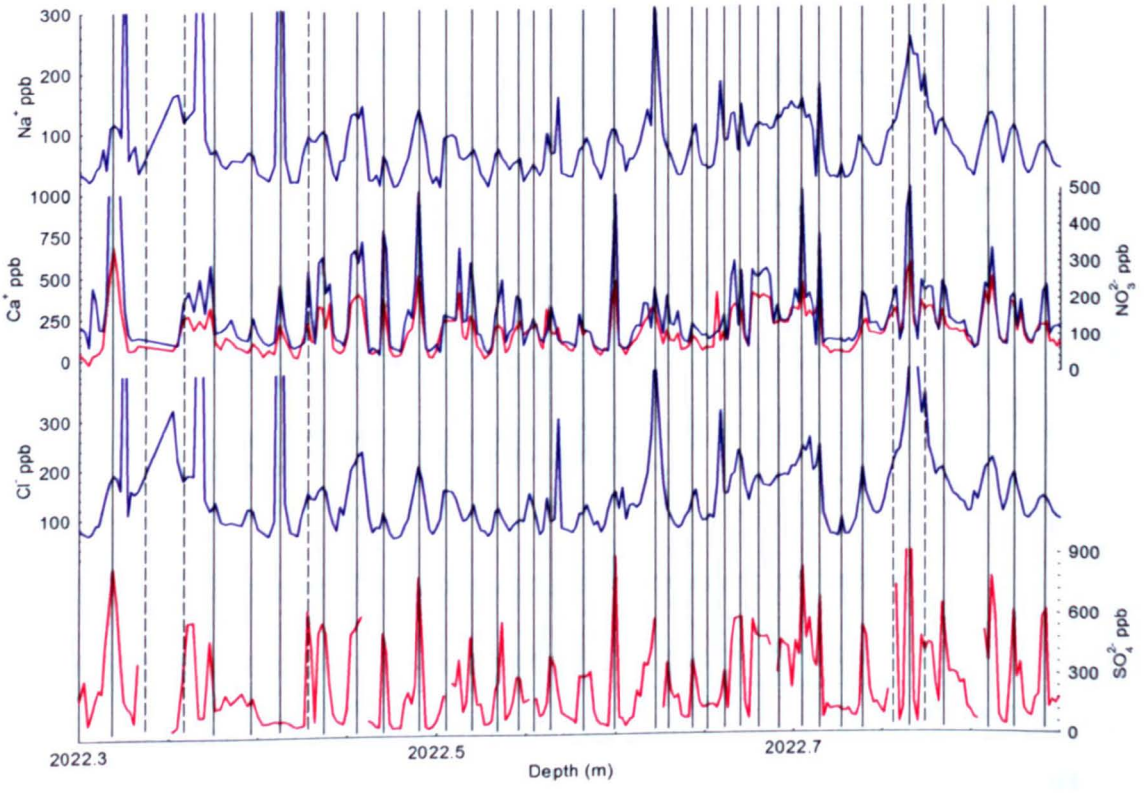

Figure 11.5. Annual layer counting of (top to bottom) sodium, calcium (red), nitrate (blue), chloride and sulphate between depths 2022.3 to 2022.85 m.

A total of 108 spring peaks were confidently marked between depths 2021.25 m and 2022.9 m, as shown in figures 11.3 to 11.5, with 6 peaks marked with dashed lines to indicate uncertainty.

Annual layer counting of section A & B – 2068.6 to 2071.3 m:

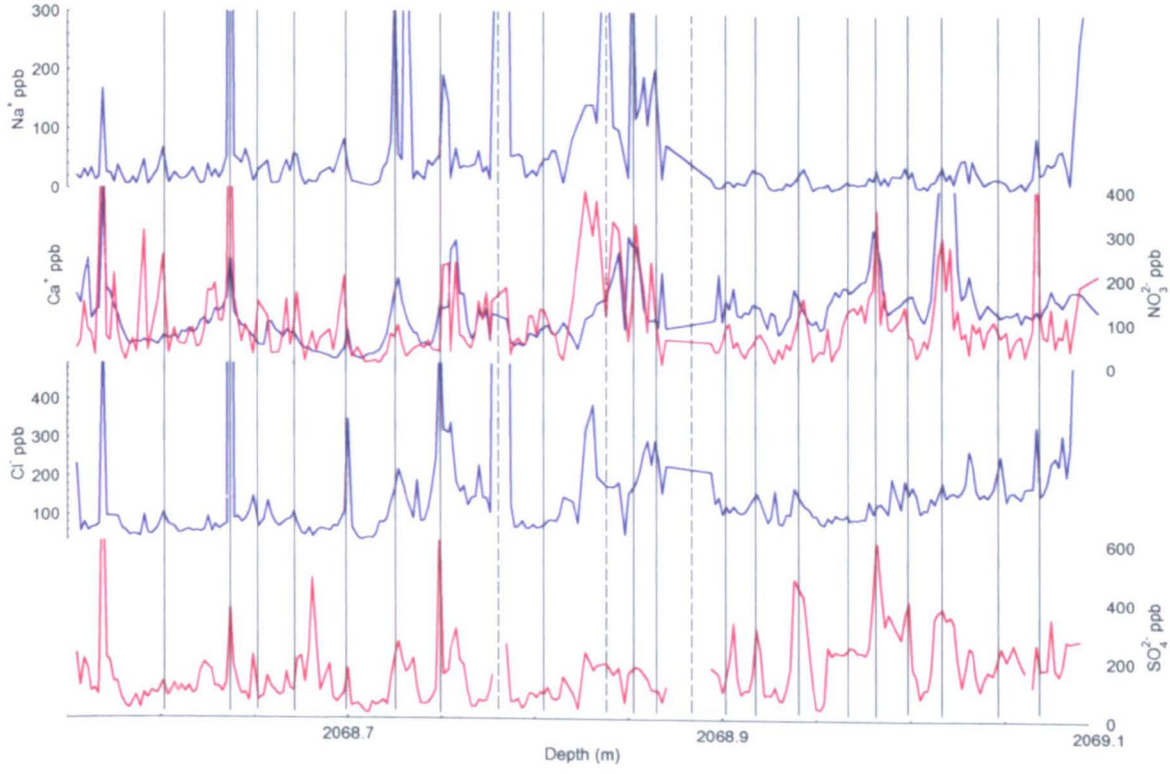

Figure 11.6. Annual layer counting of (top to bottom) sodium, calcium (red), nitrate (blue), chloride and sulphate between depths 2068.55 to 2069.10 m.

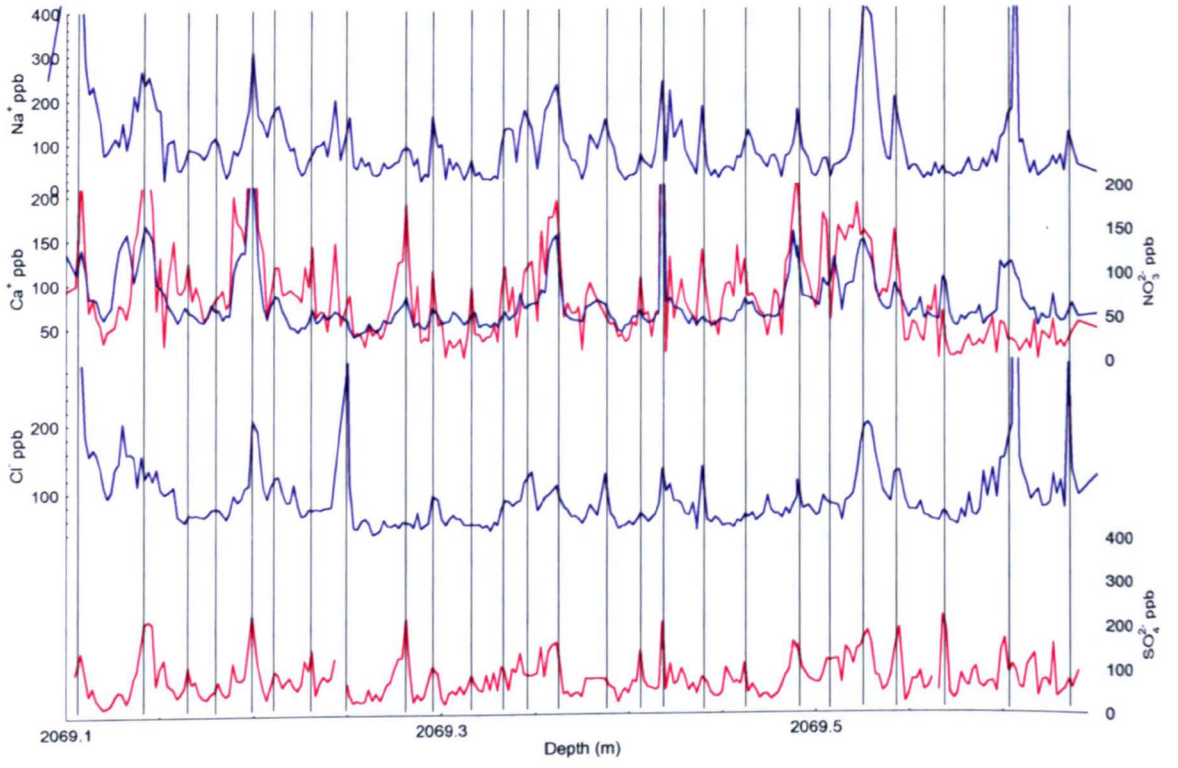

Figure 11.7. Annual layer counting of (top to bottom) sodium, calcium (red), nitrate (blue), chloride and sulphate between depths 2069.10 to 2069.65 m.

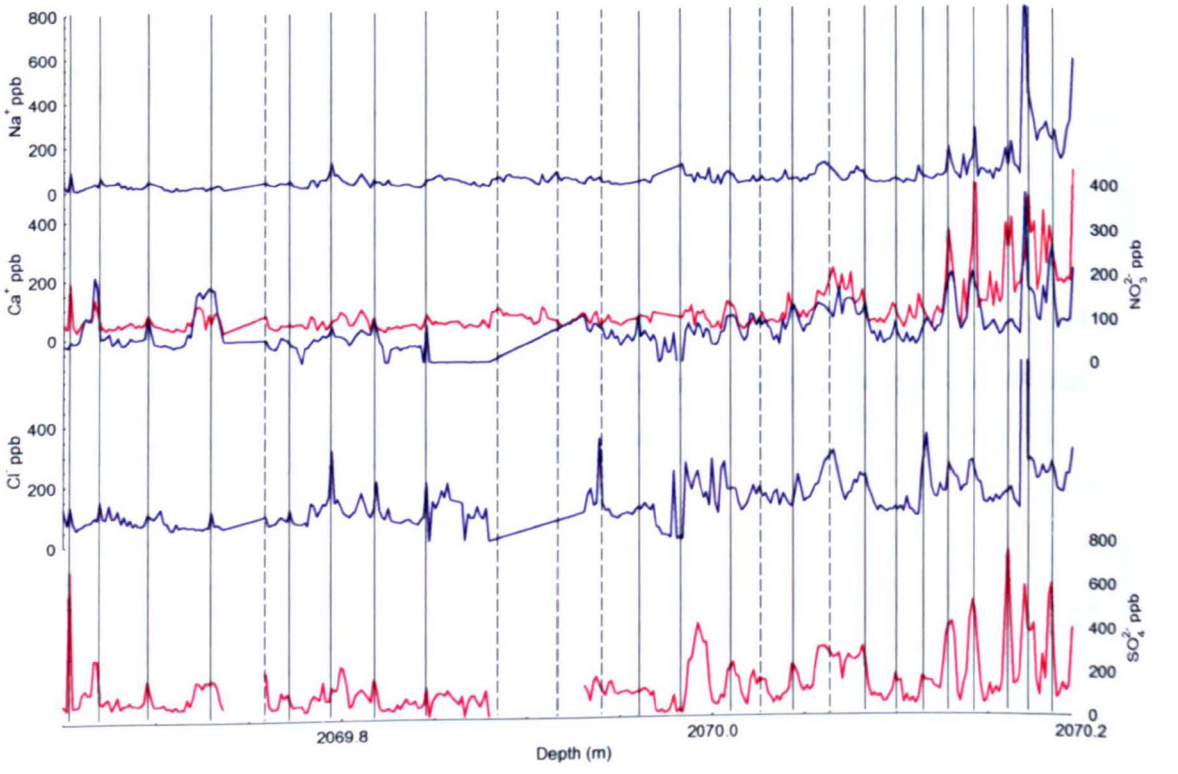

Figure 11.8. Annual layer counting of (top to bottom) sodium, calcium (red), nitrate (blue), chloride and sulphate between depths 2069.65 to 2070.20 m.

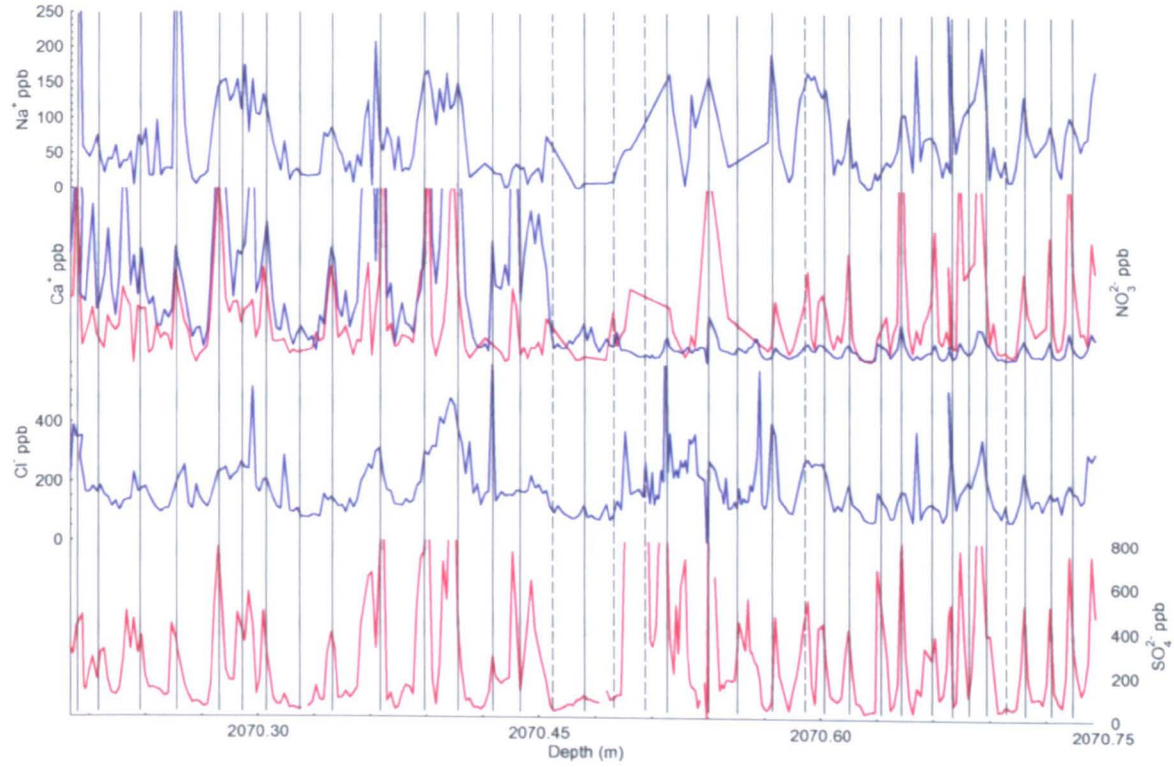

Figure 11.9. Annual layer counting of (top to bottom) sodium, calcium (red), nitrate (blue), chloride and sulphate between depths 2070.20 to 2070.75 m.

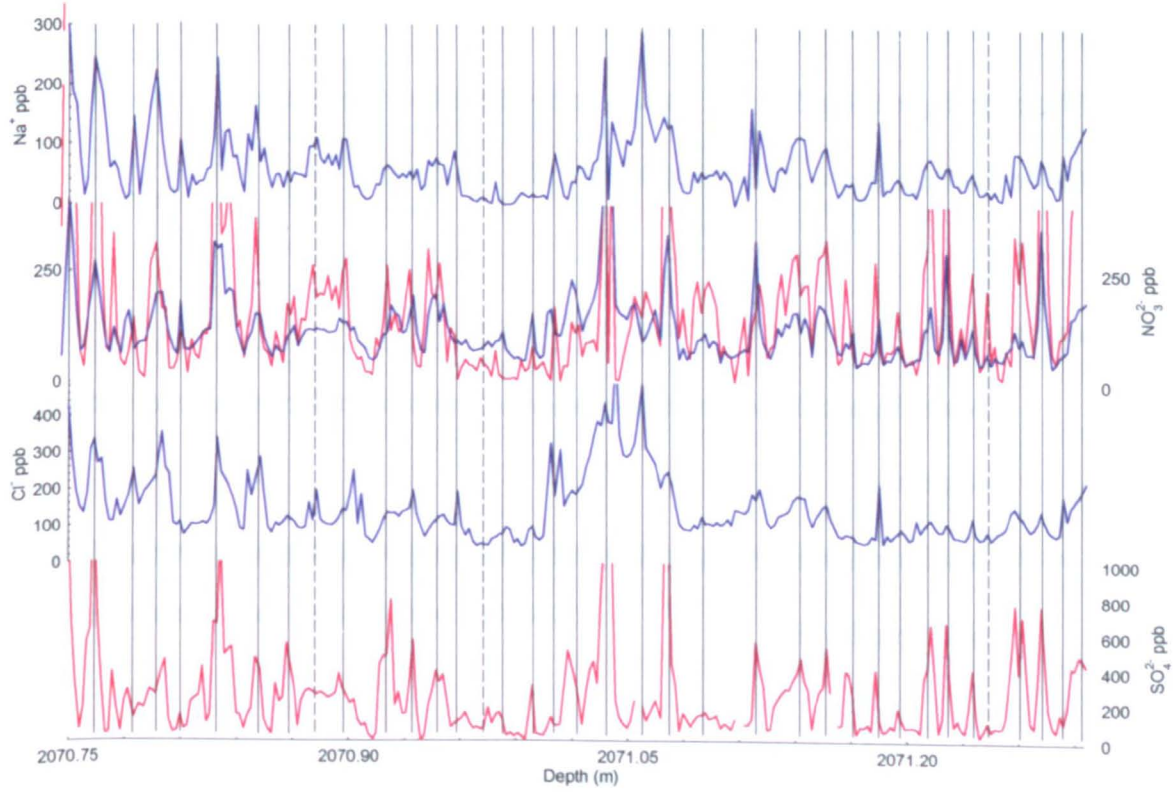

Figure 11.10. Annual layer counting of (top to bottom) sodium, calcium (red), nitrate (blue), chloride and sulphate between depths 2070.75 to 2071.30 m.

Interstadial

The ice from the interstadial, where the annual layers were slightly thicker, was harder to count. During this period the location of the different ions appears similar to that of the stadial, with most of the annual layers observed as a spring peak in all five ions at approximately the same depth. However as shown in figure 11.6 to 11.8 the signal is messy with several additional peaks in deposition occurring throughout the annual cycle.

Large deposition changes in Greenland have been seen in the chemical record (chapter 10) during the warming transition. The changes indicate a large shift in atmospheric circulation, mobilization and uplift, and conditions in source location. All of these factors could alter the seasonality of depositions to Greenland however, for the benefit of counting the annual layers it was still assumed that there was only one peak in deposition during an annual cycle, believed to occur during the spring.
The counting during this section was more subjective than during the glacial however the following rules were applied to try and constrain it.

An annual layer must (where possible) contain:

- A single, synchronous peak in all ions; calcium, chloride, nitrate, sodium and sulphate.
- A winter minimum following the spring peak, where concentrations return to near zero levels.

The layer counting during the warming transition (sections A & B) is shown in figures 11.6 to 11.10 for the length of the chemical record during the warming transition. A

total of 132 spring peaks were confidently assigned between depths 2068.6 m and 2071.3 m, with 15 spring peaks marked with a dashed line to indicate uncertainty.

11.3 Comparison with independent dating- GICC05

The new GICC05 dating for the last glacial period [Anderson et al., 2006] was produced using CFA, ECM, and visual stratigraphy. The layer thickness in the sections of ice analysed in this thesis has been compared between this thesis and GICC05 in figures 11.11 and 11.12.

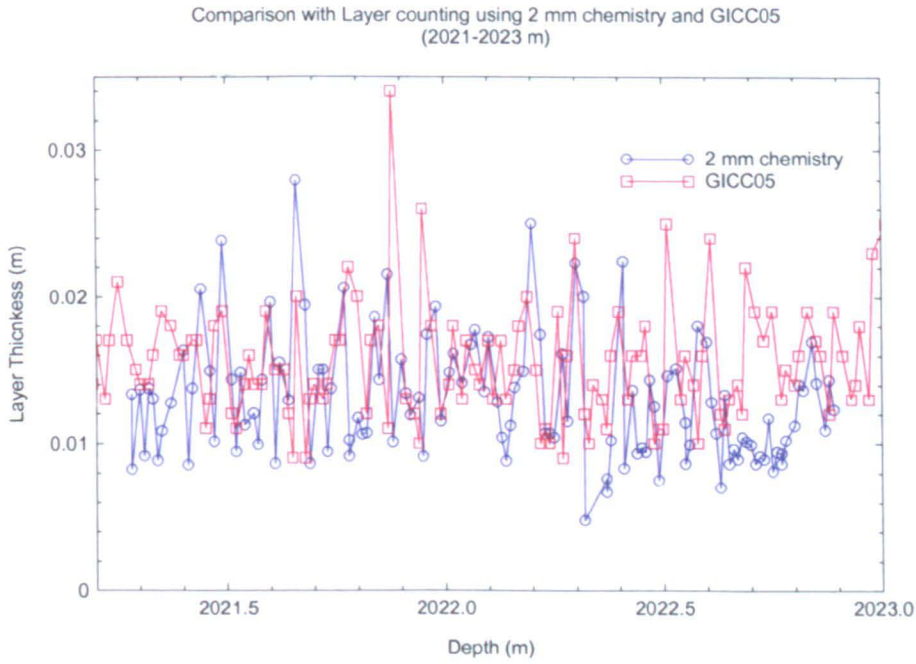

Figure 11.11. Comparison with 2 mm layer count from this thesis (blue) and GICCO5 (red) for the cooling transition, between 2021.30 m and 2022.90 m.

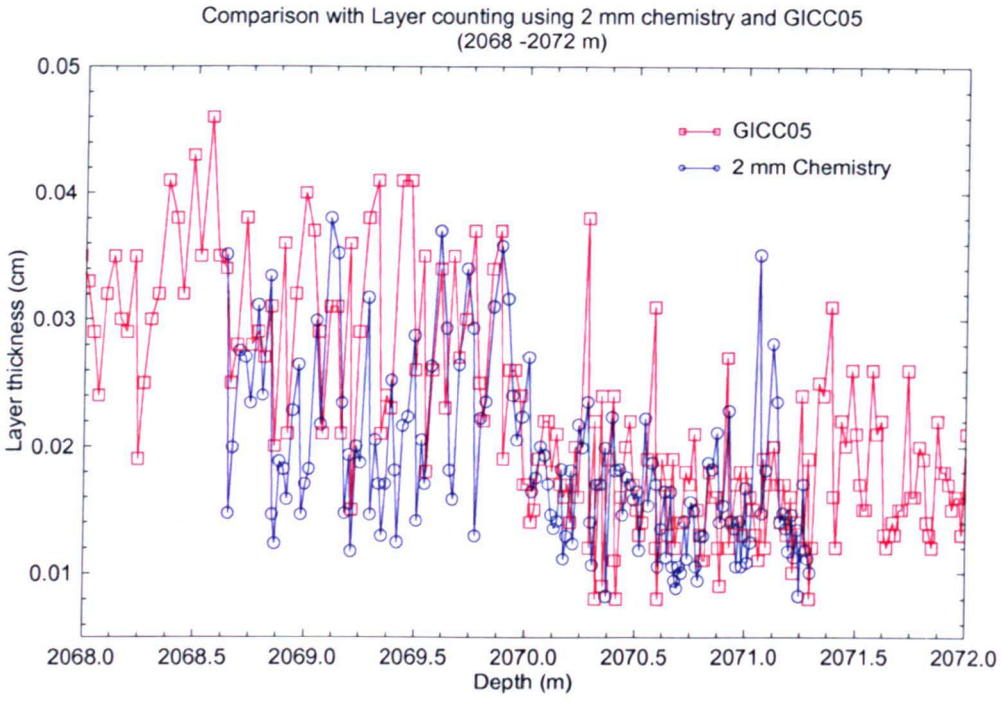

Figure 11.12. Comparison with 2 mm layer count from this thesis (blue) and GICC05 (red) from the warming transition between 2068.60 m and 2071.30 m.

The layer counting using the 2 mm chemistry with 5 ions during the cooling period (section D) is shown in figures 11.3 and 11.5. A total of 108 years and 6 uncertain years were counted compared to 105 with 5 uncertain years counted using the GICC05 method. During the warming transition (Fig 11.6 to 11.10), which included stadial and interstadial ice, 132 years with 15 uncertain years were counted using the 2 mm chemistry, compared to 129 with 9 uncertain years in GICC05. The layer thickness determined from the two methods has been compared in figures 11.11 and 11.12, which shows a generally good agreement, with the number of years in each section within the error of both methods.

Despite the good agreement, the number of years counted using the 2 mm chemistry is consistently higher than the number of years counted using the GICC05 method.

The reason for this is probably the increased resolution of the 2 mm data compared to that of the GICC05 data.

During the Holocene and the late glacial the resolution of the CFA record was greater than the annual thickness, and therefore a powerful tool for annual layer counting in the GICC05 method. However by the mid- early glacial the annual layer thickness of the ice was significantly lower that the temporal resolution of the CFA meaning that distinguishing annual layers was increasingly difficult. This is shown in figure 11.13 where the CFA has been overlaid on the 2 mm chemistry during the warming transition. The single broad peaks in the CFA are actually seen as many individual peaks corresponding to several years in the counting. The CFA was therefore unsuitable for layer counting in this period.

The annual layer counting around DO-8 was therefore heavily reliant on visual stratigraphy (VS), conductivity and to a lesser extent ECM. The VS, conductivity, CFA and 2 mm chemistry records have been combined in figure 11.13 for the warming transition; between 2070.0 m to 2070.4 m. The years determined using the GICC05 method are marked as dots on the conductivity record and the years determined using my counting are shown as vertical lines. Open (smaller) dots indicate uncertain years in the GICC05 record and dashed lines indicate uncertainty in my counting method.

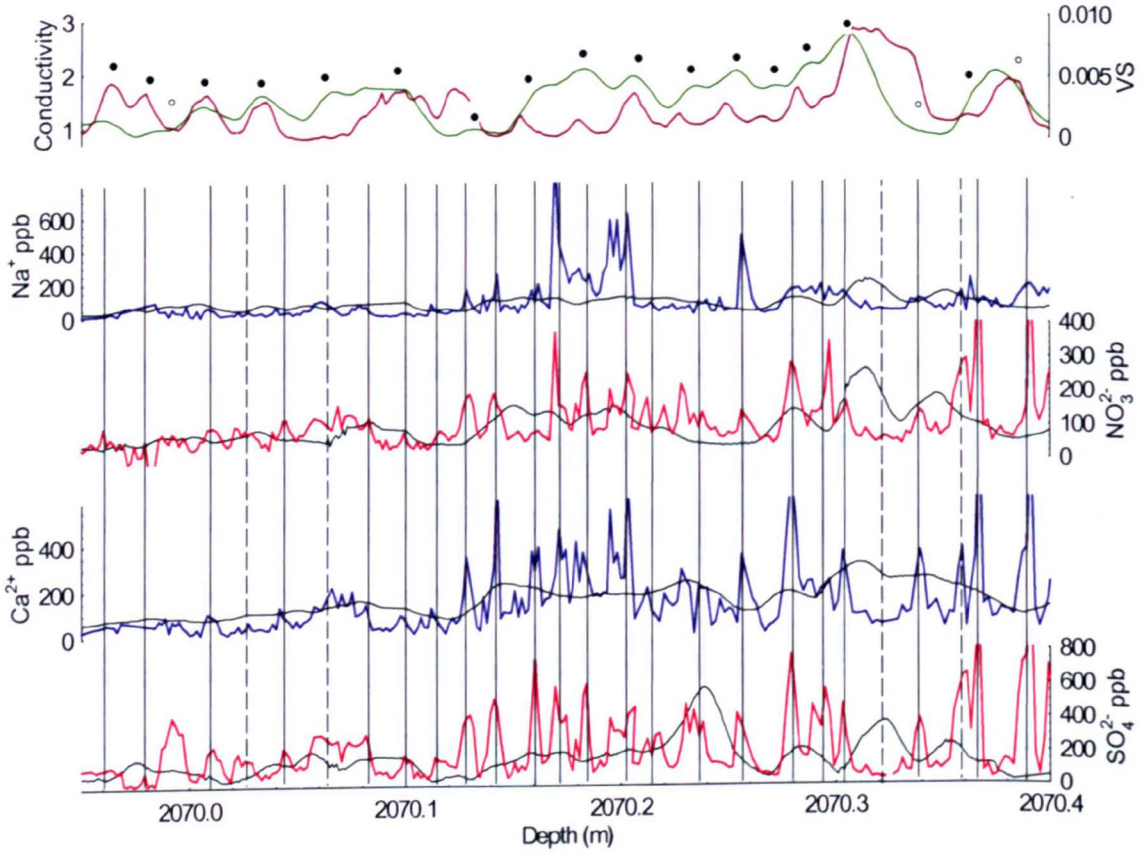

Figure 11.13. Top graph; Visual stratigraphy (brown), and conductivity (green). Bottom four graphs (top to bottom); sodium, nitrate, calcium and sulphate at 2 mm resolution between 2070 – 2070.4 m, CFA of each ion overlaid in black. Dots in top graph represent years counted using GICC05, open dots represent questionable years according to GICC05. Solid lines represent confident years and dashed lines represent questionable years counted in this thesis.

11.4 Accumulation rate

The snow accumulation rate during the warming transition has been calculated using the layer thickness determined by the annual layer counting of the new high-resolution chemical record. A Dansgaard-Johnsen model was used, as described in chapter 6.

The accumulation rate is shown in figure 11.14 across the warming transition. The accumulation rate increases by 33 %, from 5.4 cm ice/year before the warming to 8.1 cm ice/year after the warming. This is a change from an average annual layer thickness of 1.5 cm before the warming transition to 2.2 cm after the warming. The transition in accumulation begins later than the transitions in $\delta^{18}O$ at a depth of 2070.10 m, (determined in the same way as the isotopes and chemistry, red horizontal lines in fig 11.14) however the termination is reached earlier, at a depth of 2069.95 m.

The accumulation rate was calculated using a Dansgaard-Johnsen model (described in chapter 6 [Johnsen and Dansgaard, 1992; Johnsen et al., 1995]) plotted on figure 11.14 (dashed black curve) at approximate decadal resolution. Given the dependence on the $\delta^{18}O$ record, the features and transition points from the model derived accumulation profile are the same as the $\delta^{18}O$ record. This contradicts the annual layer determined accumulation transition, which begins and ends faster than the $\delta^{18}O$ record.

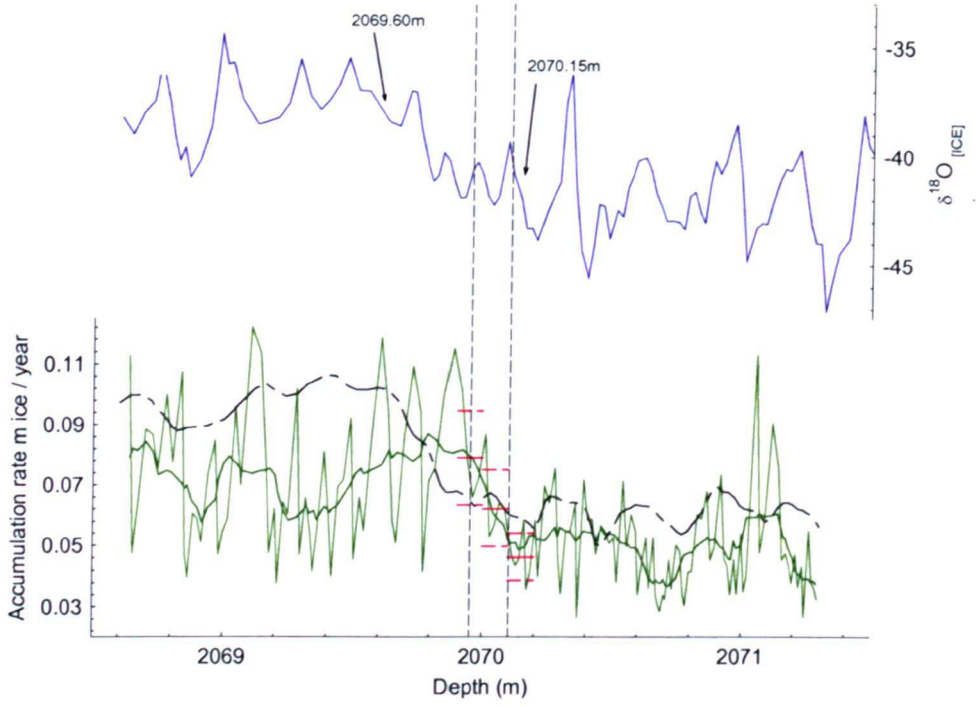

Figure 11.14. Top; Oxygen isotopes (blue) at 2 cm resolution, arrows and depth labels showing onset and termination of warming transition. Bottom: accumulation rate at annual (thin green) and decadal (thick green, smoothed by a factor of 10) resolution derived from annual layer counting and decadal resolution from model-derived rate (dashed black, smoothed by a factor of 9[16]). Vertical dashed lines indicate onset and termination of accumulation transition.

The average accumulation rate derived from annual layer counting and the Dansgaard-Johnsen model are compared for the period before and after the warming in table 11.1. The model derived accumulation rates are consistently higher than the annual layer counted rate, especially during the period after the warming (interstadial, section B) with an average rate more than 1 cm a year higher in the model derived method. A better agreement is observed during the period before the warming (stadial, section A) when accumulation and temperatures are lowest. This suggests a change in

[16] Annual resolution not available because the $\delta^{18}O$ used in model is at 2 cm resolution, therefore record smoothed to 18 cm based on an average annual layer thickness of 1.8cm to give an approximate decadal record.

the relationship between $\delta^{18}O$ and temperature during the onset of the interstadial, or an overestimate of the relationship between accumulation rates and $\delta^{18}O$ in the model.

	Accumulation rate cm yr^{-1}	
	Annual layer derived	Model derived
Average before warming (A)	5.45	6.04
Average after warming (B)	8.14	9.21

Table 11.1 Comparison of the average accumulation rate, before and after the transition, derived from annual layer counting and the Dansgaard-Johnsen model.

11.5 Seasonality

The deposition of marine and continental aerosols to Greenland varies throughout the year, which enables the annual layer to be determined. It was shown that the annual cycle during the stadial, when temperatures were at the coldest, was dominated by a single synchronous peak and trough in all species. For the ice from the interstadial, the annual cycle was less clear, with more than one peak throughout the year indicating a change in seasonality.

The annual layers for the whole of the warming transition have been determined and plotted in figures 11.6 to 11.10, showing a total of 132 years with 15 uncertain years. Using this information the strength of seasonal deposition could be analysed using a method of determining the peaks and troughs within the annual cycle.

In many species the minimum is observed during the summer months, with a second smaller peak in deposition during the late summer/ autumn. Due to ice thinning, resulting in a small number of data points each year, it is hard to determine all the

seasons within an annual layer. For this reason it has been assumed that peaks indicate a spring maximum and troughs a summer minimum. In this way the maximum and minimum values within the annual cycle could be determined in order to assess the change in seasonal strength across the transition.

The spring maximum value has been determined for all years in which enough ice was available to provide a reliable maximum and minimum. Care was taken to ensure that only years with more than 5 data points and a distinctive seasonal cycle (which included a maximum and minimum) were used, to capture a full year. In sections where ice was broken, damaged or cut to a larger size (such as at section ends), there were not enough data points within an annual layer to confidently determine the maximum and minimum and as such these years were removed. In general there are clear maximum and minimums in the glacial to allow a degree of confidence that the maximum value within each year is in fact the spring peak and not an additional peak. In the interstadial however (as discussed in section 11.2), the annual signal was less clear.

The maximum and minimum within each annual cycle has been plotted in figures 11.15 to 11.18.

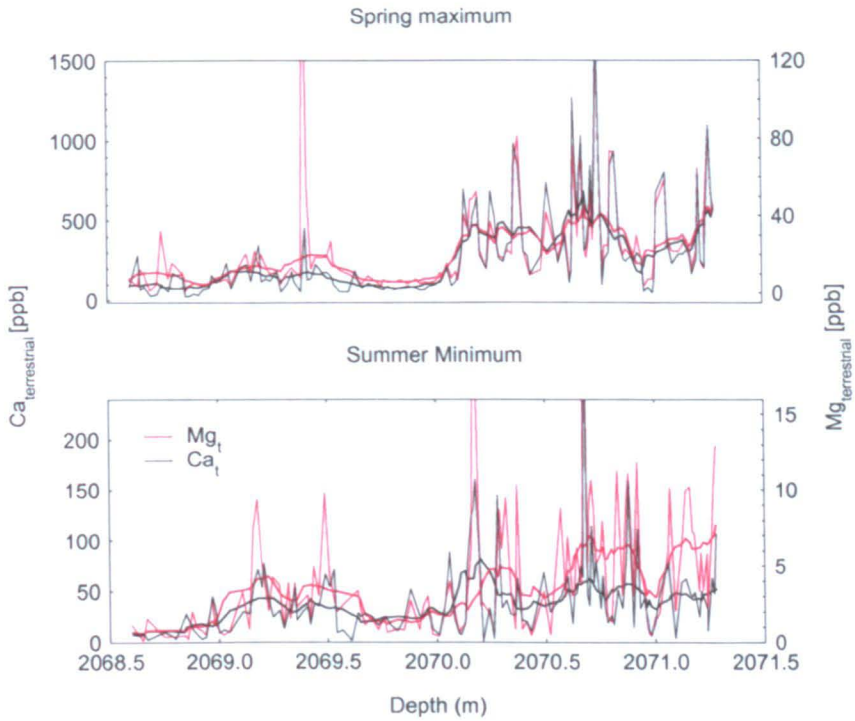

Figure 11.15 Spring (maximum), and summer (minimum) for terrestrial calcium (black) and terrestrial magnesium (red) during the warming transition. Thin curves indicate annual data and thick curves are 10 years averaged.

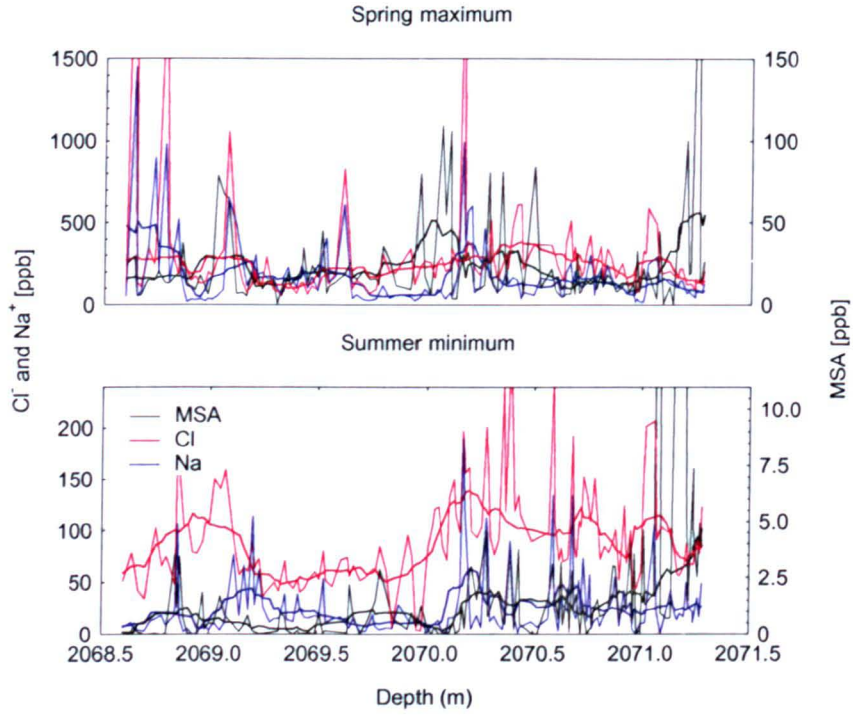

Figure 11.16 Spring (maximum) and summer (minimum) for chloride (red), sodium (blue) and MSA (black) during the warming transition. Thin curves indicate annual data and thick curves are 10 years averaged.

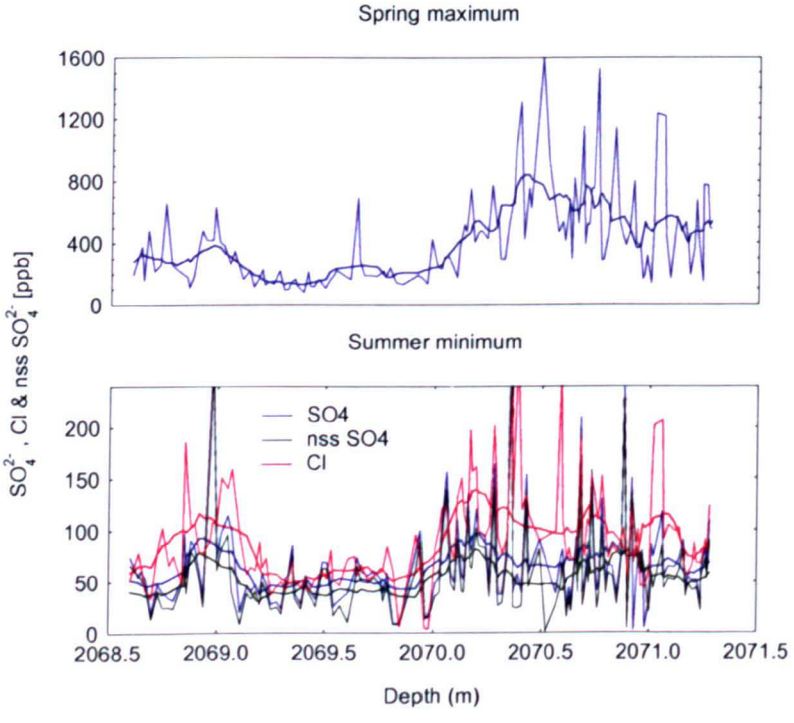

Figure 11.17 Spring (maximum), and summer (minimum) of chloride (red), sulphate (blue) and non-sea-salt sulphate (black) during the warming transition. Thin curves indicate annual data and thick curves are 10 years averaged.

	Concentration [ppb]												
	Na^+	Na^+ marine	K^+	Mg^{2+}	Mg^{2+} terrestrial	Ca^{2+}	Ca^{2+} terrestrial	F^-	MS^-	Cl^-	NO_3^{2-}	SO_4^{2-}	n.s.s. SO_4^{2-}
	Spring Maximum												
Average before warming	135.6	115.8	34.1	34.1	32.7	449.2	444.3	8.9	40.0	258.2	188.4	585.1	564.3
Average after warming	95.0	91.2	23.7	7.8	7.3	90.6	88.5	9.7	22.1	220.4	103.4	228.6	216.5
% Decrease in maximum	29.9	21.2	30.5	77.1	77.7	79.8	80.1		44.8	14.6	45.1	60.9	61.6
	Summer Minimum												
Average before warming	28.9	22.3	5.8	6.1	5.6	51.7	52.0	1.2	4.0	108.1	61.7	75.6	63.7
Average after warming	10.3	8.3	4.6	1.7	1.5	22.7	21.4	0.4	0.8	58.4	38.7	46.3	37.5
% Decrease in minimum	64.4	62.8	20.7	72.1	73.2	56.1	58.8	66.7	80.0	46.0	37.3	38.8	41.1

Table 11.2. Average annual maximum and minimum before and after the warming transition and the percentage decrease.

The concentrations of all ions drop considerably immediately after the warming transition, remaining low for several years until a depth of 2069.6 m (Chapter 10). For the benefit of investigating the change in seasonal strength at the transition, the years before the warming have been compared to the years immediately following the warming. The changes in the average concentrations of the annual maximum and minimum are shown in table 11.1 along with the percentage change at the transition.

A significant change in the spring maximum and summer minimum is observed for all species during the warming transition. With the exception of fluoride, the average concentration of the spring peak and the summer trough is higher during the stadial than the interstadial, however the magnitude of the change is different for the marine and continental species.

Calcium and sulphate show only a relatively small change (decreasing 56% and 39% respectively) in the concentration of the summer minimum while the percentage change for the concentration of the spring peak is much greater (80% and 61% respectively). The marine ions, sodium and chloride, show a larger change in the concentration of the summer minimum than the spring maximum; decreasing 64 %, and 46% respectively for the summer minimum and 30 % and 15% for the spring maximum. Therefore it appears that changes in summer-time deposition is greatest for the marine species while spring deposition changes are the dominant factor in the continental species.

Shape of the seasonal cycle

The annual layers have been used to determine the shape of the seasonal cycle (with respect to the location of deposition) and how it changed throughout the warming transition. The concentration of each ion within a determined year has been divided into twelve increments by a robust cubic spline interpolation routine (using a programme written in MatLab), representing each month of the year. As with the investigation of seasonal strength, only years with greater than 5 data points and a clear seasonal cycle with a distinct minimum and maximum were used. The location of deposition (seasonal cycle) of each year can then be averaged to give a general cycle for each ion during the stadial, the transition and the interstadial, as shown in figures 11.18 and 11.19.

The period during the transition (red curve in figs 11.18 and 11.19) is only based on three years (representing the final chemistry step) and is therefore less robust than the period before and after the warming, which is an average of 79 and 45 years respectively.

In figure 11.18 calcium and sulphate have been compared during the stadial, the interstadial and during the transition. Both calcium and sulphate show a large change in the strength (concentration) of the spring maximum and summer minimum during the transition, as observed earlier. The general shape of the seasonal cycle is similar both before and after the transition, with a broad maximum and minimum at approximate 6-month intervals of each other. The decrease in deposition from the absolute maximum to the absolute minimum takes slightly longer during the

interstadial than during the stadial; possibly indicating longer winters or additional spring deposition.

The general shape of the seasonal cycle for the marine ions (sodium and chloride) appears to have changed, during the interstadial than the stadial, with the location of the minimum slightly earlier and a shorter period of low deposition.

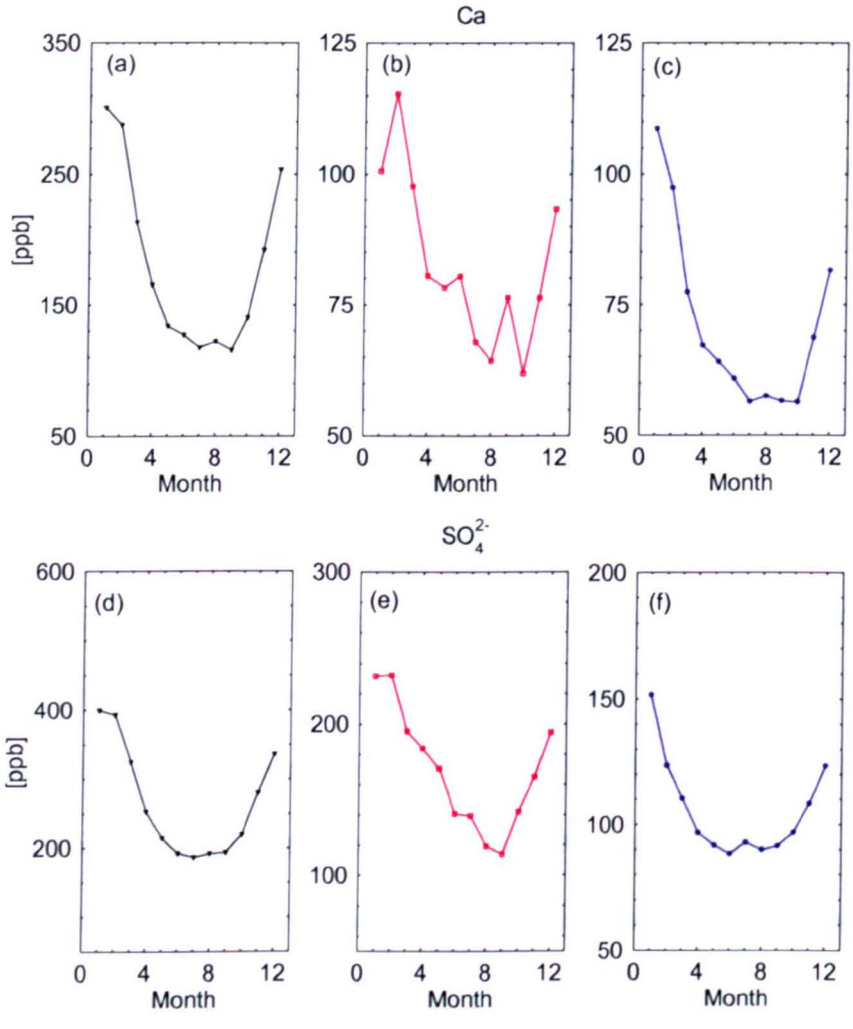

Figure 11.18. Comparison of the seasonal cycle in calcium (top) and sulphate (bottom) during the stadial (black), the transition (red) and the interstadial (blue). Note the changing left-hand axis.

There is a distinct change in the seasonal cycle in the transition years (red curves on fig 11.19) for both species. Sodium shows a shift in the maximum values, peaking later in the year; during months 3 / 4 compared to months 12/1 before and after the transition. Chloride however peaks earlier in the year; during months 11/12 compared to 12/1.

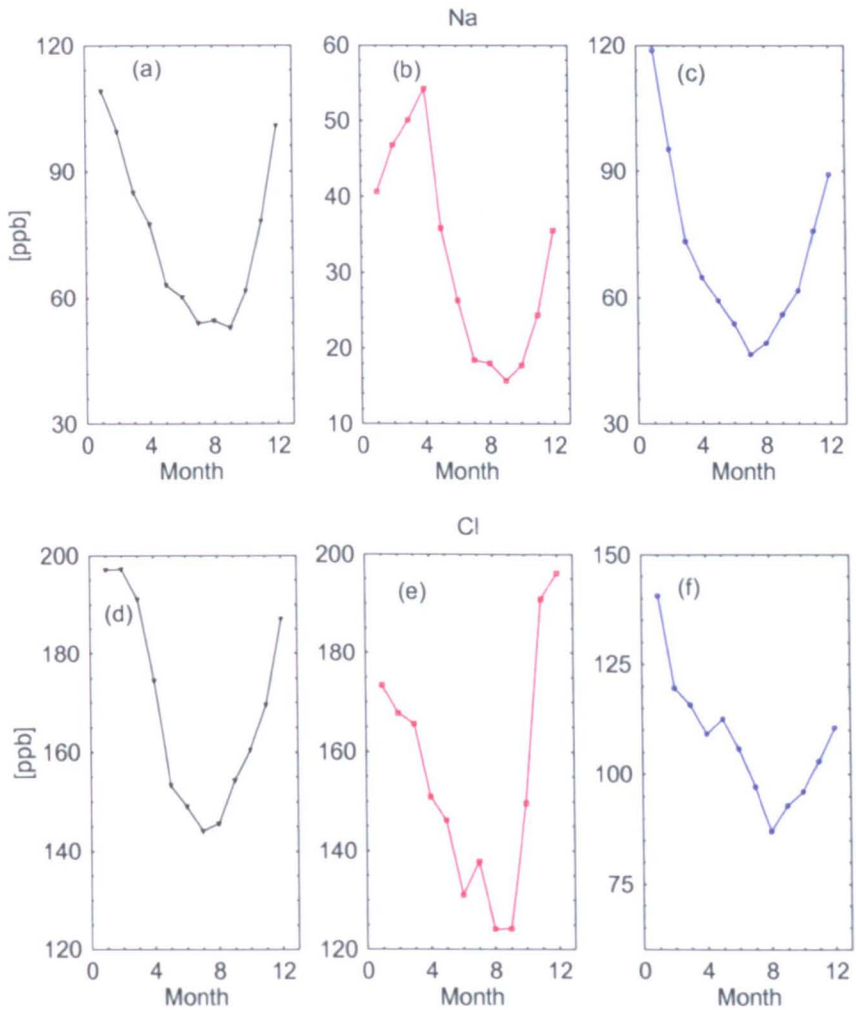

Figure 11.19 Comparison of the seasonal cycle in sodium (top) and chloride (bottom) during the stadial (black), the transition (red) and the interstadial (blue). Note the changing left-hand axis.

11.6 Summary of annual layer counting, accumulation and seasonality at DO-8

Annual layer counting has been carried out using five ions from NGRIP during the warming transition at the onset of DO-8 and during the cooling transition at the termination of DO-8. A total of 132 years were confidently counted during the warming transition with 15 years marked as uncertain. This compares well to the independently dated GICC05 age-scale that confidently marked 129 years with 9 uncertain years over the same period.

The accumulation rate was calculated from the true layer thickness determined by annual layer counting. An increase of 33 % was observed during the warming transition with the annual layer thickness decreasing from an average of 1.5 cm during the stadial to 2.2 cm during the interstadial.

A change in seasonality is observed at the warming transition at the onset of DO-8. For the continental and non-marine species (Ca_t, Mg_t, NO_3^-, SO_4^{2-}, K^+) the change in spring deposition is greatest however for the marine and non-continental species (Na^+, Cl^-, F^-, MSA) the change in summer deposition is greatest. This change in seasonality is also reflected in the shape of the seasonal cycle with a longer period of summer deposition observed in calcium during the stadial than the interstadial. For the marine ions, sodium and chloride, there is a shift in the location of the spring maximum.

Chapter twelve

DO-8: Discussion

DO-8: Discussion

The warming transition into DO-8 began approximately 38,166[17] years ago, according to the GICC05 age scale [Andersen et al, 2006] based on the transition in the deuterium excess. It is observed in the NGRIP ice core as an abrupt jump in average mean annual temperature of over 13 °C, from a period of extreme cold during the stadial to a warm period during the interstadial. The event is clearly seen in the isotope record, the accumulation rate (as determined by the annual layer counting) and in the chemical deposition to Greenland.

12.1 Precursors to the warming transition

Oxygen and deuterium

The average mean annual temperature after the warming transition (for the length of ice analysed) remains relatively constant at approximately 12 °C lower than present day temperatures at Summit Greenland. However, the stadial period before the warming transition is far from stable.

During the coldest glacial period, there are several large and abrupt changes in the isotope record, some of which (if truly reflecting temperature) indicate temperature increases of more than 28 °C in just 2-4 years (figure 9.1, p.194). The most abrupt jumps occur at 2070.33 m – 2070.4 m and 2071.3 m in the oxygen and deuterium record. The signature of both events is the same; first there is an abrupt temperature decrease to absolute minimum values. Following this, there is a jump to significantly

[17] The ages and the durations of the transition have been determined from annual layer counting. The transition point in the deuterium excess record at 2069.95 m corresponding to an age of 38,161 years BP (1950) based on the GICC05 age-scale [Andersen at al., 2006] has been chosen as a reference with years above and below this counted using the 2 mm chemical record.

warmer temperatures for a short period before temperatures drop again in an equally abrupt step to background levels.

During the larger of the two (at 2070.33 m -2070.4 m), temperatures rise from among the lowest in the record to among the highest; reaching a maximum just 0.84 °C lower than present day temperatures at Summit. The temperature excursion is the largest in the oxygen isotope record from the small section of ice analysed in this thesis and is the largest single excursion of the surrounding 100 m [NGRIP members 2004]. The second highest oxygen jump is 1.25 ‰ (±0.05‰) smaller in amplitude and occurs during the cooling transition out of DO-8. Although significant, the jump at 2070.33 m is short-lived and temperatures drop again after approximately 5 years to background values. However, from this point onwards the isotopic signal never drops below the pre-warming average and instead values rise steadily until a constant interstadial temperature is reached.

Deuterium excess

The record of deuterium excess (see fig 9.1, p194) appears in-phase with oxygen and deuterium (and therefore temperature) for most of the stadial period. The same abrupt jumps in the oxygen and deuterium record during the stadial are observed as synchronous increases in the deuterium excess. The largest and most abrupt occurs at 2070.33 m to 2070.4 m, where values rise by as much as 11.45 ‰ (±1.4‰), with smaller deuterium excess deviations occurring at 2071.0 m and 2071.3 m. The amplitude of the deuterium excess jumps appears to increase with time; getting larger the closer they get to the final warming transition.

The deuterium excess in polar snow generally preserves the oceanic conditions at source and an increase is expected in response to enhanced moisture recycling, expected if sea-surface temperatures (SSTs), source temperatures or the relative humidity increase [Masson-Delmotte et al., 2005]. The abrupt shifts in deuterium excess above the glacial average (7.73 ‰ ±1.4 ‰) imply a change in moisture source, possibly to a warmer location. This could imply either a southward shift in atmospheric circulation to a region of warmer SSTs or possibly be an indicator of warmer waters entering the North Atlantic.

12.2 The onset of DO-8

The most robust change in chemical deposition and isotopic composition is the final warming transition that marks the onset of interstadial 8. Compared with the abrupt temperature jumps in the ice during the glacial, the final transition is observed as a gradual change in the isotopes, taking several years to stabilize. The point at which the transition starts is hard to determine graphically, although it would appear that it happens following one of the largest isotope spikes between 2070.33 m and 2070.4 m (fig 9.1, p.194).

Oxygen and Deuterium

The point at which the isotope record (and therefore temperatures) consistently rises above the stadial background was determined at 2070.15 m, representing the onset of the warming transition at approximately 38,177[16] years BP. In a period of approximately 16 years, temperatures (inferred from the $\delta^{18}O$ record) increase by almost 13 °C until they stabilize after a depth of 2069.8 m. The transition takes place in a series of abrupt jumps with both the first and final steps taking place in less than

two years, a similar duration to the larger less robust jumps observed during the stadial period.

Deuterium excess

It is only after the warming transition has begun in the isotope record (fig 9.1, p.194) that the relationship with deuterium excess changes from in-phase to out-of-phase. The sudden drop occurs at a depth of 2069.95 m, (approximately 38,166 yrs BP 1950 [Andersen et al., 2006]) eleven years after the onset of the transition in $\delta^{18}O$ (fig 12.1). This point has been chosen as the reference for dating, using the GICC05 age at this depth [Andersen et al., 2006] as a central point for the annual layer counting of the 2 mm chemical record. The transition is the fastest of all records investigated (isotopes and chemistry) taking place in a single year and indicates a significant change in source location or condition. The sudden drop in deuterium excess at a time when temperatures in Greenland are increasing could indicate a northward shift in source area, to a region of colder waters with less evaporation, consistent with the idea of retreating sea ice as the North Atlantic warms following strengthened THC.

Chemical deposition

The precursor climate switches appear to be robust in the isotope record and the record of chemical deposition (fig 10.5 & 10.6, p.21 & 216), the largest of which is coincident with the onset of the chemical transition into DO-8. The transition point in the terrestrial chemical record (calcium) was determined using 5 cm and 10 cm running averages, in the same way as the isotopes. The transition was determined to occur in three steps starting at a depth of 2070.35 m (38,188 years BP), coincident with the abrupt isotope and deuterium excess switch. The second step occurs at

2070.10 m, followed by a third and final jump at 2070.05 m, after which concentrations in all species remain low for more than 20 years. For the marine ions the transition in sodium is observed at a depth of 2070.1 m however the transition is not clearly defined for chloride and MSA.

The shape of all steps follows the same pattern. They are first seen as an abrupt decrease below background concentrations to near interstadial levels. Concentrations remain low for a few years before returning to the stadial average in an equally rapid step. The pattern is observed three times until the last transition at 2070.05 m (38,170 years BP), where the concentrations do not return to pre-interstadial levels.

What changes first?

The location of the transition, as determined by the isotopes and the chemistry, is shown in figure 12.1. The transition is first observed in the chemical record at a depth of 2070.35 m, corresponding to an age of 38,188 years BP. The chemical transition is short, lasting only 18 years, occurring in three distinct steps. Following the onset in the chemistry it is a further 11 years before the isotopes appear to show an increase. The transition in the chemistry is complete, with concentrations stabilized at the interstadial level, almost 19 years before the isotopes stabilize.

The deuterium excess is the last to show a change, with the transition occurring 22 years after the onset of the chemical transition and 11 years after $\delta^{18}O$ and δd begins to increase. However, the deuterium excess transition is the most rapid, taking place in a single year. Therefore it is the $\delta^{18}O$ and δd that is last to stabilize, at a depth of

2069.8 m (38,161 years BP), 27 years after the transition is first observed in the chemistry.

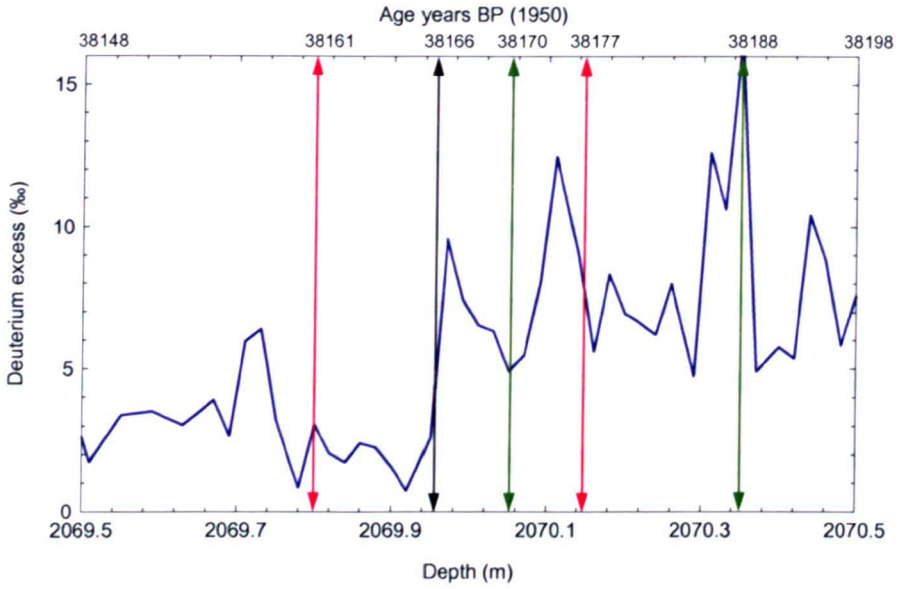

Figure 12.1 Transition points determined from the isotope record (red arrows), the deuterium excess record (black arrow) and the chemical record (green arrows) for DO-8 shown on the deuterium excess record (2 cm resolution). The age-scale is based on annual layer counting with deuterium excess transition point at 2069.95 m used as a reference point.

Accumulation

The annual layers of each ion were counted during the warming transition and show good agreement with the new GICC05 age-scale [Andersen et al., 2006], improving the confidence in this method. The annual layer thickness increased from an average of 0.15 cm during the stadial to 0.22 cm during the interstadial, representing an increase in accumulation of 33 % during the warming transition. The onset of the accumulation transition was determined at a depth of 2070.1 m; slightly lagging the $\delta^{18}O$ transition however stabilizing earlier, at a depth of 2069.95 m.

Seasonality

The new age-scale determined from the annual layer counting of the 2 mm chemical record was also used to investigate the change in seasonality during the warming transition. For the continental and non-marine species (Ca^{+}, Mg^{2+}, SO_4^{2-}, K^{+}, NO_3^{2-}) the greatest change in seasonal strength was observed in the spring maximum (fig 11.15 and 11.17, p.251 and 252). The decrease at the warming transition was large with concentrations dropping 62 % for non-sea-salt sulphate and 80 % for calcium. This compared to a drop in the summer minimum of 41 % for non-sea-salt sulphate and 56 % for calcium. There is little change in the shape of the average seasonal cycle, which shows a broad maximum during the winter/ spring months and a broad minimum during the summer months; however the period of deposition is slightly longer during the interstadial.

For the marine and non-continental species (Na^{+}, Cl^{-}, MSA, F^{-}) there is also a large change in the spring maximum and summer minimum (fig 11.16, p.252). The percentage change in deposition at the transition is greatest in the summer minimum; indicating a greater change in summer deposition than winter/ spring deposition as the temperatures get warmer. This contradicts theories by Denton et al., (2005) that wintertime seasonality changes were dominant. The evidence that summertime deposition was also larger (for marine and non-continental species) prior to the warming indicates that both summers and winters were colder, at least in Greenland.

Changes in North Atlantic circulation have been proposed as a mechanism for the exceptionally cold stadials; with theories of THC weakening or shutdown. If deepwater formation and sinking diminished then the warm waters from the tropical

Atlantic would no longer be pulled northward. Sea ice would form more readily in the colder North Atlantic waters forming a lid lasting most of the year [Overpeck et al., 1997]. The insulating sea ice would prevent relatively warm ocean water from heating the adjacent landmasses and act as an amplifier, reflecting sunlight and further cooling the region. Under these conditions it would be expected that summer temperatures in Greenland and the North Atlantic would be colder and drier.

The shape of the seasonal cycles appears to change for the marine species with a generally more complex signal during the interstadial that the stadial. For all ions, including the continental species, the transition period is observed as a messy seasonal cycle with peaks of deposition throughout the year, not just during the winter period. However, the short duration of the transition means that the shape of the seasonal cycle during the transition period is not as robust as it is only an average of 5 years. The comparison of the cycle before and after the warming gives a better indication of the change, because it is an average of several decades of data.

For the continental species, there is little change in the shape, however for chloride and MSA there appears to be a much stronger springtime peak during the interglacial. The additional (or stronger) deposition could be a result of a northward shift in the sea ice zone, bringing the source (from sea ice break-up) closer to Greenland.

12.3 Cooling

Following the warming transition at the onset of DO-8, the temperature (inferred from the isotopes) remains relatively warm for several hundred years before cooling slowly back to extreme glacial temperatures. The cooling transition was investigated in the NGRIP ice core for two sections between 2021.2 m to 2022.9 m (section D) and

2026.2 m to 2028.2 m (section C). The isotopes reveal no major excursions or temperature deviations in these two sections of ice and instead show a gradual decline, with slopes of just 0.02 ‰/m and 0.03 ‰/m respectively. The coldest ice analysed, 2021.2 m to 2022.9 m, (also the youngest ice analysed) has an average oxygen isotope value of -42.84 ‰ corresponding to an inferred temperature almost 24 °C colder than present day Summit Greenland. The older ice, 2026.2 m to 2028.2 m (section C) is 3.28 °C warmer than section D, with similar average temperatures to those before the warming transition. The rate of deposition is doubled between section C and D for calcium, chloride and sulphate, and quadrupled for sodium, despite a rate decrease in the $\delta^{18}O$ from 0.02 ‰yr^{-1} to just 0.01 ‰ yr^{-1} (Table 10.5, p.229).

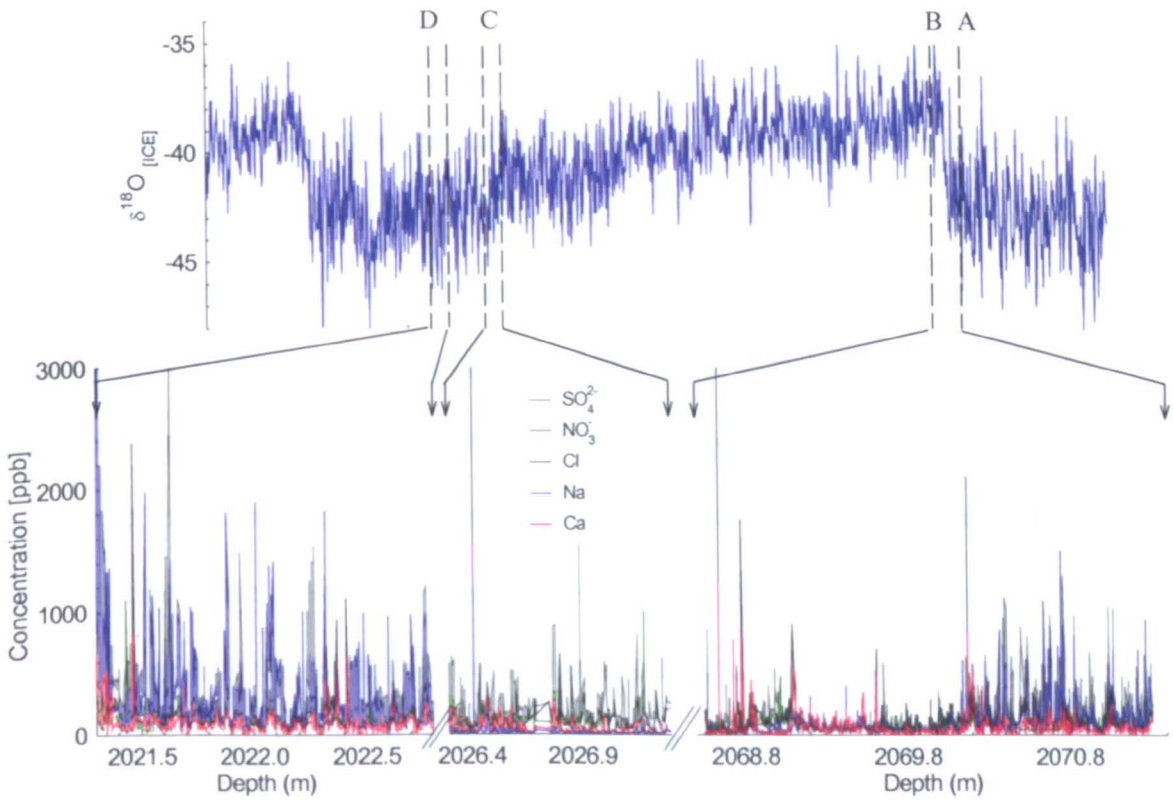

Figure 12.2 (also fig 10.12, p.226) DO-8 from NGRIP, oxygen isotopes (top blue curve) [NGRIP members 2004] and chemistry (bottom curves) at 2 mm resolution.

The total record of chemical deposition is plotted in figure 12.2 along with the isotope record for the whole of DO-8. It shows that the lowest concentrations in most ions is observed during the warmest periods B and C, with the greatest deposition observed during the final part of the cooling in section D.

12.4 The anatomy of Dansgaard-Oeschger event 8

The shifts in the isotope record in the period prior to the warming transition are both large and abrupt. They are not only significant within the record obtained in this thesis but are the largest transitions of the surrounding 100 meters. If the record were to truly reflect surface temperatures at summit Greenland then the abrupt jumps would indicate an increase of almost 28 °C in less than 5 years.

The evidence that the deuterium excess undergoes a significant shift broadly in-phase with oxygen and deuterium would imply that these abrupt jumps represent more than just a temperature signal. The increase of more than 9 ‰ in deuterium excess at 2070.33 m to 2070.4 m (fig 10.7) indicates either a significant alteration in the moisture source location or the source conditions. This could mean a southward shift to warmer waters or possibly be an indicator of an increase in the SSTs in the North Atlantic.

It has been shown that sea surface temperatures in the North Atlantic increased by as much as 3-5 °C during the interstadial 8 [Bond et al., 1993; Curry and Oppo, 1997; Sachs and Lehman, 1999; Hendy and Kennett, 1999], and therefore it is expected that this increase would be observed in the isotope record. If the deuterium excess is truly

indicating warmer SSTs it is interesting that it occurs prior to the warming transition, in a period when background temperatures are still extremely cold.

Paleoclimate records from the tropical Atlantic [Hughen et al., 1996; Peterson et al., 2000], the tropical pacific [Bard et al., 1997; Stott et al., 2002], the Indian ocean [Burns et al., 2003; 2004] and Asia [Wang et al., 2001] support the theory DO events in Greenland coincided with a warming of the tropical deep basin water. The result of the warming in the tropics would be an increase in the strength of the THC northerlies, transporting warm saline water into the North Atlantic. This mechanism has been proposed as a tropical precursor to DO events and maybe even a tropical trigger [Hendy et al., 2002; Broecker, 2003; Denton et al., 2005].

Knorr and Lohmann (2003) proposed that warmer southern oceans triggered the interstadials in the northern hemisphere; attributed to local Milankovitch forcing or tropical SST anomalies. A three-dimensional ocean circulation model was used to show an abrupt resumption of the interglacial mode of the THC is observed when the southern ocean is warmed gradually. The southern ocean warming and reduction in sea ice extent enhances mass transport into the Atlantic, via the warm Indian Ocean and the cold Pacific route, resulting in increased northern hemisphere temperatures and reduced southern hemisphere temperatures [Knorr and Lohmann, 2003]. This is consistent for the observations that the most recent deglaciation that warming in the southern hemisphere preceded that of the northern hemisphere by more than 1,000 years [Sowers and Bender, 1995].

The model results show an increase in THC strength irrespective of increased melt water entering the North Atlantic from retreating North American and Scandinavian ice sheets. A mechanism normally associated with reduced NADW formation [Stocker and Wright, 1991; Marshall and Clarke, 1999] and THC shutdown [Renssen et al., 2002].

12.5 Comparison with oxygen isotope record at DO-7

Dansgaard-Oeschger event 7 occurs at approximately 35 kyr BP [Andersen et al, 2006] and is less extreme and shorter in duration than DO-8. However based on the oxygen isotope record [NGRIP members 2004] there appears to be similar abrupt jumps, at the onset of DO-7 as those observed at the onset of DO-8. The largest occur at 2011.9 m and 2009.85 m and are the most extreme isotope excursions within the surrounding 100 m of ice. The two events are compared in figure 12.3 and show that the two significant jumps at the onset of DO-7, at 2011.9 m and 2009.85 m, are approximately comparable in amplitude and location (within the record), with respect to the final transition, as the jumps at 2071.3 m and 2070.4 m at the onset of DO-8.

Both DO-7 and DO-8 events start with a sudden rapid drop to extreme negative isotope values (and therefore extreme cold temperatures), approximately 70 years before the final warming transition begins. Temperatures remain cold for only a few years and then increase rapidly to extreme high temperatures before returning to baseline values. Approximately 50 years later the second abrupt jump occurs, however within 10 years of this final jump (firstly to extreme cold and then to extreme warm) the temperatures rise consistently and do not return to the extreme cold stadial temperatures for several hundred years.

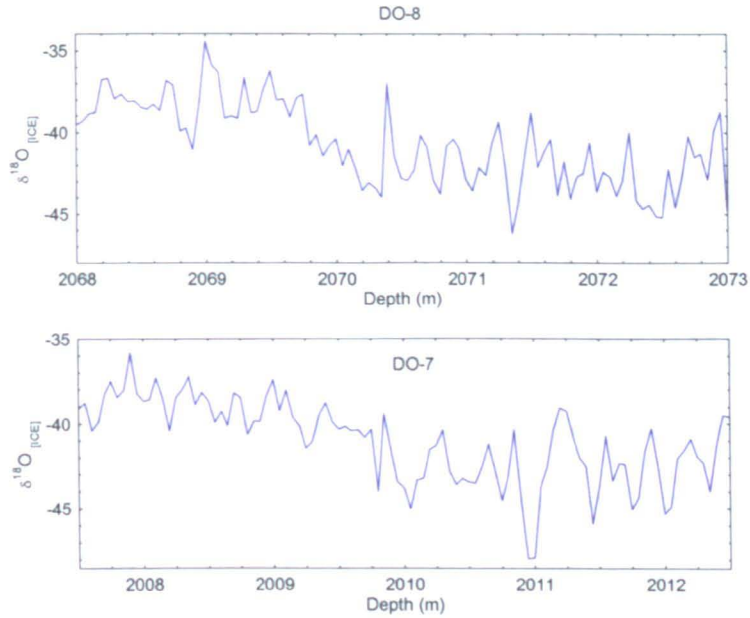

Figure 12.3 Comparison of $\delta^{18}O$ from NGRIP at 2 cm resolution [NGRIP members, 2004] for DO-8 (top) and DO-7 (bottom).

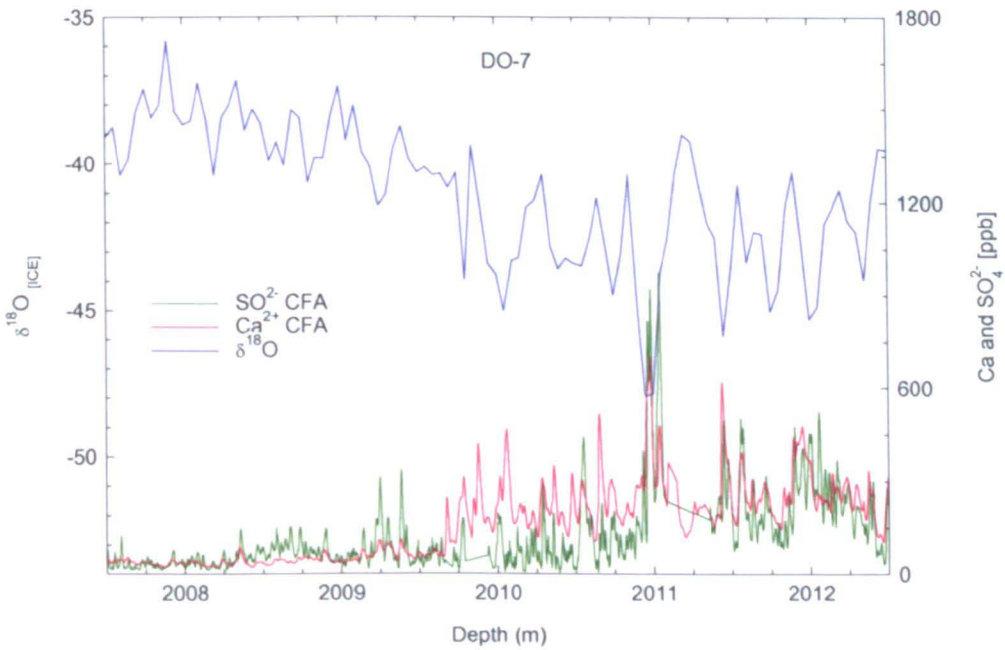

Figure 12.4 Sulphate (from CFA, green), calcium (from CFA, red) and $\delta^{18}O$ (2 cm resolution, blue) at the onset of DO-7

The chemical record at the onset of DO-7, from the NGRIP CFA [Courtesy of Mathias Bigler] also appears to show similarities to that of DO-8. As shown in figure 12.4, the concentration of calcium and sulphate increase dramatically during the most negative $\delta^{18}O$ excursion at 2011.9 m, decreasing rapidly as the isotope values return to the stadial average. It is only after this point that the concentrations (especially for sulphate) start to decrease, in a similar way to the 2 mm chemistry record from DO-8. The CFA record is at a lower resolution than the 2 mm chemical record, however this could represent the onset of the transition in the chemistry at DO-7, which also appears to precede the isotope record.

A better comparison of the two events would be made using the same high-resolution chemical and deuterium excess records, however they are unavailable at this time. Based on the lower resolution record, there are similarities in the $\delta^{18}O$ and chemical deposition, at the onset of the warming transition in both DO events. This shows that the results from this thesis, proposing precursor events and that the chemical transition began and ended prior to the isotope transition are not unique to DO-8 and are likely to be representative of other DO events.

Chapter thirteen

Conclusions

Conclusions

In this thesis the most prominent cold event in the Holocene, the 8.2 kyr event, and one of the longest and strongest interstadials, DO-8 have been investigated. The findings are summarized below.

The 8.2 kyr event

- **Extreme central event, lasting 69 years, within a 160.5-year period of colder temperatures.** The 8.2 kyr event was determined statistically; from the isotope records of four Greenland ice cores (NGRIP, GRIP, GISP2 and Dye 3), as a central event of extreme negative isotope values lasting 69 ± 2 years. Surrounding this extreme period, the isotopic values are consistently lower that the Holocene average for a period of 160.5 ± 5.5 years. The duration was determined from the annual layer counting of nine ions from the new sub seasonal chemical record and compares well to the independently dated GICC05 record.

- **Comparison of Greenland isotopic records.** All four deep ice cores from Greenland show a similar period of decreased values on a decadal resolution However, the comparison of the new high-resolution (1 cm) isotope records from GRIP and GISP2, during the 8.2 kyr event, revealed differences in the isotopic signal at sub annual resolution. The presence of an extreme spike of negative values, which dominates the GRIP record, is not observed in the same section of the GISP2 core, despite the two cores being drilled only 30

km apart. The conclusions from this comparison are that caution should be used when using isotope records at greater than annual or even decadal resolution as features are not robust even within two cores influenced by the same climate regime.

- **Small changes in deposition.** The high resolution chemical analysis of a 20 meter section of the GRIP core during the period determined as the 8.2 kyr event revealed very little change in deposition during this abrupt cold event. There are periods of increased deposition within the record observed as a 27 % increase in calcium, a 12 % increase in chloride and a 23 % increase in sodium; with greater deposition during the central event than the whole event. The increases are significant within the 20 m section of GRIP ice analysed but not significant within the Holocene.

- **Difference from previously published deposition changes.** These findings contradict previously published deposition increases of 60 % for calcium, chloride and sodium from Alley et al (1997). Reanalysis of the GISP2 data used in that study revealed that the increases were heavily biased by the statistics used. The increase was based on the difference between the highest and the lowest concentrations within the section, which in the case of chloride was influenced by a single extreme data point. By removing the extreme data point (which was not accompanied by a similar increase in sodium and therefore could not be considered of marine origin), and calculating the increases based on the average concentrations from the surrounding 1,000

years, the new increases for calcium, chloride and sodium were 18 %, 9 % and 10 % respectively.

Dansgaard-Oeschger event 8

- **Precursor events observed in the isotope and the marine record.** The sharp spikes in the deuterium excess record, from values considerably lower than average to values considerably higher than average, indicate abrupt changes in oceanic source conditions. Increasing SSTs have been proposed for the increase of 11.75 ‰ in just 2-4 years.

- **Oceanic trigger.** Increased deposition of marine species, sodium, chloride and MSA are observed in-phase with the deuterium excess increases in the period prior to the warming transition.

- **Chemistry changes first.** The onset of the warming transition is first observed in the chemical record with a sharp decrease in all ions occurring in three distinct steps. The greatest change is observed in terrestrial components, calcium and magnesium, which decrease by 70 %. The marine species show a smaller magnitude of change decreasing by 47 % for sodium and 34 % for chloride.

- **Followed by the temperature.** The temperatures begin to increase approximately 11 years after the first steps are observed in the chemistry

- **Isotope transition lasts 16 years.** The onset and the termination of the transition in the isotopes were determined statistically as the point at which values were significantly outside the expected value, set by the mean and standard deviation. Compared to short duration of the transition in deuterium excess, the transition in oxygen and deuterium is more gradual.

- **Chemistry transition completed 18 years before the isotopes stabilize.** The concentration of all ions has reached interglacial levels just four years after the increase is observed in the isotopes.

- **Abrupt decrease in deuterium excess.** The abrupt decrease, in anti-phase to the oxygen and deuterium record, occurs in less than 2 years indicating a significant change in source conditions. The change is observed approximately 11 years after the onset in the isotope record, four years after the final chemical transition and coincident with the onset of lower concentrations of MSA.

- **Change in seasonality.** The change in deposition at the warming transition is observed as a change in both summer and spring deposition. The decrease in summer deposition is dominant for the marine and non-continental species, while the decrease in springtime deposition is dominant for the continental and non-marine species.

Summary

Improving our understanding of the 8.2 kyr event is of great importance to the modelling community and policy makers because the event occurred during temperatures that were similar or even warmer than present day. Despite different initial conditions (primarily the existence of the Laurentide ice sheet in North America), it is a good scenario for testing model parameters of THC slowdown and future climate change. The need to improve our understanding of the response to a freshening of the north Atlantic is especially relevant following recent evidence that the meridional overturning circulation (MOC) has shown a 30 % decline in recent decades [Bryden et al., 2005].

It is therefore beneficial for future research that the event in Greenland has been defined and the duration confidently determined. The new deposition increases will better constrain model parameters of atmospheric circulation patterns.

The Dansgaard-Oeschger climate oscillations, unlike the 8.2 kyr event, occurred under very different initial conditions than present day. The large and abrupt increases from extreme cold to relatively warm glacial temperatures have been observed globally, affecting oceanic and atmospheric conditions.

The magnitude of warming is approximately double that of the 8.2 kyr cooling, with the abrupt jump taking place in less than a decade. However, the change in deposition observed in the new chemical record is significantly greater, almost 13 times greater for some species, indicating that the oceanic and atmospheric changes associated with DO-8 were much larger. The 8.2 kyr event is believed to have been triggered by the

outburst flooding of Lake Agassiz, resulting in a slowing or complete shutdown of the THC. If the precursor events observed in the isotope, deuterium and chemical records from NGRIP during DO-8 are believed, they too could be indicative of an oceanic trigger.

Future work

Modelling:

The new results from the 8.2 kyr event, as observed in Greenland, have improved the model constraints relating to the duration and strength of the event. New simulations are needed to determine the effects on MOC under the shorter event duration. Is the effect of THC still large? Do the models show a global response to the freshwater input into the North Atlantic?

The new high-resolution chemical and isotope record from DO-8 offers better parameters to improve modelling of Dansgaard-Oeschger events. Can the models simulate the changes proposed in this thesis that a tropical or ocean trigger initiated the abrupt warming?

Contamination:

The collection of the chemical record from GRIP during this thesis has shown that ice cores are subject to contamination in long-term storage. This could greatly affect the way that ice cores are stored and indeed the value in doing so. A further study of ice cores, which have been in long-term storage, is needed. What is the cause of the

contamination? And how is it propagating into the ice? How reproducible are the chemical records from other deep ice cores?

Small volume/ high-resolution:

The new high-resolution method of IC analysis for small sample volumes, developed in this thesis, has shown that a sub-annual record of chemical deposition at depths can be achieved. This will enable further study of sections of interest during the last glacial. A comparison of the same resolution record from other Dansgaard-Oeschger events, such as DO-7, would confirm the anatomy of DO events discussed here. Is the pattern and rate of changes the same for all DO events?

Dating:

The analysis of the new high-resolution chemical record from NGRIP has shown that annual layers can be counted in ice that has been strongly compressed. The layer counting is comparable to the independent GICC05 dating however the new 2mm resolution record is able to pick up features, which the GICC05 method (reliable on the lower resolution CFA) cannot. Improvements are need to in the resolution of the CFA and the speed of the IC method.

Layer counting:

Both dating methods (the 2mm record and GICC05), although comparable, have highlighted the user dependence of annual layer counting. A study of the reliability of layer counting is needed, using a large number of counters, to determine how reproducible layer counting is.

Deposition:

In order to understand the layer counting we must first determine the true location of the different ions within the annual layer. A study was carried out by Whitlow et al (1992) however the comparison of the stadial and interstadial ice in this thesis showed a difference in the location of the spikes, from either a synchronous peak in all species to an offset. When during the year are the ions deposited? Is there post-depositional movement within the cores that affects the location in the annual layer? Do temperature, atmospheric circulation or ice compression and post-depositional processes affect the location?

References

Ahn, J., Wahlen, M., Deck, B.L., Brook, E.J., Mayewski, P.A., Taylor, K.C., White, J.W.C, 2004. A record of atmospheric CO2 during the last 40,000 years from the Siple Dome, Antarctica ice core. Journal of Geophysical Research, 109(D13): D13305.

Alley, R.B., Meese, D.A., Shuman, C.A., Gow, A.J., Taylor, K.C., Grootes, P.M., White, J.W.C., Ram, M., Waddington, E.D., Mayewski, P.A., Zielinski, G.A., 1993. Abrupt snow accumulation increase at end of YD. Nature, 362: 527-529.

Alley, R.B., and Anandakrishnan, S, 1995. Variations in melt-layer frequency in the GISP2 ice core. Annals of Glaciology, 21: 64-70.

Alley, R.B., Mayewski, P.A., Sowers, T., Stuiver, M., Taylor, K.C., Clark, P.U., 1997. Holocene climate instability: a prominent widespread event 8200 y ago. Geology, 25: 483-486.

Alley, R. B., 2000. The Younger Dryas cold interval as viewed from central Greenland. Quaternary Science Reviews 19: 213-226.

Alley, R.B., Anandakrishnan, S., Jung, P., 2001. Stochastic resonance in the North Atlantic. Paleoceanography, 16(2): 190-198.

Alley, R.B., Hanson, B., 2003. The two-mile time machine: Ice cores, abrupt climate change, and our future. Professional Geographer, 55 (4): 538-540.

Alley, R.B., and Agustsdottir, A.M., 2005. The 8k event: cause and consequences of a major Holocene abrupt climate change. Quaternary Science Reviews, 24((10-11)): 1123-1149.

Altabet, M.A., Higginson, M.J., Murray, D.W., 2002.The effect of millennial-scale changes in Arabian Sea denitrification on atmospheric CO2.Nature, 415:159-162.

Andersen, K. K., Svensson, A., Johnsen, S., Rasmussen, S.O., Bigler, M., Rothlisberger, R., Ruth, U., Siggaard-Andersen, M-l., Steffensen, J.P., Dahl-Jensen, D., Vinther, B.M., Clausen, H.B. (Submitted). The Greenland Ice Core Chronology 2005, 15-42 kyr. Part 1:Constructing the time scale. Quaternary Science Reviews.

Baldini, J.U.L., McDermott, F., Fairchild, I.J., 2002. Structure of the 8200-year cold event revealed by a speleothem trace element record. Science, 296: 2203-2206.

Barber, D.C., Dyke, A., Hillaire-Marcel, C., Jennings, A.E., Andrews, J.T., Kerwin, M.W., Bilodeau, G., McNeely, R., Southon, J., Morehead, M.D., Gagnon, J.M., 1999. Forcing of the cold event 8,200 years ago by catastrophic drainage of Laurentide lakes. Nature, 400: 344-348.

Bard, E., Rostek, F., Sonzogni, C, 1997. Interhemispheric synchrony of the last deglaciation inferred from alkenone palaeothermometry. Nature, 385(6618): 707-710.
Bard, E., 1999. Paleoclimate - Ice age temperatures and geochemistry. Science (284): 5417.

Barrie, L.A., 1995. Arctic Aerosols: Composition, Sources and Transport. In: Delmas, R.J. (Editor), Ice Core Studies of Global Biogeochemical Cycles. Global Environmental Change. NATO ASI Series, pp. 1-22.

Barron, E.J., 1987. Eocene equator-to-pole surface temperatures: A significant climate problem. Paleoceanography, 2: 729-739.

Bauch, A.H., Erlenkeuserb, H., Spielhagena, R.F., Struckc, U., Matthiessend,J., Thieded, J., and Heinemeiere, J, 2001. A multiproxy reconstruction of the evolution of deep and surface waters in the sub arctic Nordic seas over the last 30,000 yr. Quaternary Science Reviews, 20(4): 659-678.

Beer, J., Mende, W., Stellmacher, R., 2000. The role of the sun in climate forcing. Quaternary Science Reviews, 19(1-5): 403-415.

Bender, M., Sowers, T., Dickson, M.L. Orchardo, J., Grootes, P., Mayewski, P.A., Meese, D.A., 1994. Climate correlations between Greenland and Antarctica during the past 100,000 years. Nature, 372: 663-666.

Biscaye, P.E., Grousset, F.E., Revel, M., Van der Gaast, S., Zielinski, G.A., Vaars, A., Kukla, G, 1997. Asian provenance of glacial dust (stage 20) GISP2. Journal of Geophysical Research, 102(C12): 26765-26781.

Blunier, T., Chappellaz, J., Schwander, J., Stauffere, B., Raynaud, D., 1995. Variations in atmospheric methane concentration during the Holocene epoch. Nature, 374: 46-49.

Blunier, T., and Brook, E.J., 2001. Timing of millennial-scale climate change in Antarctica and Greenland during the last glacial period. Science, 291(5501): 109-112.

Bond, G., Heinrich, H., Broecker, W., Labeyrie, L., MCManus, J., Andrews, J., Huon, S., Jantschik, R., Clasen, S., Simet, C., Tedesco, K., Klas, M., Bonani, G., Ivy, S, 1992. Evidence for massive discharges of icebergs into the North-Atlantic Ocean during the last glacial period. Nature, 360(6401): 245-249.

Bond, G., Broecker, W., Johnsen, S., MCManus, J., Labeyrie, L., Jouzel, J., Bonani, G., 1993. Correlations between climate records from North Atlantic sediments and Greenland ice. Nature, 365(6442): 143-147.

Bond, G., Showers, W., Cheseby, M., Lotti, R., Almasi, P., deMenocal, P., Priore, P., Cullen, H., Hajdas, I., Bonani, G.,, 1997. A pervasive millennial-scale cycle in North Atlantic Holocene and Glacial climates. Science, 278: 1257-1266.

Boyle, E.A., and Keigwin, L. 1987. North Atlantic Thermohaline Circulation during the past 20,000 years linked to High-latitude surface temperature. Nature, 330: 35-40.

Briffa, K.R., Osborn, T.J., Schweingruber, F.H., Harris, I.C., Jones, P.D., Shiyatov, S.G., Vaganov, E.A., 2001. Low-frequency temperature variations from a northern tree ring density network. Journal of Geophysical Research, 106(D3): 2929-2941.

Broecker, W.S., Peteet, D.M., Rind, D., 1985. Does the Ocean-Atmosphere system have more than one stable mode of operation? Nature, 315(6014): 21-26.

Broecker, W.S., 1995. The Glacial World According to Wally. Eldigio Press, Lamont-Doherty Earth Observatory of Columbia University, Palisades, NY.

Broecker, W.S., 1997. Thermohaline circulation, the Achilles heel of our climate system: Will man-made CO2 upset the current balance? . Science, 278: 1582-1588.

Broecker, W.S., Sutherland, S., Peng, T.H., 1999. A possible 20th-century slowdown of Southern Ocean deep-water formation. Science, 286(5442): 1132-1135.

Broecker, W.S., 2003. Does the trigger for abrupt climate change reside in the ocean or in the atmosphere? Science, 300 (5625): 1519-1522.

Brook, E.J., Sowers, T., Orchardo, J., 1996. Rapid variations in atmospheric methane concentrations during the past 110,000 years. Science, 273: 1087-1093.

Bryden, H.L., Longworth, H.R., Cunningham, S.A., 2005. Slowing of the Atlantic meridional overturning circulation at 25 degrees N. Nature, 438(7068): 655-657.

Burns, S.J., Fleitmann, D., Matter, A., Kramers, J., and Al-Subbary, A. A., 2003. Indian Ocean Climate and an Absolute Chronology over Dansgaard-Oeschger Events 9 to 13. Science, 301: 1365-1367.

Burns, S.J., 2004. Indian Ocean climate and an absolute chronology over Dansgaard-Oeschger events 9 to 13 (vol 301, pg 1365, 2003). Science, 305(5690): 1567-1567.

Cacho, I., Grimalt, J.O., Canals, M., 2002. Response of the Western Mediterranean Sea to rapid climatic variability during the last 50,000 years: a molecular biomarker approach. Journal of Marine Systems, 33-34: 253-272.

Caldeira, K., and J.F. Kasting., 1992. Susceptibility of the early Earth to irreversible glaciation caused by carbon dioxide clouds. Nature. 359: 226-228.

CD-ROM, 1997. The Greenland Summit Ice Cores, Available from the National Snow and Ice Data Centre, University of Colorado at Boulder, and the World Data Centre-A for Paleoclimatology, National Geophysical Data Centre, Boulder, Colorado.

Chappellaz, J., Blunier, T., Raynaud, D., Barnola, J.m., Schwander, J., Stuffer, B., 1993. Synchronous changes in atmospheric CH_4 and Greenland climate between 40 & 8 kyr BP. Nature, 366: 443-445.

Clark, P.U., 2001. Freshwater forcing of abrupt climate change during the last glaciation. Science, 293(5528): 283-287.

Clark, P.U., Pisias, N.G., Stocker, T.F., Weaver, A.J., 2002. The role of the thermohaline circulation in abrupt climate change. Nature, 415 (6874): 863-869.

Clarke, G.K.C., Leverington, D.W., Teller, J.T., and Dyke A.S., 2004. Paleohydraulics of the last outburst flood from glacial Lake Agassiz and the 8200 BP cold event. Quaternary Science Reviews, 23(3-4): 389-407.

CLIMAP Project Members, 1981. Sea-Surface Temperature Anomaly Maps for August and February in the Modern and Last Glacial Maximum. Geological Society of America bulletin, Map Chart Sec. MC-36.

Crowley, T.J., Lowery, T.S., 2000. How warm was the medieval warm period? AMBIO, 29(1): 51-54.

Cuffey, K.M., Alley, R.B., Grootes, P.M., Bolzan, J.M., Anandakrishnan, S., 1994. Calibration of the $\delta^{18}O$ isotopic paleothermometer for central Greenland, using borehole temperatures. Journal of Glaciology, 40(135): 341-349.

Cuffey, K.M., Clow, G.D., Alley, R.B., Stuiver, M.,Waddington, E.D., Saltus, R.W, 1995. Large Arctic temperature-change at the Wisconsin-Holocene glacial transition. Science, 270(5235): 455-458.

Curran, M.A.J., van Ommen, T. D., Morgan, V. I., Phillips, K. L., Palmer, A.S., 2003. Ice Core Evidence for Antarctic Sea Ice Decline Since the 1950s. Science, 302: 1203-1206.

Curry, W.B., and Oppo, D.W, 1997. Synchronous, high frequency oscillations in tropical sea surface temperatures and North Atlantic Deep Water production during the last glacial cycle. Paeoceanography, 12(1): 1-14.

Dahl-Jensen, 2002. The NGRIP deep drilling programme. Annals of Glaciology, 35: 1-4.

Daley, T., Barber, K., Street-Perrott, A., Loader, N., Hughes, P., 2006. Peat Bog Progress Report. ISOMAP-UK, University of Southampton, pp. 1-8.

Dansgaard, W., 1964. Stable isotopes in precipitation. Tellus, 16: 436-467.

Dansgaard, W., 1985. Greenland Ice Core Studies. Palaeogeography Palaeoclimaology Palaeoecology, 50((2-3)): 185-187.

Dansgaard, W., Johnsen, S.J., Clausen, H.B., Dahl-Jensen, D., Gundestrup, N.S., Hammer, C.U., Hvidberg, C.S., Steffensen, J.P., Sveinbjornsdottir, A.E., Jouzel, J., Bond, G., 1993. Evidence for general instability of past climate from a 250-kyr ice core record. Nature, 364: 218-220.

De Angelis, M., Steffensen, J.P., Legrand, M., Clausen, H., Hammer, C., 1997. Primary aerosol (sea salt and soil dust) deposited in Greenland ice during the last climatic cycle: Comparison with east Antarctic records. Journal of Geophysical Research, 102(C12): 26681-26698.

Denton, G.H., Karlen, W., 1977. Holocene and glacial tree-line variations in white river valley and Skolai pass, Alaska and Yukon Territory. Quaternary Research, 7(1): 63-111.

Denton, G.H., Alley, R.B., Comer, G.C., Broecker, W.S, 2005. The role of seasonality in abrupt climate change. Quaternary Science Reviews, 24(10-11): 1159-1182.

Duplessy, J.C., Labeyrie, L., Arnold, M., Paterne, M., Duprat, J., van Weering, T.C.E., 1992. Changes in surface salinity of the North Atlantic Ocean during the last deglaciation. Nature, 358: 485-488.

Dyke, A.S., Dale, J.E., McNeely, R.N., 1996. Marine mollusks as indicators of environmental change in glaciated North America and Greenland during the last 18,000 years. Geographie Pysique et Quaternaire, 50(2): 125-184.

Emmerich., R., 2004. The Day After Tomorrow. Twentieth Century Fox, USA.

Epstein, S., Mayeda, T.K. 1953. Variation of 18O content of waters from natural sources. Geochimica et Cosmochimica Acta 4(5): 213-224.

EPICA community members, 2004. Eight glacial cycles from an Antarctic ice core. Nature, 429: 623-628.

Esper, J., Cook, E.R., Schweingruber, F.H., 2002. Low-frequency signals in long tree-ring chronologies for reconstructing past temperature variability. Science, 295(5563): 2250-2253.

Fairchild, I. J., Smith, C.L., Baker, A., Fuller, L., Spötl, C., Mattey, D., McDermott, F., E.I.M.F, 2006. Modification and preservation of environmental signals in speleothems. Earth-Science Reviews, **75**: 105-153.

Fisher, D.A., Koerner, R.M., Reeh, N., 1995. Holocene climatic records from Agassiz ice cap, Ellesmere Island, NWT, Canada. Holocene, 5(1): 19-24.

Fleitmann, D., Burns, S.J., Mudelsee, M., Neff,U., Kramers, J., Mangini, A., Matter, A., . 2003. Holocene forcing of the Indian monsoon recorded in a stalagmite from Southern Oman. Science, 300: 1737-1739.

Fuhrer, K., Neftel, A., Anklin, M., Maggi, V, 1993. Continuous measurements of hydrogen peroxide, formaldehyde, calcium and ammonium concentrations along the GRIP ice core from summit, Central Greenland. Atmospheric Environment Part A, 27(12): 1873-1880.

Fuhrer, K., Wolff, E. W., Johnsen, S. J., 1999. Timescales for dust variability in the Greenland Ice Core Project (GRIP) ice core in the 100,000 years. Journal of Geophysical Research, 104(D24): 31043-31052.

Gagan, M.K., Ayliffe, L.K., Scott-Gagan, H., Hantoro, W.S., McCulloch, M.T, 2002. Coral reconstruction of abrupt tropical cooling 8,000 years ago. Geochimica et cosmochimica acta, 66(15A): A255-A255.

Garnett, E.R., Gilmour, M.A., Rowe, P.J., Andrews, J.E., Preece, R.C., 2004. Th-230/U-234 dating of Holocene tufas: possibilities and problems. Quaternary Science Reviews, 23(7-8): 947-958.

Gasse, F., Van Campo, E., 1994. Abrupt post-glacial climate events in West Asia and North Africa monsoon domains. Earth and Planetary Science Letters, 126: 435-456.

Gasse, F., 2000. Hydrological changes in the African tropics since the Last Glacial Maximum. Quaternary Science Reviews, 19(1-5): 189-211.

Gentry, D., 2003. Precise dating of Dansgaard-Oeschger climatic oscillations in Western Europe from stalagmite data. Nature, 421: 833-837.

GRIP Project Members, 1993. Climate instability during the last interglacial period recorded in the GRIP ice core. Nature, 364: 203-207.

Grootes, P.M., 1993. Comparison of the oxygen isotope records from GISP2 and GRIP Greenland ice cores. Nature, 366: 552-554.

Grootes, P.M, and Stuiver, M., 1997. Oxygen 18/16 variability in Greenland snow and ice with 10-3–to 105-year time resolution,. Journal of Geophysical Research, 102C: 26455–26470.

Grousset, F.E., Labeyrie, L., Sinko, J.A., Cremer, M., Bond, G., Duprat, J., Cortijo, E., Huon, S., 1993. Patterns of ice-rafted detritus in the glacial North-Atlantic (40-degrees-N). Paleoceanography, 8(2): 175-192.

Gundestrup, N. S., Johnsen, S.J., Hansen, S. B., Shoji, H., Talalay, P., and Wilhelms, F (2002). Sticking deep ice core drills: Why and how to recover. Memoirs of National Institute of Polar Research, Special Issue **56**: 181-195.

Heinrich, H., 1988. Origin and consequences of cyclic ice rafting in the northeast Atlantic Ocean during the past 130,000 years. Quaternary Research, 29(2): 142-152.

Hendy, I.L., and Kennett, J.P, 1999. Latest Quaternary North Pacific surface-water responses imply atmosphere-driven climate instability. Geology, 27(4): 291-294.

Hendy, I.L., Kennett, J.P., Roark, E.B., Ingram, B.L, 2002. Apparent synchronicity of sub millennial scale climate events between Greenland and Santa Barbara Basin, California from 30-10 ka. Quaternary Science Reviews, 21(10): 1167-1184.

Hong, Y.T., Hong, B., Lin, Q.H., Zhu, Y.X., Shibata, Y., Hirota, M., Uchida, M., Leng, X.T., Jiang, H.B., Xu, H., Wang, H., Yi, L., 2003. Correlation between Indian Ocean summer monsoon and North Atlantic climate during the Holocene. Earth and Planetary Science Letters, 211(3-4): 371-380.

Huang, B., 2004. Remotely forced variability in the tropical Atlantic Ocean. Climate Dynamics, 23(2): 133-152.

Hughen, K.A., Overpeck, J.T., Peterson, L.C., Trumbore, S., 1996. Rapid climate changes in the tropical Atlantic region during the last deglaciation. Nature, 380: 51-54.

Hvidberg, C.S., 2002. The NGRIP ice-core logging procedure: description and evaluation. Annals of Glaciology, 35: 5-8.

IPCC, 1995. Climate Change 1995: Impacts, Adaptations and Mitigation of Climate Change: Scientific-Technical Analyses. In: R.T. Watson, Zinyowera, M.C., Moss, R.H., (Editor), Contribution of Working Group II to the Second Assessment of the Intergovernmental Panel on Climate Change. Cambridge University Press, UK.

IPCC, 2001. Climate Change 2001: IPCC Third Assessment Report, Working group 2: Impacts, Adaptation and Vulnerability.

Johannessen, O.M., Shalina, E.V., Miles, M.W., 1999. Satellite evidence for an Arctic sea ice cover in transformation. Science, 286(5446): 1937-1939.

Johnsen, S.J., Clausen, H.B., Dansgaard, W., Fuhrer, K., Gundestrup, N., Hammer, C.U., Iversen, P., Jouzel, J., Stauffer, B., Steffensen, J.P., 1992. Irregular glacial interstadials recorded in a new Greenland ice core. Nature, 359: 311-313.

Johnsen, S.J., Dahl-Jensen, D., Dansgaard, W., Gundestrup, N, 1995. Greenland palaeotemperatures derived from GRIP bore hole temperature and ice core isotope profiles. Tellus, 47b: 624-629.

Johnsen, S.J., Clausen, H.B., Dansgaard, W., Gundestrup, N.S., Hammer, C.U., Andersen, U., Andersen, K.K., Hvidberg, C.S., Dahl-Jensen, D., Steffensen, J.P., Shoji, H., Sveinbjornsdottir, A.E., White, J., Jouzel, J., Fisher, D, 1997. The delta O-18 record along the Greenland Ice Core Project deep ice core and the problem of possible Eemian climatic instability. Journal of Geophysical Research, 102(C12): 26397-26410.

Johnsen, S.J., Dahl-Jensen, D., Gundestrup, N., Steffensen, J.P., Clausen, H.B., Miller, H., Masson-Delmotte, V., Sveinbjörnsdottir, A.E., White, J., 2001. Oxygen isotope and palaeotemperature records from six Greenland ice-core stations: Camp Century, Dye-3, GRIP, GISP2, Renland and NorthGRIP. Journal of Quaternary Science, 16: 299-307.

Jones, P.D., Briffa, K.R., Barnett, T.P., Tett, S.F.B., 1998. High-resolution palaeoclimatic records for the last millennium: interpretation, integration and comparison with General Circulation Model control-run temperatures. Holocene, 8(4): 455-471.

Jones, P.D., Mann, M.E., 2004. Climate over past millennia. Reviews of Geophysics, 42(2).

Jouzel, J., Lorius, C., Petit, J.R., Genthon, C., Barkov, N.I., Kotlyakov, V.M, Petrov, V.M, 1987. Vostok ice core - A continuous isotope temperature record over the last climatic cycle (160,000 years). Nature, 329(6138): 403-408.

Jouzel, J., Alley, R.B., Cuffey, K.M., Dansgaard, W., Grootes, P.M., Hoffmann, G., Johnsen, S.J., Koster, R.D., Peel, D., Shuman, C.A., Stievenard, M., Stuiver, M., White, J.W.C., 1997. Validity of the temperature reconstruction from water isotopes in ice cores. Journal of Geophysical Research, 102: 26471-26487.

Keigwin, L.D., and Jones, G. A., 1994. Western North-Atlantic evidence for millennial-scale changes in ocean circulation and climate. Journal of Geophysical Research, 99(C6): 12397-12410.

Kennish, M.J., 2001. Practical Handbook of Marine Science. Marine Science Series. CRC press LLC.

Klitgaard-Kristensen, D., Sejrup, H.P., Haflidason, H., Johnsen, S., Spurk, M, 1998. A regional 8200 cal. yr BP cooling event in northwest Europe, induced by final stages of the Laurentide ice-sheet deglaciation? Journal of Quaternary Science, 13(2): 165-169.

Knorr, G., and Lohmann, G, 2003. Southern Ocean origin for the resumption of Atlantic thermohaline circulation during deglaciation. Nature, 424(6948): 532-536.

Knudsen, K.L., Jiang, H., Jansen,J., Eiríksson,J., Heinemeier,J., and Seidenkrantz, M. - S., 2004. Environmental changes off North Iceland during the deglaciation and the Holocene: foraminifera, diatoms and stable isotopes. Marine Micropaleontology, 50(3-4): 273-305.

Kobashi, T., Severinghaus, J.P., Brook, E.J., Grachev, A., 2003. Speed and magnitude of abrupt climate change at 8,200 yrs B.P. from the Greenland Ice Core (GISP2). Eos Transactions of the American Geophysical Union, 84 (46) (Fall Meeting Supplement): Abstract PP41D-04.

Labeyrie, L.D., Duplessy, J-C., Duprat, J., Juillet-Leclerc, A., Moyes. J., Michel, E., Kallel, N., and Shackleton, N.J., 1992. Changes in vertical structure of the North Atlantic Ocean between glacial and modern times. Quaternary Science Reviews, 11: 401-413.

Langway, C.C., Osada, K., Clausen, H. B., Hammer,C. U., Shoji, H, 1995. A 10-century comparison of prominent bipolar volcanic events in ice cores. Journal of Geophysical Research, 100(D8): 16,241–16,248.

Legrand, M., Hammer, C., DeAngelis, M., Savarino, J., Delmas, R., Clausen, H., Johnsen, S.J, 1997. Sulfur-containing species (methanesulfonate and SO_4) over the last climatic cycle in the Greenland Ice Core Project (central Greenland) ice core. Journal of Geophysical Research, 102(C12): 26663-26679.

Leuenberger, M.C., Lang, C., Schwander, J, 1999. Delta(15)N measurements as a calibration tool for the paleothermometer and gas-ice age differences: A case study for the 8200 BP event on GRIP ice. Journal of Geophysical Research, 104(D18): 22163-22170.

Leverington, D.W., Mann, J.D., Teller, J.T, 2002. Changes in the bathymetry and volume of glacial Lake Agassiz between 9200 and 7700 C-14 yr BP. Quaternary Research, 57(2): 244-252.

Magaritz, M., 1993. Synchronized changes in regional water balance since the mid-Holocene. Climatic Change, 24: 179-185.

Magny, M., Begeot, C., Guiot, J., Peyron, O, 2003. Contrasting patterns of hydrological changes in Europe in response to Holocene climate cooling phases. Quaternary Science Reviews, 22(15-17): 1589-1596.

Mann, M.E., Bradley, R.S., Hughes, M.K., 1999. Northern hemisphere temperatures during the past millennium: Inferences, uncertainties, and limitations. Geophysical research letters, 26(6): 759-762.

Mann, M.E., Jones, P.D., 2003. Global surface temperatures over the past two millennia. Geophysical Research Letters, 30(15).

Marshall, J.S., and Clarke, G.K.C., 1999. Modelling North American freshwater runoff through the last glacial cycle. Quaternary Research, 52: 300-315.

Masson-Delmotte V, L.A., Stievenard M, Cattani O, Falourd S, Jouzel J, Johnsen SJ, Jensen DD, Sveinsbjornsdottir A, White JWC, Popp T, Fischer H, 2005. Holocene

climatic changes in Greenland: Different deuterium excess signals at Greenland Ice Core Project (GRIP) and NorthGRIP. Journal of Geophysical Research, 110(D14): D14102.

Mayewski, P.A., Meeker, L.D., Whitlow, S., Twickler, M.S., Morisson, M.C., Bloomfield, P., Bond, G.C., Alley, R.B., Gow, A.J., Grootes, P.M., Meese, D.A., Ram, M., Taylor, K.C., Wumkes, W., 1994. Changes in atmospheric circulation and ocean ice cover over the North Atlantic during the last 41,000 years. Science, 263(5154): 1747-1751.

Mayewski, P.A., Meeker, L.D., Twickler, M.S., Whitlow, S.I., Yang, Q., Lyons, W.B., Prentice. M., 1997. Major features and forcing of high-latitude Northern hemisphere atmospheric circulation using a 110,000-year-long glaciochemical series. Journal of Geophysical Research, 102: 26345-26366.

McDermott, F., Mattey, D.P., Hawkesworth, C., 2001. Centennial-Scale Holocene climate variability revealed by a high-resolution speleothem $\delta^{18}O$ record from SW Ireland. Science, 294: 1328-1331.

Meese, D.A., Gow, A.J., Alley, R.B., Zielinski, G.A., Grootes, P.M., Ram, M., Taylor, K.C., Mayewski, P.A., Bolzan, J.F, 1997. The Greenland Ice Core Project 2 depth-age scale: Methods and results. Journal of Geophysical Research, 102: 26411-26423.

Menounos, B., Kochb,J., Osbornc,G., Clagueb, J., and Mazzucchid, D., 2004. Early Holocene glacier advance, southern Coast Mountains, British Columbia, Canada. Quaternary Science Reviews, 23(14-15): 1543-1550.

Moberg, A., Sonechkin, D.M., Holmgren, K., Datsenko, N.M., Karlen, W., 2005. Highly variable Northern Hemisphere temperatures reconstructed from low- and high-resolution proxy data. Nature, 433 (7026):(7026): 613-617.

Morrison, J., Brockwell, T., Merren, T., Fourel, F. & Phillips, A.M. 2001. On-line high-precision stable hydrogen isotopic analyses of nanoliter water samples. Annals of Chemistry. 73, 3570-3575.

Muscheler, R., Beer, J., Vonmoos, M., 2004. Causes and timing of the 8200 yr BP event inferred from the comparison of the GRIP Be-10 and the tree ring Delta C-14 record. Quaternary Science Reviews, 23((20-22)): 2101-2111.

NCR, 2002. Abrupt Climate Change: Inevitable surprises. National Academy Press, Washington DC: pp.80

Neff, U., Burnes, S.J., Mangini, A., Mudelsee, M., Fleitmann, D., Matter, A., 2001. Strong coherence between solar variability and the monsoon in Oman between 9 and 6 kyr ago. Nature, 411: 290-293.

Nesje, A., and Dahl, S.O., 2001. The Greenland 8200 cal.yr BP event, detected in loss-on-ignition profiles in Norwegian lacustrine sediment sequences. Journal of Quaternary Science, 16: 155-166.

North Greenland Ice Core Project Members, 2004. High-resolution record of Northern Hemisphere climate extending into the last interglacial period. Nature, 431(7005): 147-151.

NSIDC, 2005. http://nsidc.org/data/gisp_grip/.

O'Brien, S.R., Mayewski, P.A., Meeker, L.D., Meese, D.A., Twickler, M.S., Whitlow, S.I., 1995. Complexity of Holocene climate as reconstructed from a Greenland ice core. Science, 270(5244): 1962-1964.

O'Dwyer, J., Isaksson, E., Vinje, T., Jauhiainen, T., Moore, J., Pohjola, V., Vaikmae, R., van de Wal, R.S.W, 2000. Methanesulfonic acid in a Svalbard ice core as an indicator of ocean climate. Geophysical Research Letters, 27(8): 1159-1162.

Oerlemans, J., 2005. Extracting a climate signal from 169 glacier records. Science, 308(5722): 675-677.

Overpeck, J., Hughen, K., Hardy, D., Bradley, R., Case, R., Douglas, M., Finney, B., Gajewski, K., Jacoby, G., Jennings, A., Lamoureux, S., Lasca, A., MacDonald, G., Moore, J., Retelle, M., Smith, S., Wolfe, A., Zielinski, G, 1997. Arctic environmental change of the last four centuries. Science, 278(5341): 1251-1256.

Pasteur, E.C., Mulvaney, R., Peel, D. A., Saltzman, E. S. Whung, P.-Y, 1995. A 340-year record of biogenic sulphur from the Weddell Sea area, Antarctica. Annals of Glaciology, 21: 169-174.

Peterson, L.C., Haug, G.H., Hughen, K.A., Rohl, U, 2000. Rapid changes in the hydrologic cycle of the tropical Atlantic during the last glacial. Science, 290(5498): 1947-1951.

Petit, J.R., White, J.W.C, Young, N.W., Jouzel, J., Korotkevich, Y.S., 1991. Deuterium excess in recent Antarctic snow. Journal of Geophysical Research, 96(D3): 5113-5122.

Putnins, P., 1970. The Climate of Greenland, World Survey of Climatology: Climate of the Polar Regions: Chapter 2. Elsevier, Amsterdam, pp. 3–128.

Rahmstorf, S., 1995. Bifurcations of the Atlantic thermohaline circulation in response to changes in the hydrological cycle. Nature, 378: 145-149.

Rankin, A.M., Wolff, E.W., Martin, S., 2002. Frost flowers: Implications for tropospheric chemistry and ice core interpretation. Journal of Geophysical Research, 107(D23).

Rasmussen, S.O., Andersen, K. K., Svensson, A. M.,Steffensen, J. P., Vinther, B. M., Clausen, H. B., Siggaard-Andersen, M.-L., Johnsen, S. J., Larsen, L. B., Bigler, M., Röthlisberger, R., Fischer, H., Goto-Azuma, K., Hansson, M. E., and Ruth, U., 2006. A new Greenland ice core chronology for the last glacial termination. Journal of Geophysical Research, 111(D6).

Renssen, H, Goosse, H, Fichefet, T., Campin, J.M., 2001. The 8.2 kyr BP event simulated by a global atmosphere-sea-ice-ocean model. Geophysical research letters, 28(8): 1567-1570.

Renssen, H., Goosse, H., Fichefet, T., 2002. Modelling the effect of freshwater pulses on the early Holocene climate: The influence of high-frequency climate variability. Paleoceanography, 12(2).

Risebrobakken, B., Jansen, E., Andersson, C., Mjelde, E. & Hevrøy, K., 2003. A high-resolution study of Holocene paleoclimatic and paleoceanographic changes in the Nordic Seas. Paleoceanography, 18: 1029.

Rohling, E.J., Mayewski, P. A., Hayes, A., Abu-Zied, R. H. & Casford, J. S. L., 2002. Holocene atmosphere-ocean interactions: records from Greenland and the Aegean Sea. Climate Dynamics, 18: 587-593.

Rohling, E.J., and Palike, H., 2005. Centennial-scale climate cooling with a sudden cold event around 8,200 years ago. Nature, 434 (7036): 975-979.

Rosen, P., Segerstrom, U., Eriksson, L., Renberg, I., Birks, H.J.B., 2001. Holocene climatic change reconstructed from diatoms, chironomids, pollen and near-infrared spectroscopy at an alpine lake (Sjuodjljaure) in northern Sweden. Holocene, 11(5): 551-562.

Rothlisberger, R., Bigler, M., Hutterli, M., Sommer, S., Stauffer, B., Junghans, H.G., Wagenbach, D, 2000. Technique for continuous high-resolution analysis of trace substances in firn and ice cores. Environmental Science & Technology, 34(2): 338-342.

Rousseau, D.D., Preece, R., Limondin-Lozouet, N., 1998. British late glacial and Holocene climatic history reconstructed from land snail assemblages. Geology, 26(7): 651-654.

Sachs, J.P., and Lehman, S.J., 1999. Subtropical North Atlantic Temperatures 60,000 to 30,000 Years Ago. Science, 286(5440): 756 - 759.

Schiller, A., Mikolajewicz, U., Voss, R, 1997. The stability of the North Atlantic thermohaline circulation in a coupled ocean-atmosphere general circulation model. Climate Dynamics, 13(5): 325-347.

Schott, C., Waddington, E.D., Raymond, C.F., 1992. Predicted time-scales for the GISP2 and GRIP boreholes at Summit, Greenland. Journal of Glaciology, 38(128): 162-168.

Schulz, H., von Rad, U., Erlenkeuser, H., 1998. Correlation between Arabian Sea and Greenland climate oscillations of the past 110,000 years. Nature, 393(6680): 54-57.

Schwartz, P., and Randall, D, 2003. An abrupt climate change scenario and its implications for United States security. Pentagon, USA.

Seppa, H., Birks, H.J.B., 2001. July mean temperature and annual precipitation trends during the Holocene in the Fennoscandian tree-line area: pollen-based climate reconstructions. Holocene, 11(5): 527-539.

Severinghaus, J., 1999. Abrupt climate change at the end of the last glacial period inferred from trapped gasses in polar air. Science, 286: 930-934.

Shackleton, N.J., and Pisias, N. G., 1985. The carbon cycle and atmospheric CO2: Natural variations archean to present; Washington, DC, 303-317 pp.

Shuman, B., Bartlein, P., Logar, N., Newby, P., Webb, T., 2002. Parallel climate and vegetation responses to the early Holocene collapse of the Laurentide Ice Sheet. Quaternary Science Reviews, 21(16-17): 1793-1805.

Sirocko, F., Sarnthein, H., Erlenkeusers, H., Lange, H., Arnold, M., Duplessy, J.C., 1993. Century-scale events in monsoonal climate over the past 24,000 years. Nature, 364: 322-324.

Sowers, T., and Bender, M, 1995. Climate records covering the last deglaciation. Science, 269: 210-214.

Spooner, I., Douglas, M.S.V., Terrusi, L., 2002. Multiproxy evidence of an early Holocene (8.2 kyr) climate oscillation in central Nova Scotia, Canada. Journal of Quaternary Science, 17(7): 639-645.

Spurk, M., Leuschner, H. H., Baillie, M. G. L., Briffa, K. R. & Friedrich, M., 2002. Depositional frequency of German subfossil oaks: climatically and non-climatically induced fluctuations in the Holocene. Holocene, 12: 707-715.

Staubwasser, M., Sirocko, F., Grootes, P. M. & Erlenkeuser, H., 2002. South Asian monsoon climate change and radiocarbon in the Arabian Sea during early and middle Holocene. Paleoceanography, 17.

Stipp, D., 2004. The Pentagon's Weather Nightmare, Fortune magazine.

Stocker, T.E., and Wright, D.G, 1991. Rapid transitions of the ocean's deep circulation induced by changes in surface water fluxes. Nature, 351: 729-232.

Stocker, T. F., Johnsen, S.J. 2003. A minimum thermodynamic model for the bipolar seesaw. Paeoceanography 18(4).

Stocker, T. F., Johnsen, S.J. 2005. A minimum thermodynamic model for the bipolar seesaw (vol 18, pg 1087, 2003). Paeoceanography 20(1).

Stott, L., Poulsen, C., Lund, S., Thunell, R, 2002. Super ENSO and global climate oscillations at millennial time scales. Science, 297(5579): 222-226.

Street-Perrott, F.A., Roberts, N., 1983. Fluctuations in closed-basin lakes as an indicator of past atmospheric circulation patterns. In: F.A. Street-Perrott, Beran, M., Ratcliffe, R. (Editor), Variations in the Global Water Budget. D. Reidel Publishing Company, pp. 331-345.

Street-Perrott, F.A., Perrott, A.R., 1990. Abrupt climate fluctuations in the tropics: The influence of the Atlantic Ocean circulation. Nature, 358: 607-612.

Stuiver, M., Grootes, P.M., and Brazunias, T.F., 1995. The GISP2 $\delta^{18}O$ record of the past 16,500 years and the role of the Sun, ocean and volcanoes. Quaternary Research, 44: 341–354.

Svensson, A., Biscaye, P.E., Grousset, F.E., 2000. Characterization of late glacial dust in the GRIP. Journal of Geophysical Research, 105(D4): 4637-4656.

Taylor, K.C., Hammer, C.U., Alley, R.B., Clausen, H.B., Dahl-Jensen, D., Gow, A.J., Gundestrup, N.S., Kipfstuhl, J. Moore, J.C., Waddington, E.D, 1993. Electrical-conductivity measurements from the GISP2 and GRIP Greenland ice cores. Nature, 366(6455): 549-552.

Teller, J.T., Leverington, D.W., Mann, J.D, 2002. Freshwater outbursts to the oceans from glacial Lake Agassiz and their role in climate change during the last deglaciation. Quaternary Science Reviews, 21(8-9): 879-887.

Thomas, E.R., Wolff, E.W.W., Mulvaney, R., Steffensen, J.P., Johnsen, S.J., Arrowsmith, C., Vaughn, B., White, J.W.C., Popp, T., 2006. The 8.2 kyr event from Greenland ice cores. Quaternary Science Reviews. doi: 10.1016

Van Campo, E., Gasse, F., 1993. Pollen-and diatom-inferred climatic and hydrological changes in Sumxi Co Basin (western Tibet) since 13,000 yr BP. quaternary Research, 39: 300-313.

Vaughan, D.G., Marshall, G.J., Connolley, W.M., King, J.C., Mulvaney, R., 2001. Climate change - Devil in the detail. Science, 293(5536): 1777-1779.

Vinther, B.M., Clausen, H. B., Johnsen, S. J., Rasmussen, S. O., Andersen, K. K., Buchardt, S.L., Dahl-Jensen, D., Seierstad, I. K., Siggaard-Andersen, M-L., Steffensen, J. P., Svensson, A., Olsen J. and Heinemeier, J., 2006. A synchronized dating of three Greenland ice cores throughout the Holocene. Journal of Geophysical Research, 111(D13): D13102

Von Grafenstein, U., Erlenkeuser, H., Muller, J., Jouzel, J., Johnsen, S.J, 1998. The cold event 8200 years ago documented in Oxygen isotope records of precipitation in Europe and Greenland. Climate Dynamics, 14: 73-81.

Von Grafenstein, U., Erlenkeuser, H., Brauer, A., Jouzel, J., Johnsen, S.J, 1999. A mid-European decadal isotope-climate record from 15,500 to 5000 years B.P. Science, 284: 1654-1657.

Wang, Y.J., Cheng, H., Edwards, R.L., An, Z.S., Wu, J.Y., Shen, C.C., Dorale, J.A., 2001. A high-resolution absolute-dated Late Pleistocene monsoon record from Hulu Cave, China. Science, 294(5550): 2345-2348.

Welch, K.A., Mayewski, P.A., Whitlow, S.I, 1993. Methansulfonic-acid in coastal Antarctic snow related to sea-ice extent. Geophysical research letters, 20(6): 443-446.

Whitlow, S., Mayewski, P.A., Dibb, J.E., 1992. A comparison of major chemical-species seasonal concentration and accumulation at the South Pole and Summit, Greenland. Atmospheric Environment Part A, 26(11): 2045-2054.

Whung, P.Y., Saltzman, E.S., Spencer, M.J., Mayewski, P.A., Gundestrup, N, 1994. 200-Year record of biogenic sulfur in the south Greenland ice core (20D). Journal of Geophysical Research, 99(D1): 1147-1156.

Wiersma, A., P, and Renssen, H, 2006. Model-data comparison for the 8.2 ka BP event: confirmation of a forcing mechanism by catastrophic drainage of Laurentide Lakes. Quaternary Science Reviews, 25(1-2): 63-88.

Xia, Q., Zhao, J., Collerson, K.D, 2001. Early-Mid Holocene climatic variations in Tasmania, Australia: multi-proxy records in a stalagmite from Lynds Cave. Earth and Planetary Science Letters, 194: 177-187.

Yu, Z.C., Eicher, U., 1998. Abrupt climate oscillations during the last deglaciation in central North America. Science, 282(5397): 2235-2238.

Yuan, D., Cheng, H., Edwards, R.L., Dykoski, C.A., Kelly, M.J., Zhang, M., Qing, J., Lin, Y., Wang, Y., Wu, J., Dorale, J.A., An, Z., Cai. Y., 2004. Timing, duration, and transitions of the Last Interglacial Asian monsoon. Science, 304: 575-578.

ELSEVIER

Quaternary Science Reviews ▮ (▮▮▮▮) ▮▮▮–▮▮▮

QSR

The 8.2 ka event from Greenland ice cores

Elizabeth R. Thomas[a,*], Eric W. Wolff[a], Robert Mulvaney[a], Jorgen P. Steffensen[b], Sigfus J. Johnsen[b], Carol Arrowsmith[c], James W.C. White[d], Bruce Vaughn[d], Trevor Popp[d]

[a]*British Antarctic Survey, Natural Environment Research Council, High Cross, Madingley Road, Cambridge CB3-0ET, UK*

[b]*Department of Geophysics, The Niles Bohr Institute for Astronomy, Physics and Geophysics, University of Copenhagen, Juliane Maries Vej. 30, DK-2100 Copenhagen, Denmark*

[c]*NERC Isotope Geosciences Laboratory, British Geological Survey, Kingsley Dunham Center, Keyworth, Nottingham NG12-5GG UK*

[d]*Institute of Arctic and Alpine Research, Boulder, Colorado, USA*

[e]*Department of geological Sciences and Environmental Studies Program, University of Colorado, Boulder, Colorado 80309, USA*

Received 27 January 2006; received in revised form 3 May 2006; accepted 21 July 2006

Abstract

We present a collection of high-resolution chemistry and stable isotope records from the plateau of the Greenland ice cap during the cold event 8200 yr ago. Using a composite of four records, the cold event is observed as a 160.5 yr period during which decadal-mean isotopic values were below average, within which there is a central event of 69 yr during which values were consistently more than one standard deviation below the average for the preceding period. Four cores in north, south, and central Greenland show differences at decadal and shorter timescales; it is not yet clear if this represents significant spatial differences in response. The results show clear evidence for colder temperatures and a decrease in snow-accumulation rate. However, the changes in chemical concentrations for the ions looked at here are small, suggesting only minor changes in atmospheric circulation for this event. Apart from the decrease in methane concentration, Greenland ice cores give only weak evidence for effects outside the North Atlantic region.

1. Introduction

Much has been written about the event recorded in palaeoclimate records at approximately 8200 yr before present (BP) (often known as the 8.2 or 8 k event) (**Alley and Agustsdottir, 2005**; **Rohling and Palike, 2005**). In the Greenland ice core records, where it was first clearly noted, it is the outstanding climatic cooling of the Holocene period. The 8.2 ka BP event as observed in the Greenland ice cores, has been described as being a rapid cooling of 6 ± 2 °C at Summit, Greenland (**Johnsen et al., 1992**; **Dansgaard, 1993**; **Alley et al., 1997**). A more recent study, using $\delta^{15}N$ in N_2 as a calibration tool, confirms that the isotopic anomaly is due to a temperature change, with a best estimate of 7.4 K for the magnitude of temperature change (**Leuenberger et al., 1999**). The existence of a cold, dry event in North Atlantic regions is now documented; however, doubt still remains over its extent and cause.

Barber et al. (1999) proposed that the pattern of cooling implies that heat transfer from ocean to atmosphere was reduced in the North Atlantic. An increase in freshwater flux would result in a decrease in the formation of deepwater and ultimately a cooling in high latitudes (**Clark, 2001**). This amplification in freshwater budget in the North Atlantic is generally, attributed to the final stages of the deglaciation of the Laurentide and Scandinavian ice sheets.

Barber et al. (1999) concluded that the massive outflow of freshwater required to reduce the formation of deepwater was from the glacial lakes of Agassiz and Ojibway, north eastern Canada, which drained catastrophically an estimated 8470 calendar year BP (~7700 ^{14}C yr BP) releasing 2×10^{14} m^3 of lake water over a period of at most 100 yr (**Barber et al., 1999**; **Clark, 2001**). Simulations (**Clarke et al., 2004**) of sub-glacial drainage for lake Agassiz led to the suggestion that, the magnitude of the outbursts

*Corresponding author. Tel.: +44 1223 221658, fax: +44 1223 221279.
E-mail address: lith@bas.ac.uk (E.R. Thomas).

0277-3791/$ - see front matter © 2006 Elsevier Ltd. All rights reserved.
doi:10.1016/j.quascirev.2006.07.017

was ~5 Sv occurring in less than 6 months. Correlative evidence exists throughout the Labrador Sea observed as lower sea surface salinities and increased water stratification (**Knudsen et al., 2004**).

Renssen et al. (2001) used an atmosphere–sea-ice–ocean model, to study the mechanism behind the 8.2 ka BP event. They conclude that weakening of the thermohaline circulation, as a result of a freshwater pulse associated with final stages of North American deglaciation, would indeed produce a model response of atmospheric cooling consistent with proxy data. **Legrande et al. (2006)** used a fully coupled atmosphere–ocean global climate model, to simulate a short period of diminished North Atlantic deep-water formation, following a freshwater pulse, which quantitatively matched paleoclimate observations. If this is indeed the case, then the event has a particular significance as the clearest example, under geographic conditions similar to those of today, of the climatic effect of changes in the thermohaline circulation.

However, there is considerable confusion in the literature about what the 8.2 k event really is. The rapidity and relatively short duration of the 8.2 ka BP event as recorded in Greenland ice cores is often below the temporal resolution of palaeoclimate data. This combined with dating uncertainties, has made it difficult to determine the true rate of change, duration and cause of the event at different locations. **Alley and Agustsdottir (2005)** discussed the contrast between longer anomalies at some sites and the short, high-amplitude anomaly around 8.2 ka BP at others. **Rohling and Palike (2005)** have pointed out that, at most locations removed from the North Atlantic, the signals around the 8.2 k event are relatively small (not outstanding in the Holocene), and of much longer duration (several centuries) than the event recorded in Greenland. The exact relationship between this weak variability and the sharp event around the North Atlantic is unclear. Even in the region with a sharp and unique event, its description in the literature is somewhat unclear. Here, we use existing data from four Greenland ice cores, as well as new high-resolution isotopic and/or chemical data from two of them to clearly define the duration and signature of the 8.2 k event in Greenland ice cores.

2. Sample collection and analysis

The material mainly used for the new data in this study is from the European Greenland ice core Project (GRIP) core drilled to bedrock at the top of the Greenland ice cap (Summit, 72° 34°N, 37° 37°W, 3230 m above sea level) in the summer of 1992, 28 km east of the parallel US Greenland ice sheet project 2 (GISP2) core which reached bedrock a year later (**GRIP Project members, 1993**; **Mayewski et al., 1994**). Some extra isotopic measurements were also made on the GISP2 core. We refer also to existing data from the Dye 3 (**Dansgaard, 1985**) and North GRIP (NGRIP) cores (**North Greenland ice core Project Members, 2004**) (**Fig. 1**).

Fig. 1. Map of Greenland. This shows the locations of the deep ice core drilling sites in this paper: GRIP (72.5°N, 37.3°W), GISP2 (72.5°N, 38.3°W), NGRIP (75.1°N, 42.3°W), and Dye3 (65.2°N, 43.8°W).

Sections of the GRIP core from 1320 to 1340 m, corresponding to the rapid climate event at 8.2 ka, were cut and then sub-sampled using a band saw into pre-cleaned polythene containers to 1 cm resolution, about 10 samples per year. The outer surface of the core was removed and protective clothing worn to minimize contamination.

Ion chromatography (IC) was used to determine anions (Cl^-, F^-, methanesulfonate (MSA^-), NO_3^-, SO_4^{2-}) using a Dionex ICS-2500 2 mm column (0.25 mL min^{-1}) and isocratic elution (23 mM NaOH and 250 μL sample loop). The cations (Ca^{2+}, K^+, Na^+, NH_4^+, Mg^+) were determined using a Dionex IC-2000 3 mm column (0.5 mL min^{-1}) and isocratic elution (20 mM MSA^- and 250 μL sample loop).

Water isotopes were run at 1 cm resolution for $\delta^{18}O$ by the Niels Bohr Institute, University of Copenhagen, and 10 cm resolution for both $\delta^{18}O$ and deuterium at the NERC Isotope Geosciences Laboratory (NIGL) in Keyworth. Additional samples were cut and analyzed at INSTAAR in Boulder at 1 cm resolution for $\delta^{18}O$ and δD in a 2 m long section of ice from the 8.2 ka event in the GISP2 core.

Please cite this article as: Elizabeth R. Thomas et al., The 8.2 ka event from Greenland ice cores, Quaternary Science Reviews (2006), doi:10.1016/j.quascirev.2006.07.017

The concentrations we measured for Ca in the GRIP samples were significantly higher than, those determined 10 yr earlier using continuous flow analysis (Fuhrer et al., 1993) and than those found in GISP2 ice of similar age (O'Brien et al., 1995). We suspect that Ca has penetrated into the core of the samples over the long storage period, given the small size of our samples, taken from the heavily contaminated outer part of the core (Thomas, 2006). As a result our removal of the outside of the core was insufficient. We found no comparable anomalies for other ions, and indeed seasonal signals are clearly observable in many of them, so that any contamination has not obscured the natural signal. Since, high-resolution data are already available from the core (Fuhrer et al., 1993) we have used the earlier data for Ca only.

3. The timing and nature of the isotopic 8.2 k event

3.1. *Timing*

High accumulation rates in all the Greenland cores (e.g., 0.24 m ice per year at GISP2 (Meese et al., 1997) and 0.23 m ice per year at GRIP (Johnsen et al., 1992)) provide favorable conditions for the construction of annually counted age scales, using various parameters that vary seasonally. For the GISP2 core, the main methods were visual stratigraphy, electrical conductivity measurements (ECMs), and dust; the minimum of the event is estimated at 8250 yr BP (Alley et al., 1997). (Note that, despite different usages that have been employed in the ice core community, we have corrected all calculated ages to a reference "present" of 1950 AD.). The most recent dating of Greenland ice cores (known as GICC05) (Rasmussen et al., 2006) uses, from the present until the 8.2 ka event, oxygen isotope measurements (Vinther et al., 2006), mainly in the high accumulation rate Dye 3 core. The timescales of different Greenland cores can be combined or compared by matching them together using peaks in ECM, which represent discrete volcanic eruptions (Rasmussen et al., 2006; Vinther et al., 2006). The absolute $\delta^{18}O$ minimum for the last 10 ka in the GRIP ice core is observed at a depth of 1334.50 m, which has a calendar date of 8190 yr BP (8240 yrs b2k (before the year 2000 AD)), with a counting uncertainty given as 47 yr, from the new GICC05 age scale (Rasmussen et al., 2006). Using a comparison of anomalies in ^{10}Be in the GRIP ice core and ^{14}C in tree rings, (Muscheler et al., 2004) recently estimated the isotopic minimum at GRIP to be at 8150 yr BP, with an uncertainty of less than 20 yr. We conclude that the isotopic minimum occurs at an age slightly younger than 8200 yr BP.

3.2. *The nature of the event in Greenland*

In order to determine the true rate of change and duration of this event the event itself must first be defined. Discrepancies in the dating between different palaeoclimate records and ice core records from different sites have made this difficult. In Fig. 2a, we have compared the smoothed oxygen isotope data from GRIP, NGRIP, GISP2, and Dye 3 from the Younger Dryas transition to the mid-Holocene; in Fig. 2b and subsequent figures, we zoom in on the details of the event. In each case, the cores have been synchronized to the same depth scale using ECM spikes, so that we are rather confident that the depths are matched to within a few cm.

In Fig. 2a, the event at 8.2 ka BP is clearly seen as the extreme event of the Holocene in all four cores. The general shape and duration of the event is similar in all four cores, although there are substantial differences in detail at decadal timescales (Fig. 2b). The GRIP data are exceptional in having a sharp central spike, only a decade or so long that stands out even from the remainder of the event. Such a sharp event, if real, might indicate an even more extreme temperature excursion, or could represent the signal of a change in freshwater content of the surface ocean, which might be expected if the ocean was really flooded with freshwater melt.

It was to test this idea further that we analyzed a parallel section of the GRIP core at even higher (1 cm) resolution. This showed that the existence of the "spike" is robust in the GRIP core (Fig. 3) and that it embeds 1–3 yr of very low values, typical of glacial ice. However, analysis of the GISP2 ice (30 km distant) from the same section shows no such spike, at decadal or higher resolution. This obvious discrepancy between the two cores could suggest that the isotopic anomaly in the GRIP core was not a period of extremely cold winters but more likely an artifact of a build up of winter snowdrift at the GRIP site or snow ablation at the GISP2 site. In any case, there is no similar decadal scale event in the GISP2 or either of the other cores, and we do not explore this any further. Rather the event should be seen as the somewhat broader signal around it.

4. The length of the event

The next issue is to determine when the event started and finished. This has been a source of confusion in the literature because different authors have used different definitions to define the start and end of the event. To tackle this problem we have first created a composite Greenland isotope record for the event. This is done to highlight the common pattern of the signal and we will later return to look at the differences between the sites.

The composite record was formed by first placing all four cores onto a GRIP depth scale and using the volcanic ECM peaks as tie-points. The resolution at which GRIP data were available throughout the early Holocene was 27.5 cm, and all the cores are available across the event at considerably higher resolution than this. We therefore averaged all the other datasets to the same resolution (27.5 cm in GRIP depth, approximately 2.5 yr). Using the mean and standard deviation (SD) of the 27.5 cm (GRIP depth) data across the section we normalized all of the datasets so that they all had the GRIP mean and SD.

Please cite this article as: Elizabeth R. Thomas et al., The 8.2 ka event from Greenland ice cores, Quaternary Science Reviews (2006), doi:10.1016/j.quascirev.2006.07.017

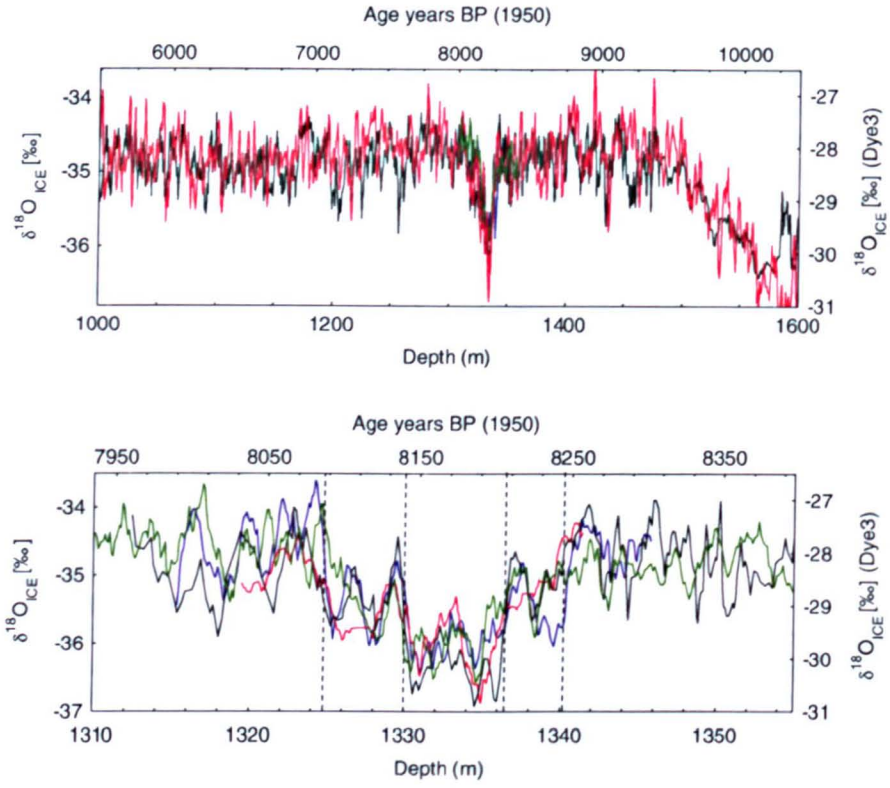

Fig. 2. Oxygen isotope ratios for the 8.2 ka event. Data are shown for GRIP (red), GISP2 (black), NGRIP (blue), and Dye 3 (green) all plotted on the GRIP depth scale and the GICC05 age scale (a) Between 1000 and 1600 m, from the mid to early Holocene, with all data smoothed to approximately 20 yr running averages; (b) between 1310 and 1355 m, with all data smoothed to approximately 10 yr running averages. Outer dashed lines indicate onset and termination of whole event and inner dashed lines indicate onset and termination of central event (see text).

Finally, we combined the normalized datasets to give a composite Greenland isotope signal across the event; a four-point running mean of the 2.5 yr resolution data, representing decadal-scale variability is also shown (**Fig. 4**). Of course, this does not represent a Greenlandic spatial average because the cores are not fully representative but it should nonetheless define the most prominent common features of the climate change occurring at this time.

To determine when the event started and ended we calculated the mean (−34.73‰) and SD (0.83‰) of the GRIP 27.5 cm data for the 1000 yr period between 9300 and 8300 yr BP (because we have normalized the data from the other sites to GRIP this should also represent the statistic for the composite).

We can now define two intervals. Between 1324.77 and 1340.12 m, the composite 27.5 cm isotopic values are consistently below the mean for the preceding 1000 yr. This can be seen as the maximum extent of the climate cooling anomaly. On the GICC05 timescale, it represents 159 yr. We also define a "central event" during which the composite signal is consistently more than 1 SD below the average of the previous 1000 yr. This core period lasts for 70 yr on the GICC05 timescale. Both periods are shown with vertical lines in **Fig. 5**, and described in **Table 1**.

The 8.2 ka event, as defined in this study, is asymmetrical in shape with considerable decadal variability in the record as shown by the presence of relatively warm spikes at around 8220 and 8160 yr BP (**Fig. 4**). The asymmetrical shape has been replicated in climate models of THC weakening (**Manabe and Stouffer, 1995**; **Renssen et al., 2001**) and the relatively warm phase in the early part of the cold event has been observed by (**Wiersma and Renssen, 2006**) in model experiments showing temporal strengthening of the THC approximately 30 yr after the freshwater perturbation was introduced.

Despite general similarities in the shape of the low-resolution isotope record in each of the Greenland cores, differences exist on the decadal and shorter resolution and hence our assessment of the onset and termination depths for the 8.2 ka event would be different in each of the cores (**Fig. 5**). It appears as if the early part of the event is most prominent in NGRIP, and the event is completed slightly earlier at Dye 3 in the south. This might indicate some kind of north–south progression of the event. However, one would want to see more duplicate cores in each region to assess the significance of these findings.

4.1. Confirming the duration of the event

Many of the chemical species in Greenland cores show annual peaks and troughs. (**Whitlow et al., 1992**) in a comparative study of seasonal concentrations of major

Please cite this article as: Elizabeth R. Thomas et al., The 8.2 ka event from Greenland ice cores, Quaternary Science Reviews (2006), doi:10.1016/j.quascirev.2006.07.017

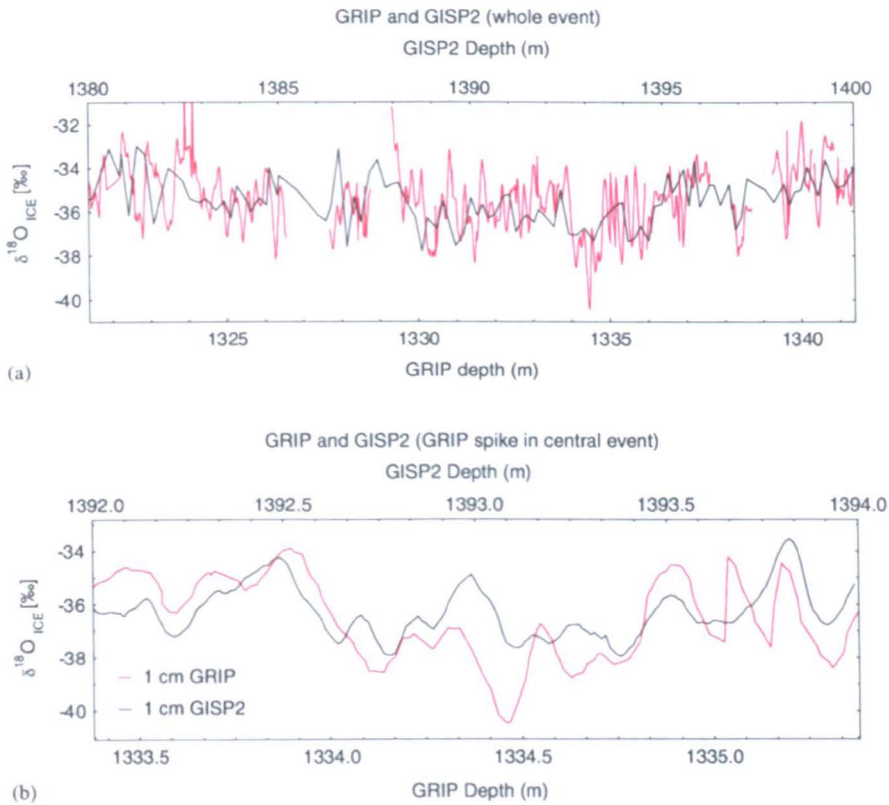

Fig. 3. High-resolution variability in the oxygen isotope record across the center of the event. Oxygen isotopes from GRIP (1 cm resolution, red) and GISP2 (5 or 1 cm resolution, black) covering the whole event (graph a) and the central event (graph b). The GRIP and GISP2 data have been aligned precisely using a volcanic ECM peak clearly seen in both records during the event.

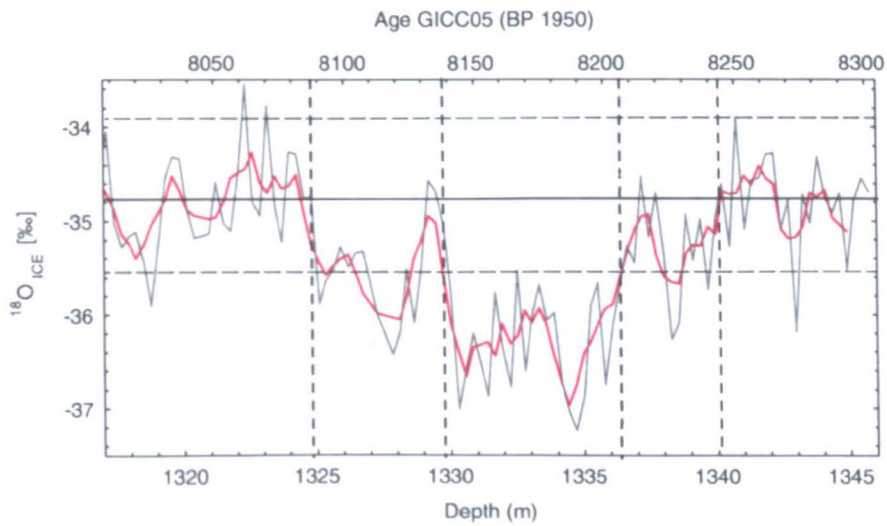

Fig. 4. Composite oxygen isotope record ratios for the 8.2 ka event for the Greenland ice cap. This is a stack of data from Dye 3, GRIP, GISP2, and NGRIP all normalized to the GRIP mean and standard deviation, and plotted on the GRIP depth scale. The composite dataset is shown as averages over 27.5 cm depth increments (approximately 2.5 yr, gray) and then as a running four-point average of this (representing decadal variability, red). Dashed vertical lines indicate the onset and termination of the central event (1329.96–1336.45 m) and the whole event (1324.77–1340.12 m), while horizontal lines are the mean and one standard deviation above and below the mean for the 27.5 cm GRIP dataset for 8.3–9.3 ka BP.

chemical species determined their seasonality within an idealized $\delta^{18}O$ curve for pre-1900 Summit Greenland. Using a combination of such species, it is possible to count the year in a section of core. This has already been done for parts of the GRIP and NGRIP cores and for some measured parameters (Rasmussen et al., 2006). Here, we use the annual peaks for the species we have measured over the 20 m section of the GRIP core, in order to

Please cite this article as: Elizabeth R. Thomas et al., The 8.2 ka event from Greenland ice cores, Quaternary Science Reviews (2006), doi:10.1016/j.quascirev.2006.07.017

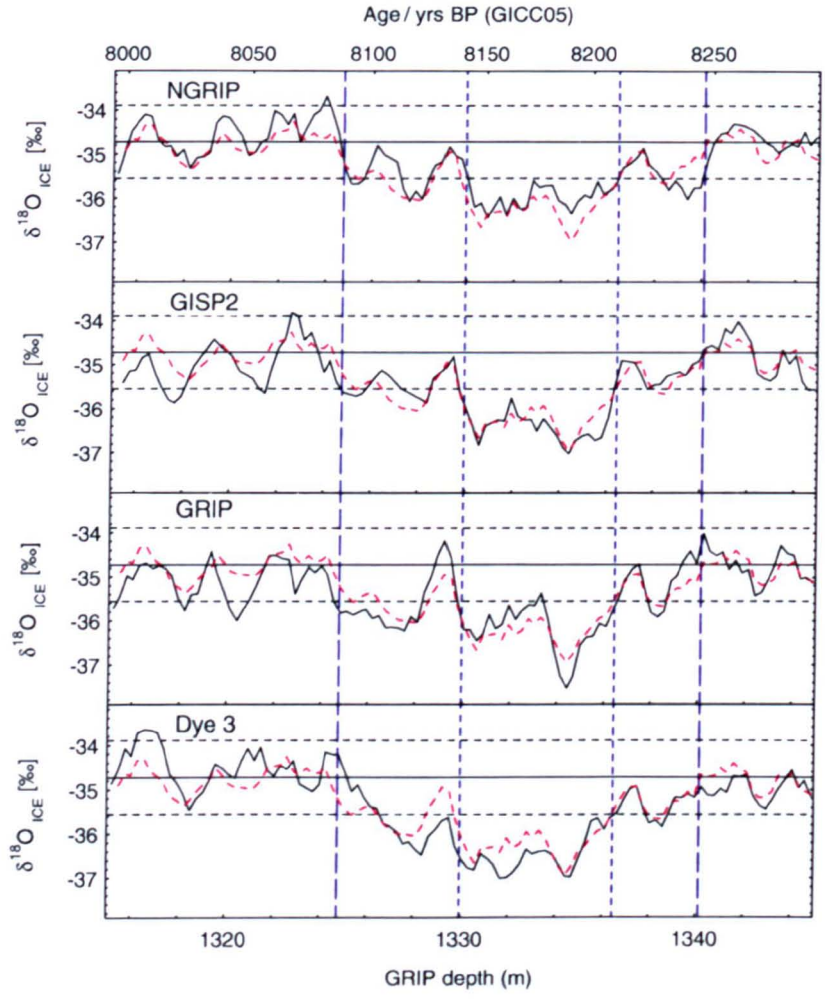

Fig. 5. Oxygen isotope ratios for the 8.2 ka event for four different Greenland sites. In each case the normalized decadally averaged data are shown on the GRIP depth scale. The dashed line is the composite stack for all four sites. Other lines as in **Fig. 3**.

Table 1
Age of markers in the 8.2 ka event

Event	Depth (GRIP m)	Age (GICC05 yr BP)	Age (GICC05 yr b2k)
Start	1340.12	8247	8297
Start central event	1336.45	8212	8262
End central event	1329.96	8141	8191
End	1324.77	8086	8136

determine the duration of the event as defined in the previous section.

The annual layers were counted using all nine species with the best reproducible results coming from sulfate, nitrate, sodium, and chloride (**Fig. 6**) An annual layer was determined as a peak in sodium and chloride followed by a peak in nitrate and sulfate approximately 6 months later. The second layer counting method is shown in **Fig. 7** using Na^+/SO_4^{2-} and NO_3^-. Dating uncertainty over the approximately 200 yr period analyzed is $\pm 4\%$ to account for missing ice over this section. Using these methods, we obtain a length for the full event of 160.5 ± 5.5 yr, and for the central event of 69 ± 2 yr. Both agree within the uncertainty with the lengths of 159 and 70 yr in GICC05 year (**Rasmussen et al., 2006**), confirming the duration using a totally independent counting method.

The length we are defining here for the full event is close to the previously published best estimate of 200 yr (**Alley et al., 1997**); the period during which methane in the GRIP core is significantly below its normal envelope is of similar length (**Spahni et al., 2003**). The duration estimated for the isotopic anomaly in Ammersee, Germany (**von Grafenstein et al., 1998**) is also 200 yr. A much shorter duration of isotopic anomaly was previously reported in a speleothem record from Ireland (**Baldini et al., 2002**). However, this has recently been identified as an analytical artifact (**Fairchild et al., 2006**). Events of longer duration at sites away from the North Atlantic have also been associated with the 8.2 ka event, but it is not yet clear whether some of them represent the same event

Please cite this article as: Elizabeth R. Thomas et al., The 8.2 ka event from Greenland ice cores, Quaternary Science Reviews (2006), doi:10.1016/j.quascirev.2006.07.017

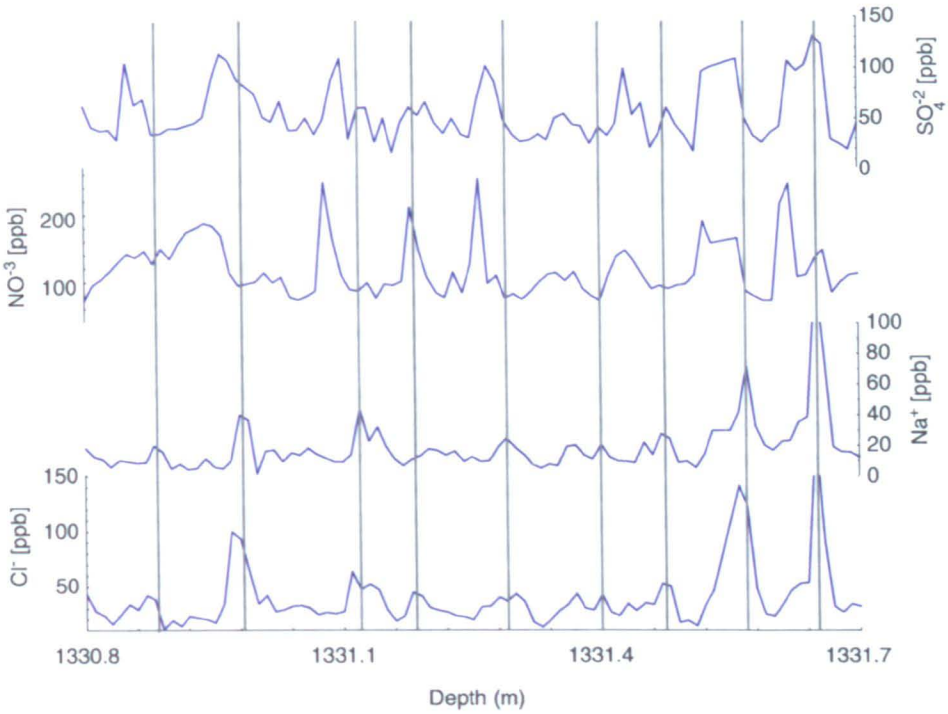

Fig. 6. Annual layer counting of Sulphate (top), nitrate, sodium, and chloride (bottom) in the GRIP core. Grey vertical lines indicate year.

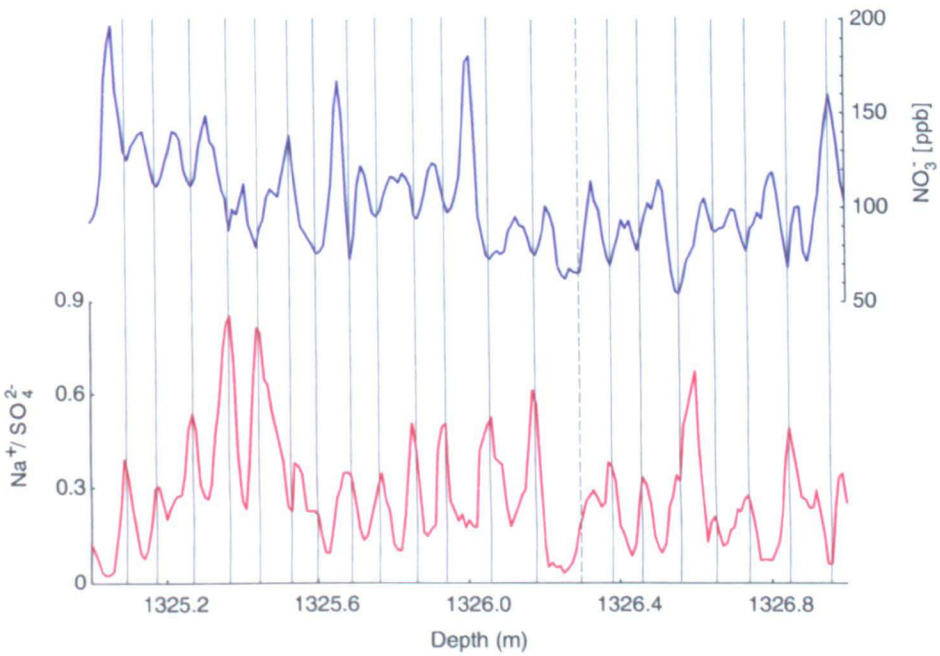

Fig. 7. Annual layer counting using Na^+/SO_4^{2-} and NO_3^- in the GRIP core. Annual layers indicated by solid lines, uncertainty indicated by dashed lines.

(Rohling and Palike, 2005). In any case, we propose that the structure and duration we have described from our Greenland composite record represents a good target for modeling studies. We now consider other parameters measured in the core.

5. Accumulation rate

The accumulation rate can be determined from the thickness of the annual layers of the chemical species providing ice thinning is accounted for. The annual layers

Please cite this article as: Elizabeth R. Thomas et al., The 8.2 ka event from Greenland ice cores, Quaternary Science Reviews (2006), doi:10.1016/j.quascirev.2006.07.017

are gradually stretched and thinned under the vertical compression and longitudinal stress in the ice sheet. Using a Dansgaard–Johnsen type model, assuming thinning is proportional to burial, the mean accumulation rate for the central event is 0.16 m of ice per year (**Fig. 8**). This is a decrease of 9% from the average during the 200 yr period surrounding the event and 31% from the mean Holocene value.

6. Chemistry

Atmospheric loading is reflected by the chemical composition in Summit ice (**O'Brien et al., 1995**), and is an indicator of changes occurring further from Greenland. The marine input (determined from Na and Cl concentrations) represents some combination of the vigor of atmospheric circulation and the location and strength of marine sources, while the continental component (inferred by the concentrations of Ca) is indicative of long range atmospheric transport and the strength of the source, believed to be in Asia (**Biscaye et al., 1997**; **Svensson et al., 2000**).

We now have detailed chemical profiles across the 8.2 ka event at GRIP (**Fig. 9**); our motivation was to study the phasing of changes in chemical and isotopic proxies across the event. We also re-examine the chemical profiles from GISP2 (**O'Brien et al., 1995**) across a wider section of core (**Fig. 10**). In the detailed GRIP record, some short periods of high concentration are observed within the period of the event. However, these are not unusual in the longer perspective provided by the longer Ca and NH_4 records in the GRIP core (**Fuhrer et al., 1993**). In earlier discussions of the 8.2 ka event in Greenland, it was suggested that significant changes in chemical concentration occurred over the event, and this has been used to imply some significant changes in atmospheric circulation affecting a larger region than the isotopic indicators cover.

The evidence for a change in atmospheric circulation was first reported by **Alley et al. (1997)** as an increase in calcium and chloride of 60% from background values. These percentage increases were calculated based on the difference between the maximum value at the peak of the event and the values just outside the event (**Alley et al., 1997**; **Alley and Agustsdottir, 2005**). We propose that the comparison of the period average with that of a longer Holocene record, gives a better indication of change.

Unfortunately, the high variability in our data, for sea salt in particular, precludes the use of the short section of data from the GRIP core for a similar calculation; we do not have a long enough section from either side of the event to make meaningful statistical comparisons. We note however that the Ca concentration (**Fig. 9**) (**Fuhrer et al., 1993**) in the 70 yr central event (average 8.4 $\mu g\,kg^{-1}$) is higher, but without statistical significance, than the average concentration of the 10 sections, each about 70 yr long, which preceded it (7.1 +/−1.3 $\mu g\,kg^{-1}$).

In the light of this we returned to the original GISP2 chemical data, as made available at (**ftp:http://www.ftp.ncdc.noaa.gov/pub/data/paleo/icecore/greenland/summit/gisp2/chem/iond.txt**).

We removed a single anomalous chloride data point that is apparent in the data; this single value of 72 $\mu g\,kg^{-1}$ is not supported by the values of other sea salt ions, and therefore

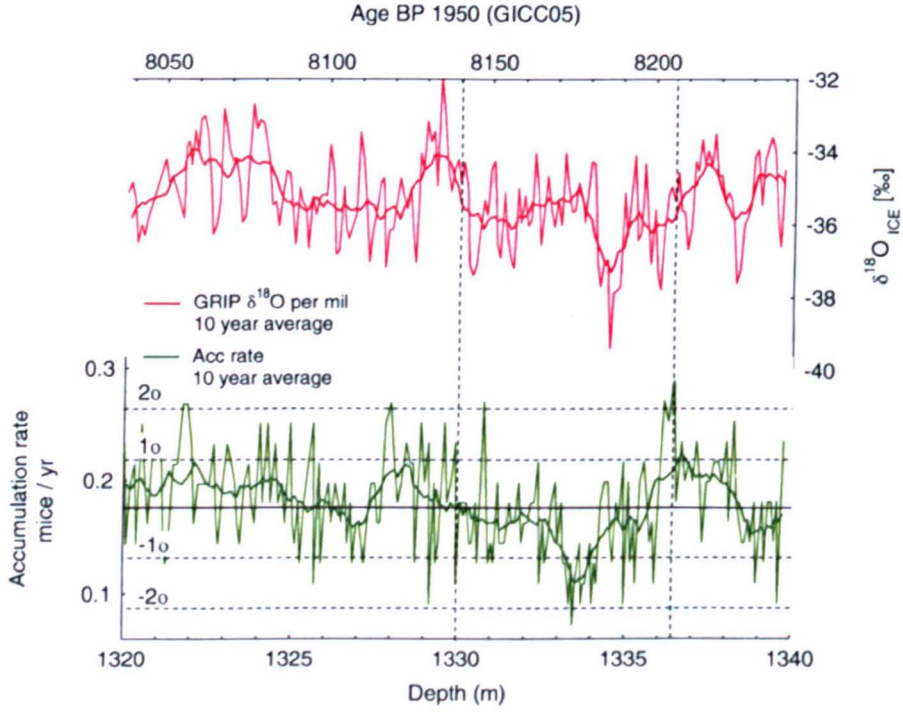

Fig. 8. Accumulation rate (meters of ice per year) derived from the average annual layer thickness derived by counting, corrected for ice thinning.

Please cite this article as: Elizabeth R. Thomas et al., The 8.2 ka event from Greenland ice cores, Quaternary Science Reviews (2006), doi:10.1016/j.quascirev.2006.07.017

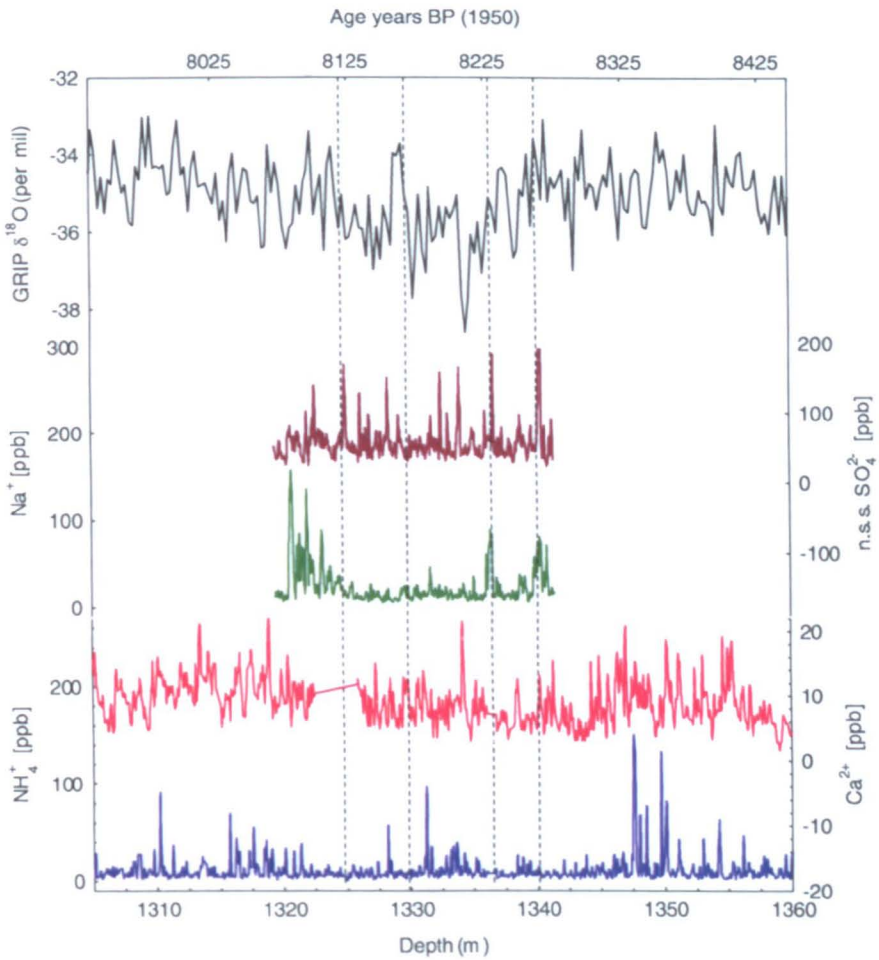

Fig. 9. High-resolution chemical data and oxygen isotopes from the GRIP ice core. Oxygen isotopes at 27 cm resolution (black); sodium (green), and non-sea salt Sulfate (brown), analyzed at 1 cm resolution using IC; calcium (red), and ammonium (blue), analyzed using CFA (Fuhrer et al., 1999). Data are shown on a GRIP depth scale and the GICC05 age scale, as approximately annual averages. Vertical dashed lines define the 8.2 ka event.

does not represent an enhancement of marine input. We have then re-plotted the data for chloride and calcium on the GRIP depth scale (for comparison with earlier figures in this paper), and included vertical lines representing the duration of the 8.2 ka event as before (Figs. 4 and 5). In order to clarify the presentation, we have plotted only 1.1 m averages (approximately decadal), and also approximately 70 yr averages (the length of the central event).

It is immediately obvious that the enhancements, when seen in the context of the data from the centuries surrounding the event, are relatively small. For chloride, neither decadal nor 70 yr average values are the highest of the section shown. However, the average value for the central event is elevated for several decades, by about 15% compared to the 1000 yr period centered on the event. These increases are much smaller than those reported previously (Alley and Agustsdottir, 2005), partly because the single anomalous data point was included in the 20 yr averages shown there, but also because of the different methodology used to estimate the change during the event.

For Ca, there is a clear increase in concentration across the event, although only for the period of the central event is it unusual compared to the surrounding period. Specifically, the average value in the central event is elevated about 35% compared to the average for the 1000 yr surrounding (but excluding) it. High values are sustained in the decadal values throughout the central event. Thus, we agree that statistically significant increases occurred but due to different methodologies they are smaller than have been reported previously. The relatively small changes compared to the normal variability prevent us from making any statement about the phasing of chemical and isotopic changes.

7. Discussion and concluding remarks

The cold event 8200 yr ago is observed in central Greenland as a 160.5 yr period of reduced isotopic ratios, within which there is a central event of 69 yr during which values were significantly below the Holocene average. Comparison of the isotope record from four cores, two of which are located just 30 km apart, highlighted variability between the records at decadal and shorter timescales; it is not yet clear if this represents significant spatial differences

Please cite this article as: Elizabeth R. Thomas et al., The 8.2 ka event from Greenland ice cores, Quaternary Science Reviews (2006), doi:10.1016/j.quascirev.2006.07.017

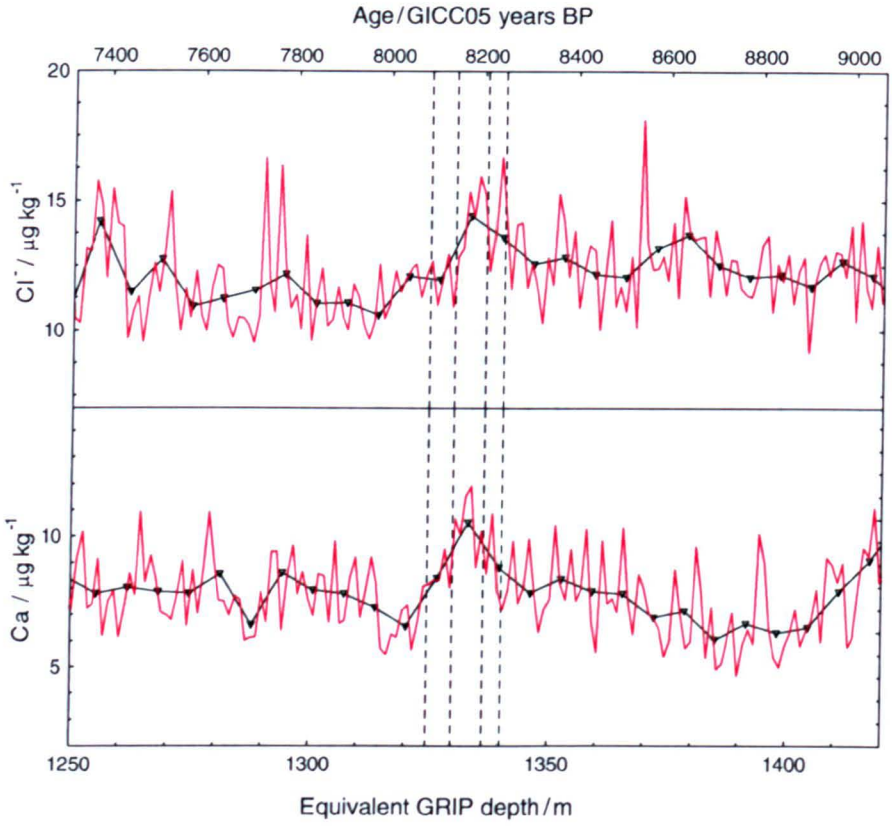

Fig. 10. Chemical data from the GISP2 ice core, derived from data previously shown in **O'Brien et al. (1995** and **Alley and Agustsdottir (2005)**. Data are shown on a GRIP depth scale, as approximately decadal and 70 year averages. Vertical dashed lines define the 8.2 ka event.

in response. Re-examination of chemical data, based on a different methodology, show smaller changes in chemical deposition over Greenland accompanying this cold event than those reported previously.

The small increase in Cl could reflect a small increase in storminess, or in sea ice production at the onset of colder conditions around Greenland; the small increase in Ca could reflect small changes in Asian conditions or in transport strength. However, it is worth noting that similar increased Ca concentrations are also observed in the GISP2 dataset between 5 and 6 ka BP, which are not accompanied by an isotopic signal, and that the Cl increase is not unusual in the Holocene. We conclude that there is only weak evidence in the Greenland ice cores for a significant change (outside the Holocene norm) beyond the North Atlantic region during the 8.2 ka event. Only methane (**Blunier et al., 1995**) (which we do not discuss here) shows a clear signal that might derive from further a field.

The 8.2 ka event has often been compared to the much larger Younger Dryas event (**Alley et al., 1997**; **Alley and Agustsdottir, 2005**) which punctuated the termination of the last glacial with a proposed mechanism of flood outburst from the final deglaciation of the Laurentide ice sheet (**Broecker et al., 1988**; **Alley, 2000**) The proposed mechanism for the 8.2 ka event is similar. The estimated temperature change at the 8.2 ka event is about 40% of that at the Younger Dryas, and the changes in accumulation rate and methane show a similar proportionality. However, the increases in chemical deposition for the Younger–Dryas transition were in excess of 600% for calcium and 200% for chloride. The small increase in Ca and Cl during the 8.2 ka event (about 5% of that observed in the Younger Dryas) suggests that the larger-scale atmospheric response during the event was very subdued, and certainly not proportional to the local climatic signal in the North Atlantic.

Interest in this event is currently high, with increasing numbers of paleoclimate data recording this period, which is seen as a suitable test-bed for the ability of models to predict the climatic effects of changes in thermohaline circulation. It is important therefore that we consider exactly what event we are referring to when reporting paleoclimate findings. There was a definite cold period in Greenland that occurred 8200 yr ago as shown by the decrease in isotope ratios and accumulation rates observed in all four deep ice cores drilled in Greenland, and by the evidence from ^{15}N in N_2 in the air bubbles, that confirms that a temperature decrease occurred. Several corroborative records across northern Europe exist which suggests that these cold conditions spread further than just Greenland. However, beyond the North Atlantic, the evidence that we are seeing the same sharp event gets weaker. It has previously been suggested that the event

Please cite this article as: Elizabeth R. Thomas et al., The 8.2 ka event from Greenland ice cores, Quaternary Science Reviews (2006), doi:10.1016/j.quascirev.2006.07.017

(Alley and Agustsdottir, 2005; Rohling and Palike, 2005) observed as a sudden change in records such as the Greenland one is superimposed on a longer, less unique event seen elsewhere. We concur with this view: while the broad context of climate variability is clearly important, we recommend that the term "8.2 ka event" be reserved for signals of a timing and duration similar to that reported here.

Acknowledgments

We thank Richard Alley, Jonathan Holmes, and an anonymous reviewer for their helpful comments. The Natural Environment Research Councils RAPID climate change program supported this work. Data provided by the National Snow and Ice Data Center, University of Colorado at Boulder, and the WDC-A for Paleoclimatology, National Geophysical Data Center, Boulder, Colorado.

References

Alley, R.B., 2000. The Younger Dryas cold interval as viewed from central Greenland. Quaternary Science Reviews 19, 213–226.

Alley, R.B., Agustsdottir, A.M., 2005. The 8 k event: cause and consequences of a major Holocene abrupt climate change. Quaternary Science Reviews 24 (10–11), 1123–1149.

Alley, R.B., Mayewski, P.A., Sowers, T., Stuiver, M., Taylor, K.C., Clark, P.U., 1997. Holocene climate instability: a prominent widespread event 8200 year ago. Geology 25, 483–486.

Baldini, J.U.L., McDermott, F., Fairchild, I.J., 2002. Structure of the 8200 yr cold event revealed by a speleothem trace element record. Science 296, 2203–2206.

Barber, D.C., Dyke, A., Hillaire-Marcel, C., Jennings, A.E., Andrews, J.T., Kerwin, M.W., Bilodeau, G., McNeely, R., Southon, J., Morehead, M.D., Gagnon, J.M., 1999. Forcing of the cold event 8200 yr ago by catastrophic drainage of laurentide lakes. Nature 400, 344–348.

Biscaye, P.E., Grousset, F.E., Revel, M., Van der Gaast, S., Zielinski, G.A., Vaars, A., Kukla, G., 1997. Asian provenance of glacial dust (stage 20) GISP2. Journal of Geophysical Research 102 (C12), 26765–26781.

Blunier, T., Chappellaz, J., Schwander, J., Stauffere, B., Raynaud, D., 1995. Variations in atmospheric methane concentration during the Holocene epoch. Nature 374, 46–49.

Broecker, W.S., Andree, M., Wolfli, W., Oeschger, H., Bonani, G., Kennett, J., Peteet, D., 1988. The chronology of the last deglaciation: implications to the cause of the Younger Dryas event. Paeoceanography 3, 1–19.

Clark, P.U., 2001. Freshwater forcing of abrupt climate change during the last glaciation. Science 293 (5528), 283–287.

Clarke, G.K.C., Leverington, D.W., Teller, J.T., Dyke, A.S., 2004. Paleohydraulics of the last outburst flood from glacial Lake Agassiz and the 8200 BP cold event. Quaternary Science Reviews 23 (3–4), 389–407.

Dansgaard, W., 1985. Greenland ice core studies. Palaeogeography, Palaeoclimaology and Palaeoecology 50 (2–3), 185–187.

Dansgaard, W., 1993. Evidence for general instability of past climate from a 250 kyr ice core record. Nature 364, 218–220.

Fairchild, I.J., Smith, C.L., Baker, A., Fuller, L., Spötl, C., Mattey, D., McDermott, F., E.I.M.F., 2006. Modification and preservation of environmental signals in speleothems. Earth-Science Reviews 75, 105–153.

Fuhrer, K., Neftel, A., Anklin, M., Maggi, V., 1993. Continuous measurements of hydrogen peroxide, formaldehyde, calcium and ammonium concentrations along the GRIP ice core from summit, Central Greenland. Atmospheric Environment Part A 27 (12), 1873–1880.

Fuhrer, K., Wolff, E.W., Johnsen, S.J., 1999. Timescales for dust variability in the Greenland ice core Project (GRIP) ice core in the 1,00,000 year. Journal of Geophysical Research 104 (D24), 31043–31052.

GRIP Project Members, 1993. Climate instability during the last interglacial period recorded in the GRIP ice core. Nature 364, 203–207.

Johnsen, S.J., Clausen, H.B., Dansgaard, W., Fuhrer, K., Gundestrup, N., Hammer, C.U., Iversen, P., Jouzel, J., Stauffer, B., Steffensen, J.P., 1992. Irregular glacial interstadials recorded in a new Greenland ice core. Nature 359, 311–313.

Knudsen, K.L., Jiang, H., Jansen, J., Eiriksson, J., Heinemeier, J., Seidenkrantz, M.-S., 2004. Environmental changes off North Iceland during the deglaciation and the Holocene: foraminifera, diatoms and stable isotopes. Marine Micropaleontology 50 (3–4), 273–305.

LeGrande, A.N., Schmidt, G.A., Shindell, D.T., Field, C.V., Miller, R.L., Kock, D.M., Faluvegi, G., Hoffmann, G., 2006. Consistent simulations of multiple proxy responses to an abrupt climate change event. 103(4), 837–842.

Leuenberger MC, L.C., Schwander, J., 1999. Delta (15)N measurements as a calibration tool for the paleothermometer and gas–ice age differences: a case study for the 8200 BP event on GRIP ice. Journal of Geophysical Research 104 (D18), 22163–22170.

Manabe, S., Stouffer, R.J., 1995. Simulation of abrupt climate-change induced by freshwater input to the North Atlantic Ocean. Nature 378 (6553), 165–167.

Mayewski, P.A., Meeker, L.D., Whitlow, S., Twickler, M.S., Morisson, M.C., Bloomfield, P., Bond, G.C., Alley, R.B., Gow, A.J., Grootes, P.M., Meese, D.A., Ram, M., Taylor, K.C., Wumkes, W., 1994. Changes in atmospheric circulation and ocean ice cover over the North Atlantic during the last 41,000 year. Science 263 (5154), 1747–1751.

Meese, D.A., Gow, A.J., Alley, R.B., Zielinski, G.A., Grootes, P.M., Ram, M., Taylor, K.C., Mayewski, P.A., Bolzan, J.F., 1997. The Greenland ice core Project 2 depth-age scale: methods and results. Journal of Geophysical Research 102, 26411–26423.

Muscheler, R., Beer, J., Vonmoos, M., 2004. Causes and timing of the 8200 year BP event inferred from the comparison of the GRIP Be-10 and the tree ring Delta C-14 record. Quaternary Science Reviews 23 (20–22), 2101–2111.

North Greenland ice core Project Members, 2004. High-resolution record of Northern Hemisphere climate extending into the last interglacial period. Nature 431 (7005), 147–151.

O'Brien, S.R., Mayewski, P.A., Meeker, L.D., Meese, D.A., Twickler, M.S., Whitlow, S.I., 1995. Complexity of Holocene climate as reconstructed from a Greenland ice core. Science 270 (5244), 1962–1964.

Rasmussen, S.O., Andersen, K.K., Svensson, A.M., Steffensen, J.P., Vinther, B.M., Clausen, H.B., Siggaard-Andersen, M.-L., Johnsen, S.J., Larsen, L.B., Bigler, M., Röthlisberger, R., Fischer, H., Goto-Azuma, K., Hansson, M.E., Ruth, U., 2006. A new Greenland ice core chronology for the last glacial termination. Journal of Geophysical Research 111 (D6), D06102.

Renssen, H., Goosse, H., Fichefet, T., Campin, J.M., 2001. The 8.2 kyr BP event simulated by a global atmosphere–sea-ice–ocean model. Geophysical Research Letters 28 (8), 1567–1570.

Rohling, E.J., Palike, H., 2005. Centennial-scale climate cooling with a sudden cold event around 8200 year ago. Nature 434 (7036), 975–979.

Spahni, R., Schwander, J., Fluckiger, J., Stauffer, B., Chappellaz, J., Raynaud, D., 2003. The attenuation of fast atmospheric CH_4 variations recorded in polar ice cores. Geophysical Research Letters 30 (11), 1571.

Please cite this article as: Elizabeth R. Thomas et al., The 8.2 ka event from Greenland ice cores, Quaternary Science Reviews (2006), doi:10.1016/j.quascirev.2006.07.017

Svensson, A., Biscaye, P.E., Grousset, F.E., 2000. Characterization of late glacial dust in the GRIP. Journal of Geophysical Research 105 (D4), 4637–4656.

Thomas, E.R., 2006. High-resolution analysis of rapid climate change from Greenland ice cores. PhD Thesis, British Antarctic Survey, Open University.

Vinther, B.M., Clausen, H.B., Johnsen, S.J., Rasmussen, S.O., Andersen, K.K., Buchardt, S.L., Dahl-Jensen, D., Seierstad, I.K., Siggaard-Andersen, M-L., Steffensen, J.P., Svensson, A., Olsen, J., Heinemeier, J., 2006. A synchronized dating of three Greenland ice cores throughout the Holocene. Journal of Geophysical Research 111 (D13), D13102.

von Grafenstein, U., Erlenkeuser, H., Muller, J., Jouzel, J., Johnsen, S.J., 1998. The cold event 8200 year ago documented in oxygen isotope records of precipitation in Europe and Greenland. Climate Dynamics 14, 73–81.

Whitlow, S., Mayewski, P.A., Dibb, J.E., 1992. A comparison of major chemical-species seasonal concentration and accumulation at the South Pole and Summit, Greenland. Atmospheric Environment Part A 26 (11), 2045–2054.

Wiersma, A.P., Renssen, H., 2006. Model-data comparison for the 8.2 ka BP event: confirmation of a forcing mechanism by catastrophic drainage of Laurentide lakes. Quaternary Science Reviews 25 (1–2), 63–88.

Please cite this article as: Elizabeth R. Thomas et al., The 8.2 ka event from Greenland ice cores, Quaternary Science Reviews (2006), doi:10.1016/j.quascirev.2006.07.017